

132839

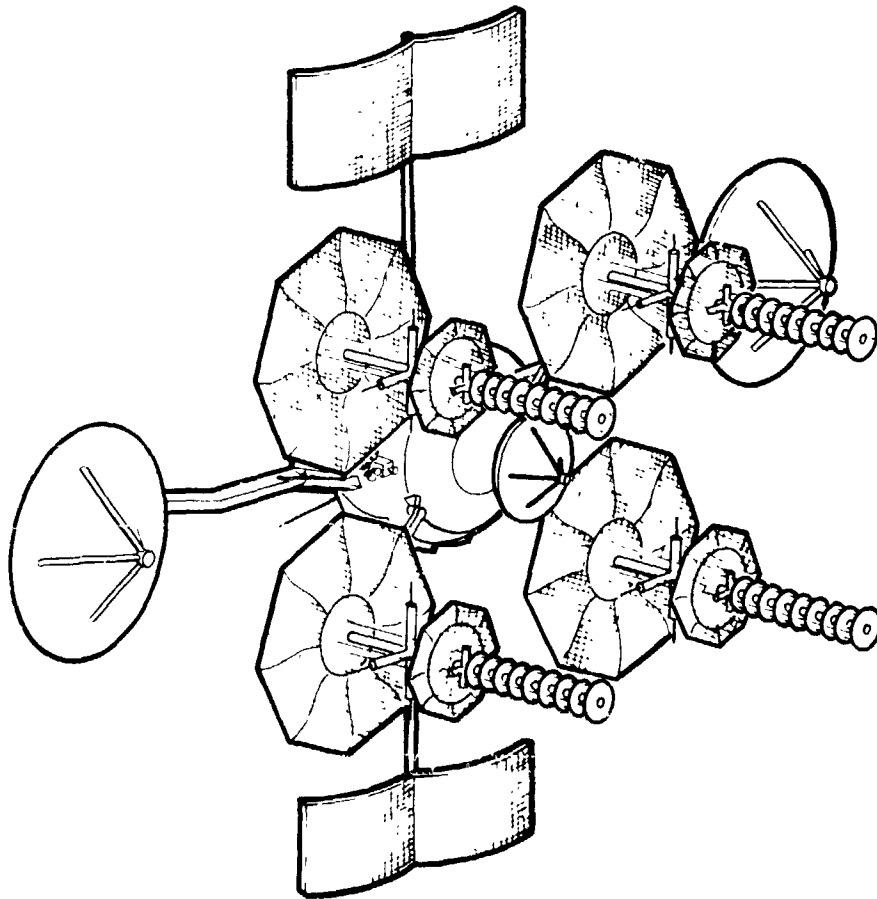
SD 72-SA-0133-4

PART I FINAL REPORT

TRACKING & DATA RELAY SATELLITE SYSTEM CONFIGURATION & TRADEOFF STUDY

VOLUME IV SPACECRAFT & SUBSYSTEM DESIGN

NASA-CR-132839 TRACKING AND DATA RELAY
 SATELLITE SYSTEM CONFIGURATION AND
 TRADEOFF STUDY. VOLUME 4: SPACECRAFT
 AND SUBSYSTEM DESIGN, (NORTH AMERICAN
 ROCKWELL CORP.) 390 P HC \$11.50 CSEL 22E
 N74-10809
 UAClas
 21311
 63/31



OCTOBER 1972

SUBMITTED TO
 GODDARD SPACE FLIGHT CENTER
 NATIONAL AERONAUTICS & SPACE ADMINISTRATION



IN ACCORDANCE WITH
 CONTRACT NAS5-21705

PART I FINAL REPORT

**TRACKING & DATA RELAY SATELLITE SYSTEM
CONFIGURATION & TRADEOFF STUDY**

**VOLUME IV
SPACECRAFT & SUBSYSTEM DESIGN**

Tom Hill

T. E. Hill
TDRS STUDY MANAGER

OCTOBER 1972

SUBMITTED TO
GODDARD SPACE FLIGHT CENTER
NATIONAL AERONAUTICS & SPACE ADMINISTRATION



Space Division
North American Rockwell

IN ACCORDANCE WITH
CONTRACT NAS5 21705

PRECEDING PAGE BLANK NOT FILMED

FOREWORD

This report summarizes the results of Part I of the study conducted under Contract NAS5-2107, Tracking and Data Relay Satellite Configuration and Systems Trade-off Study - 3-Axis Stabilized Configuration. The study was conducted by the Space Division of North American Rockwell Corporation for the Goddard Space Flight Center of the National Aeronautics and Space Administration.

The study is in two parts. Part I of the study considered all elements of the TDRS system but emphasized the design of a 3-axis stabilized satellite and a telecommunications system optimized for support of low and medium data rate user spacecraft constrained to be launched on a Delta 2914. Part II will emphasize upgrading the spacecraft design to provide telecommunications support to low and high, or low, medium and high data rate users, considering launches with the Atlas/Centaur and the Space Shuttle.

The report consists of the following seven volumes.

- | | |
|--|-----------------|
| 1. Summary | SD 72-SA-0133-1 |
| 2. System Engineering | SD 72-SA-0133-2 |
| 3. Telecommunications Service System | SD 72-SA-0133-3 |
| 4. Spacecraft and Subsystem Design | SD 72-SA-0133-4 |
| 5. User Impact and Ground Station Design | SD 72-SA-0133-5 |
| 6. Cost Estimates | SD 72-SA-0133-6 |
| 7. Telecommunications System Summary | SD 72-SA-0133-7 |

Acknowledgment is given to the following individuals for their participation in and contributions to the conduct of this study:

M.A. Cantor	North American Rockwell	System Engineering and Spacecraft Design
A.A. Nussberger	"	Electrical Power
W.C. Shail	"	"
R.E. Oglevie	"	Stabilization and Control
A.F. Boyd	"	"
R.W. Yee	"	Propulsion
A.D. Nusenow	"	Thermal Control
T.F. Rudiger	"	Flight Mechanics
J.W. Collins	"	Satellite Design
P.H. Dirnbach	"	Reliability
W.F. Deutsch	"	Telecommunications Design
S.H. Tuskel	"	Operations Analysis
A. Forster	"	Cost
A.F. Anderson	"	Integration
T.T. Moji	AIL-Division of Cutler-Hammer	Telecommunications Design
L. Swartz	"	"
D.M. DeVito	The Magnavox Company	Telecommunication System Analysis
D. Cartier	"	Ground Station Design
R.H. French	"	Operations Analysis
G. Shaughanian	"	User Transponder Design

PRECEDING PAGE BLANK NOT FILMED



TABLE OF CONTENTS

VOLUME I

Section	Page
1.0 SUMMARY	1-1
1.1 SYSTEM CONCEPT	1-3
1.2 SATELLITE LAUNCH AND DEPLOYMENT	1-7
1.2.1 Deployment Analysis	1-7
1.2.2 Launch Analysis	1-8
1.2.3 Launch and Deployment Profile	1-11
1.3 TELECOMMUNICATIONS DESIGN	1-13
1.3.1 Telecommunications System Analysis	1-13
1.3.2 Telecommunications Subsystem Design	1-25
1.3.3 Telecommunications Relay Performance	1-29
1.4 SPACECRAFT MECHANICAL AND STRUCTURAL DESIGN	1-35
1.5 ELECTRICAL POWER SUBSYSTEM	1-51
1.6 ATTITUDE STABILIZATION AND CONTROL SUBSYSTEM	1-54
1.7 AUXILIARY PROPULSION SUBSYSTEM	1-57
1.7.1 Reaction Control Subsystem	1-57
1.7.2 Apogee Motor	1-60
1.8 THERMAL CONTROL	1-60
1.9 RELIABILITY	1-64
1.10 USER TRANSPONDER DESIGN	1-66
1.10.1 LDR Transponder	1-66
1.10.2 MDR Transponder	1-66
1.11 NETWORK OPERATIONS AND CONTROL	1-68
1.12 TDRS GROUND STATION	1-77
1.13 RECOMMENDATIONS	1-82

VOLUME II

2.0 SYSTEM ENGINEERING	2-1
2.1 MISSION ANALYSIS	2-1
2.1.1 Network Configuration	2-1
2.1.2 TDRS Operational Plan	2-6
2.1.3 Performance Sensitivity	2-19
2.1.4 TDRS On-Orbit Payload Capability	2-21
2.1.5 Launch and Deployment Profile	2-22
2.1.6 Launch and Deployment Timeline	2-27
2.2 NETWORK OPERATIONS AND CONTROL	2-33
2.2.1 TDRS System Concept	2-33
2.2.2 Primary System Elements and Their Operational and Functional Interfaces	2-37
2.2.3 TDRSS Functional Analysis	2-48
2.2.4 TDRS Operational Phase Sequence of Events	2-113
2.3 SYSTEM RELIABILITY ANALYSIS	2-139

VOLUME III

Section	Page
3.0 TELECOMMUNICATIONS SYSTEM ANALYSIS	3-1
3.1 RELAY SYSTEM REQUIREMENTS AND CONSTRAINTS	3-1
3.1.1 Design Goals	3-1
3.1.2 System Design Criteria	3-1
3.1.3 Telecommunication System Description	3-3
3.2 THE INTERFERENCE PROBLEM	3-4
3.2.1 Radio Frequency Interference	3-6
3.2.2 "Trash Noise" and Its Effect on the TDRS Channels	3-11
3.2.3 The TDRS User Propagation Path	3-16
3.3 FREQUENCY SELECTION	3-21
3.3.1 Frequency Trades	3-21
3.3.2 Frequency Plan	3-25
3.4 MODULATION AND CODING	3-25
3.4.1 Impact of Forward Error Control on the Medium and Low Data Rate Users	3-25
3.4.2 Voice Coding for Manned Users of the Tracking and Data Relay Satellite System	3-32
3.5 RELAY SYSTEM PERFORMANCE ANALYSIS	3-37
3.5.1 Forward (Command) Link Communications Performance	3-39
3.5.2 Return (Telemetry) Link Communications Performance	3-44
3.5.3 TDRS Tracking Performance	3-51
3.5.4 Pseudo-Random Code Acquisition and Tracking	3-67
3.5.5 Manned User Performance	3-76
3.6 REFERENCES	
4.0 TDRS TELECOMMUNICATION SUBSYSTEM	4-1
4.1 TELECOMMUNICATION SYSTEM REQUIREMENTS	4-7
4.1.1 Design Goals and Criteria	4-7
4.1.2 Requirements and Constraints	4-10
4.2 TELECOMMUNICATION SYSTEM DESIGN DESCRIPTION	4-12
4.2.1 Frequency Plan	4-12
4.2.2 Functional Description	4-22
4.2.3 Telecommunications Subsystem Size, Weight, and Power Summary	4-30
4.3 LOW DATA RATE LINK	4-32
4.3.1 Return Link	4-32
4.3.2 LDR Antenna	4-61
4.3.3 LDR Transponder	4-68

Section	Page
4.3.4 Performance Specification for LDR Transponder	4-81
4.3.5 Size, Weight, and Power Summary for LDR Transponder	4-86
4.4 MEDIUM DATA RATE LINK	4-87
4.4.1 MDR System Analysis and Trades	4-87
4.4.2 MDR Antennas	4-95
4.4.3 MDR Transceiver	4-100
4.4.4 Performance Specification for MDR Transponder	4-110
4.5 TDRS/GS LINK	4-119
4.5.1 System Analysis and Trades	4-119
4.5.2 TDRS/GS Link Antenna	4-124
4.5.3 TDRS/GS Transceiver	4-128
4.5.4 Performance Specification for the TDRS/GS Link Transponder	4-146
4.5.5 Size, Weight, and Power Summary of TDRS/GS Link Transponder	4-150
4.6 FREQUENCY SOURCE	4-151
4.6.1 System Analysis and Tradeoffs	4-151
4.6.2 Detailed Description of the Frequency Source	4-153
4.6.3 Performance Specification for the TDRS Frequency Source	4-157
4.6.4 Size, Weight, and Power Summary for TDRS Frequency Source	4-161
4.7 TRACKING, TELEMETRY, AND COMMAND SYSTEM	4-162
4.7.1 Mechanization Trades	4-163
4.7.2 Detailed Description of TT&C Transponder	4-163
4.7.3 Performance Specification for the TDRS Tracking, Telemetry and Command Subsystem	4-170
4.7.4 Size, Weight, and Power Summary for TT&C	4-172
4.8 TDRS TRACKING/ORDER WIRE TRANSPONDER	4-173
4.8.1 System Analysis and Trades	4-173
4.8.2 Detailed Description of TDRS Tracking Order Wire	4-175
4.8.3 Performance Specification for TDRS Tracking/Order Wire Transponder	4-177
4.8.4 Size, Weight, and Power Summary for the TDRS Tracking/Order Wire Transponder	4-179
4.9 Ku-BAND BEACON	4-179
4.9.1 System Description	4-179
4.9.2 Performance Specification of the Ku-Band Beacon	4-181
4.9.3 Size, Weight, and Power Summary of the Ku-Band Beacon	4-181

VOLUME IV

Section		Page
5.0	SPACECRAFT MECHANICAL AND STRUCTURAL DESIGN	5-1
5.1	TDRS BASELINE CONFIGURATION	5-2
	5.1.1 Deployed Configuration	5-2
	5.1.2 Launch Configuration	5-2
5.2	SPACECRAFT BODY STRUCTURE	5-6
5.3	ANTENNA MECHANICAL DESIGN	5-9
	5.3.1 MDR Antennas	5-9
	5.3.2 LDR UHF-VHF Array Structural Construction	5-9
	5.3.3 TDRS/GS Antenna	5-10
	5.3.4 TT&C Antennas	5-10
	5.3.5 Ku- and S-Band Tracking/ Order Wire Antennas	5-13
5.4	SOLAR ARRAY PANELS AND DRIVE MECHANISM	5-13
	5.4.1 Solar Panels	5-13
	5.4.2 Drive Mechanism	5-14
5.5	SUBSYSTEMS INSTALLATION	5-14
5.6	ACCESSIBILITY AND SERVICING PROVISIONS	5-21
5.7	MASS PROPERTIES	5-21
5.8	SUBSYSTEM INTEGRATION	5-21
6.0	ATTITUDE STABILIZATION AND CONTROL SUBSYSTEM (ASCS)	6-1
6.1	PERFORMANCE REQUIREMENTS	6-1
6.2	DISTURBANCE TORQUES AND MOMENTUM STORAGE REQUIREMENTS	6-3
	6.2.1 Solar Pressure Torques	6-3
	6.2.2 Antenna Gimbaling Disturbances	6-8
	6.2.3 Momentum Storage Requirements	6-8
6.3	SYSTEM MECHANIZATION TRADE STUDIES	6-13
	6.3.1 Transfer Orbit and Deployment Phase	6-13
	6.3.2 On-Orbit Phase Torquer and Momentum Storage Subsystem Trades	6-15
	6.3.3 Attitude Determination Sensor Trades	6-22
6.4	BASELINE SYSTEM DESCRIPTION	6-25
	6.4.1 Spin Stabilized Control Mode	6-25
	6.4.2 Three-Axis Stabilized Control System	6-30
6.5	APS Performance Requirements	6-33
	6.5.1 Propellant Requirements	6-33
	6.5.2 Thruster Performance Requirements	6-36
	6.5.3 Reaction Jet Configuration	6-39

Section		Page
7.0	PROPULSION SYSTEM	7-1
7-1	APS REQUIREMENTS AND CRITERIA	7-1
7-2	ANALYSIS AND TRADE STUDIES	7-2
7-3	SUBSYSTEM DESIGN	7-7
	7.3.1 Description	7-7
	7.3.2 Performance	7-8
7-4	DESIGN CONSIDERATIONS	7-16
	7.4.1 Operating Life	7-16
	7.4.2 Thrust Vector Alignment	7-17
	7.4.3 Performance Verification	7-17
7-5	APOGEE MOTOR	7-17
8.0	ELECTRICAL POWER SUBSYSTEM (EPS)	8-1
8.1	EPS SUMMARY	8-1
	8.1.1 Alternative Concepts	8-3
	8.1.2 Requirements	8-5
	8.1.3 EPS Description	8-13
8.2	PRIMARY POWER GENERATION ASSEMBLY	8-15
	8.2.1 Solar Array Function and Description	8-15
	8.2.2 Solar Array Assembly Characteristics	8-18
	8.2.3 Operational Constraints and Growth Considerations	8-20
8.3	ENERGY STORAGE ASSEMBLY	8-22
	8.3.1 Function and Description	8-22
	8.3.2 Assembly Characteristics	8-24
	8.3.3 Growth Considerations	8-26
8.4	POWER CONDITIONING ASSEMBLY	8-26
	8.4.1 Function and Description	8-26
	8.4.2 Power Conditioning Assembly Characteristics	8-28
	8.4.3 Operational Constraints and Growth Considerations	8-30
8.5	DISTRIBUTION, CONTROL AND WIRING ASSEMBLY	8-31
	8.5.1 Function and Description	8-31
	8.5.2 Assembly Characteristics	8-31
8.6	EFFECT OF BATTERY CAPABILITY OF TDRS VOICE TRANSMISSION	8-33
9.0	THERMAL CONTROL	9-1
9.1	REQUIREMENTS	9-1
	9.1.1 Mission Requirements	9-1
	9.1.2 Heat Rejection Loads	9-1
	9.1.3 Temperature Limits	9-4
	9.1.4 Design Constraints and Problem Areas	9-4

Section		Page
9.2	SYSTEM DESCRIPTION	9-7
	9.2.1 Louver Radiator	9-7
	9.2.2 Multilayer Insulation	9-10
	9.2.3 Thermal Control Coatings	9-13
	9.2.4 Equipment Component Placement	9-13
9.3	ALTERNATE CONCEPTS	9-15
	9.3.1 Passive Design	9-15
	9.3.2 Variable Conductance Heat Pipe Radiator	9-15
9.4	SUBSYSTEM THERMAL CONTROL	9-16
	9.4.1 APS	9-16
	9.4.2 Solar Array Panel	9-18
	9.4.3 Antennas	9-22
	9.4.4 Apogee Motor	9-22
	9.4.5 Excess Power Dissipation	9-23
9.5	SYSTEM DEFINITION	9-25
10.0	RELIABILITY	10-1
	10.1 DEFINITIONS	10-1
	10.2 RELIABILITY GOALS AND CRITERIA	10-2
	10.3 SUBSYSTEM ANALYSIS	10-5
	10.3.1 Telecommunications	10-5
	10.3.2 Structure and Mechanics	10-13
	10.3.3 Attitude Control	10-13
	10.3.4 Auxiliary Propulsion Subsystem (APS).	10-13
	10.3.5 Electrical Power	10-15
	10.3.6 Thermal Control	10-15
	10.4 SINGLE FAILURE POINT SUMMARY	10-18
	10.5 RELIABILITY PROGRAM FOR IMPLEMENTATION PHASE	10-24
VOLUME V		
11.0	USER SPACECRAFT IMPACT	11-1
	11.1 USER SPACECRAFT TRANSPONDER CONCEPTS AND TRADES	11-1
	11.1.1 LDR Transponder	11-1
	11.1.2 MDR Transponder	11-5
	11.2 USER SPACECRAFT TRANSPONDER MECHANIZATION	11-7
	11.2.1 LDR Transponder	11-7
	11.2.2 MDR Transponder	11-15
	11.3 CONCLUSIONS	11-19
12.0	TDRS GROUND STATION DESIGN	12-1
	12.1 REQUIREMENTS AND CONSTRAINTS	12-1
	12.1.1 Uplink Requirements and Constraints	12-1
	12.1.2 Downlink Requirements and Constraints	12-3



Section		Page
12.2	TDRS GROUND STATION	12-4
	12.2.1 TDRS GS Antenna Subsystem	12-4
	12.2.2 Antenna Site Analysis	12-5
12.3	ANTENNA SITE ISOLATION ANALYSIS	12-6
12.4	Ku-BAND GROUND STATION ANTENNA	12-6
	12.4.1 TDRS Ground Station Receiver Front End	12-8
	12.4.2 TDRS Ground Station FM Demodulator and Demultiplexer.	12-8
	12.4.3 TDRS Ground Station LDR Processing	12-9
	12.4.4 TDRS Ground RF Transmitter	12-9
	12.4.5 TDRS Ground Station FDM Multiplexing	12-9
	12.4.6 TDRS Ground Station Frequency Source	12-10
	12.4.7 TDRS Ground Link Backup Mode	12-10
12.5	DESIGN CONSIDERATIONS	12-11
	12.5.1 Signal Categories	12-11
	12.5.2 LDR Command/Tracking (Uplink).	12-11
	12.5.3 LDR Telemetry	12-13
	12.5.4 LDR/MDR Tracking (Downlink)	12-13
	12.5.5 MDR Command (P/BU)/Uplink Voice (P/BU)/Tracking	12-13
	12.5.6 MDR Telemetry (P/BU)	12-14
	12.5.7 TDRS Order Wire	12-14
	12.5.8 MDR Downlink Voice (P/BU) (Manned User)	12-17
	12.5.9 TDRS Command/Tracking (P/BU)	12-17
	12.5.10 TDRS Telemetry (P/BU)	12-17
	12.5.11 TDRS Tracking (Downlink) (P/BU)	12-17
	12.5.12 Ground Station/Network Communications	12-19
12.6	CONCEPT DESCRIPTION	12-19
	12.6.1 LDR Command/Tracking (Uplink).	12-20
	12.6.2 LDR Telemetry	12-20
	12.6.3 LDR/MDR Tracking (Downlink)	12-21
	12.6.4 MDR Command (P/BU)/Uplink Voice (P/BU) Tracking	12-21
	12.6.5 MDR Telemetry (P/BU)	12-21
	12.6.6 TDRS Order Wire	12-22
	12.6.7 MDR Downlink Voice (P/BU) (Manned User)	12-22
	12.6.8 TDRS Command/Tracking (P/BU)	12-22
	12.6.9 TDRS Telemetry (P/BU)	12-23
	12.6.10 TDRS Tracking (Downlink) (P/BU)	12-23
	12.6.11 Ground Station/Network Communications	12-23
	12.6.12 Demodulation Tracking Unit	12-23
	12.6.13 Modulation Unit	12-25
	12.6.14 Control and Monitor Subsystem.	12-26
12.7	CONCLUSIONS AND RECOMMENDATIONS	12-31

VOLUME VI

Section	Page
13.0 COSTING	13-1
13.1 INTRODUCTION	13-1
13.1.1 Cost Analysis	13-1
13.1.2 TDRSS Program Cost Estimates	13-1
13.2 TDRSS BASELINE DESCRIPTION	13-3
13.2.1 TDRSS Operational Concept	13-3
13.2.2 TDRS Design Concept	13-5
13.2.3 TDRS Technical Characteristics	13-5
13.3 TDRSS COSTING REQUIREMENTS	13-5
13.3.1 Costing Ground Rules	13-5
13.3.2 Costing Work Breakdown Structure	13-9
13.3.3 Schedules	13-10
13.4 SPACECRAFT COST ANALYSIS	13-14
13.4.1 Cost Methodology	13-14
13.4.2 Alternate Cost Models Description	13-15
13.4.3 TDRS Cost Estimates Based on Alternate Cost Models	13-17
13.4.4 Selected TDRS Cost Models	13-19
GLOSSARY	13-25
APPENDIX 13A. SAMSO/NR NORMALIZED COST MODEL	13A-1

VOLUME VII

14.0 TELECOMMUNICATIONS SYSTEM SUMMARY	14-1
14.1 INTRODUCTION	14-1
14.2 SYSTEM SERVICE AND PERFORMANCE SUMMARY	14-4
14.2.1 LDR Return Link	14-4
14.2.2 LDR Forward Link	14-6
14.2.3 MDR Link Performance	14-8

Section	Page
14.3 LINK BUDGET	14-12
14.3.1 LDR Return Link Budget	14-12
14.3.2 LDR Forward Link Budget.	14-14
14.3.3 MDR Return Link Budget	14-14
14.3.4 MDR Forward Link Budget.	14-17
14.3.5 TDRS/GS Return Link Budget	14-17
14.3.6 TDRS/GS Forward Link Budget	14-20
14.3.7 Tracking/Order Wire	14-24
14.3.8 Ku-Band Beacon	14-24
14.4 SUBSYSTEM TERMINAL CHARACTERISTICS	14-24
14.4.1 TDRS Telecommunication Subsystem	14-24
14.4.2 User Transponder Design.	14-26
14.4.3 Ground Station Terminal Characteristics	14-33



PRECEDING PAGE BLANK NOT FILMED

ILLUSTRATIONS

Figure		Page
5-1	TDRS Baseline Configuration	5-3
5-2	Spacecraft Body Configuration	5-7
5-3	UHF-VHF Backfire Array Element	5-11
5-4	Solar Panel Array	5-15
5-5	Equipment Shelf - Front View	5-17
5-6	Equipment Shelf - Rear View	5-18
5-7	Propulsion System Installation	5-19
5-8	Integrated Subsystem Block Diagram	5-27
6-1	Attitude Determination and Pointing Accuracy Budget	6-4
6-2	Solar Pressure Disturbance Histories	6-6
6-3	Attitude Error Versus Momentum Bias	6-9
6-4	Spin Stabilized ASCS Configuration Trades:	
	Nutation Control	6-14
6-5	ASCS Torquer Trades	6-16
6-6	Momentum Storage Subsystem Configurations	6-18
6-7	Reaction Wheel Weight	6-20
6-8	Attitude Determination Subsystem Trades	6-23
6-9	Attitude Stabilization and Control System	6-27
6-10	Active Nutation Control System Block Diagram	6-28
6-11	Momentum Storage Subsystem Arrangement	6-31
6-12	On-Orbit Stabilization and Control Logic	6-32
6-13	Minuteman Gyro/Nutation Damper	6-34
6-14	APS Engine Arrangement	6-39
7-1	Auxiliary Propulsion System Trades	7-2
7-2	Auxiliary Propulsion System Baseline Configuration	7-7
7-3	Thrust Pressure Versus Propellant Consumed	7-9
7-4	Pressurant/Propellant Tank	7-12
7-5	Fill and Drain Valve	7-12
7-6	Latching Valve	7-14
7-7	Explosive Actuated Valve (N/O)	7-14
7-8	Propellant Filter	7-15
7-9	Thruster Valve	7-15
8-1	TDRS Major EPS Assemblies	8-1
8-2	Eclipse Periods	8-2
8-3	EPS Trade Tree	8-4
8-4	Battery Requirements - Maximum Eclipse Period - 2 NiCd Batteries	8-5
8-5	Time Required to Charge Batteries	8-6
8-6	Average Battery Charge Efficiencies	8-12
8-7	Electrical Power Subsystem Block Diagram	8-14
8-8	Solar Panel Array Configuration	8-16
8-9	Schematic of Shunt Dissipator	8-17
8-10	Solar Array Characteristics	8-19



Figure		Page
8-11	Solar Array Panel Eclipse Temperature Versus Thermal Capacitance	8-19
8-12	Degradation of Maximum Power of Hoffman N/P Si Solar Cells Under 1 Mev Electron Bombardment	8-20
8-13	Baseline Battery Capability Maximum Eclipse	8-24
8-14	Statistical Data for Nominal 12 Ampere - Hour Cells	8-26
8-15	Power Conditioning Packaging Concept	8-29
8-16	Breadboard Parts Regulators Unit	8-30
8-17	TDRS Voice Transmission Battery Capability	8-34
8-18	TDRS Voice Transmission Sunlight Period (Non-Eclipse Season)	8-35
9-1	Louver Panel Heat Rejection Versus Sun Angle	9-9
9-2	TDRS Louver Radiator Heat Rejection	9-9
9-3	Louver Operating Characteristics	9-11
9-4	TDRS Mean Temperature Versus Heat Load	9-12
9-5	Temperature at End of Transfer Orbit Versus Power Load	9-12
9-6	Transfer Orbit Attitude to Maintain 40 F	9-12
9-7	Thruster Temperature Distribution	9-17
9-8	Required Heating Power For Propellant Tank	9-19
9-9	Solar Array Panel Temperature Transfer Orbit	9-21
9-10	Solar Array Panel Allowable Duration From Despin to Deployment	9-21
9-11	Solar Array Panel Eclipse Temperature Versus Thermal Capacitance	9-22
9-12	Thermal Control Subsystem	9-24
10-1	Satellite Reliability Estimates	10-3
10-2	System Reliability Versus Satellite Reliability	10-3
10-3	Reliability Diagram of Communication Subsystem	10-7
10-4	Reliability Logic Diagram of Tracking, Telemetry and Command Subsystem	10-9
10-5	Reliability Logic Diagram of Structure and Mechanisms	10-15
10-6	Reliability Logic Diagram of Attitude Control Subsystem	10-16
10-7	Reliability Logic Diagram of Auxiliary Propulsion Subsystem	10-18
10-8	Reliability Logic Diagram of Electrical Power Subsystem	10-20

TABLE

Table		Page
5-1	Design Constraints	5-1
5-2	Baseline TDRS Spacecraft Characteristics	5-5
5-3	Weight Summary	5-22
5-4	Weight Estimate by Subsystem	5-23
5-5	Preliminary Moments of Inertia	5-26
6-1	ASCS Performance Requirements Summary	6-1
6-2	Summary of Momentum Requirements Due to Solar Pressure Torques	6-5
6-3	Control Available from Momentum Storage Subsystem Configurations	6-19
6-4	Momentum Storage Subsystem Trade Data	6-21
6-5	Yaw Sensing Gyro Candidates	6-24
6-6	G6 Gyro History - Minuteman	6-24
6-7	Gyro and Momentum Wheel Comparison	6-25
6-8	TDRS ASCS Component Characteristics	6-26
6-9	Auxiliary Propulsion System Impulse Requirements and Criteria	6-35
6-10	Summary of APS Thruster Requirements for the Various Maneuvers	6-37
6-11	Reaction Jet Duty Cycle (Number of On-Off Cycles per Jet)	6-38
6-12	Jet Select Logic	6-40
6-13	Summary of APS Thruster Arrangement Requirements	6-40
7-1	Propellant Requirements	7-1
7-2	Propulsion Trade Summary	7-3
7-3	Expulsion System Comparison	7-5
7-4	Positive Expulsion Tanks with EPT-10 Diaphragms for Hydrazine Service	7-6
7-5	APS - Hardware List	7-10
7-6	Modified CTS Motor Performance and Weight Data	7-19
7-7	CTS Motor Characteristics	7-20
8-1	EPS Major Design Drivers	8-2
8-2	EPS Sizing Requirements	8-7
8-3	Electrical Load Chart (watts)	8-8
8-4	Telecommunication Service (LDR) Voice Transmission Requirements	8-9
8-5	Estimated Battery Life Consumed in 5 Years	8-10
8-6	Variations in MDR Power Requirements	8-11
8-7	Transfer Orbit Energy Requirements	8-11
8-8	EPS Component Efficiency (Sizing Model).	8-12
8-9	Electrical Power Subsystem Weights	8-15
8-10	Solar Array Assembly Weight Summary	8-18
8-11	Array Performance Factors	8-21

Table		Page
8-12	Eclipse Period Maximum Energy Requirements	8-23
8-13	Nickel Cadmium Battery Cell Characteristics	8-25
8-14	Power Conditioning Assembly Weight Summary	8-30
8-15	Telecommunication Service Transmission Power Requirements	8-33
9-1	Mission Thermal Requirements	9-2
9-2	Thermal Control System Heat Rejection Loads	9-3
9-3	Temperature Requirements of TDRS Components	9-5
9-4	Performance of Louver Radiator	9-8
9-5	Equipment Temperatures	9-14
9-6	APS Thermal Design Requirements	9-19
10-1	Probability of Mission Success	10-4
10-2	Preliminary Subsystem Reliability Goals	10-4
10-3	Failure Mode Effects Analysis - Communications	10-11
10-4	Failure Mode Effects Analysis - TT&C	10-14
10-5	Failure Mode Effects Analysis - Attitude Control	10-17
10-6	Failure Mode Effects Analysis - Auxiliary Propulsion	10-19
10-7	Failure Mode Effects Analysis - Electrical Power	10-21
10-8	Single Failure Point Summary	10-23

5.0 SPACECRAFT MECHANICAL AND STRUCTURAL DESIGN

The TDR spacecraft provides the support for and integrates the various antenna systems and solar array panels, and encloses and protects the communications, electrical power, attitude control, and propulsion subsystems in both the launch and deployed environments. The deployable elements are properly packaged to withstand the structural and vibrational loads experienced during launch on the Delta 2914 booster and the spinning accelerations imposed during third stage burn and transfer orbit. After apogee motor burnout, despin and stabilization maneuvers, the antennas and solar panels are deployed to their extended positions.

The evolution of the spacecraft design proceeded within the design constraints summarized in Table 5-1.

Table 5-1. Design Constraints

Constraint	Derived From
Max. payload: 788 lb (357.5 kg), including burned-out apogee motor case	Delta 2914 capability
Maximum size	Delta 8-ft (2.44 m) shroud
No shadowing on solar cells	Power loss cannot be tolerated
RCS Sys. temperature > 40 F (4.4 C)	Hydrazine freezes
Electronics Temperature < 110 F (43 C)	Reliability
RCS jets operable in stowed configuration	Stability and pointing require- ments in transfer orbit
Unfurlable antenna dishes not desired	Reliability, surface control and minimum cost
Clear sensor FOV before and after deployment	Stability and pointing require- ments

Areas that were of primary concern in the development of the final baseline design were packaging and deployment mechanization, antenna design and sizing, weight control, and optimization of the configuration for support of multiple user spacecraft. Several trade studies and alternates were considered, and are summarized in Appendix 5A. These include:

- Alternate spacecraft body shapes and construction
- Single and dual drive for solar panels
- Solar panel shape, size and method of packaging
- Jettisonable apogee motor installation
- MDR antenna maximum size and furlable types
- LDR array VHF-VHF design in several frequency sizes
- LDR FTCV and AGIPA design antennas
- Blockage and reflective study relationship of MDR to LDR antennas
- Propulsion system alternates
- Equipment shelf arrangements

5.1 TDRS BASELINE CONFIGURATION

Figure 5-1 illustrates the arrangement of antennas and solar array panels symmetrically grouped around the central spacecraft body. The two MDR parabolic reflector antennas are supported on struts on each side of the symmetrically spaced LDR UHF-VHF 4-element array of back-fire antennas with the body mounted TDRS/GS antenna in the center. The one-degree-of-freedom solar panels are deployed above and below the spacecraft beyond the solar shadow limits of the antennas. Telemetry and command VHF omni whip antennas located around the rear of the spacecraft are utilized during launch and spacecraft orbital maneuvers prior to deployment of the primary antennas. The baseline characteristics are summarized in Table 5-2.

5.1.1 Deployed Configuration

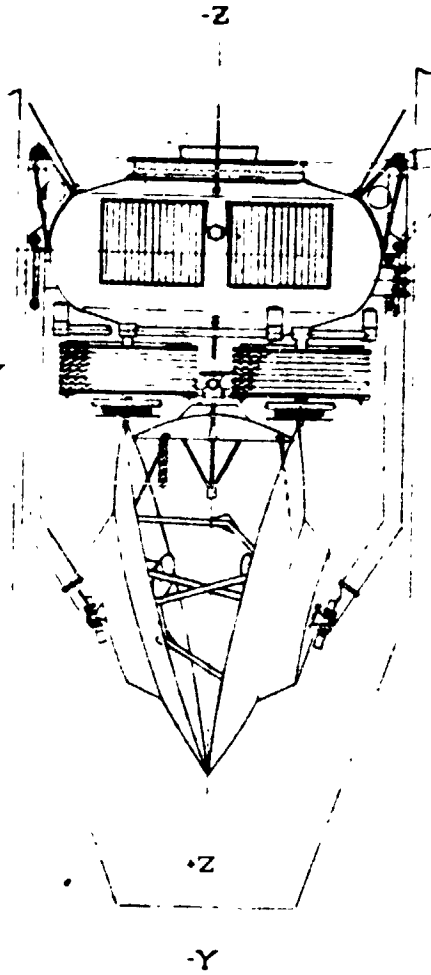
As shown in Figure 5-1, the spacecraft achieves its deployed configuration by extending the solar arrays, the two MDR antennas aft to their positions on each side of the spacecraft, and deploying the four elements of the LDR UHF-VHF array laterally and then extending them forward. The LDR antenna is deployed laterally by spring loaded linkage joints which lock into the extended position. Release of the deployable elements is initiated by solenoid activation of packaging and restraint latches by ground commands. After the lateral deployment the LDR antenna elements are extended forward by motor driven "STEM" units mounted at the rear of the elements and the extended "STEM's" become the center rod supports for the disc elements.

5.1.2 Launch Configuration

The spacecraft is packaged for launch within the 8-ft (2.44 m) shroud of the Delta 2914 as shown in Figure 5-1. The MDR antennas are folded forward in a face-to-face position with slight mutual rotation to allow the antenna feeds and supports to clear each other. The 3-ft (.915 m) dia. TDRS/GS dish antenna is located at the front of the spacecraft between the rear rims of the angled MDR dishes. The LDR array is packaged into four cylindrical shapes and positioned around the TDRS/GS antenna behind the MDR dishes

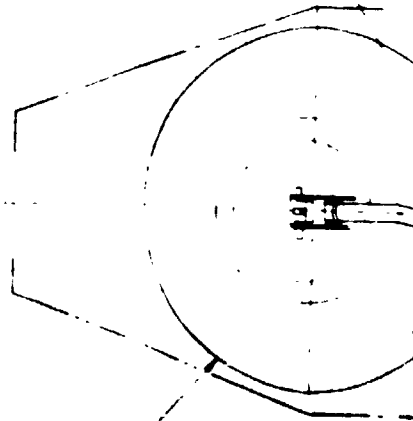
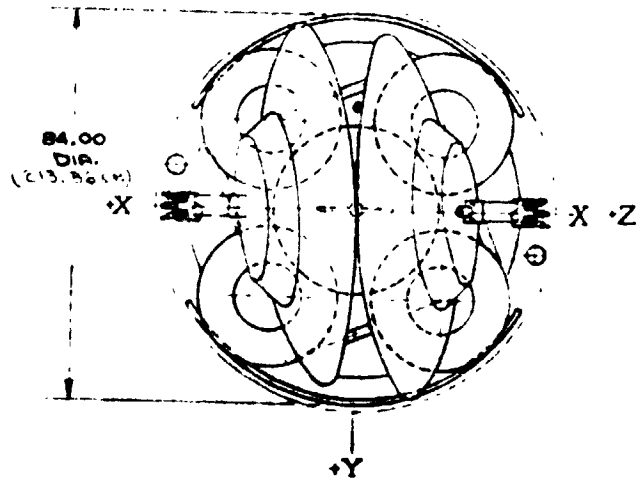
FOLDOUT FRAME

SOLAR PANEL ARRAY
NOT SHOWN IN THIS
VIEW FOR 3/4 CLARITY



FAIRING ENVELOPE (REF.)
THOR-DELTA 8 FT DIA.
NOSE FAIRING

(.91 +)
3.0 FT. DIA ANTENNA
(GROUND LINK)

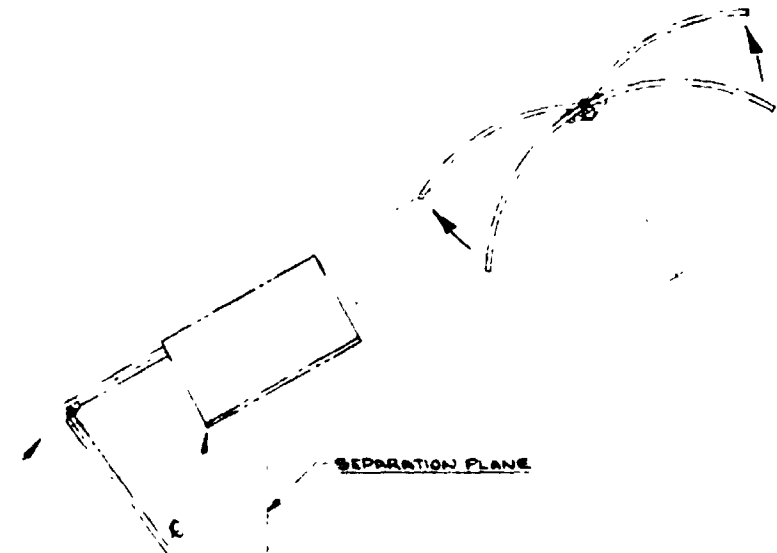
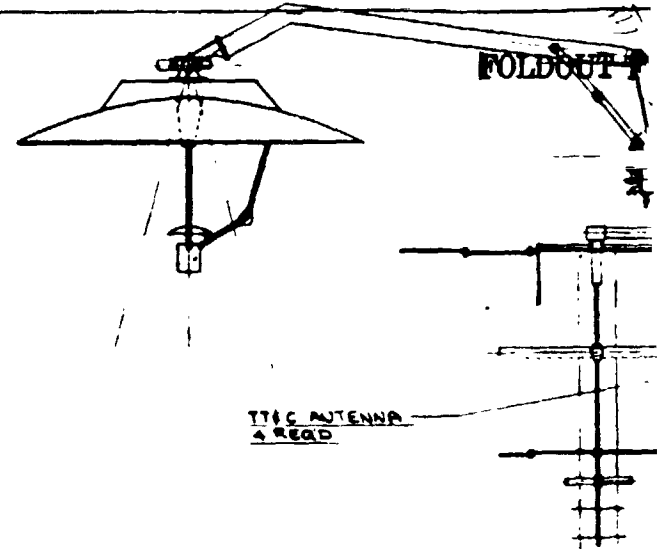


(2.0M)
6.5 FT. DIA. ANTENNA
RETRACTED POSITION
Z REQ.

UMF VMP AS
RETRACTE
4.8 REQ.

TDRS LAUNCH (PACKAGED) CONFIGURATION
(1/20 SCALE)

FOLDOUT FRAME



SOLAR PANEL ARRAY
2 REGR (1.18 - 2.41)
(TOTAL AREA 85.952 FT.)

38.9
(1.0154 m)

138.30
(4.011 m)
3.524

SEPARATION PLANE

86.00
DIA.
(REF.)
2.184 m

2.50
(0.762 m)

-Z

+X

48.75
(1.482 m)
123.33 m

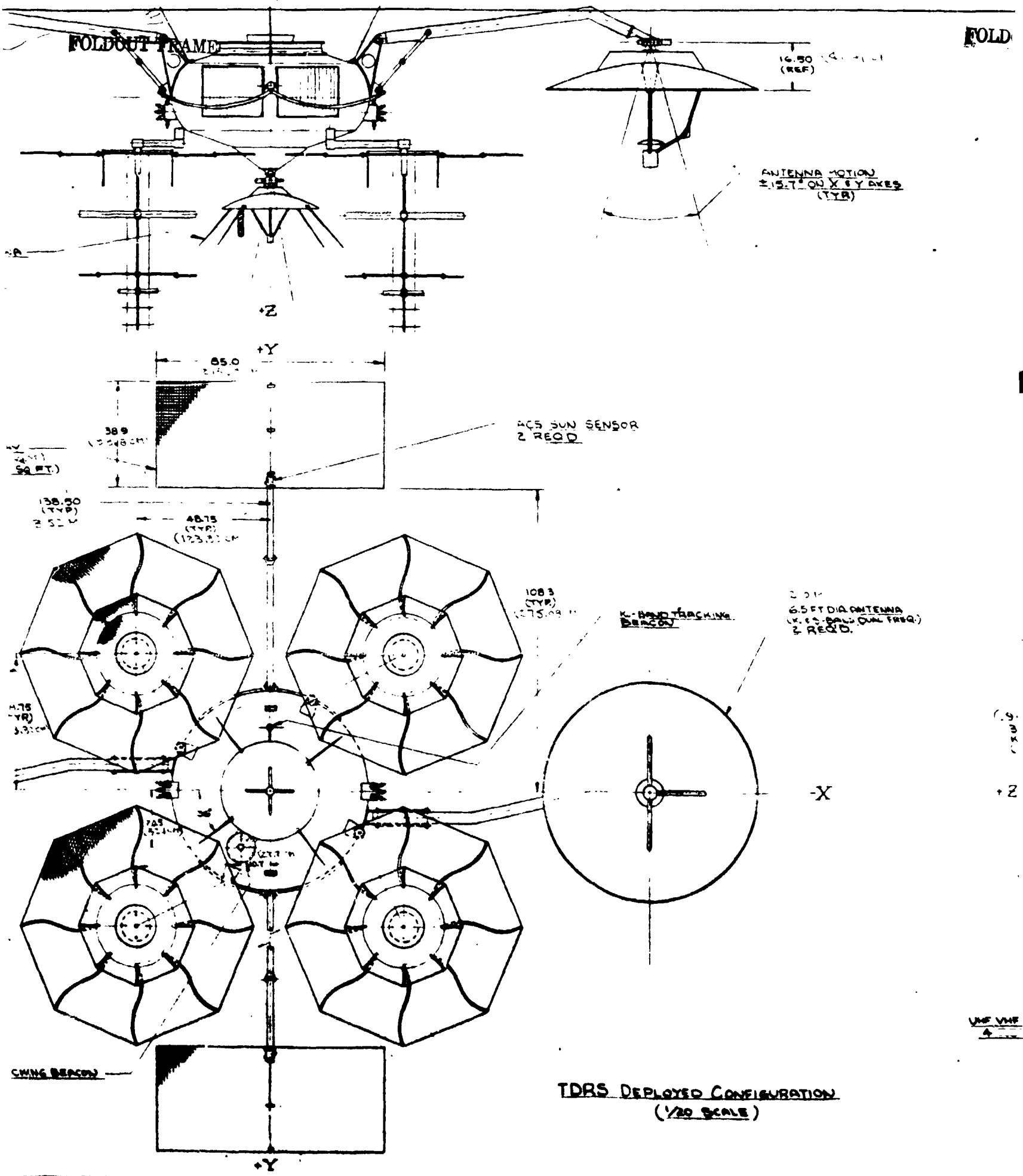
2.03
(0.618 m)
1

SOLAR PANEL ARRAY
RETRACTED/ FOLDED
2 REGR

EVENT
WIGG

3-BAND TRACKING BEACON

FOLD



TDRS DEPLOYED CONFIGURATION
(1/20 SCALE)

FOLDOUT FRAME

REVISIONS	
LTR	DESCRIPTION
A	ADDED K _U -BAND SUBREFLECTOR TO MDR RE
	5-BAND K _U -BAND TRACKING BEACONS, E
	SET TTIC ANTENNAS

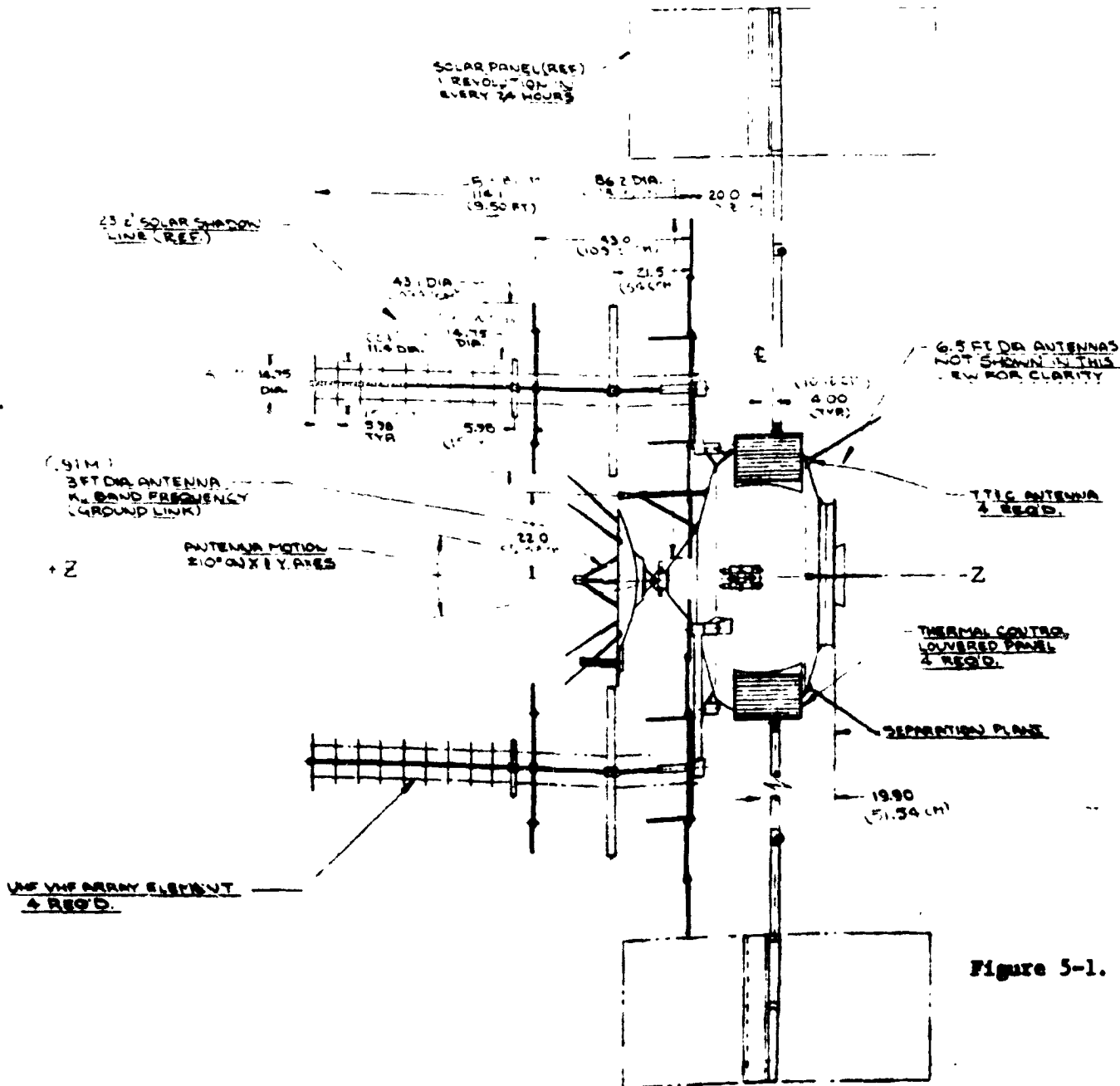


Figure 5-1. TDRS Baseline Config

REVISIONS			
LTR	DESCRIPTION	DATE	CHK BY
A	ADDED K-BAND SUBREFLECTOR TO MDR REFLECTORS	8-7-78	WEDOUT
	5-BAND K-BAND TRACKING BEACONS, E PWD		
	SET TTIC ANTENNAS		

FRAM

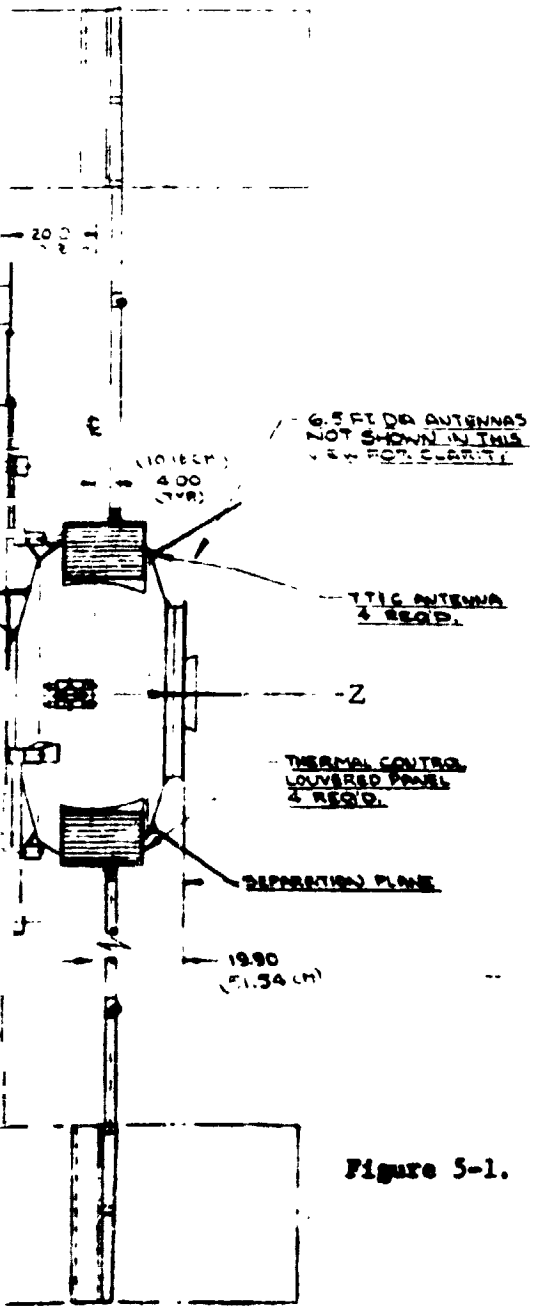


Figure 5-1. TDRS Baseline Configuration

5-3,5-4

Table 5-2. Baseline TDRS Spacecraft Characteristics (English Units)

Component or System	Description	Location	Weight (lb)
ANTENNAS			
MDR (Ku- and S-band)	(2) 6.5 ft. dia. parabolic reflector, 2-axis gimbal	Centerline at 138.5 inches each side of S/C centerline	67.9
LDR (UHF-VHF)	(1) Backfire array with four elements	Centerline each element 48.75 inches from X and Y axes	31.6
TDRS/GS (Ku-band)	(1) 3.0 ft. dia. parabolic reflector, 2-axis gimbal	On centerline at front of spacecraft body	14.8
TT&C (VHF)	(4) Omni whip antenna	Equally spaced around rear spacecraft body	3.0
	(4) Omni whip antenna	Equally spaced around TDRS/GS dish	
Tracking Beacon (S-band)	(1) Helix - ground plane	Front spacecraft body	.3
Tracking Beacon (Ku-band)	(1) Conical horn	Front spacecraft body	.3
SOLAR ARRAY	(2) 32.9 in. x 85.0 in. panels (total area 45 sq ft)	108.3 in. above and below spacecraft centerline	58.6
COMMUNICATION SYS.	MDR, LDR, ground link, TT&C equipment	Mounted on forward surface of spacecraft equip. shelf	122.2
PROPULSION SYSTEM	(16) Hydrazine thrusters (2) Tanks, valves, plumbing	Mounted on equipment shelf with thrusters at sides of spacecraft body	38.4
Apogee Motor	(1) CTS motor (propellant 688 pounds)	On S/C centerline	50.0 (burned out)
Propellant + N ₂	(Two 65-degree, 15-day station changes)	Propellant tanks on spacecraft equipment shelf	49.3
ATTITUDE CONTROL SYSTEM	(2) Reaction wheels (1) Gyro package, logic and sensors	Mounted on equipment shelf, sensors on spacecraft body and solar arrays	57.7
ELECT. POWER SYSTEM	(2) Batteries, charge regulators, logic, meters, cabling	Mounted on aft surface of equipment shelf	97.0
THERMAL CONTROL SYSTEM	(4) Louvered shutters and heaters on ACS thrusters, cabling, thermocouples	Louver assembled on top and bottom of body	23.9
SPACECRAFT BODY STRUCTURE	Internal conical shells and transverse honeycomb equipment shelf; outer shells aluminum honeycomb	Spacecraft centerline	91.0
Total Weight			656.0
Contingency			82.0
Allowable Payload			738.0
Empty Apogee Motor Case			50.0
Initial in Orbit			788.0

Table 5-2A. Baseline TDRS Spacecraft Characteristics (International Units)

Component or System	Description	Location	Weight (kg)
ANTENNAS			
MDR (Ku- and S-band)	(2) 2.0 m dia. parabolic reflector, 2-axis gimbal	Centerline at 351.8 cm each side of S/C centerline	30.8
LDR (UHF-VHF)	(1) Backfire array with four elements	Centerline each element 123.8 cm from X and Y	14.4
TDRS/GS (Ku-band)	(1) 0.9 m dia. parabolic reflector, 2-axis gimbal	On centerline at front of spacecraft body	6.71
TT&C (VHF)	(4) Omni whip antenna (4) Omni whip antenna	Equally spaced around rear spacecraft body Equally spaced around TDRS/GS dish	1.36
Tracking Beacon (S-band)	(1) Helix - ground plane	Front spacecraft body	.136
Tracking Beacon (Ku-band)	(1) Conical horn	Front spacecraft body	.136
SOLAR ARRAY	(2) 96.8 cm x 316.0 cm panels (total area 4.18 sq m)	274 cm above and below spacecraft centerline	26.6
COMMUNICATION SYS.	MDR, LDR, ground link, TT&C equipment	Mounted on forward surface of spacecraft equip. shelf	55.5
PROPULSION SYSTEM	(16) Hydrazine thrusters (2) Tanks, valves, plumbing	Mounted on equipment shelf with thrusters at sides of spacecraft body	17.4
Apogee Motor	(1) CTS motor (propellant 312 kg)	On S/C centerline	22.7 (burned out)
Propellant + N ₂	(Two 65-degree, 15-day station changes)	Propellant tanks on spacecraft equipment shelf	22.4
ATTITUDE CONTROL SYSTEM	(2) Reaction wheels (1) Gyro package, logic and sensors	Mounted on equipment shelf, sensors on spacecraft body and solar arrays	25.2
ELECT. POWER SYSTEM	(2) Batteries, charge regulators, logic, meters, cabling	Mounted on aft surface of equipment shelf	44.0
THERMAL CONTROL SYSTEM	(4) Louvered shutters and heaters on ACS thrusters, cabling, thermocouples	Louver assembled on top and bottom of body	10.8
SPACECRAFT BODY STRUCTURE	Internal conical shells and transverse honeycomb equipment shelf; outer shells aluminum honeycomb	Spacecraft centerline	41.3
Total Weight			297.6
Contingency			37.2
Allowable Payload			334.8
Empty Apogee Motor Case			22.7
Initial in Orbit			357.5

forward of the structural body of the spacecraft. The solar array panels are folded down around the top and bottom of the spacecraft allowing room on each side for clearance with the side-mounted booms of the MDR antennas and the ACS thrusters.

5.2 SPACECRAFT BODY STRUCTURE

The spacecraft structural body (Figure 5-2) consists of inner aluminum tapered cones around the apogee motor, a transverse equipment shelf of aluminum honeycomb and the outer body shells of aluminum honeycomb that close off and protect the internal equipment and thermal louvers.

The inner conical shell surrounds and supports the apogee motor and provides a machined rear flange that mates with the Delta 3731A attach fitting. This shell is 0.040 in. (.102 cm) aluminum welded to the rear flange. Spring pads and internal stiffeners at the rear of the cone accommodate the spring separation system of the Delta attach fittings. The forward end of the inner shell is closed with a front cone section also of 0.040 inch (.102 cm) alum.

The apogee motor is installed on the spacecraft centerline by an accurately machined titanium ring attached to the apogee motor flange and is bolted to the inner structural cone. The attachment ring is located along the Z-axis of the spacecraft to accurately position the apogee motor. The motor nozzle extends 2.5 in. (6.35 cm) beyond the separation plane. The apogee motor is not jettisoned after burnout and remains in the spacecraft body.

The equipment shelf is an aluminum honeycomb transverse bulkhead that provides the primary mounting surface for the equipment. It is made of 1.50 in. (3.81 cm) thick aluminum honeycomb core with 0.010 in. (.025 cm) aluminum face sheets in a main bulkhead shape and four insert panels. Equipment is mounted on both the bulkhead and the insert panels for simultaneous and sequential subsystems installation and checkout during manufacture.

The outer body shells enclosing the equipment are bonded 0.50 in. (1.27 cm) thick aluminum honeycomb core with 0.010 in. (.025 cm) reinforced fiberglass face sheets. The shell halves are bolted to the inner shell structure and the outer rim of the equipment shelf through angle clips.

Four thermal control louvered shutter assemblies are positioned at North-South extremities of the body such that at least one-half the shutter radiator area is always shadowed from solar radiation. These individually thermal operated louvers are of the overlap design and have high rigidity to withstand launch shock and vibration loads when in their normally-warm open position.

Machined aluminum fittings bolted to the equipment shelf edges and through the outer body shell provide pivot points for the support booms of the MDR antennas and the swing-arm support links for the UHF-VHF array elements. Mounting blocks for the VHF TT&C omni whip antennas are bolted through the rear outer shell. The TDRS/GS antenna gimbal mounting flange is bolted to the forward face of the front closeout shell cone on the spacecraft centerline.

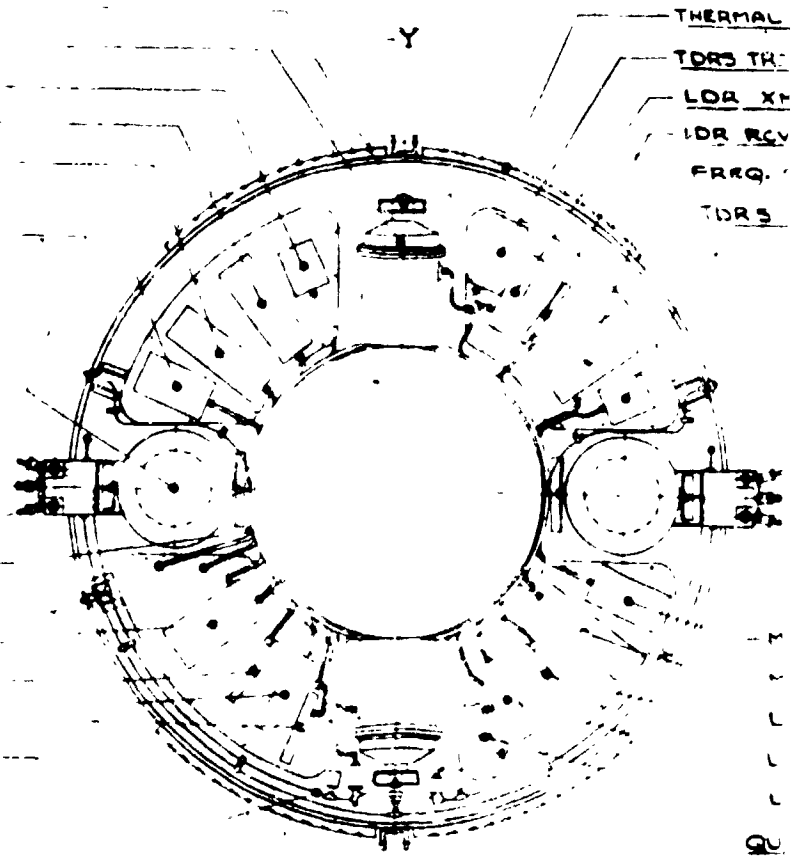
FOLDOUT FRAME

- ACS HORIZON SENSOR (2)
- ACS REACTION WHEEL (2)
- TDRS/GS XMTR
- TDRS/GS RCVR
- MDR RECVR (2)
- MDR XMTR (2)
- PROPUL SYS TANK (2)

QUADRANT 1

- RF CABLE / WIRE HARNESSSES
- FREQ. SOURCE (2)
- LDR RCVR
- LDR XMTR
- LDR XMTR COVER
- PROPUL SYS.

QUADRANT 3



SECTION A-A
(VIEW LOOKING AT)
(1/10 SCALE)

THERMAL CONTROL
LOUVERED SHUTTER
+ REQD

FOLDOUT FRAME

CONTROL LOUVER PANEL (4)

RACKING RCVR

XMTR

CVI

SOVACE (REF.)

TRACKING XMTR

QUADRANT 2

X

LDR XMTR

LDR RCVR

LDR RCVR

LDR XMTR

LDR SUMMING UNIT

QUADRANT 4

SOLAR PANEL DRIVE ACTUATOR (2)

TELEMETRY CONTROL LOUVER PANEL (4)

ACS ELECTRONICS MODULE

ACS ACCELEROMETER (2)

BATTERY (2)

ACS SPINNING HORIZON SENSOR (2)

THRUSTER CLUSTER (2)

QUADRANT 2

TFC LOGIC

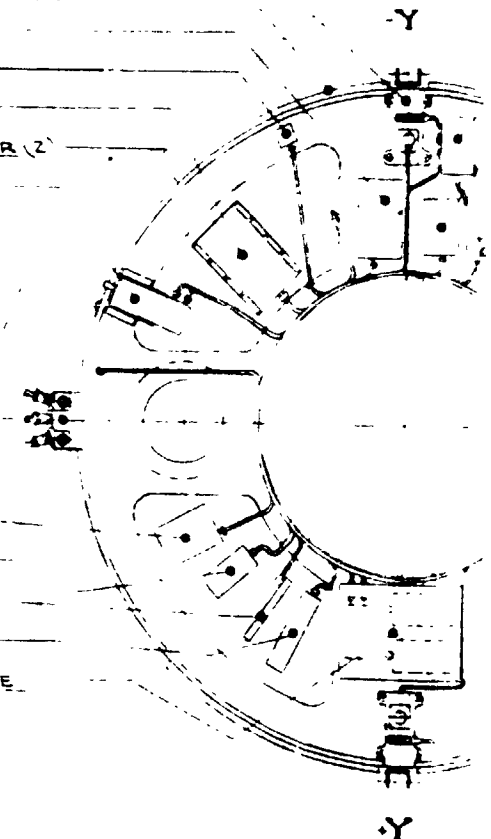
TFC TRANSCIEVER

LDR RCVR

LDR XMTR

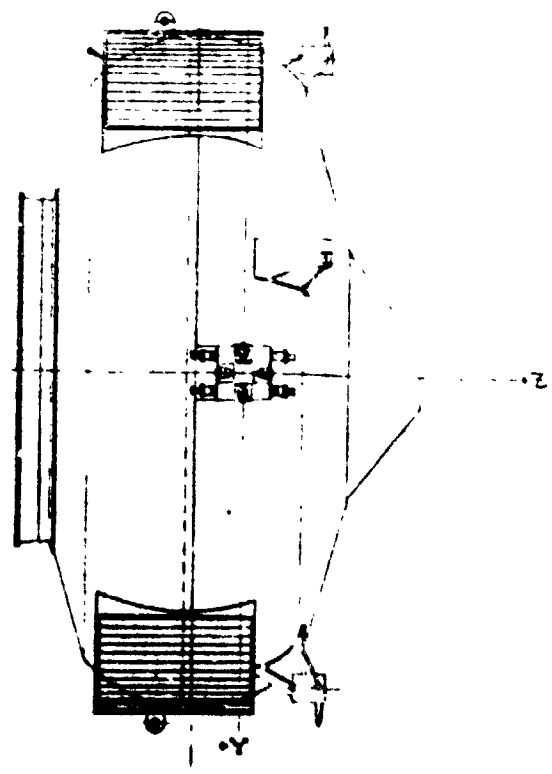
ELECT. POWER CONTROL MODULE

QUADRANT 4

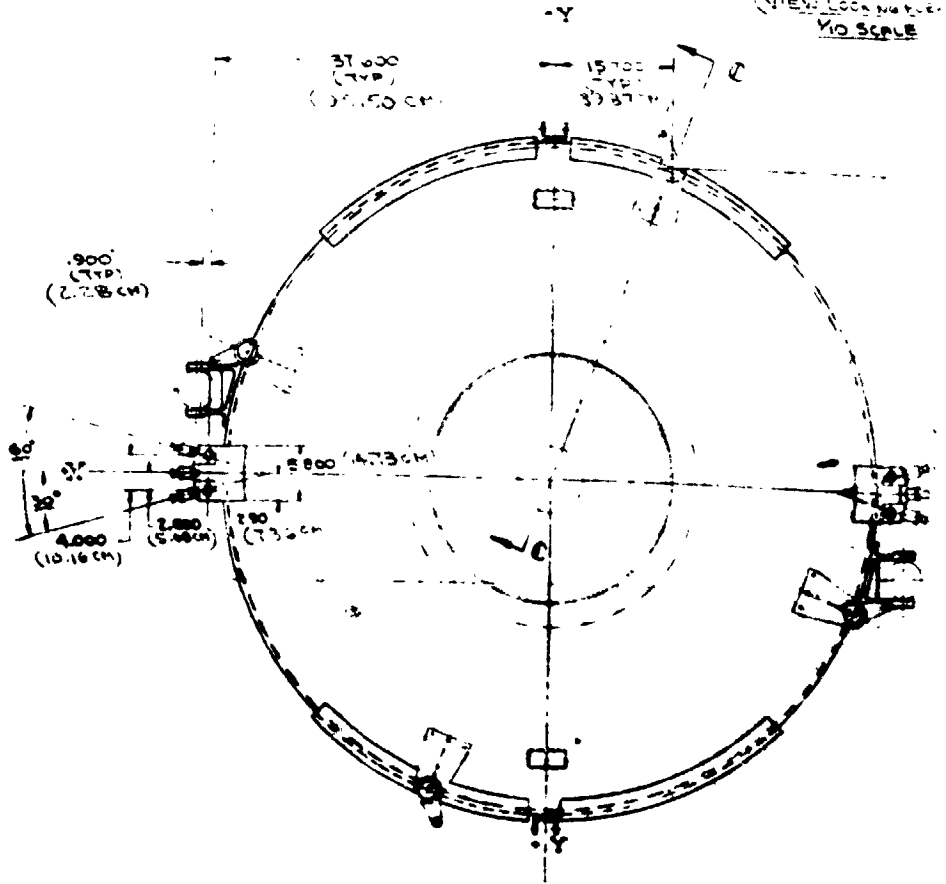


SECTION B-B
(VIEW LOOKING FROM
Y TO X)
1/16" SCALE

1.45 (11.0)
18.00
7.00



SIDE VIEW - EXTERNAL
(1/16" SCALE)



FRONT VIEW

3
POLYMER BOARD

- AMP. HR. METER (2)
- TDRS/GS ANTENNA ELECTRONICS
- MDR ANTENNA ELECTRONICS
- ELEC. POWER & SIGNAL HARNESS

QUADRANT 1

MDR ANTENNA (REF)

ACS GYRO

BATTERY

ACS ACCELEROMETER

QUADRANT 3

SECTION B-B
(VIEW FROM 10 DEGREE)
NO SCALE

SUPPORT FITTING VHF ARRAY
& REOD

32.100
(440)
(81.58 CM)

(9.1)
16.70
(REF)
19.20
(38.41 CM)

(27.86 CM)
8.000
(78)

UHF VHF ARR
(REF)

TDRS/GS
K-BASE GEORADAR
30 FT ANTENNA
(9.1M) (REF)

SECTION C-C
(VIEW FROM 10 DEGREE)
NO SCALE

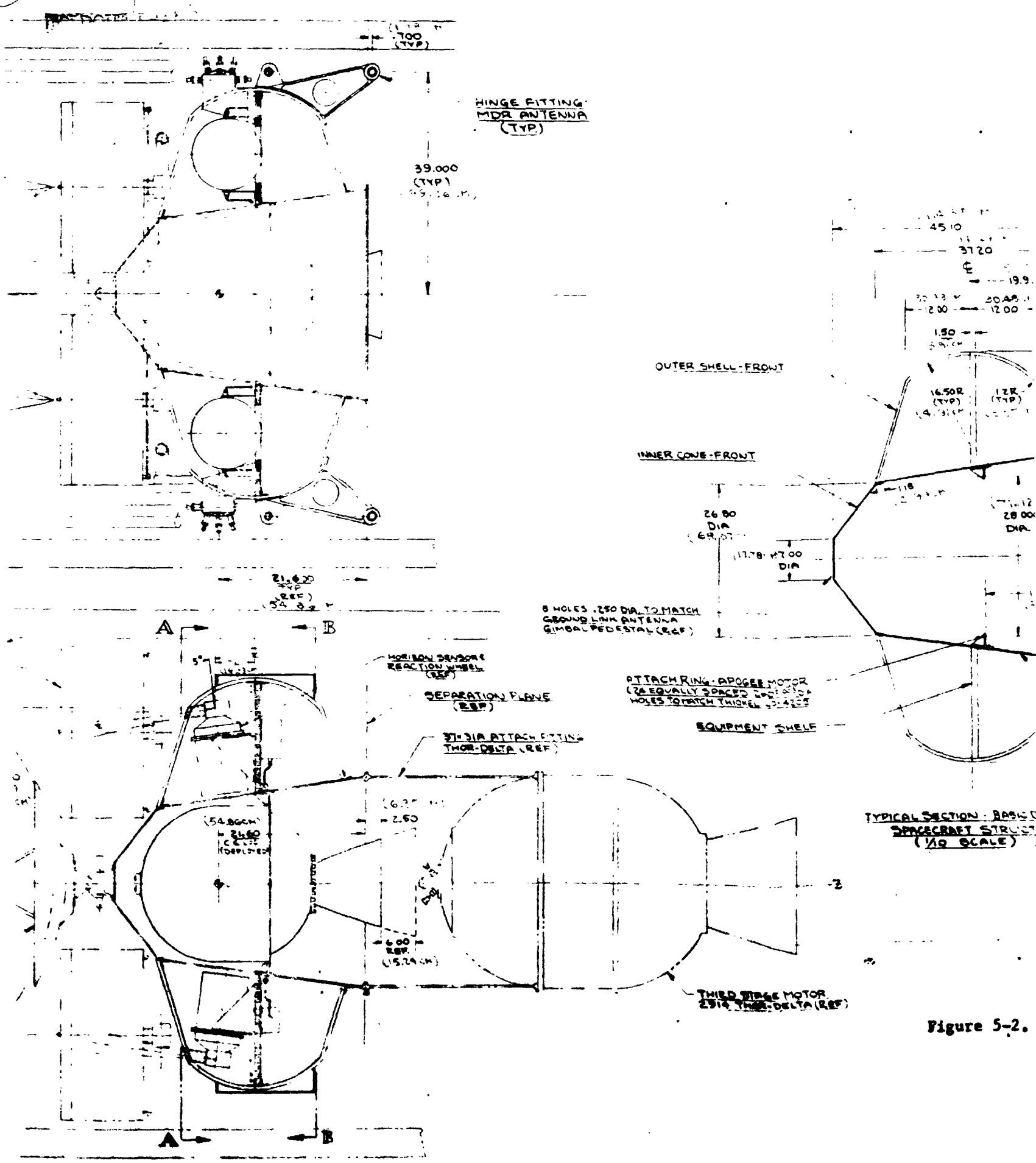


Figure 5-2.

REVISIONS			
LTR	DESCRIPTION	DATE	CHK BY
A	REVISED EQUIPMENT SHELF EQUIP ARRANGEMENT	8-3-72	J.W.C

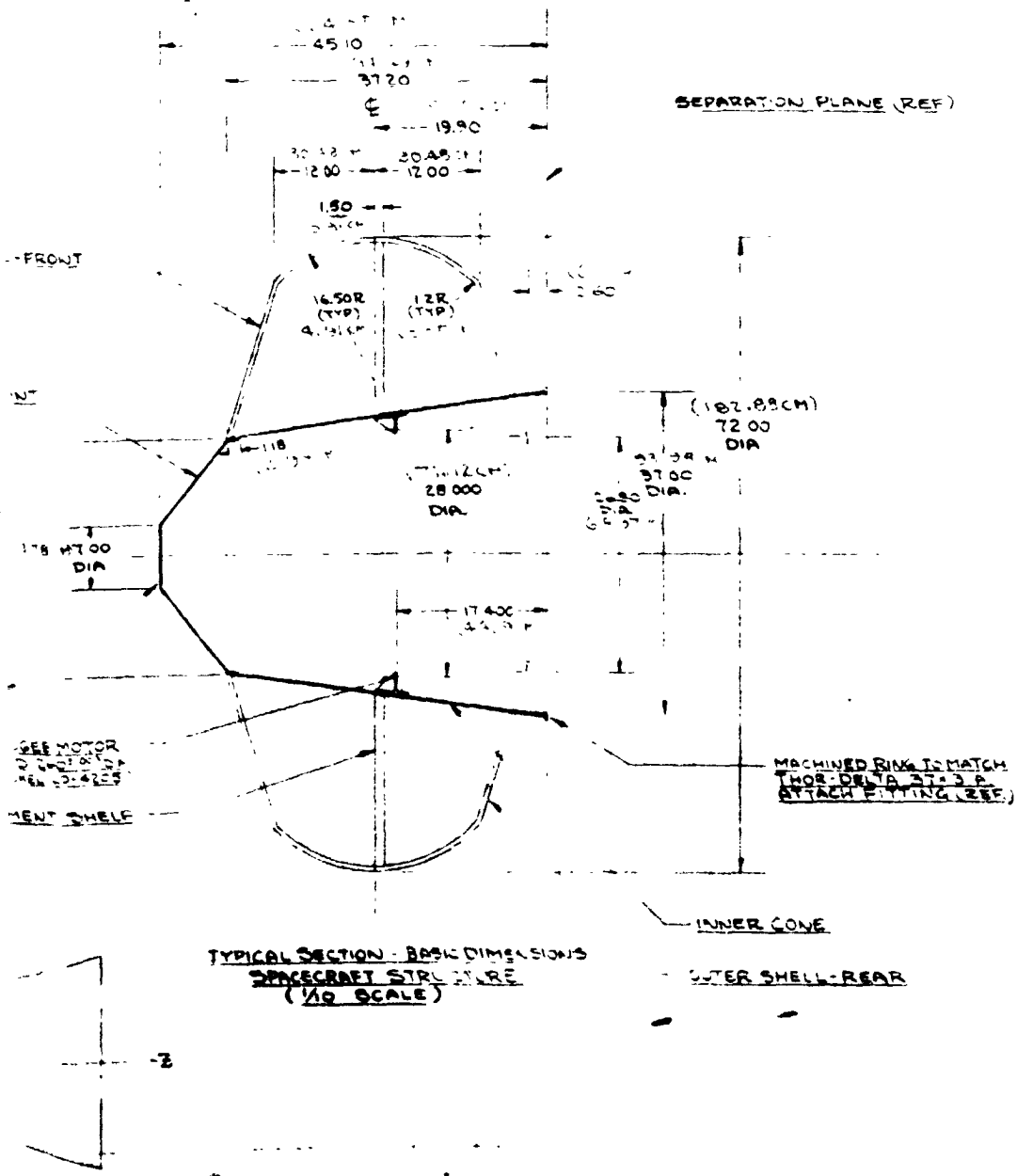


Figure 5-2. Spacecraft Body Configuration

5.3 ANTENNA MECHANICAL DESIGN

The primary considerations in locating the various antenna systems are: mutual blockage or reflective interferences; symmetry of the spacecraft to minimize effects of solar pressure; shadowing of solar panels; effects on packaging or deployment arrangements; and minimum weight with high rigidity of structure and support linkages.

5.3.1 MDR Antennas

The two MDR antennas are dual Ku- and S-band frequency, 6.5 ft (2 m) in diameter, solid face, parabolic reflectors with two-axis gimbals. They are mounted on tubular booms and deployed 138.50 in. (3.53 m) outboard on each side of the spacecraft. As shown in Figure 5-1, the packaging of the 8 ft (2.44 m) shroud in conjunction with the volume required for the spacecraft body, solar arrays, and packaged UHF-VHF array elements limits the two solid face antennas to a maximum of 6.5 ft (2 m) diameter. Solid face reflectors were chosen over furlable antennas because they meet all ERP and G/T requirements and for simplicity, accuracy of surface tolerances suitable for Ku-band antenna frequencies, weight, rigidity and reliability.

The 6.5 ft (2 m) diameter reflector is a panel with 0.50 in. (1.27 cm) aluminum core and 0.005 in. (.013 cm) face sheets bonded with epoxy adhesive. Accurately machined bonding tooling and NR-developed techniques permit consistent surface tolerances of 0.004 in. (.010 cm) RMS with peaks of 0.008 in. (.020 cm). A formed sheet metal hub is riveted and bonded to the rear of the reflector and attaches the antenna gimbal drive assembly and the feed support system. The S-band feed and Ku-band subreflector mounted at the reflector focal point, are supported by aluminum struts from the front face. The antenna is driven ± 15.7 degrees on two axes. The gimbal drive utilizes redundant electric stepper motors on each axis and is driven in autotrack for Ku-band operation or programmed open-loop for S-band by ground commands. Dry film lubricants are used throughout the gimbal mechanisms to avoid the need for sealing the moving elements and to withstand the temperature range. Dual Ku- and S-band rotary joints are supplied across each axis.

5.3.2 LDR UHF-VHF Array Structural Construction

The LDR antenna is a dual back fire UHF-VHF array with four elements spaced uniformly around the spacecraft centerline as shown in Figure 5-1. Each element consists of a series of discs-on-rod, a UHF dipole and mesh ground plane, and a VHF dipole and mesh ground plane. When deployed, each element is supported and positioned by a swing arm support link that places the element centerline at 48.75 inches (1.24 m) from the X and Y axes.

Lightweight structure and high porosity mesh materials reduce the unbalanced solar pressure, weight, and c.g. travel of the array to a minimum consistent with adequate rigidity and handling characteristics. The central rod is a "STEM" element that is retracted into its case at the rear of the antenna when the array element is packaged in the launch configuration. The two ground planes are light frame mesh covered structures that are partially folded (to 30 in. (.76 m) dia.) for packaging. The cross

dipoles are thin wall aluminum tubing welded to the central hubs which contain the RF coaxial connectors. The discs on the control rod are thin reinforced fiberglass plates with high porosity aluminized mylar face sheets for reflectivity. The discs, dipoles and UHF ground plane are positioned and properly spaced along the control stem by a dacron cord system extending from the front disc to the rear ground plane when the antenna is deployed.

To package the UHF-VHF array elements in the available space with the other antennas and spacecraft body, each array element must be packaged in a volume 30 in. (.76 m) dia. by 16 in. (.41 m) long, and must be deployed with a simple, lightweight, reliable arrangement with no loose packaging parts. To accomplish this, as shown in Figure 5-3, the two large diameter ground planes fold down on spring-loaded arms which are equally spaced around a central mesh-frame disc of 30 in. (.76 m) dia. The VHF dipole assembly is reduced to the 30-in. (.76 m) dia. by compressing the spring-loaded dipole extensions. The discs, the UHF dipole, and ground plane, and VHF dipole are closely stacked against the front of the STEM actuator. The folded mesh rims of the two ground planes are folded into the space between the two ground plane discs in their stacked position. The ground plane arms are spring-loaded and restrained by lock pin shafts that extend forward from a locking disc behind the VHF ground plane. To release the mesh arms and allow the ground plane meshes to extend to their full diameters, this locking disc is rotated on the case of the STEM by a cable system activated by the lateral deployment of the support struts. This small rotation releases the mesh arms from the lock pin shafts and extends the mesh surfaces.

5.3.3 TDRS/GS Antenna

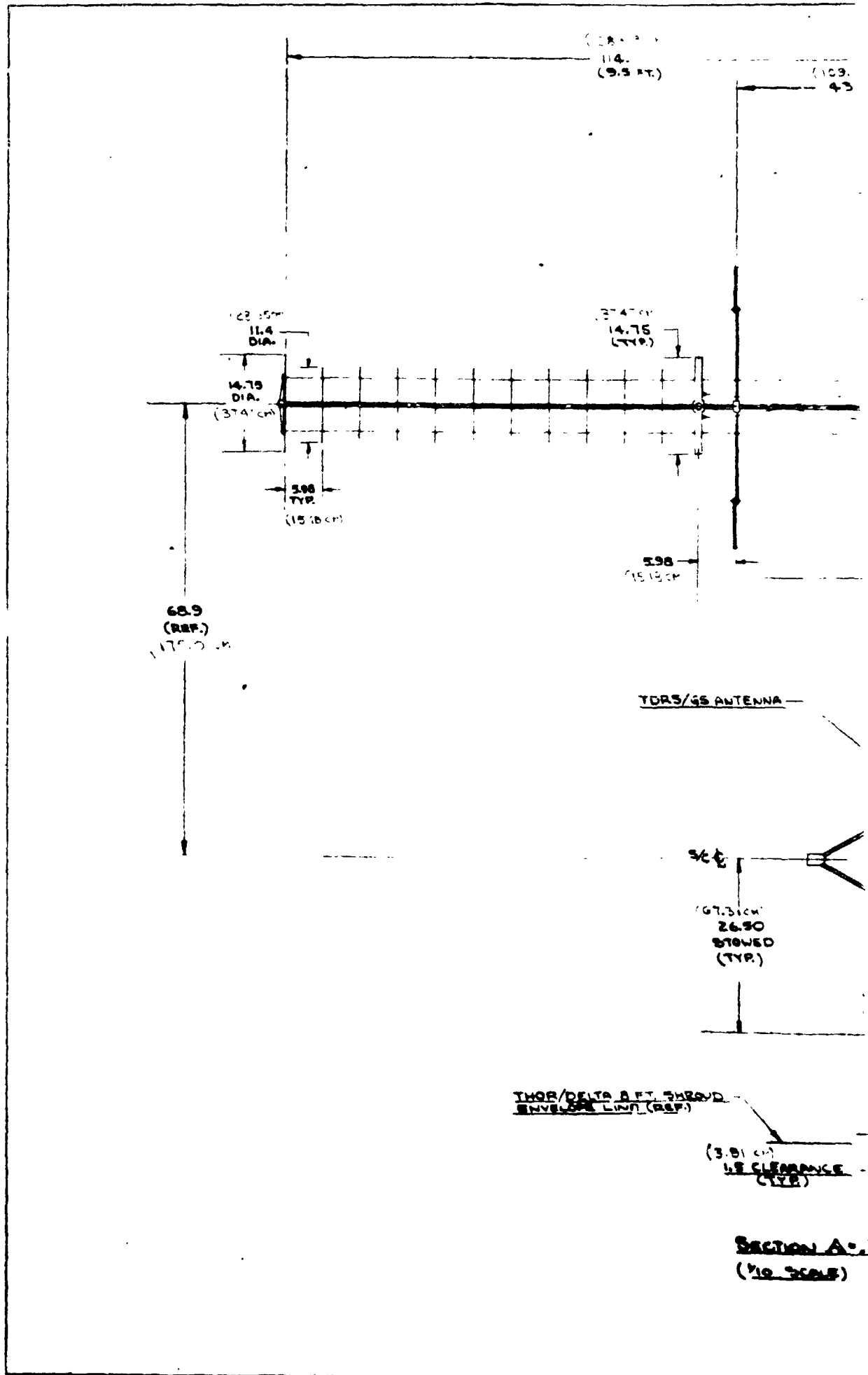
The ground link antenna is a 3-ft (.9 m) dia. Ku-band parabolic reflector located on the centerline of the spacecraft forward of spacecraft body. To provide clearance without blockage or reflective problems for the antenna beam between the LDR array elements, the antenna is positioned fore and aft as shown in Figure 5-1.

The TDRS/GS antenna is similar in construction to the MDR antennas. It is a one-piece solid face aluminum honeycomb panel with 0.50 in. (1.27 cm) alum. core and 0.005 in. (.013 cm) alum. face sheets bonded with epoxy adhesive. The 0.040 in. (.101 cm) alum. hub is riveted and bonded to the back of the reflector panel and supports the two-axis gimbal and the feed-at-focus feed package support tubes at the reflector face. The two-axis ± 10 degrees gimbal drive is similar to but smaller than the MDR gimbal drives described earlier. Ku-band rotary joints are included across each axis. The rear mounting flange of the gimbal is bolted to the front face of the spacecraft body front closeout cone.

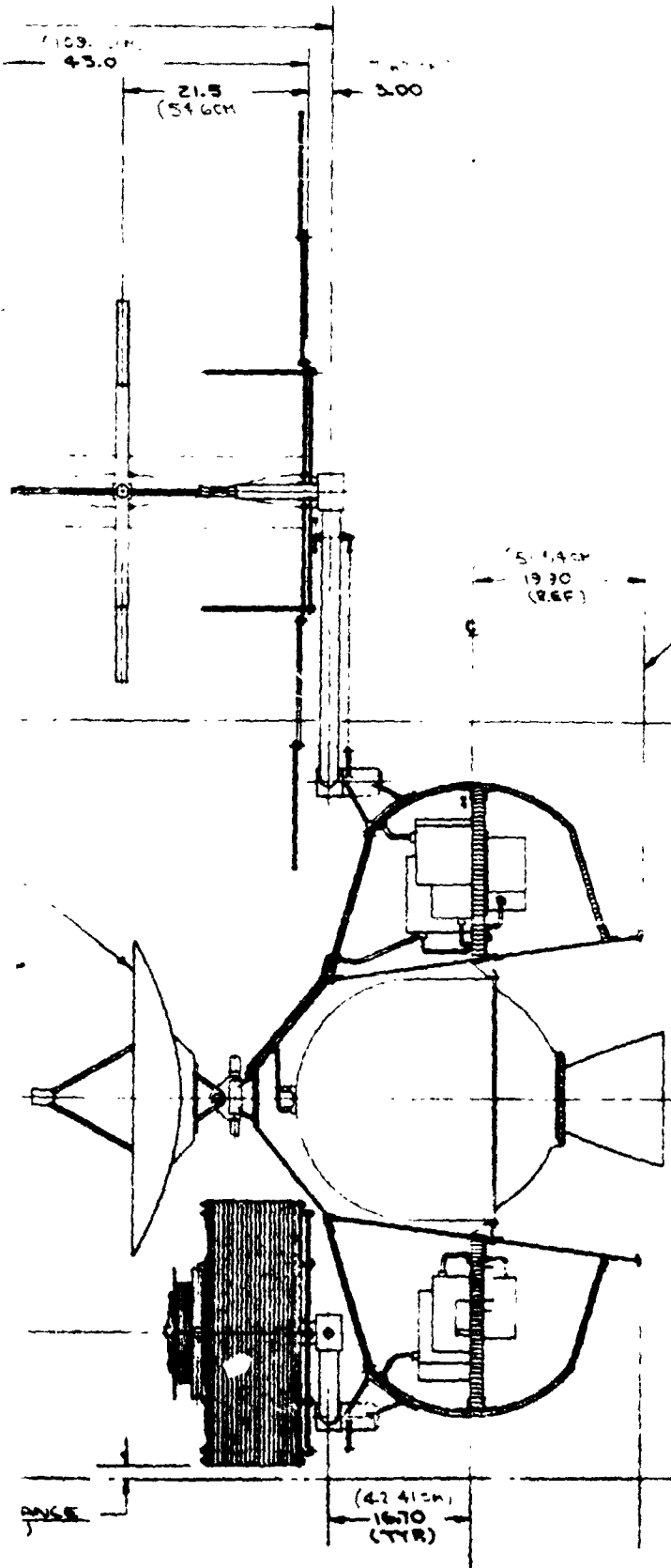
5.3.4 TT&C Antennas

The tracking telemetry and command back-up antennas are VHF omni whips. One set of four whips located radially around the rear of the spacecraft is utilized during launch when the primary antennas are in their stowed position. As shown in Figure 5-1, these TT&C antennas are behind the stowed

FOLDOUT FRAME



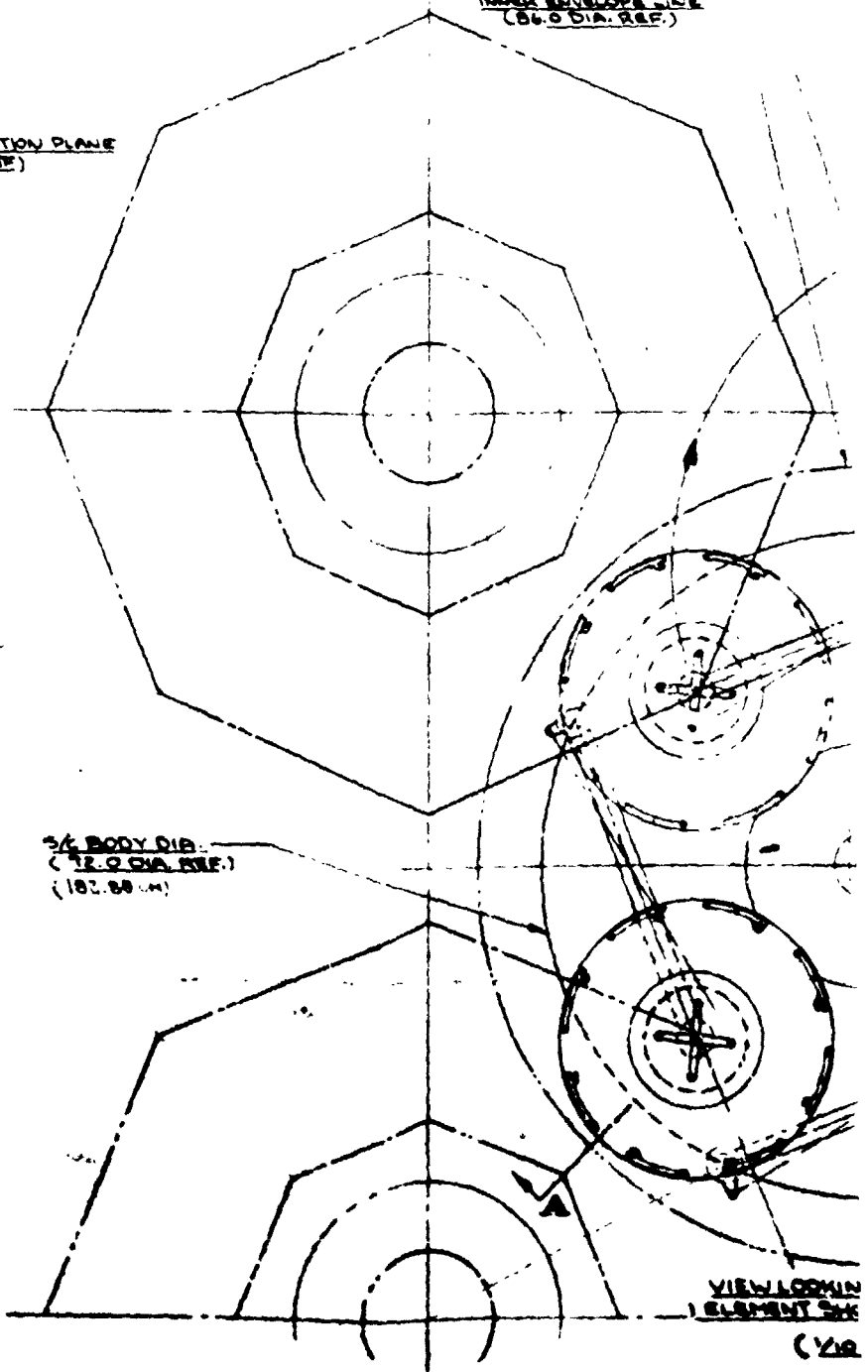
FOLDOUT FRAME



SEPARATION PLANE
(REF)

DIRECTION OF LATERAL
DEPLOYMENT (TYP.)

THOR DELTA 8 FT SHROUD
INNER ENVELOPE LINE
(86.0 DIA. REF.)



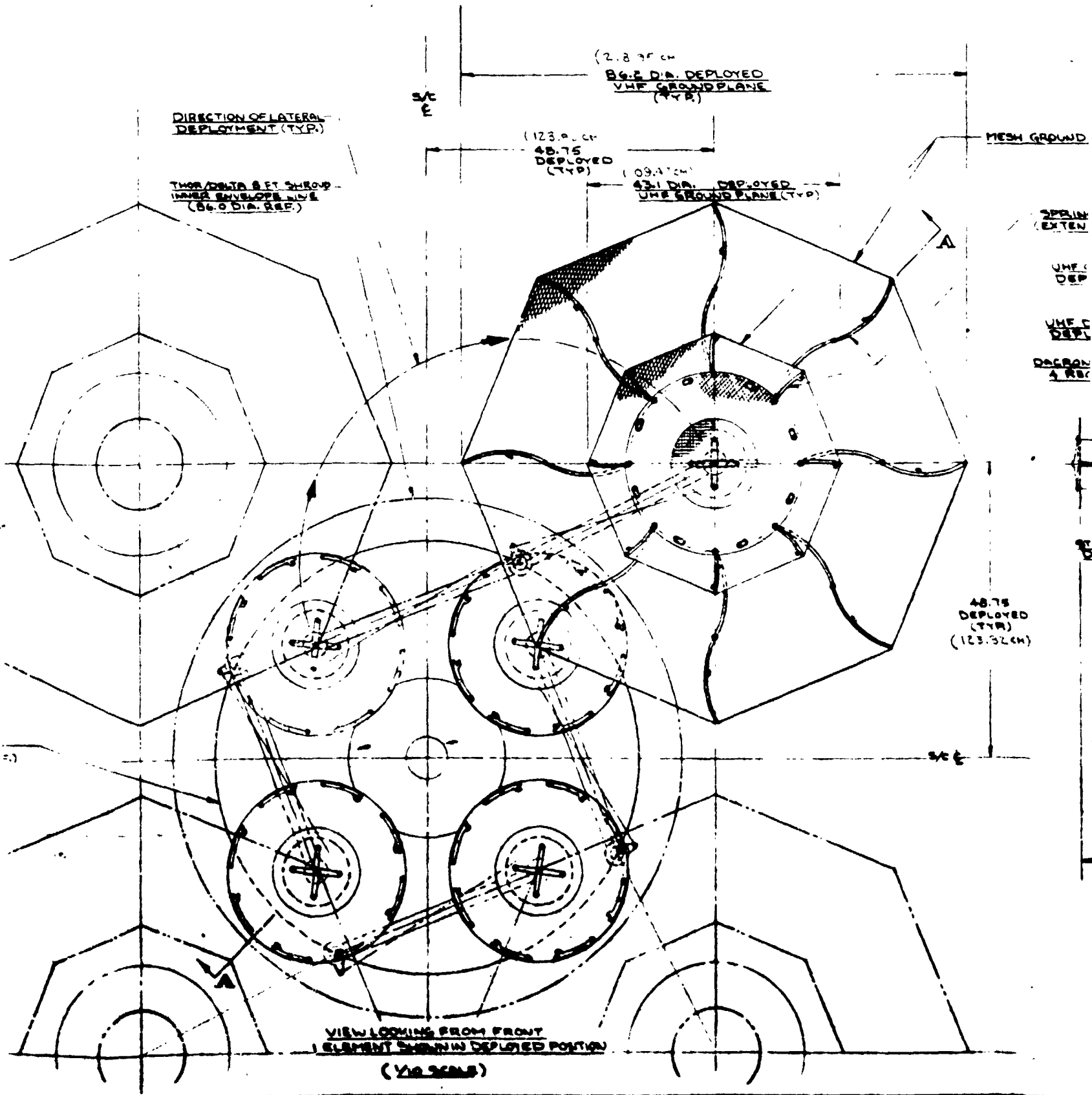
5/8 BODY DIA.
(12.0 DIA. REF.)
(182.88 mm)

VIEW LOOKING
ELEMENT 2

(1/2)

N.A.A.
(REF)

FOLDOUT FRAME



FOLDOUT FRAME

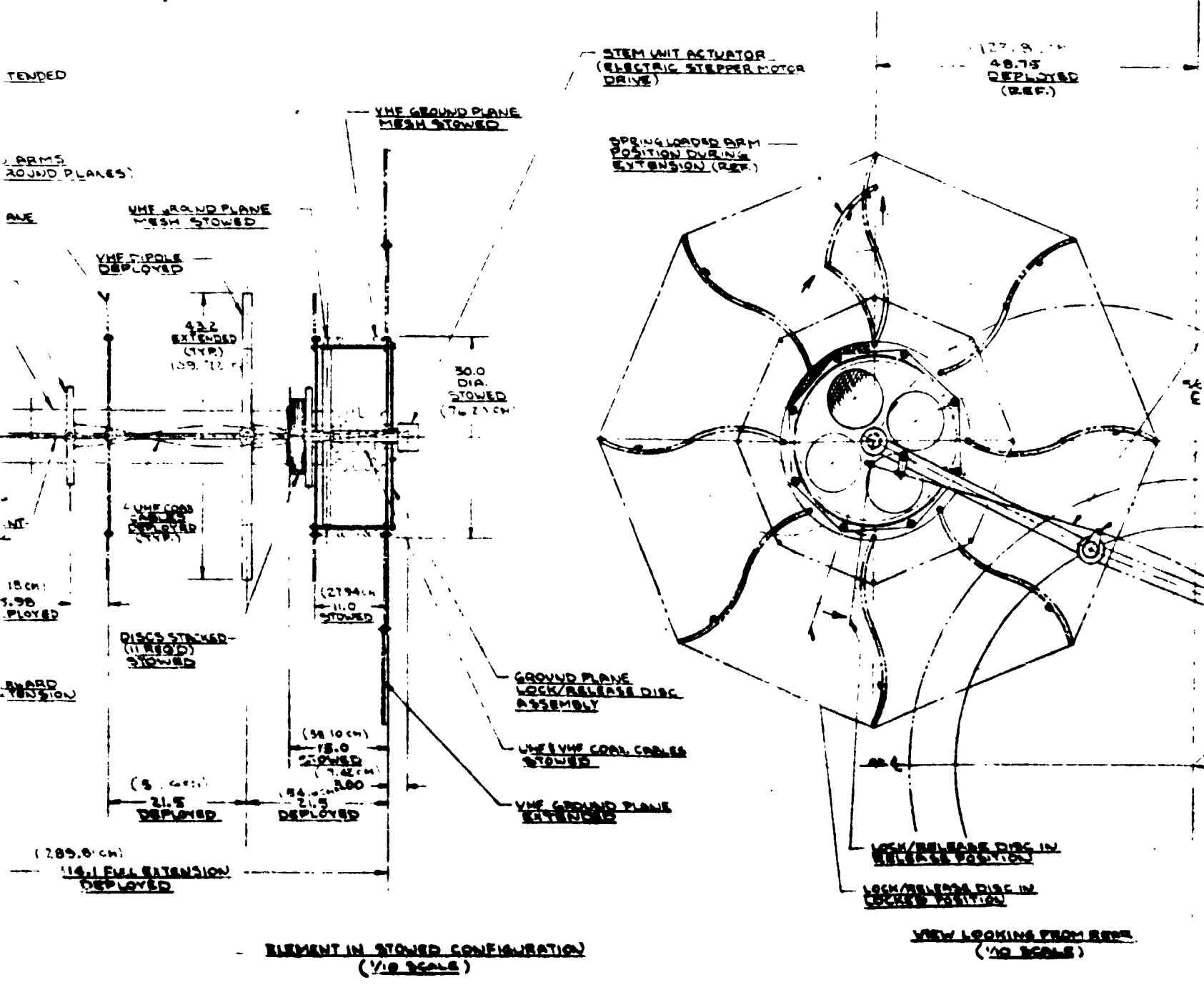


Figure 5-3. UHF

MIT ACTUATOR
RIG STEPPER MOTOR

127.5
48.75
DEPLOYED
(REF.)

4 LOADED ARM
TWIN DURING
EXTENSION (REF.)

GROUND PLANE ARM
RELEASE CABLE

CABLE POINT OFFSET ON FIXED
SUPPORT ARM FITTING.

STOWED ELEMENT POSITION
(REF.)

26.50
REF.
(TYP.)
(67.31 cm)

LOCK/RELEASE DISC IN
RELEASE POSITION

LOCK/RELEASE DISC IN
LOCKED POSITION

VIEW LOOKING FROM REAR
(NO SCALE)

Figure 5-3. UHF-VHF Backfire Array Element

5-11,5-12



solar panels and after the shroud is jettisoned they have a clear field-of-view to the ground tracking stations. After three-axis stabilization and deployment of the primary antennas, a T&C backup to the TDRS/GS Ku-band link is supplied by another set of the VHF omni-whip antennas mounted around the rim of the TDRS/GS Ku-band antenna.

5.3.5 Ku and S-band Tracking/Order Wire Antennas

Ku and S-band tracking beacons are mounted on the forward side of the spacecraft body adjacent to and offset from the TDRS/GS antenna. The Ku-band acquisition beacon antenna consists of a section of waveguide which terminates into a conical horn with a peak gain of nominally 12 dB and a 31-degree FOV. The S-band acquisition beacon/order wire antenna is a 2-in. (5.1 cm) dia. helix mounted on an 10" (25.4 cm) ground plane to provide performance comparable with the Ku-band beacon antenna.

5.4 SOLAR ARRAY PANELS AND DRIVE MECHANISM

The solar array panels are deployed to the positions shown in Figures 5-1 and 5-4, and rotate at one revolution in 24 hours to maintain solar illumination on the front of the array.

5.4.1 Solar Panels

To package the solar array in the launch configuration, the panels are constructed on a radius that permits the panels to fold around the top and bottom of the body. The gaps between the panels permit clearance for the MDR antenna booms and operation of the ACS thrusters in the launch configuration. The solar panel support links fold forward and under the solar panels and are restrained during launch loading by solenoid operated latch-release mechanisms. In this position the solar panels are active and provide limited electrical power during the spinning sequence.

After stabilization of the spacecraft at synchronous orbit, ground commands activate solenoids to release the linkage. Spring-loaded fittings extend the solar panels and lock the joints. As the panels extend, spring loaded hinges, between the panel halves and the support link, which are also released by the solenoid mechanism, extend the solar panel halves forward from their circular stowed configuration to provide a flatter shape for increased efficiency. After full panel deployment, the panel drive actuators at the base of the linkage system orient the solar panel sun sensors with the sun and begin the 1 rev/day to maintain solar alignment.

Each solar panel consists of two halves mounted to the center support link. Each half is a curved aluminum honeycomb substrate on which the solar cells, cover glasses and internal connections are bonded. The substrate panels are .75-in. (1.91 cm) alum. honeycomb core with 0.008-in. (.02 cm) alum. face sheets bonded with epoxy adhesive. The centerline hinges and support links are symmetrically located so that substrate and structural details are

identical in each panel half. The linkage struts are 2.12 in. (5.11 cm) dia aluminum tubes with machined end fittings containing the torsion springs and latching systems. The solar aspect sensors are mounted directly below the solar panel on the topmost link.

5.4.2 Drive Mechanism

The drive system consists of two actuators driven by electric stepper motors mounted on the rear surface of the equipment shelf, and supports and rotates the deployed panels. The stepper motor is either driven by ground command for initial solar acquisition and minor realignments or an automatic mode of one revolution per day after alignment and solar acquisition. Section A-A on Figure 5-4 illustrates details of a typical actuator as proposed by Spar Aerospace Products.

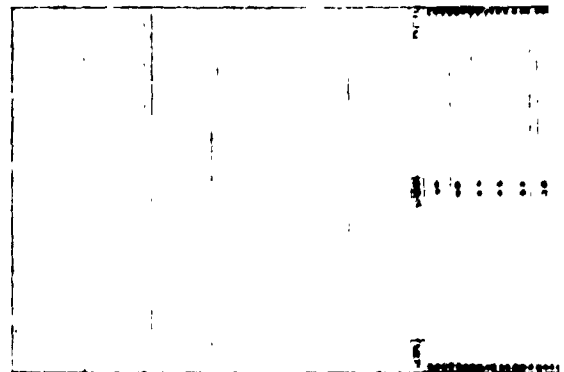
The drive is a composite brush/slip ring power transfer device on a .75-in (1.91 cm) dia shaft mounted between two bearings. The bearing at one end is rigidly mounted while the one at the other end is diaphragm mounted to apply a small preload to the bearings and to apply thermal compensation. The actuator is driven by a 1.8 degree stepper motor operating through a single pass harmonic reducer. This approach is favored because of its reliability and suitability compared to a spur gear train. In a very compact package a reduction of 120:1 can give a step angle of .015 degrees: (.26 mrad).

The power transfer provides 4 power rings and 10 signal rings with power and signal leads running inside the shaft to the rotor and the power and signal collector to the stator mounted on the side of the actuator case.

5.5 SUBSYSTEMS INSTALLATION

Most of the satellite equipment is installed on the front and back faces of the equipment shelf to provide proper c.g. location, eliminate c.g. travel during use of expendables, and provide ease of assembly, servicing and checkout. Figures 5-5 and 5-6 illustrate front and rear views of the equipment bulkhead with the subsystems installed. First, the propulsion system is installed on the blank equipment shelf which serves as an installation, checkout and shipping fixture. The propulsion subsystem installation is shown in Figure 5-7. Centerlines of tanks and ACS thruster clusters coincide with the c.g. location in the deployed configuration eliminating c.g. travel due to propellant expenditure which could cause misalignment of c.g. and the thruster centerline. All propulsion lines and valves are located around the shelf periphery leaving the central portion available for later installation of RF and electrical cable runs and harnesses. After assembly and checkout of the propulsion system on the shelf, the attitude control system is installed and checked out. The communication system components are mounted on honeycomb panel inserts which match the equipment

FOLDOUT FRAME



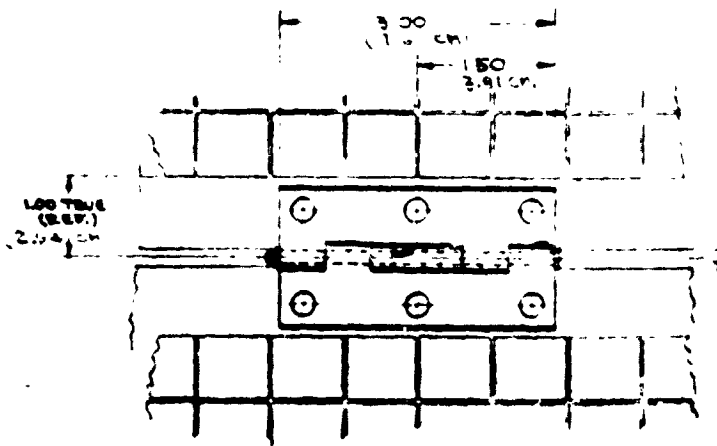
3 SETS OF
STRINGS TO
SHUNT & WIPER
CIRCUIT.

3 SETS OF
STRINGS TO
CIRCUIT

3 SETS OF
STRINGS TO
CIRCUIT

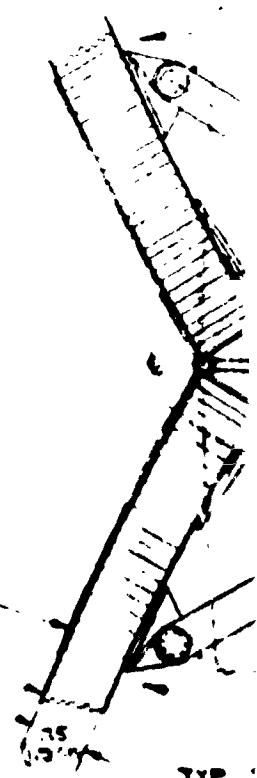
TRUE VIEW OF SOLAR ARRAY 2
(TYP FOR BOTH ARRAYS)
1/2 SCALE

AREA 5002
AREA SUBSTRATE
NUMBER OF CELLS PER ARRAY
NUMBER OF STRINGS PER ARRAY
NUMBER OF CELLS PER STRING



SOLAR CELL
(REV.)

SUBSTRATE ASSEMBLY
400 PAGE SHEETS, 6mm
CELLS TO CELL - 0.5mm
CELL TO CELL - 0.5mm
(SEE 12/7/68, 67)



TYP.

2
COLDOUT FRAME

44 80
 113 77
 45 80
 (84 CELLS AT
 97% PACKING FACT)
 (25 CM)

38 90
 48 CELLS AT
 97% PACKING FACT
 (38 90 CM)

SINGLE STRING OF
 12 (2 CM x 2 CM) CELLS

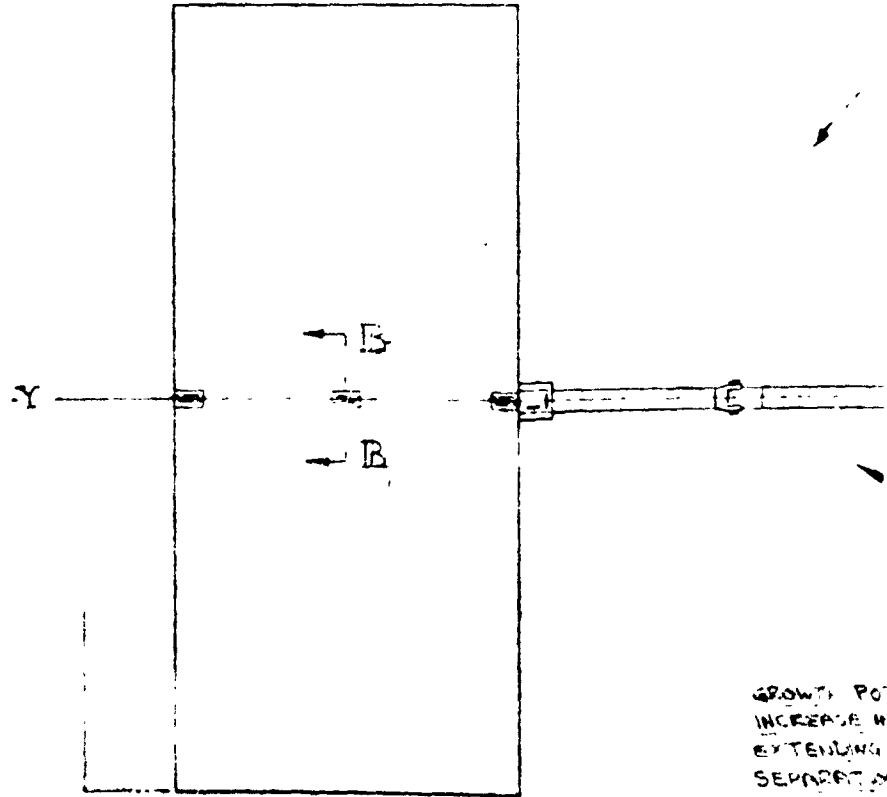
(1.5 CM)
 6.49 9 CELL DTH (TYP)
 ONE SET OF 6 STRINGS
 WITH 12 CELLS / STRING

SETS OF
 6 CELLS TO
 CUTE
 3 SETS OF
 STRINGS TO
 CROWN

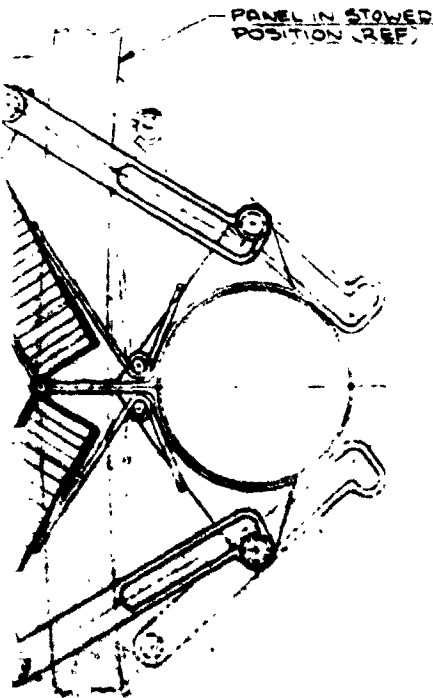
(RAY SURFACE
 RAYS)

(2.2 SQ M)
 23.7 SQ FT
 24.2 SQ FT (2.22 SQ M)
 12
 51.84

PROJECTED AREA 22.5 SQ FT
 (2.09 SQ M)



GROWTH POT
 INCREASE IN
 EXTENDING
 SEPARATION



PANEL IN STOWED
 POSITION (REF.)

SECTION B - B
 THROUGH EACH HINGE
 FULL SCALE

FOLDOUT FRAME

REVISIONS	
LR	DESCRIPTION
A	ADDED SECTION A-A

MOUNTED BEARING
 THERMAL COMPENSATION
 POWER & SIGNAL CABLES

VICE - STACKPOLE
 ES ON COIN SILVER
 RINGS
 WAL RINGS

- FITTING - SPRING OPERATED
 TO DEPLOY - LATCH TO LOCK
 IN DEPLOYED CONFIG. (TYP)

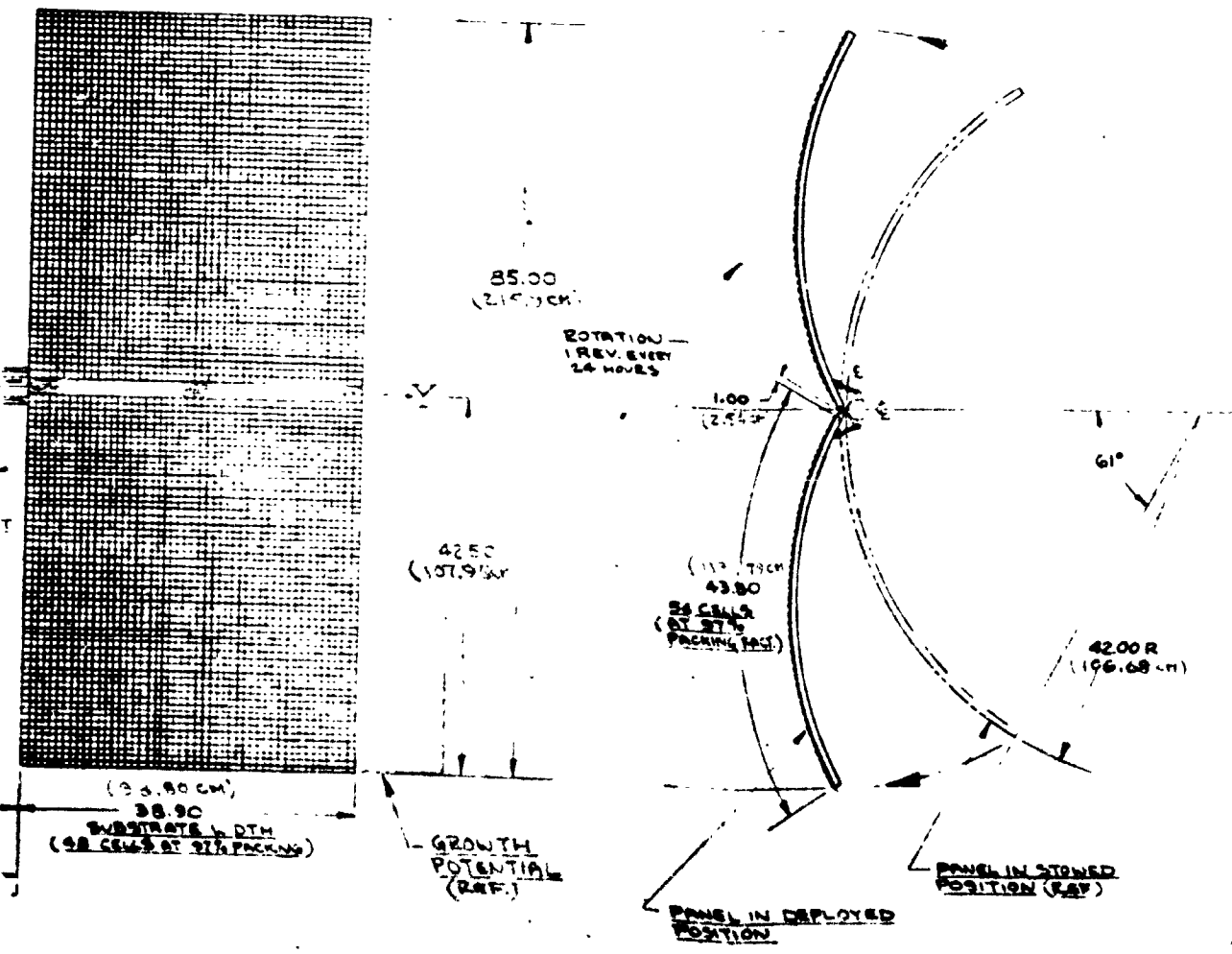


Figure 5-4, Solar Panel

REVISIONS		DATE CHG. BY
LR	DESCRIPTION	
A	ADDED SECTION A-A	10-12 J.W.C.

BOLDBOUT NAME

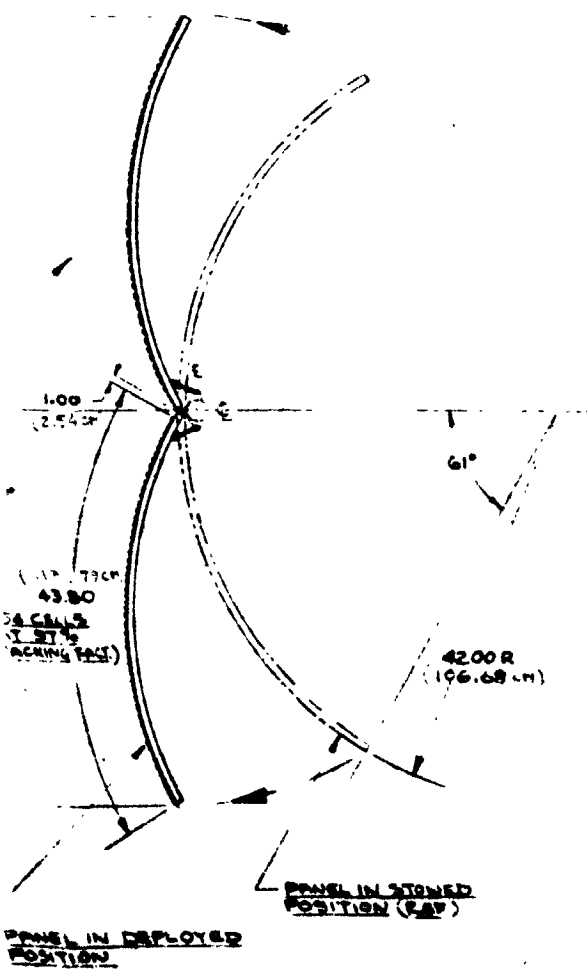
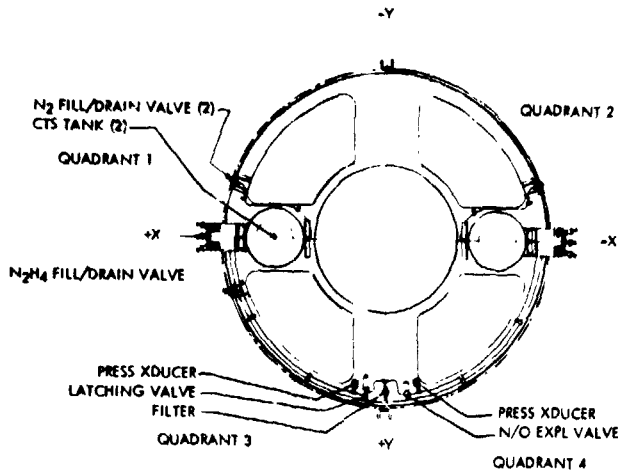


Figure 5-4. Solar Panel Array

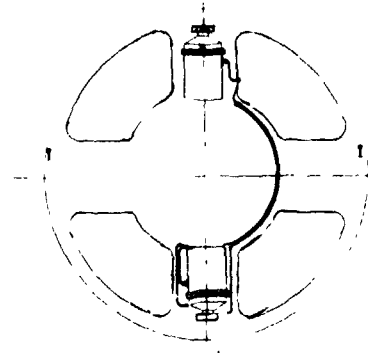
5-15,5-16

PROPULSION SYSTEM INSTALLATION

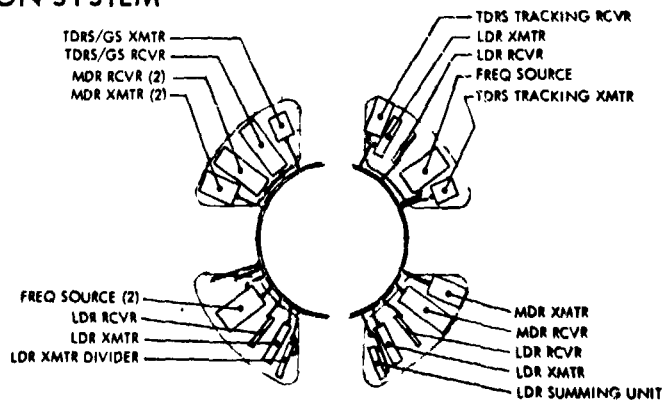


ACS REACTION WHEELS

ACS HORIZON SENSOR (2)
ACS REACTION WHEEL (2)



COMMUNICATION SYSTEM



FINAL ASSEMBLY

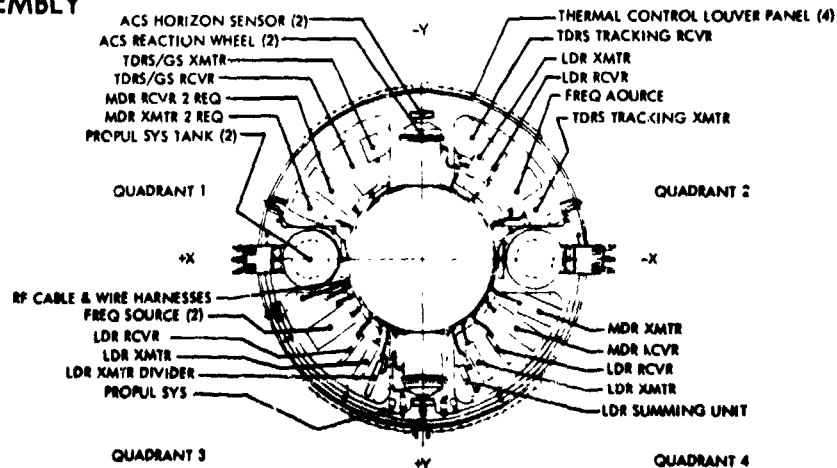
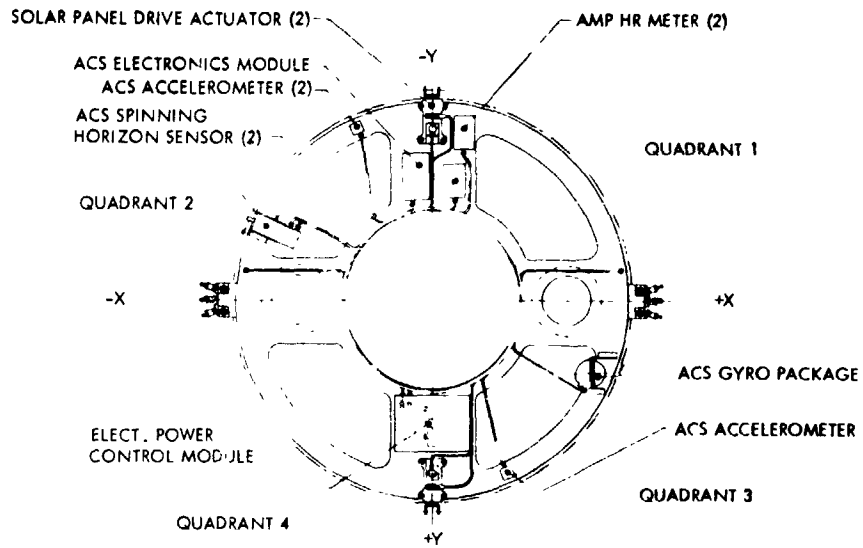
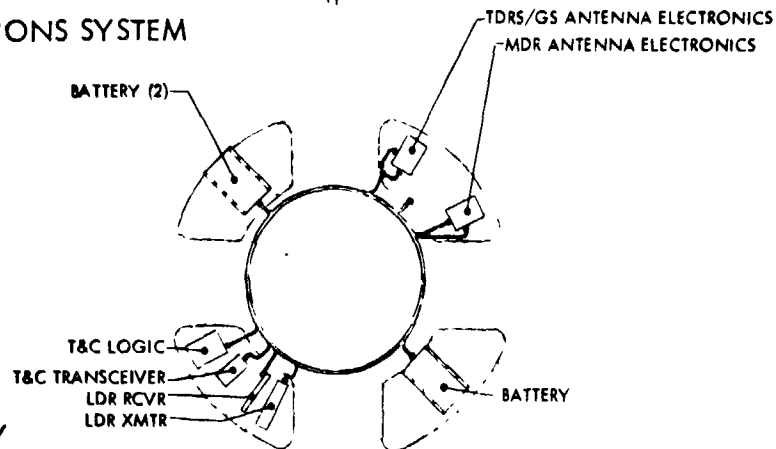


Figure 5-5. Equipment Shelf-Front View

ACS & ELECTRIC POWER SYSTEM



COMMUNICATIONS SYSTEM



FINAL ASSEMBLY

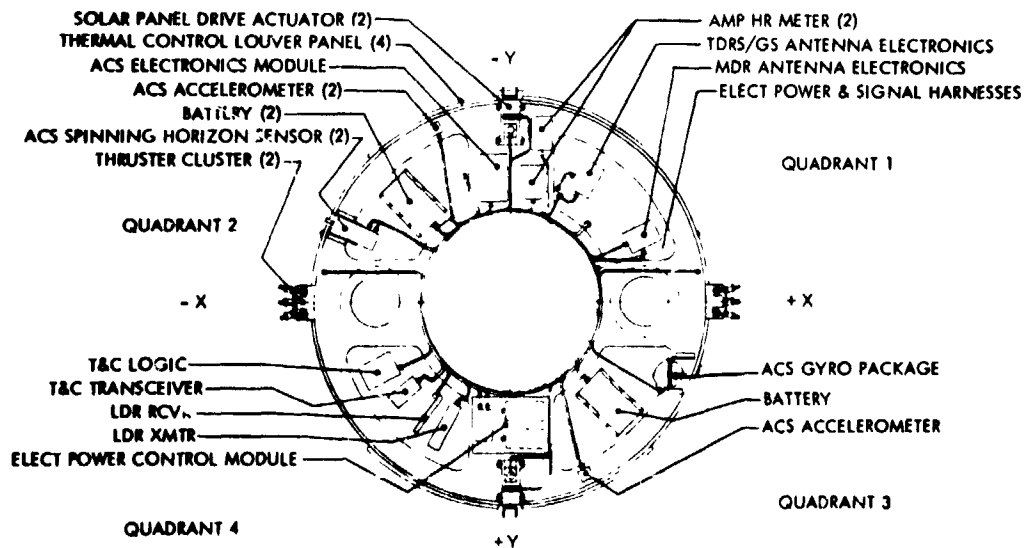
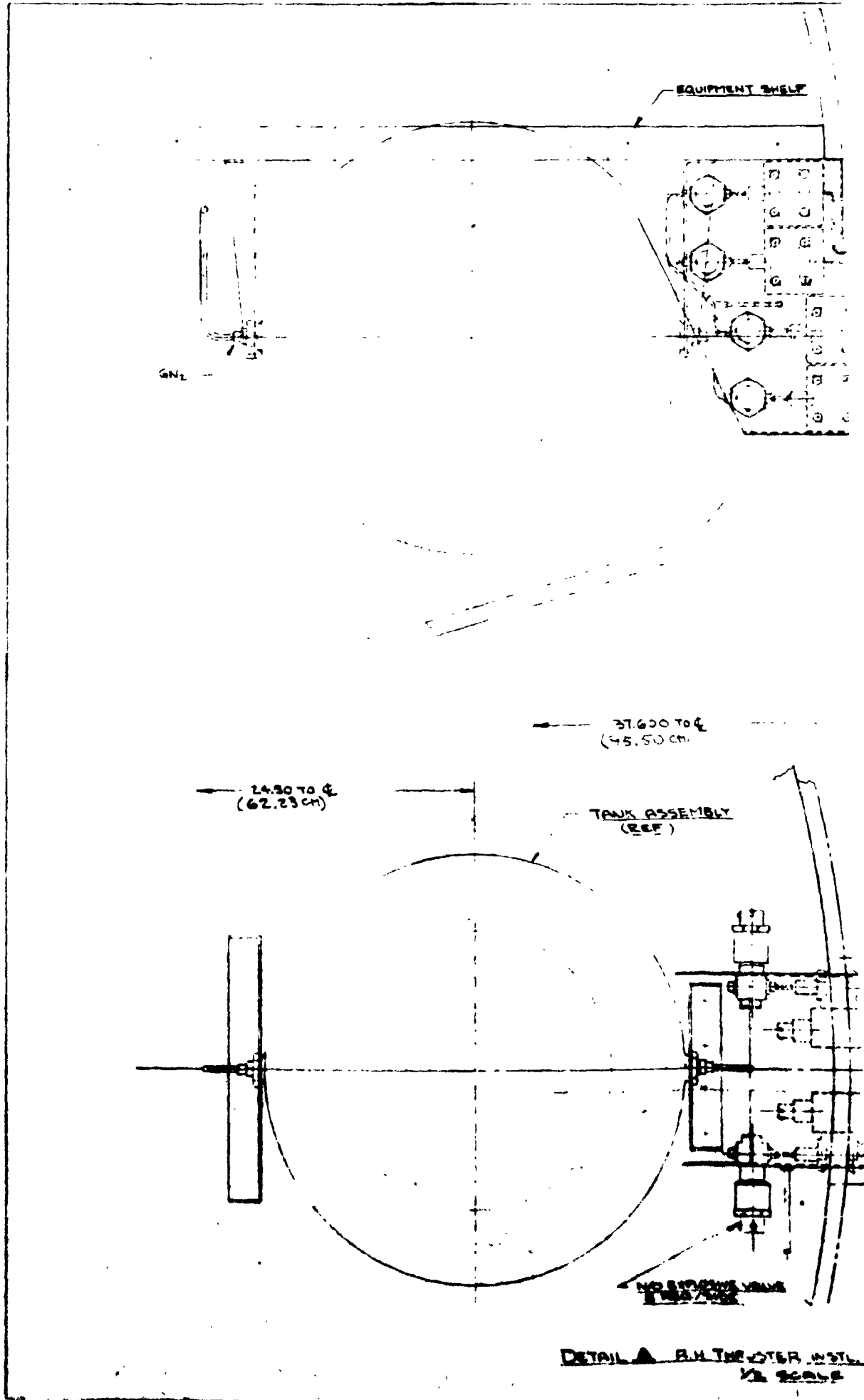


Figure 5-6. Equipment Shelf-Rear View

FOLDOUT FRAME



EQUIPMENT SHELF

GN₂

37.60 TO C
(45.50 cm)

24.80 TO C
(62.23 cm)

TANK ASSEMBLY
(REF)

NO STAYS OR BRACES
TO BE USED

DETAIL A ON THE OTHER SIDE
1/2 SCALE

FOLDOUT FRAME

FOLDOUT

21.60 TO SP.
(REF.)

1.700
43.30"

1.980
50.30"

21.60
(REF.)
54.60"

1.700
43.30"

SOLAR PANEL ARRAY
STOWED CONFIGURATION
(REF.)

COMMUNICATIONS MODULE (REF.)
(TYP.)

GN₂ LINE TO TANK
1 L-R REQ.

GN₂ FILL/DRAIN VALVE
2 REQ.

20°
(TYP.)

20°

N₂ FILL/DRAIN VALVE

N₂ LINE (TO TANKS)

N₂ LINE (TO THRUSTERS)

COMMUNICATIONS MODULE
(REF.)

PRESSURE TRANSDUCER
LATCHING VALVE

VIEW LOOKING AFT
1/2 SCALE

34.62
(87.93 CM)

1.50
38.10"

1.80
45.70"

SECTION A-A
(EVAL. 2-65)

THERMAL INSULATION
COVER TUB
(NOT SHOWN FOR CLARITY)

THRUSTER CHAMBER
8 REQ. / 2 DR.

30°
TYP.

1.000
25.40"

RADIATION SHIELD - TYP.
ON ALL THERMISTERS
(NOT SHOWN FOR CLARITY)

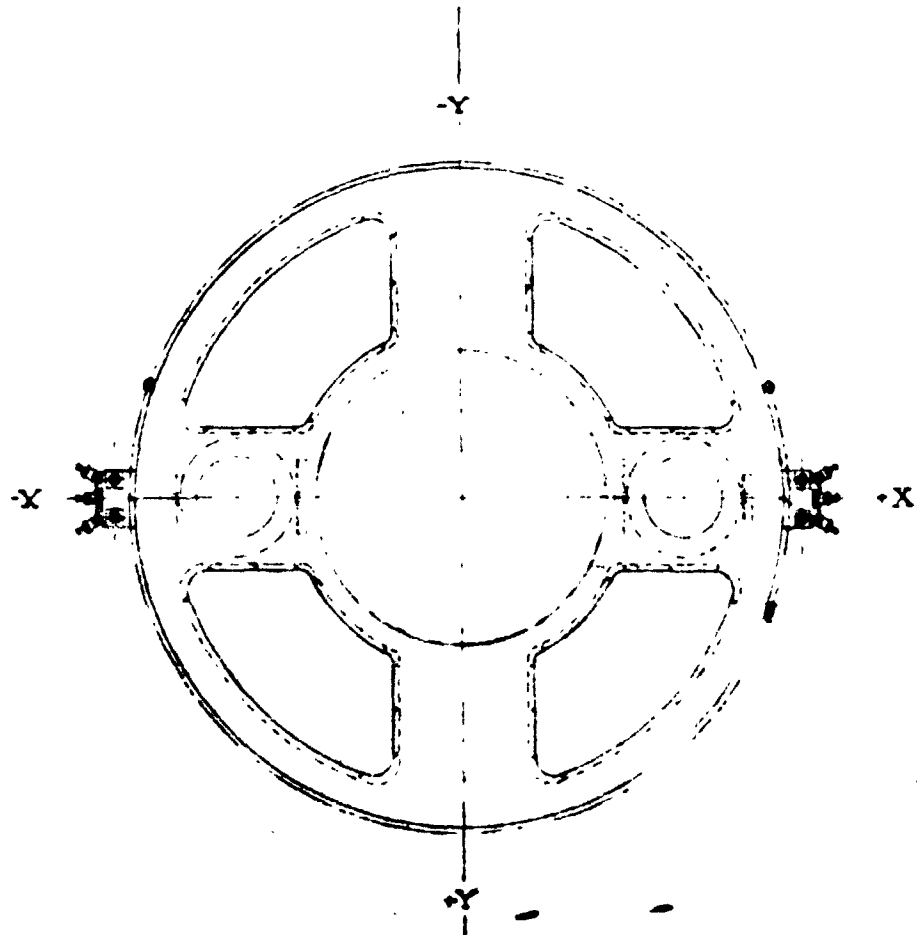
TRANSFER VALVE
REQ. / SIDE

WELD TYPE W/SP.
WITH 90° SOLDER
TUB

IN OPPOSITE

4.
FOLDOUT FRAME

LTR
A
D
E
B
S



VIEW LOOKING FORWARD
NO SCALE

Figure 5-7. Propulsion Syst

5
**FOLDOUT FRAME
 REVISIONS**

LTR	DESCRIPTION	DATE CHG BY
A	REVISED THRUSTER ARRANGEMENT (WAS 15° OFFSET IN BOTH YAW & PITCH AXES. ROLL WAS PROVIDED BY COUPLE PRODUCED BY DISPLACED YAW THRUSTERS)	6-26-72 JWC

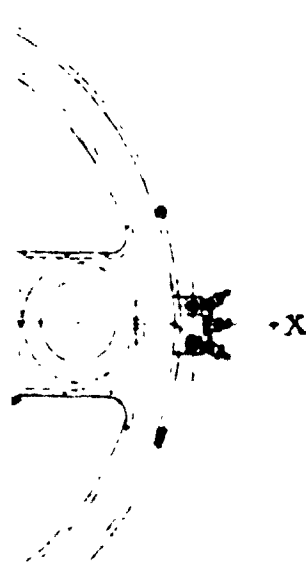


Figure 5-7. Propulsion System Installation

5-19, 5-20

SD 72-82-0133

TRDS Revision 5th Edition 1173-20

shelf cutouts, and are interconnected for bench checkout and testing as a subsystem unit. The communications panel inserts are then attached to the equipment shelf and the electrical power subsystem is installed on the rear face of the shelf and all cabling installed and tested.

5.6 ACCESSIBILITY AND SERVICING PROVISIONS

The spacecraft equipment located on the equipment shelf provides convenient servicing through access panels on the front and rear outer body shells. At initial installation, the subsystems are mounted on the shelf prior to the assembly of the outer body shells and are fully exposed for checkout. Propulsion system fill and drain valves are accessible and convenient with the spacecraft in the stowed configuration. All launch restraints and solenoid release mechanisms are visible for prelaunch checkout and inspection. Prelaunch electrical check points are adjacent to the MDR antenna attachment fittings and are readily accessible. The spacecraft terminates at the separation plane of the Delta attach fitting with only minor structural overhang at the interface. The motor extends 2.5 in. aft of the separation plane and the four whip antennas extend aft of the separation plane. Access to the Delta third stage motor through the existing access holes in the attach fitting is not compromised and remains clear and convenient.

Access to and visual inspection of the mating Delta clamp securing the TDRS to the attach fitting is clear of structure and convenient for mating prior to launch.

5.7 MASS PROPERTIES

The weight summary for the TDRS is shown in Table 5-3 and subsystem weights in Table 5-4. Preliminary c.g. location and moments of inertia for both the launch and deployed configurations are summarized in Table 5-5.

5.8 SUBSYSTEM INTEGRATION

Figure 5-8 shows the integrated subsystems block diagram. Not shown in detail are all the telemetry and command interfaces and the electrical interfaces. These subsystems are described in detail in the following sections.

Table 5-3. TDRS Weight Summary

	Weight (lb)	Weight (kg)
Communications		
Electronics	122.2	55.5
Antennas	117.9	53.5
Attitude stabilization and control	57.7	26.2
Electric power	97.0	44.0
Solar array	58.6	26.6
Structure	91.0	41.3
Thermal control	23.9	10.8
Auxiliary propulsion hardware	38.4	17.4
	606.7	275.0
Propellant + N ₂ (2-65° - 15-day station changes)	49.3	22.4
Total spacecraft	656.0	297.6
Contingency	82.0	37.2
Allowable P/L (Delta 2914 + CTS apogee motor)	738.0*	334.8*
Empty apogee motor case	50.0	22.7
Initial on-orbit	788.0	357.5
Burned-out insulation	8.0	3.6
Apogee motor propellant	688.0*	312.1
Synchronous orbit injection	1484.0	673.2
Transfer orbit propellant	6.0	2.7
Delta separation weight (27° transfer orbit)	1490.0	675.9
*5 deg/day drift orbit		

Table 5-4. Weight Estimate by Subsystem (English Units)

Component	No.	C.G. Location (in)			Weight (lb)	
		X	Y	Z	Unit	Total
SPACECRAFT STRUCTURE						
Internal cones						
Forward	0	0	0	39.8		2.85
Inner	0	0	0	8.3		22.9
Shell	0	0	0	21.0		24.43
Equipment shelf	0	0	0	19.45		12.26
Motor mounting ring	0	0	0	17.4		7.59
Fittings, hardware						
		-15.2	+32.5			
		-32.5	-15.2	33.1		
		-15.2	-32.5			20.97
		-32.5	+15.2			
		+18.5	-9	4.5		
		-18.5	+9			
Total						91.0
ELECTRICAL POWER						
Solar array						
Panels	2	0	+35.0	19.0		
		0	-35.0	19.0	19.3	38.6
Drive mechanism	2	0	-32.0	14.9		
		0	-32.0	14.9	7.5	15.0
Fitting and link	2	0	-38.75	38.0		
		0	-38.75	38.0	2.5	5.0
Subtotal						58.6
Power conditioning and distribution						
Charge and discharge regulators						11.3
		0	-21.8	15.9		
Central control and logic						5.1
Packaging		0	+21.8	15.9		4.9
Shunt dissipators		0	-39.0	19.9	1.2	2.4
			-39.0	19.9		
A.H. meters	2	+3.8	-21.5	16.9	2.0	4.0
		+5.7	-30.0	16.9		
Power Conditioner	1	0	+21.8	15.9		5.0
Cabling		0	0	18.5		20.0
Subtotal						52.7
Energy storage						
Batteries	2	-20.7	-14.4	15.9	22.15	44.3
		+17.7	+17.4	15.9		
Total						156
ATTITUDE STABILIZATION & CONTROL						
Nutation sensing accelerators	2	-13.5	-30.6	18.0		
		+13.5	-30.6	18.0	0.3	0.6
Spinning horizon sensors	2	-28.7	-13.0	17.4		
		-28.7	-13.0	15.4	2.0	4.0
Spinning sun sensors	2	-28.7	+13.0	17.4		
		-28.7	13.0	15.4	1.0	2.0
Solar aspect sensors	2	0	+40.0	39.0		
		0	-40.0	39.0	2.25	4.5

Table 5-4A. Weight Estimate by Subsystem (International Units)

Component	No.	C.G. Location (cm)			Weight (kg)	
		X	Y	Z	Unit	Total
SPACECRAFT STRUCTURE						
Internal cones						
Forward		0	0	101.1		1.29
Inner		0	0	21.1		10.4
Shell		0	0	53.3		11.1
Equipment shelf		0	0	49.4		5.56
Motor mounting ring		0	0	44.2		3.44
Fittings, hardware		+38.6	+82.5			
		+82.5	-38.6	84.1		9.51
		-38.6	-82.5			
		-82.5	+38.6			
		+47.0	-22.9	11.4		
		-47.0	+22.9			
Total						41.30
ELECTRICAL POWER						
Solar array						
Panels	2	0	+88.9	48.3		
		0	-88.9	48.3	8.75	17.5
Drive mechanism	2	0	+81.3	37.8		
		0	-81.3	37.8	3.40	6.80
Fitting and link	2	0	+98.4	96.5		
		0	-98.4	96.5	1.13	2.27
Subtotal						26.60
Power conditioning and distribution						
Charge and discharge regulators		0	+55.4	40.4		51.3
Central control and logic						2.31
Packaging		0	+55.4	40.4		2.22
Shunt dissipators		0	+99.1	40.5	.544	1.09
			-99.1	40.5		
A.H. meters	2	+ 9.65	-54.6	42.9	.907	1.81
		- 1.44	-76.2	42.9		
Power conditioner	1	0	+55.4	40.4		2.27
Cabling		0	0	47.0		9.07
Subtotal						23.90
Energy storage						
Batteries	2	-52.6	-36.6	40.4	10.0	20.1
		+45.0	+44.2	40.4		
Total						70.60
ATTITUDE STABILIZATION & CONTROL						
Nutation sensing accelerators	2	-34.5	-70.7	45.7		
		+34.5	+70.7	45.7	.136	.272
Spinning horizon sensors	2	-72.9	-33.0	44.2		
		-72.9	-33.0	39.1	.907	1.81
Spinning sun sensors	2	-72.9	+33.0	44.2		
		-72.9	+33.0	39.1	.454	.907
Solar aspect sensors	2	0	+101.6	99.1		
		0	-101.6	99.1	1.02	2.04

Table 5-4. Weight Estimate by Subsystem (English Units) (Cont)

Component	No.	C.G. Location (in.)			Weight (lb)	
		X	Y	Z	Unit	Total
Reaction wheel/earth scanner assembly	2	0	+27.0	24.9	14.3	28.6
		0	-27.0	24.9		
Electronics	1	-2.9	-22.0	16.0		12.0
Yaw gyro and nutation damper	1	+28.6	+12.8	15.9		6.0
Total						57.7
AUXILIARY PROPULSION						
GN ₂ fill/drain valve	2	+33.2	-11.8	21.5	0.3	0.6
		-33.2	-11.8	21.5		
CTS tank assembly	2	+24.5	0	25.0	5.5	11.0
		-24.5	0	25.0		
Latching valve	1	+4.5	+31.0	21.5		.61
		-4.4	+31.3	21.5		
N/O expl. valve	17	+33.9	0	25.0	0.4	6.8
		-33.9	0	25.0		
Propellant fill/drain valve	1	+33.2	+11.8	21.5		0.3
Filter (15μ absolute)	1	0	+32.3	21.5		0.4
Pressure transducer	2	+6.7	+31.0	21.5	0.32	0.64
		-6.7	-31.0	21.5		
Temperature transducer	2	+24.5	0	25.0	0.3	0.6
		-24.5	0	25.0		
Temperature sensor	16	+37.6	0	25.0	0.025	0.4
		-37.6	0	25.0		
Thruster	16	+37.6	0	25.0	0.6	9.6
		-37.6	0	25.0		
Wiring and lines		0	+24.0	21.5		3.0
Thruster housing	2	+37.6	0	25.0	0.75	1.5
		-37.6	0	25.0		
Trapped propellant						3.0
Total						38.45
THERMAL CONTROL						
Louvers	4	-14.5	+32.5	18.0	3.08	12.33
		-14.5	-32.5	18.0		
		+14.5	+32.5	18.0		
		+14.5	-32.5	18.0		
Insulation		0	0	21.0		8.53
Heaters and wiring		0	0	24.0		3.0
Total						23.86
COMMUNICATIONS						
LDR Receiver	4	-15.6	+19.6	15.4	1.90	7.60
		+15.6	+19.6	23.4		
		-15.6	+19.6	23.4		
		-15.6	+19.6	23.4		
I.F. summing unit	1	-9.7	+26.0	21.9		1.3

Table 5-4A. Weight Estimate by Subsystem (International Units) (Cont)

Component	No.	C.G. Location (cm)			Weight (kg)		
		X	Y	Z	Unit	Total	
Reaction wheel/earth scanner assembly	2	0 0	+68.6 -68.6	63.5 63.5	6.49	13.0	
Electronics	1	-7.37	-55.9	40.7			5.44
Yaw gyro and nutation damper	1	+72.6	+32.5	40.5		2.72	
Total						26.2	
AUXILIARY PROPULSION							
GN ₂ fill/drain valve	2	+84.3 -84.3	-30.0 -30.0	54.6 54.6	.136	.272	
CTS tank assembly	2	+62.2 -62.2	0 0	63.5 63.5			2.49
Latching valve	1	+11.4 -11.2	+78.7 +79.5	54.6 54.6		.277	
N/O expl. valve	17	+86.1 -86.1	0 0	63.5 63.5	.181	3.08	
Propellant fill/drain valve	1	+84.3	+30.0	54.6		.136	
Filter (15 μ absolute)	1	0	+82.0	54.6		.181	
Pressure transducer	2	+17.0 -17.0	+31.0 -31.0	54.6 54.6	.145	.290	
Temperature transducer	2	+62.2 -62.2	0 0	63.5 63.5	.136	.272	
Temperature sensor	16	+95.5 -95.5	0 0	63.5 63.5	.011	.181	
Thruster	16	+95.5 -95.5	0 0	63.5 63.5	.272	4.35	
Wiring and lines		0	+61.0	54.6		1.36	
Thruster housing	2	+95.5 -95.5	0 0	63.5 63.5	.340	.680	
Trapped propellant						1.36	
Total						17.44	
THERMAL CONTROL							
Louvers	4	-36.8 -36.8 +36.8 +36.8	+82.6 -82.6 +82.6 -82.6	45.7 45.7 45.7 45.7	1.40	5.59	
Insulation		0	0	53.3			3.87
Heaters and wiring		0	0	61.0			1.36
Total							
COMMUNICATIONS							
LDR Receiver	4	-39.6 +39.6 -39.6 -39.6	+49.8 +49.8 +49.8 +49.8	39.1 59.4 59.4 59.4	.862	3.45	
I.F. summing unit	1	-24.6	+66.0	55.6			.59

Table 5-4. Weight Estimate by Subsystem (English Units) (Cont)

Component	No.	C.G. Location (in.)			Weight (lb)	
		X	Y	Z	Unit	Total
LDR (Cont.)						
Transmitter	4	-12.4	+22.0	18.4	1.12	4.5
		+12.4	+22.0	20.4		
		-12.4	+22.0	20.4		
		-12.4	-22.0	20.4		
Transmitter divider network	1	+10.8	+25.4	23.4		5.1
Antenna, including stem unit and support link	4	+19.0	+19.0	46.0	7.9	31.6
		+19.0	-19.0	46.0		
		-19.0	+19.0	46.0		
		-19.0	-19.0	46.0		
Subtotal						50.1
MDR						
Receiver No. 1	1	+19.8	-14.5	24.4		8.8
Receiver No. 2	1	-19.8	+14.5	24.4		8.8
Transmitter No. 1	1	+14.6	-11.0	21.2		13.0
Transmitter No. 2	1	-14.6	+11.0	21.2		11.0
Antenna assembly including: contr. electr., feed/microwave, support strut	2	+14.0	0	94.0	33.95	67.9
		-14.0	0	94.0		
Subtotal						109.5
TDRS/GS						
Receiver	1	+15.0	-19.4	23.9		4.7
Transmitter	1	+10.6	-24.0	20.4		6.0
Antenna assembly, including control electronics, feed/microwave components	1	0	0	56.0		14.85
Subtotal						25.55
Frequency Source	1	+20.2	+14.5	20.9		5.6
Telemetry and Command Processor	1	-23.6	+12.1	16.2		9.6
Transceiver	1	-18.8	+15.7	16.1		4.0
Antenna (+ cabling & matching net.)	8	+35.0	+35.0		.37	3.0
		+35.0	-35.0			
		-35.0	+35.0	0		
		-35.0	-35.0	0		
		+19.0	+19.0			
		+19.0	-19.0			
		-19.0	+19.0			
		-19.0	-19.0			
Subtotal						16.6
TDRS Tracking Transceiver	1	-10.8	-25.6	20.2		5.4
Antenna, helix S-band	1					.30
Subtotal						5.7
Ku-Band Tracking Beacon	1					3.6
Antenna	1					0.3
Subtotal						3.9
Cabling						
DC cabling		0	0	20.4		13.3
RF cabling		0	0	20.4		4.9
Waveguide		+18.5	-9.0	44.0	2.0	5.0
		-18.5	+9.0	44.0		
Subtotal						23.2
Total						240.17

Table 5-4A. Weight Estimate by Subsystem (International Units) (Cont)

Component	No.	C.G. Location (cm)			Weight (kg)	
		X	Y	Z	Unit	Total
LDR (Cont.)						
Transmitter	4	-31.4	+55.9	46.7		
		+31.4	+55.9	51.8		
		-31.4	+55.9	51.8		
		-31.4	-55.9	51.8	.58	2.04
Transmitter divider network	1	+27.4	+64.5	59.4		2.32
Antenna, including stem unit and support link	4	+48.3	+48.3	116.9		
		+48.3	-48.3	116.9		
		-48.3	+48.3	116.9		
		-48.3	-48.3	116.9	3.58	14.3
Subtotal						22.8
MDR						
Receiver No. 1	1	+50.3	-36.8	62.0		4.0
No. 2	1	-50.3	+36.8	62.0		4.0
Transmitter No. 1	1	+37.1	-27.9	53.8		5.9
No. 2	1	-37.1	+27.9	53.8		5.0
Antenna assembly, including control electronics, feed/microwave, support strut	2	+35.6	0	238.8	15.4	30.8
		-35.6	0	238.8		
Subtotal						49.7
TDRS/GS						
Receiver	1	+38.1	-49.3	60.7		2.14
Transmitter	1	+26.9	-61.0	51.8		2.72
Antenna assembly, including control electronics, feed/microwave components	1	0	0	142.2		6.74
Subtotal						11.6
Frequency Source	1	+51.3	+36.8	53.1		2.54
Telemetry and Command Processor	1	-60.0	+30.7	41.1		4.4
Transceiver	1	-47.8	+39.9	40.8		1.81
Antenna (+ cabling & matching net.)	8	+88.9	+88.9			
		+88.9	-88.9			
		-88.9	+88.9			
		-88.9	-88.9	0	.168	1.36
		+48.3	+48.3			
		+48.3	-48.3			
		-48.3	+48.3			
		-48.3	-48.3			
Subtotal						7.55
TDRS Tracking Transceiver	1	-27.4	-65.0	51.3		2.45
Antenna, helix S-band	1					.136
Subtotal						2.59
Ku-Band Tracking Beacon	1					1.63
Antenna	1					.136
Subtotal						1.77
Cabling						
DC cabling		0	0	51.8		6.04
RF cabling		0	0	51.8		2.22
Waveguide		+47.0	-22.9	117.8	1.13	2.27
		-47.0	+22.9	117.8		
Subtotal						10.5
Total						109.4

Table 5-5. Preliminary Moments of Inertia

Configuration	Weight		Z Center-of-Gravity (from S.P.)		Inertia					
	lb	kg	in.	cm	I _{z-z}		I _{x-x}		I _{y-y}	
					slug-ft ²	kg-m ²	slug-ft ²	kg-m ²	slug-ft ²	kg-m ²
Launch Full apogee motor Burnout apogee motor	1484	673.2	25.7	65.3	507	145	132	179	122	165
	788	357.5	26.1	66.3	94	127	119	161	108	146
Deployed Full propellant Fuel expelled	788	357.5	21.6	54.7	465	630	234	317	308	418
	738.7	335.0	21.6	54.7	458	621	234	317	301	408

*x and y center of gravity, 0.00 and 0.00

FOLDOUT FRAME

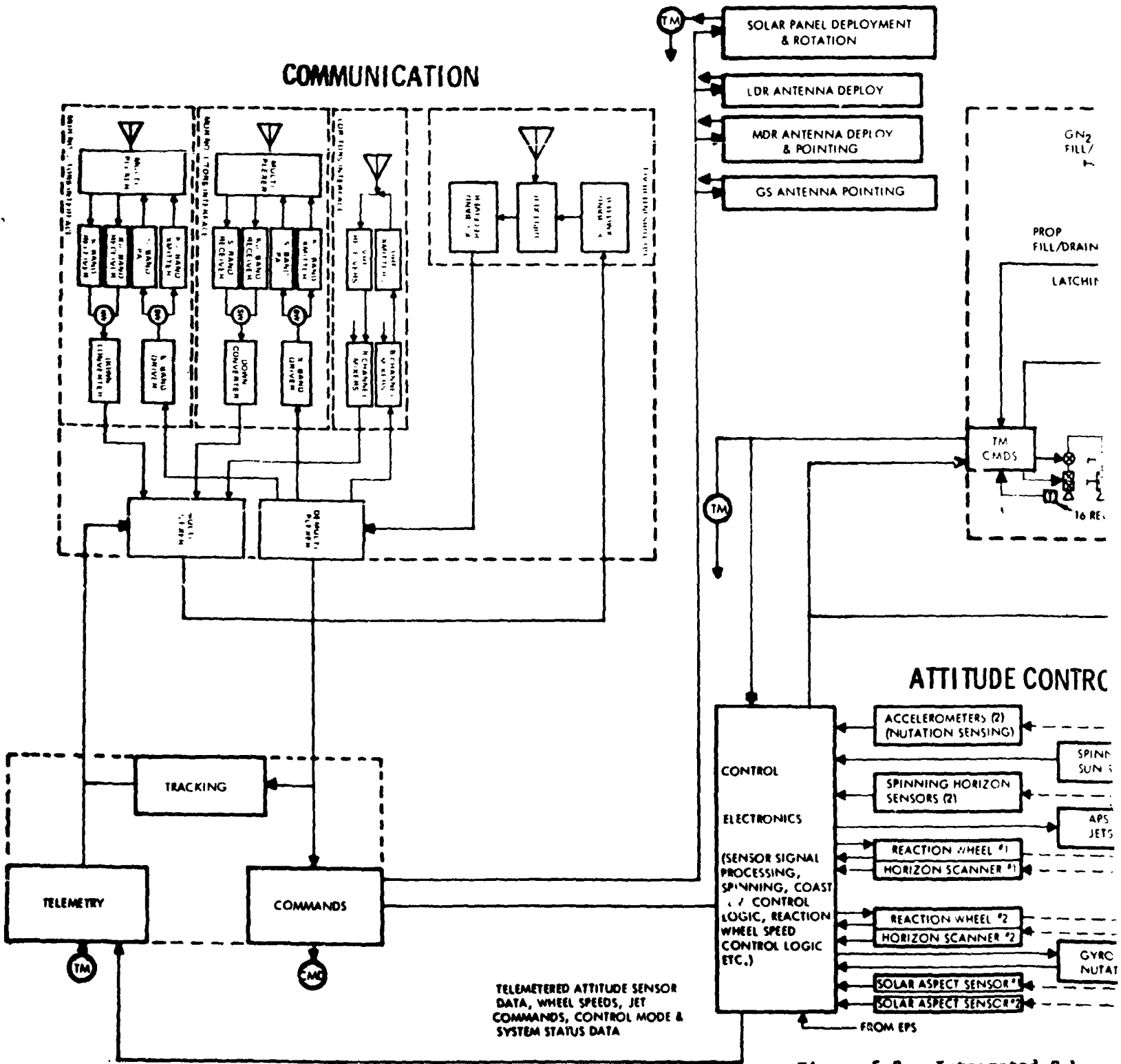
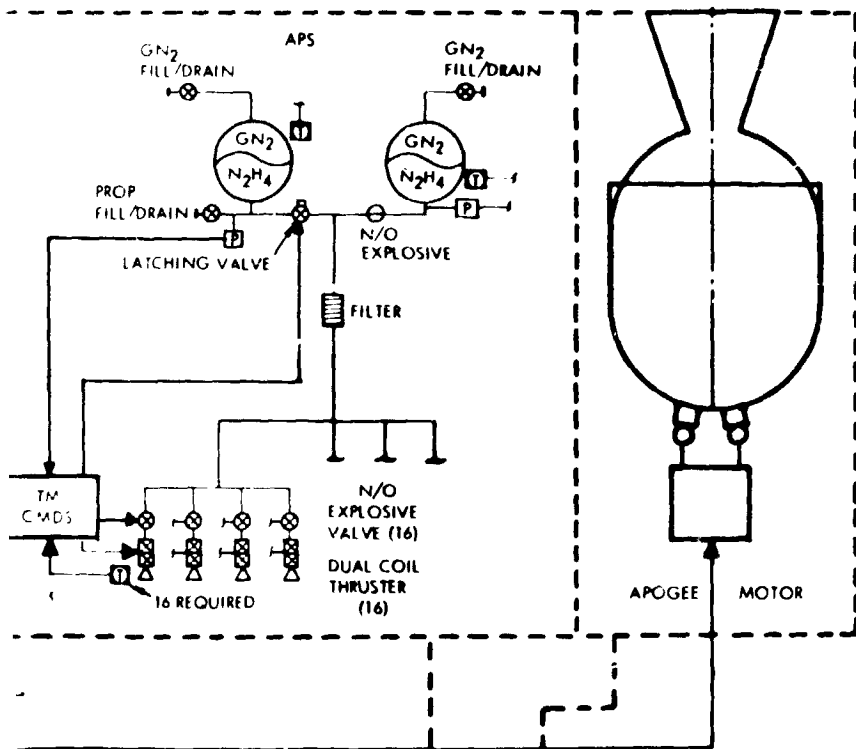
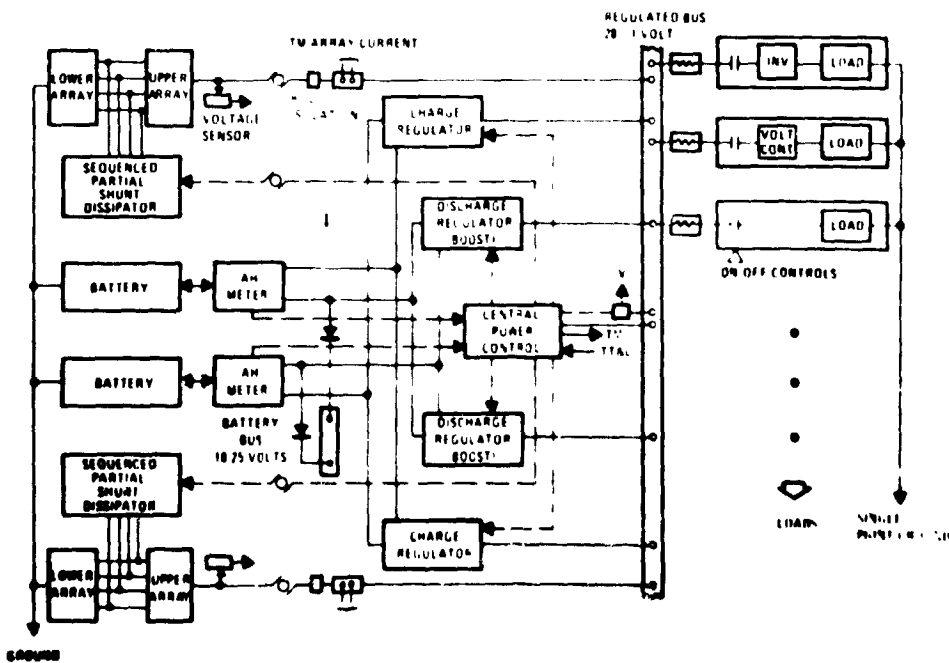


Figure 5-8. Integrated Subsystems

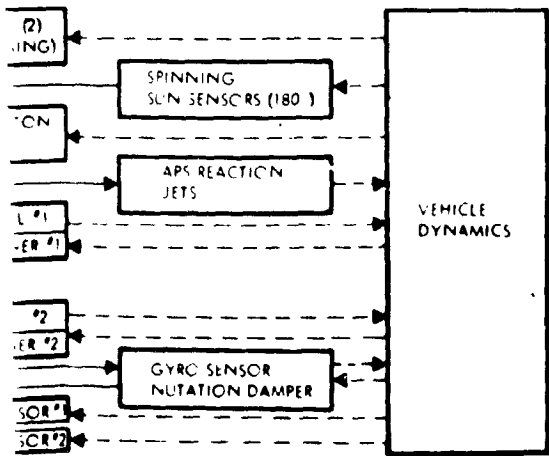
PROPULSION



ELECTRICAL POWER



MODE CONTROL



rated Subsystem Block Diagram

6.0 ATTITUDE STABILIZATION AND CONTROL SUBSYSTEM (ASCS)

The ASCS system performance requirements were determined, the disturbance torques evaluated, system mechanization trade studies performed and the baseline system defined. The selected three axis baseline system employs two momentum wheel/horizon scanner assemblies in a "V" configuration and a gas bearing gyro capable of performing the dual functions of a yaw sensor and back-up nutation damper. This system was selected over the other approaches primarily because its freedom from single point failures gives it an appreciable reliability advantage. Spin stabilization using flight proven control techniques is used during the transfer orbit and apogee motor firing. All baseline system components are existing flight qualified hardware with the exception of the horizon scanners which must be modified to operate at synchronous attitudes.

6.1 PERFORMANCE REQUIREMENTS

The ASCS performance requirements are summarized in Table 6-1. These requirements are divided into the spin stabilized mission phase and the 3-axis stabilized phase. More detailed discussion of the functional requirements, the pointing accuracy requirements, the momentum storage subsystem requirements and the auxiliary propulsion system requirements imposed by attitude control system functions are treated below.

Table 6-1. ASCS Performance Requirements Summary

<u>Spinning Phase</u>
Functional--Spin stabilized about minor axis, requires active nutation control, spin vector precession control, attitude determination and despin.
Active Nutation Control (ANC)--
Modes - Onboard Automatic + Ground Command Backup
Sense nutation as small as 0.1 deg (1.7 mrad) and to 5% accuracy at 1.0 deg (17.0 mrad)
Control nutation to less than 0.3 deg (5.2 mrad)
Nutation divergence time constant with ANC disabled-- less than 5 hours
Precession Control--Slew from TOI to SOI attitude in < 3 hours and provide spin vector attitude control errors < 0.1 deg (1.7 mrad)
Attitude Determination System--Accuracy = ± 0.2 deg (3.5 mrad) at SOI attitude, ± 1.0 deg (17.0 mrad) at any other attitude

in Figure 6-1. The numerical data is given as the total angular error except where denoted as "per axis." The upper box contains the dominant error contributions to the S/C attitude determination (i.e., errors in the knowledge of the S/C attitude). The box on the lower right contains the remainder of the error contributions to the MDR beam pointing accuracy. The budgeted MDR beam pointing accuracy of 0.447 degrees (7.8 mrad) is less than the TDRS statement of work requirement which specifies a pointing accuracy less than one-half beamwidth and an antenna beamwidth greater than one degree (.017 rad).

In the left hand box of Figure 6-1 the long term control errors are added to the attitude determination errors to yield the total pointing error of the S/C body axes. The long term control error is defined as the portion of total S/C pointing error which can be sensed and compensated for in pointing the MDR antennas. The two items which constrain this pointing accuracy are: (1) the additional MDR antenna boom length required to obtain an optically clear field of view past the LDR antenna structure and (2) the power loss of the LDR antenna when it operates in the fixed beam mode (a failure mode). One degree (.017 rad) of pointing error is budgeted as a compromise between these items and the increased weight of the ASCS to achieve tighter pointing accuracy requirements.

6.2 DISTURBANCE TORQUES AND MOMENTUM STORAGE REQUIREMENTS

The dominant disturbance torques influencing attitude control are solar pressure (long term) and antenna slewing torques (short term). The analysis defining the magnitudes of these torques and their impact on the momentum storage subsystem sizing is defined.

6.2.1 Solar Pressure Torques

An NR digital program was utilized to determine the effects of solar pressure disturbance torques. The program includes an improved solar pressure model from GSFC. The details of the analysis including the solar pressure model, the spacecraft representation and discussion of the results are presented in Appendix 6-A. Considerable data on the major components of the spacecraft is also presented to permit extrapolations for future design changes.

A summary of the momentum storage requirement due to solar pressure torques is presented in Table 6-2. Plots of the solar pressure moments (SUM-M) and angular momentum resolved into S/C body coordinates (H-B) for the total spacecraft (design case) are presented in Figure 6-2. The offset of center of pressure from center of mass is the dominant contributor to the secular momentum buildup. An MDR antenna "windmilling" situation is defined which significantly increases the momentum storage requirements. The nominal baseline S/C configuration is well balanced with respect to solar torques and a special case was devised to obtain conservative design conditions. Design techniques to minimize the torques are discussed in Appendix 6A. The momentum storage capacity required is obtained by adding the delta due to antenna "windmilling" to the design S/C case yielding the "total" values in Table 6-2.

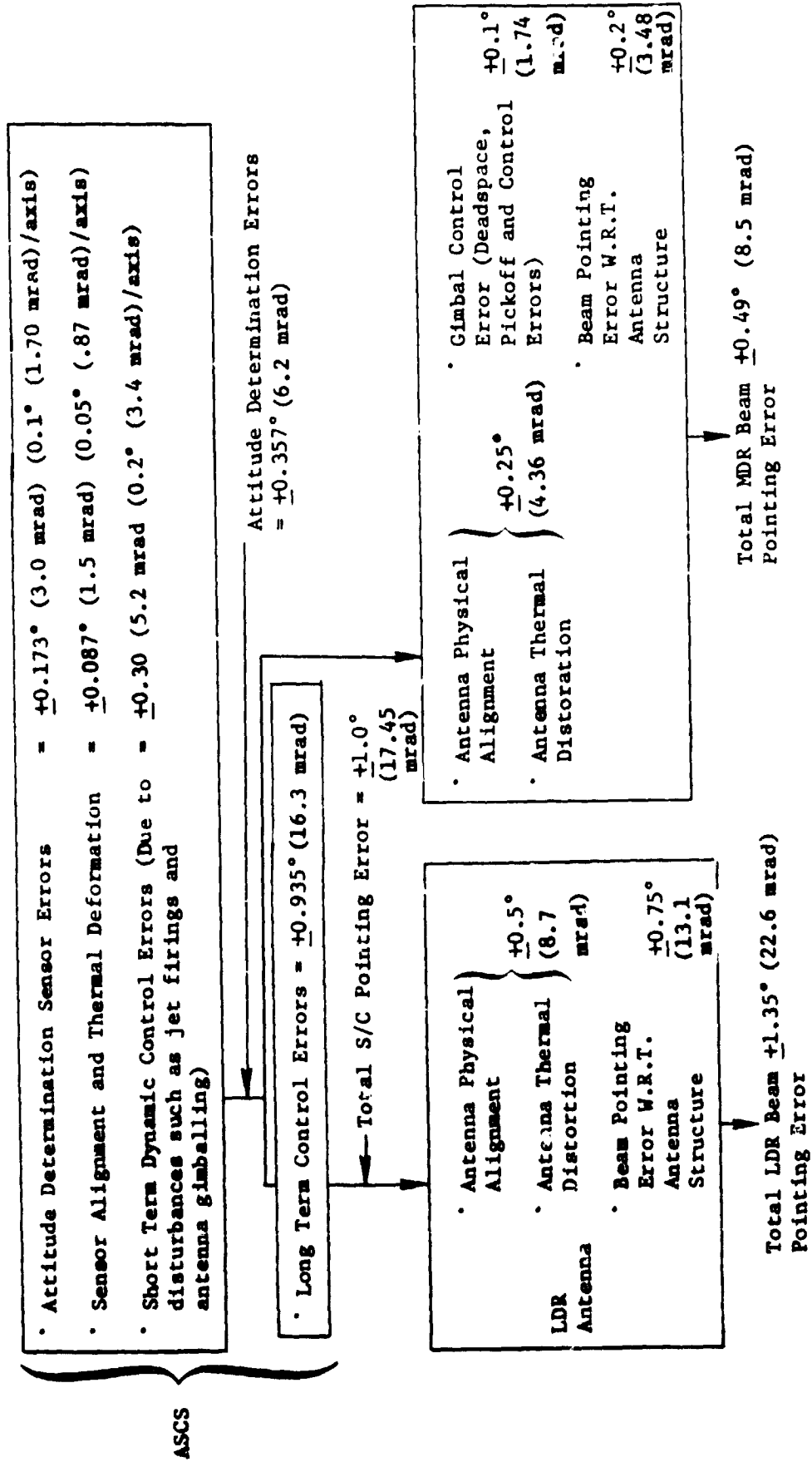


Figure 6-1. Attitude Determination and Pointing Accuracy Budget

Table 6-2. Summary of Momentum Requirements due to Solar Pressure Torques

Maximum Cyclical Variation per Orbit		Secular Growth Per Orbit		Configuration	
ft-lb-sec (kg-m ² /sec)					
$\pm\Delta H_{XB}$	$\pm\Delta H_{YB}$	$\pm\Delta H_{ZB}$	$\pm\Delta H_{XB}$		
(0.027) 0.020	(0.049) 0.036	(0.025) 0.015	(-0.016) -0.012	Total Spacecraft	Nominal S/C ($Z_{CG} = 25$ in. (63.5 cm) and $Y_{CG} = 0$)
(0.056) 0.041	(0.105) 0.077	(0.042) 0.031	(-0.016) -0.012		S/C with $Z_{CG} = 19$ in. (48 cm) and $Y_{CG} = 0$
(0.104) 0.076	(0.105) 0.077	(0.079) 0.058	(-0.127) -0.092		S/C with $Z_{CG} = 19$ in. (48 cm), $Y_{CG} = 0.6$ in. (1.5 cm) (momentum storage design cond.)
(0.123) 0.009	(0.177) 0.013	(.0085) 0.0062	(-0.016) -0.012	Spacecraft Components	Main body
(0.093) 0.068	(0.185) 0.136	(0.071) 0.052	0 0		LDR antenna
(0.035) 0.026	(0.074) 0.054	(0.030) 0.022	0 0		MDR antenna
(0.068) 0.050	(0.105) 0.084	(0.071) 0.052	0 0		Delta due to MDR antenna "windmilling"
(0.0072) 0.0053	(0.026) 0.019	(0.0071) 0.0052	0 0		
(0.172) 0.126	(0.220) 0.161	(0.150) 0.110	(-0.125) -0.092	Total (design cond. + "windmilling")	
*Secular ΔH_{YB} and $\Delta H_{ZB} = 0$					

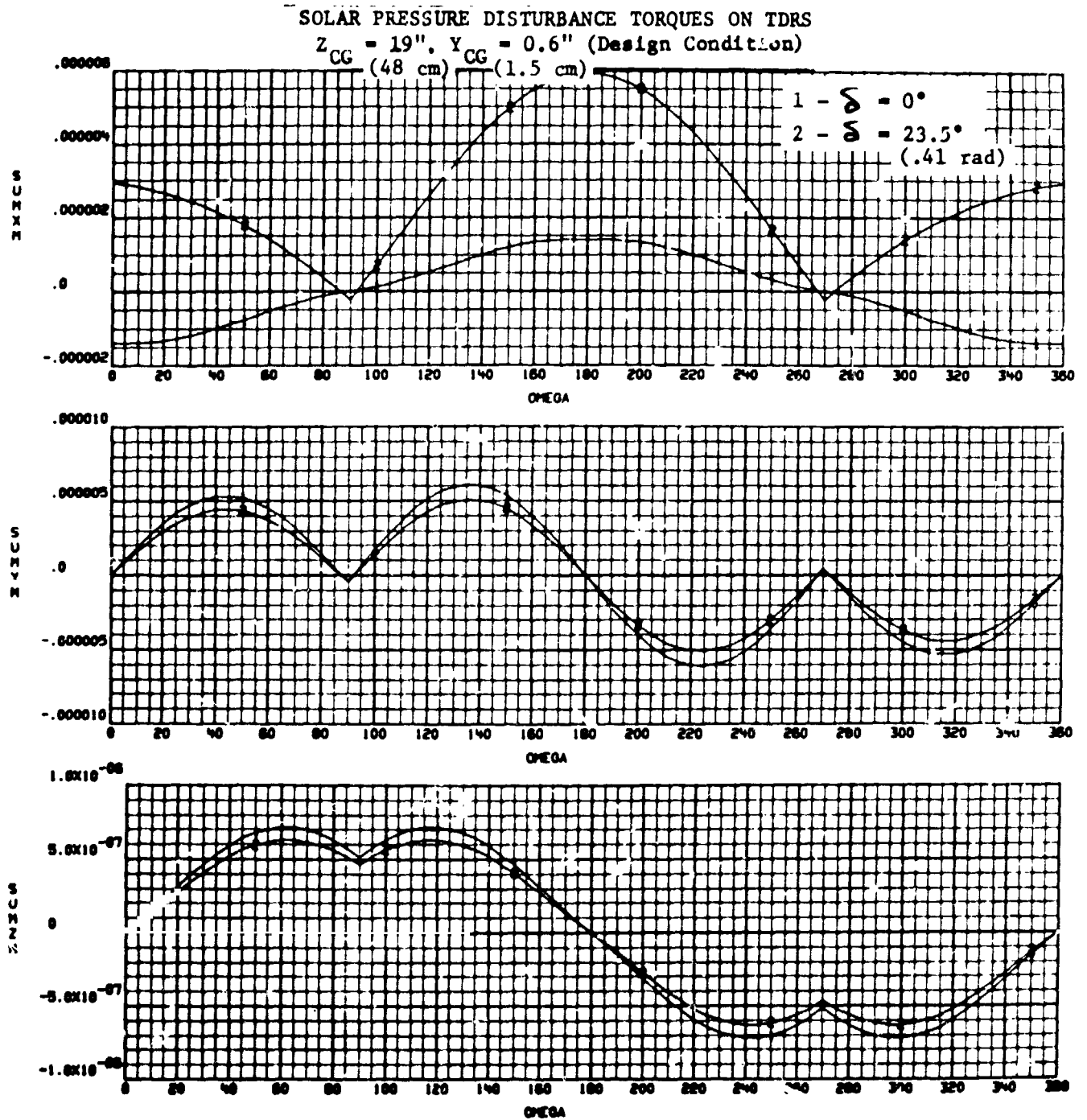


Figure 6-2a. Solar Pressure Disturbance Histories

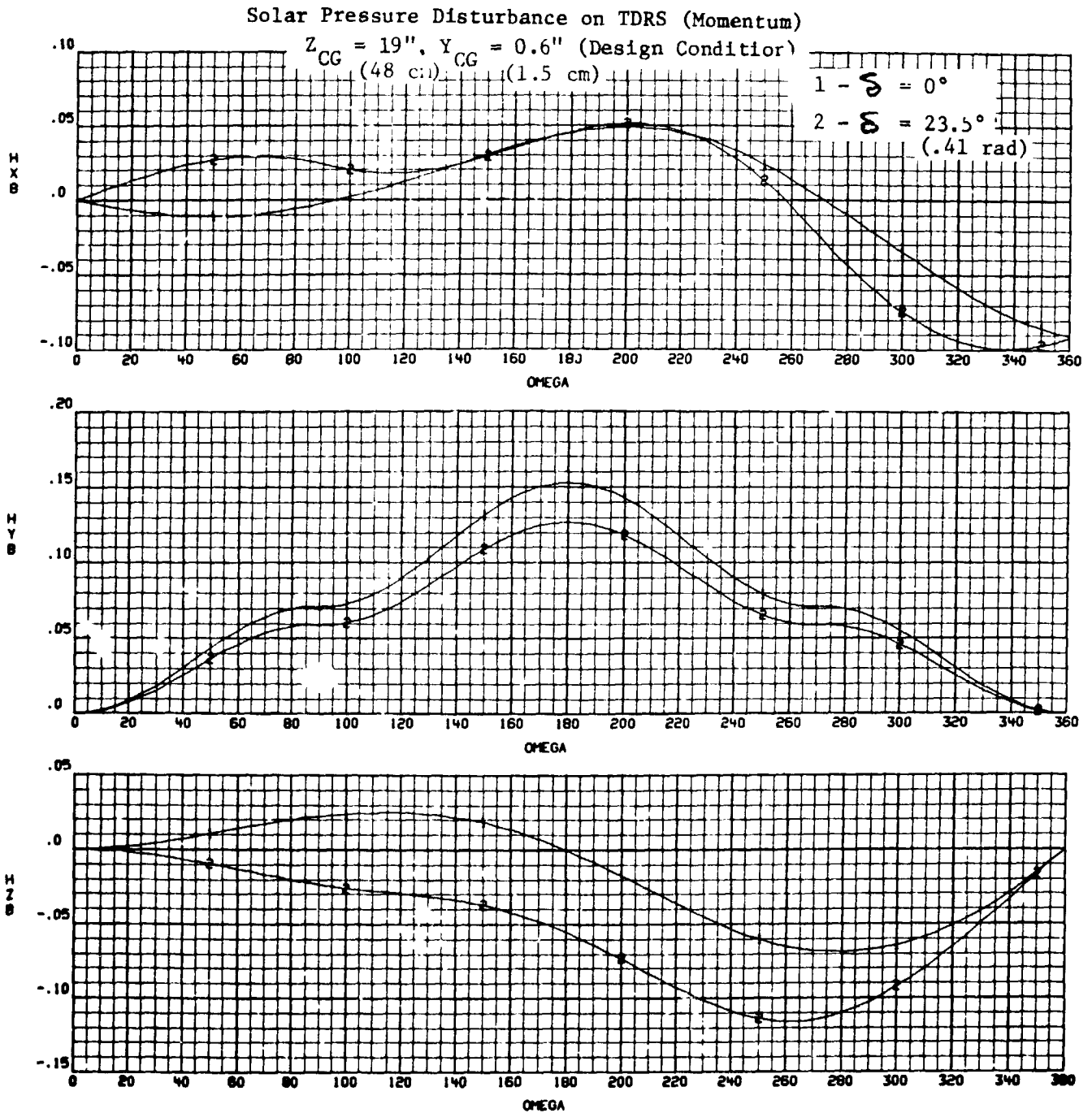


Figure 6-2b. Solar Pressure Disturbance Histories

6.2.2 Antenna Gimbaling Disturbances

A three degree-of-freedom digital simulation program was developed with in-house funding to simulate the "V" momentum bias control system concept. This digital program was thoroughly checked out and verified by an analog simulation and a hardware air bearing table evaluation in which two momentum wheels were mechanized in a "V" configuration. Excellent correlation resulted in both cases.

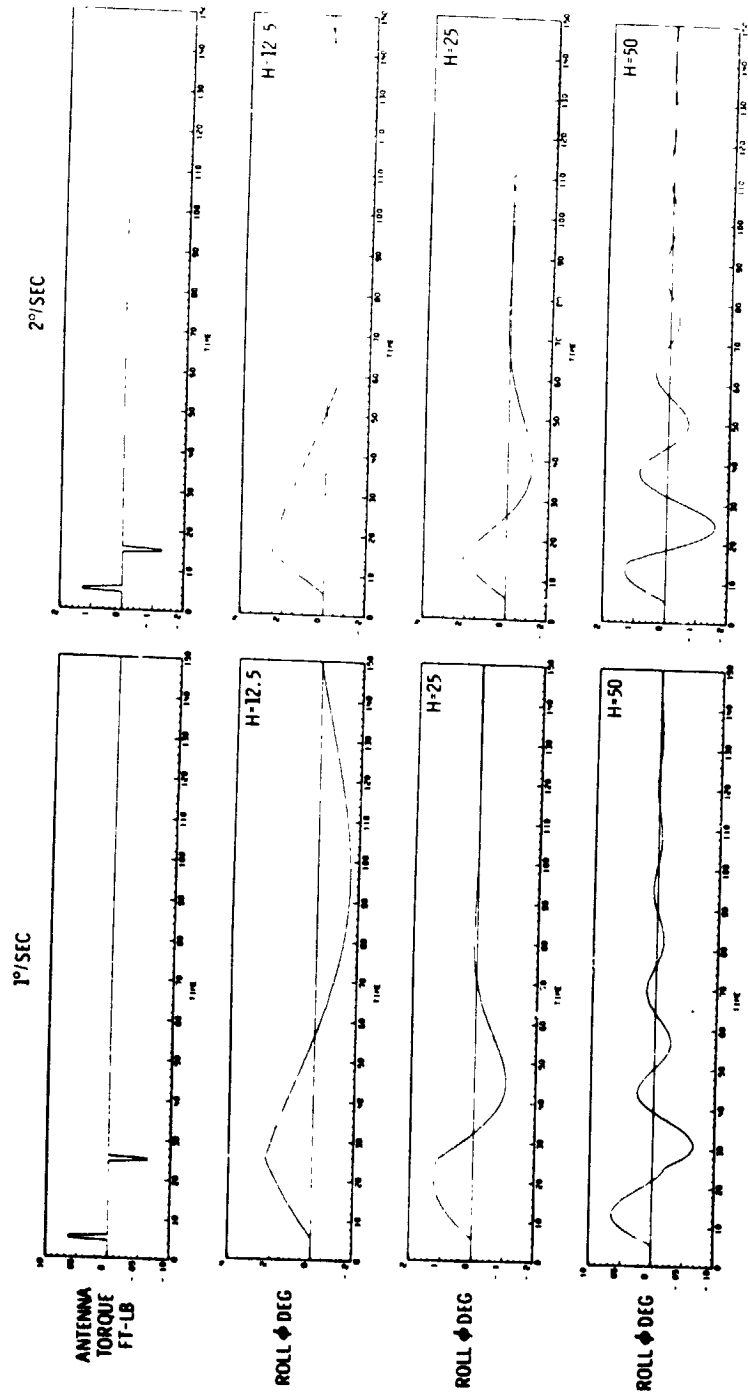
This digital program can insert antenna disturbance torques. The antenna disturbance simulation quantifies the roll and yaw transient errors and the momentum and torque values necessary for active nutation damping. No attempt was made at this time to optimize the control system gains or compensation network parameters.

The maximum antenna gimbal rate is one degree per second, and its moment of inertia is 3.61 ft-lb-sec² (4.91 kg-m²). The maximum transferable momentum is 0.063 ft-lb-sec (.085 kg-m²/sec). If this transferable momentum is introduced into the spacecraft about the X-axis (antenna roll gimbal motion) the steady-state roll error of the momentum bias ASCS [$H_B = 12.5$ ft-lb-sec (17.1 kg-m²/sec)] is 0.29 degrees (5.05 mrad). The ASCS does not reach the steady-state pointing error during an antenna reorientation maneuver. This is demonstrated in the simulated data in Figures 6-2a and 6-2b which show the spacecraft transient responses to a 20-degree (.35 rad) antenna reorientation about the roll axis at one (.017 rad) and two degrees (.034 rad) per second slew rates. For a momentum bias of 12.5 ft-lb-sec (17.1 kg-m²/sec) and a maximum antenna slew rate of one degree (.017 rad) per second the maximum transient roll attitude error is 0.2 degree (3.48 mrad) which meets the budgeted short-term control pointing accuracy requirement (0.2 degree) (3.48 mrad). Also, for this case a momentum transfer of 0.14 ft-lb-sec (0.19 kg-m²/sec) into the axis normal to the momentum bias is sufficient for nutation damping and a torque level of less than 0.001 ft-lb (.0136 m-newt) is adequate to obtain the necessary nutation damping response for this disturbance.

6.2.3 Momentum Storage Requirements

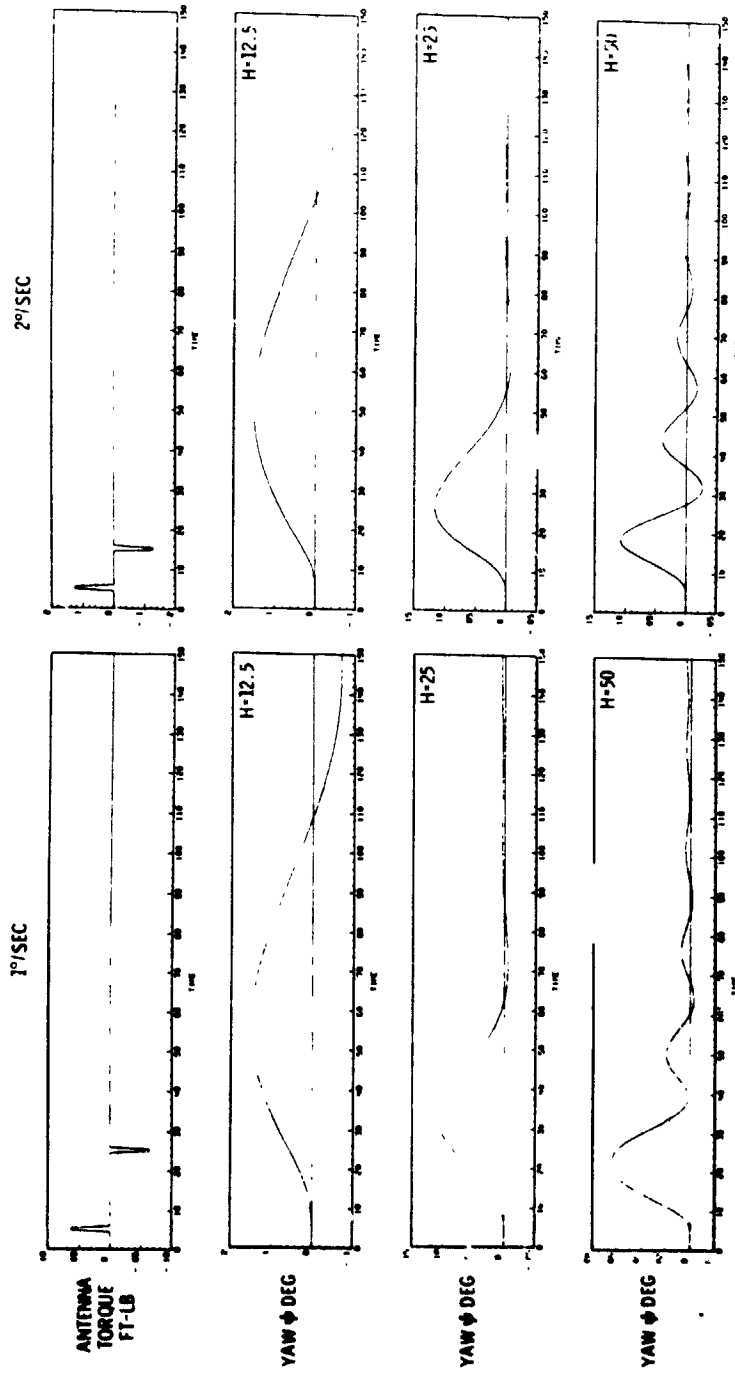
MDR antenna gimbaling produces roll, pitch and yaw attitude errors. As shown above, the 0.2° (3.48 mrad) per axis pointing accuracy budget is met with a system having a momentum bias of 12.5 ft-lb-sec (17.1 kg-m²/sec). Figure 6-3 presents attitude error versus momentum bias for several values of cross axis angular momentum. This curve assumes a pure momentum bias system without active roll control to remove roll error. The data indicate that for a ΔH_z induced by solar pressure and a momentum bias of 12.5 ft-lb-sec (17.1 kg-m²/sec) the roll attitude error will be approximately 0.5° (8.7 mrad). This meets the 0.935 degree budget for the long-term pointing error.

On the basis of the above analysis, the following momentum storage subsystem requirements were adopted:



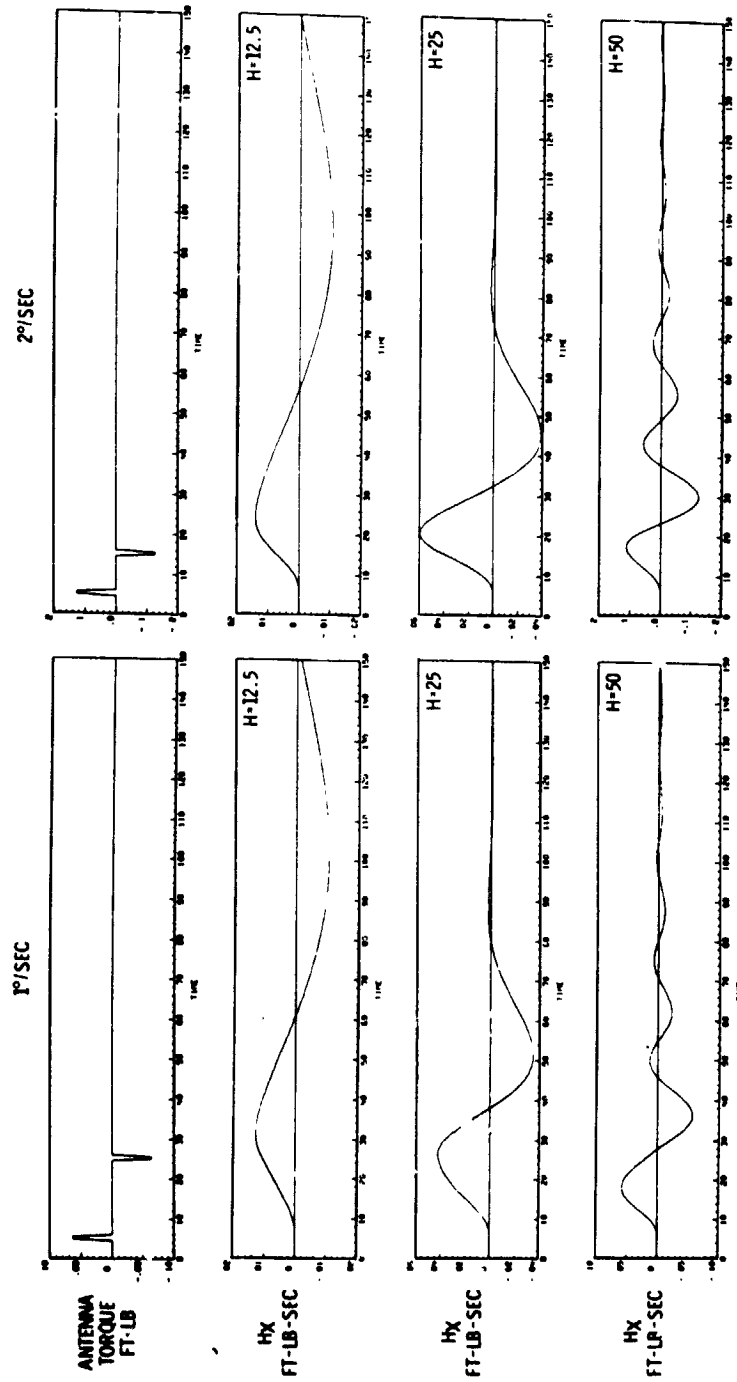
(a) ROLL ANGLE DEVIATION DUE TO MDR ANTENNA MOTION (20° DISPLACEMENT)

Figure 6-3a. Attitude Error Versus Momentum Bias



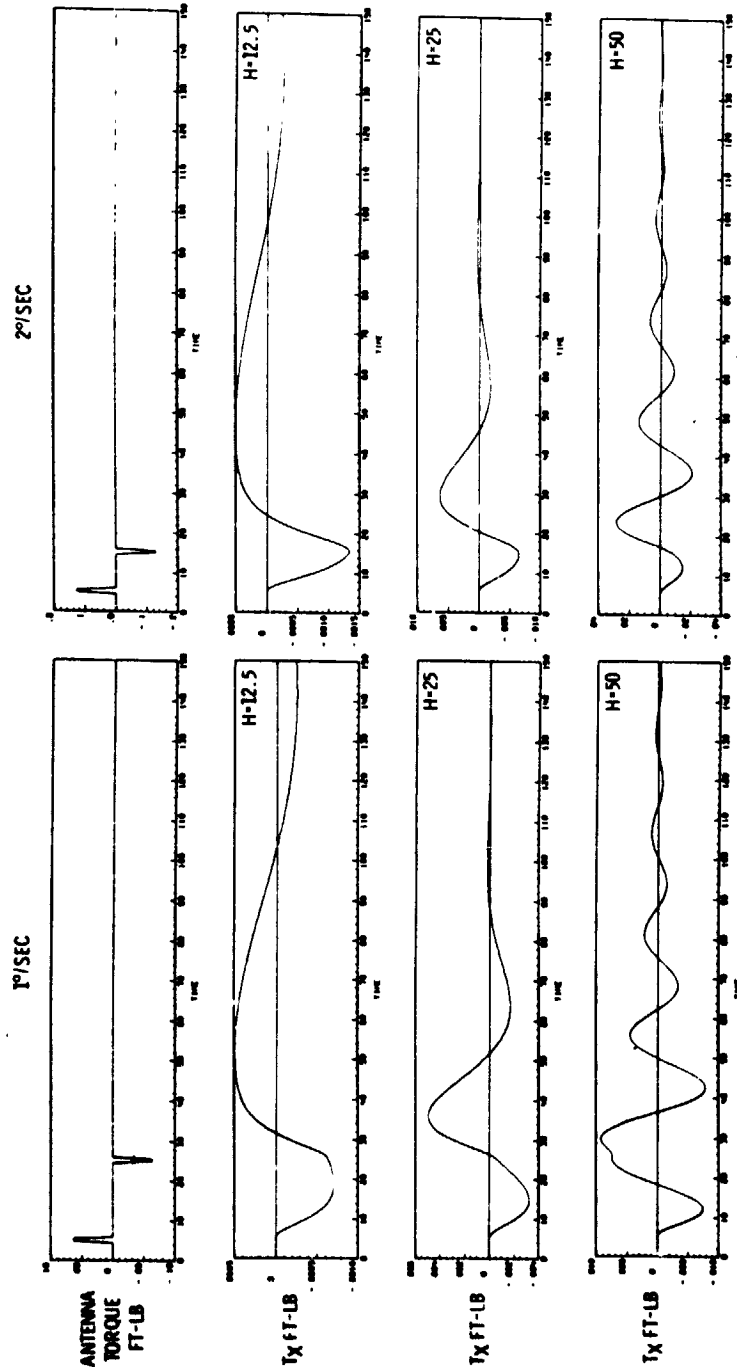
(b) YAW ANGLE DEVIATION DUE TO MDR ANTENNA MOTION (20° DISPLACEMENT)

Figure 6-3b. Attitude Error Versus Momentum Bias



(c) MOMENTUM REQUIRED FOR NUTATION DAMPING (20° ANTENNA DISPLACEMENT)

Figure 6-3c. Attitude Error Versus Momentum Bias



(d) TORQUE REQUIRED FOR NUTATION DAMPING (20° ANTENNA DISPLACEMENT)

Figure 6-3d. Attitude Error Versus Momentum Bias

$$\begin{aligned} H_{Y \text{ bias}} &= 12.5 \text{ ft-lb-sec (17.1 kg-m}^2\text{/sec)} \\ \Delta H_X &= \pm 0.02 \text{ ft-lb-sec (.027 kg-m}^2\text{/sec)} \\ \Delta H_Y &= \pm 0.25 \text{ ft-lb-sec (.34 kg-m}^2\text{/sec)} \\ \Delta H_Z &= \pm 0.2 \text{ ft-lb-sec (.27 kg-m}^2\text{/sec)} \end{aligned}$$

These requirements are adequate for active pitch and roll control, passive yaw control, active nutation damping, and momentum dumping less frequently than once per day.

6.3 SYSTEM MECHANIZATION TRADE STUDIES

The system synthesis trade studies are divided into the transfer orbit and deployment phase, operational phase momentum storage subsystem trades and attitude determination sensor selection.

6.3.1 Transfer Orbit and Deployment Phase

The transfer orbit and deployment mission phase extends from booster separation until the S/C is 3-axis stabilized in synchronous orbit. The key trades are summarized below, and the basic reason for the selection is given:

- Spin versus 3-Axis Stabilization for Apogee Motor Firing--3-axis stabilization system mechanization (such as that employed on Burner II) requires heavier, more complex and costly ASCS gear. The Burner II type system weighs 26 pounds (11.8 kg) more than the baseline spin stabilized system.
- Nutation Sensing and Control Technique (see Figure 6-4)--Minor axis spinner with reaction jet torques and accelerometer nutation sensing selected on the basis of lowest weight, cost and proven technology.

The use of a solid apogee motor facilitates the selection of spin stabilization for thrust vector control during synchronous orbit insertion. Despinning the S/C and providing 3-axis stabilization during the transfer orbit would save a small amount of propellant due to the rather large propellant requirement to precess the spinning S/C from the transfer orbit insertion attitude to the synchronous orbit insertion attitude. However, the system and operational complexity favors the use of spin stabilization during the entire transfer orbit.

The nutation control mechanization trades are depicted in Figure 6-4. Spin about a major axis of inertia is desirable because it is the stable spin axis. The alternative methods of achieving this are:

- Natural Major Axis Spinner--The slender booster shroud dimensions make it impractical to package the S/C with a minor spin axis.
- Deploy Booms--Not competitive weight-wise.
- Convert Spin from Minor to Major Axis--The structure required to support the apogee motor horizontally on the booster imposes an excessive weight penalty.

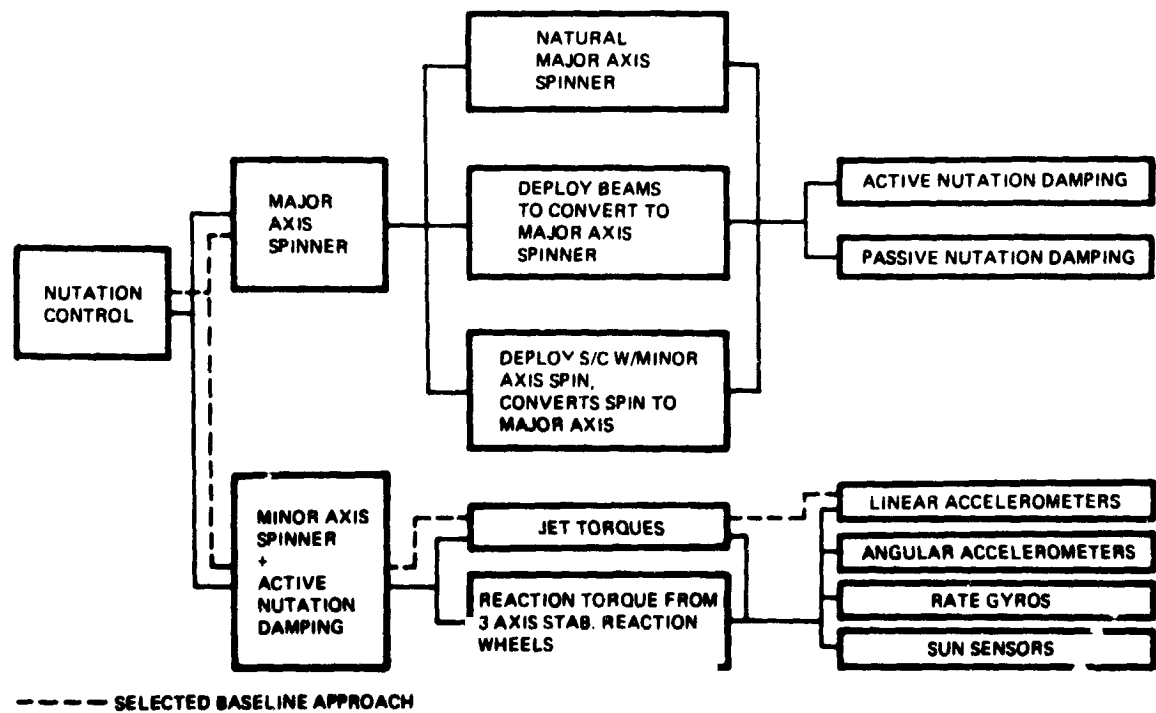


Figure 6-4. Spin Stabilized ACS Configuration Trades: Nutation Control

With the minor axis spinner the momentum wheels used in the 3-axis ASCS might be considered for active nutation damping. However, the reaction jets are used for this purpose since the propellant required is small.

Linear accelerometers are selected for the nutation sensing on the basis of lowest cost and this approach has been developed and demonstrated. Angular accelerometers are functionally more attractive but more costly. The use of sun sensors for nutation sensing is attractive since they can also be utilized for attitude determination. However, the control logic requirements will be significantly more complex than for the accelerometer system. This logic could be mechanized at the ground station but nutation damping operations cannot be conducted when the S/C is out of sight of a ground station.

6.3.2 On-Orbit Phase Torquer and Momentum Storage Subsystem Trades

The current level of 3-axis stabilization and control system technology provides several potentially viable techniques and hardware mechanization approaches. The ASCS synthesis problem, therefore, becomes one of selecting the approach best satisfying the specific TDRS requirements.

The trade study evaluation factors considered in the ASCS trades are listed according to their relative importance:

1. Reliability
2. Cost
3. Weight
4. Power
5. Performance (assuming the requirements can be met)

The attitude control torque source candidates considered for TDRS and the associated trade study logic are presented in Figure 6.5. The torque sources include the internal momentum storage/transfer devices and the external torque sources such as reaction jets. Each trade study branch in the logic diagram is numbered and the trade study methodology is presented below in the following order:

Momentum Transfer Devices Versus None
Momentum Bias Versus None
Momentum Dumping
Momentum Bias plus Transfer

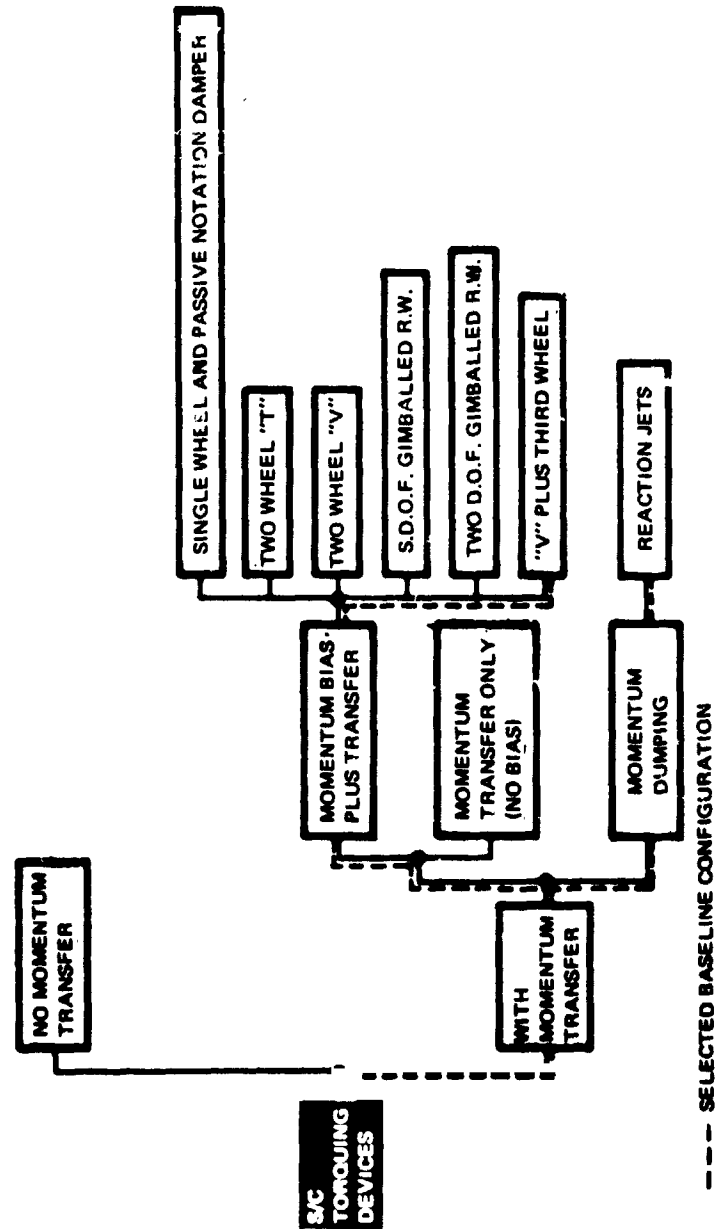


Figure 6-5. ASCS Torquer Trades

The first trade study showed that momentum transfer devices are required to prevent the antenna gimbaling disturbances from consuming excessive RCS propellant. Momentum compensation devices on the antennas themselves were not considered since these are new development items, they would not handle the cyclical solar disturbance torques, and the reaction wheel systems being considered are relatively efficient momentum compensation devices in themselves.

The second trade study concluded the weight penalty required to achieve a momentum bias system is a small penalty to incur for the elimination of active yaw sensing and control during coasting flight phases.

The third trade study is the key trade in the ASCS torquer selection and required each candidate system to be sized to the TDRS requirement. The candidate configurations in the trade study are pictorially illustrated in Figure 6-6 and their control capability briefly summarized in Table 6-3.

All of the ASCS torquer concepts in Figure 6-5 employ some form of reaction wheels. Several existing flight-qualified reaction wheels are available in the momentum range required for TDRS (< 10 ft-lb-sec) (13.6 kg-m²/sec). Figure 6-7 shows the weight for several Rendix reaction wheels. The slope of the curve is small in the region about 5 ft-lb-sec (6.8 kg-m²/sec). The penalty for conservatively sizing the reaction wheels for larger momentum than required is small, providing that appropriate reaction wheels are available in that size range. The attribute of the conservative approach is that the design becomes insensitive or unaffected by any feasible variations in predicted disturbance torques.

The passive damper system is not considered competitive since it must be relatively heavy and sophisticated to obtain adequate damping. Since antenna gimbaling disturbances will occur at frequent intervals a nutation damping time constant of less than a minute is desirable rather than one or many minutes. The nutation frequency with the momentum wheel size selection is too low for practical passive damper design.

Table 6-4 presents comparative weight, power and cost for the alternative concepts each of which meet all performance requirements. Data for the single gimbal system may be extrapolated from the data for the two-gimbal system. The "T-gyro" system differs from the "T" system in that it utilizes the G-6C gyro in the dual function of gyro and momentum transfer device. When the "V" system also uses this gyro in the same way it is converted to the "V Plus 1". The "T-gyro" system is lighter and less expensive than the other approaches. Unfortunately, this system has two single point failure modes (wheel and gyro) which could cause mission failure. Similarly, the GRASP has single point failure modes in the reaction wheel and each gimbal drive system.

To assess the impact of these single point failures, reliability calculations were run on the "V Plus 1" system and the "T" gyro system. The "V Plus 1" system is the only one with no single point failures ($R = 0.962$) and barely meets the reliability apportionment of $R = 0.96$. The estimated "T" gyro system reliability is 0.833 demonstrating the impact of the two single point failure modes. The reliability diagrams and failure rates used

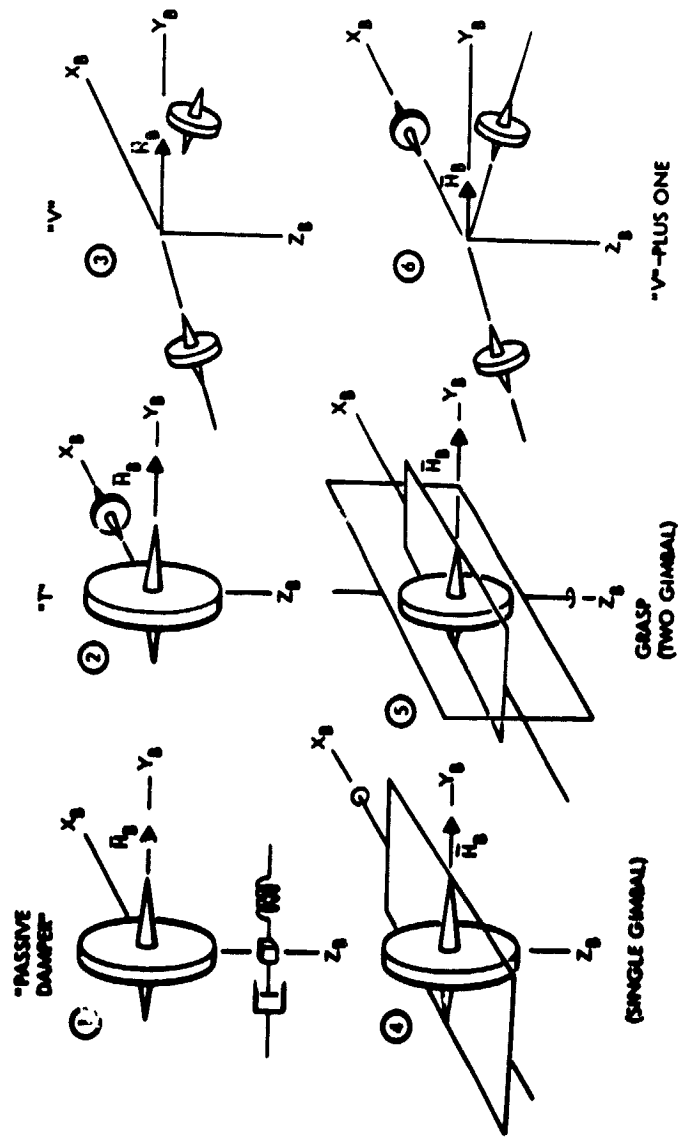


Figure 6-6. Momentum Storage Subsystem Configurations



Table 6-3. Control Available From Momentum Storage Subsystem Configurations

No.	Configuration	Control				Comment
		Nutation Damping	Roll	Pitch	Yaw	
1	Single R. W. with Speed Bias	Passive	Passive	Active	Passive	Poor Nutation Damping
2	Two R. W.'s, Large One Biased	Active	Active or Passive	Active	Passive	
3	Two R. W.'s, with Speed Bias	Active	Active or Passive	Active	Passive	
4	R. W. with Speed Bias and C.D.O.F. Gimbal	Active or Semi-Passive Gimbal Damper	Active or Passive	Active	Passive	
5	R. W. with Speed Bias and 2 D.O.F. Gimballing	Active	Active	Active	Active	Second gimbal unnecessary complexity for TDRS
6	Two R. W.'s in "V," Third R. W. Orthogonal to First Two	Active (Third wheel provides excellent damping)	Active	Active	Active	"Graceful" Performance Degradation in presence of wheel failures

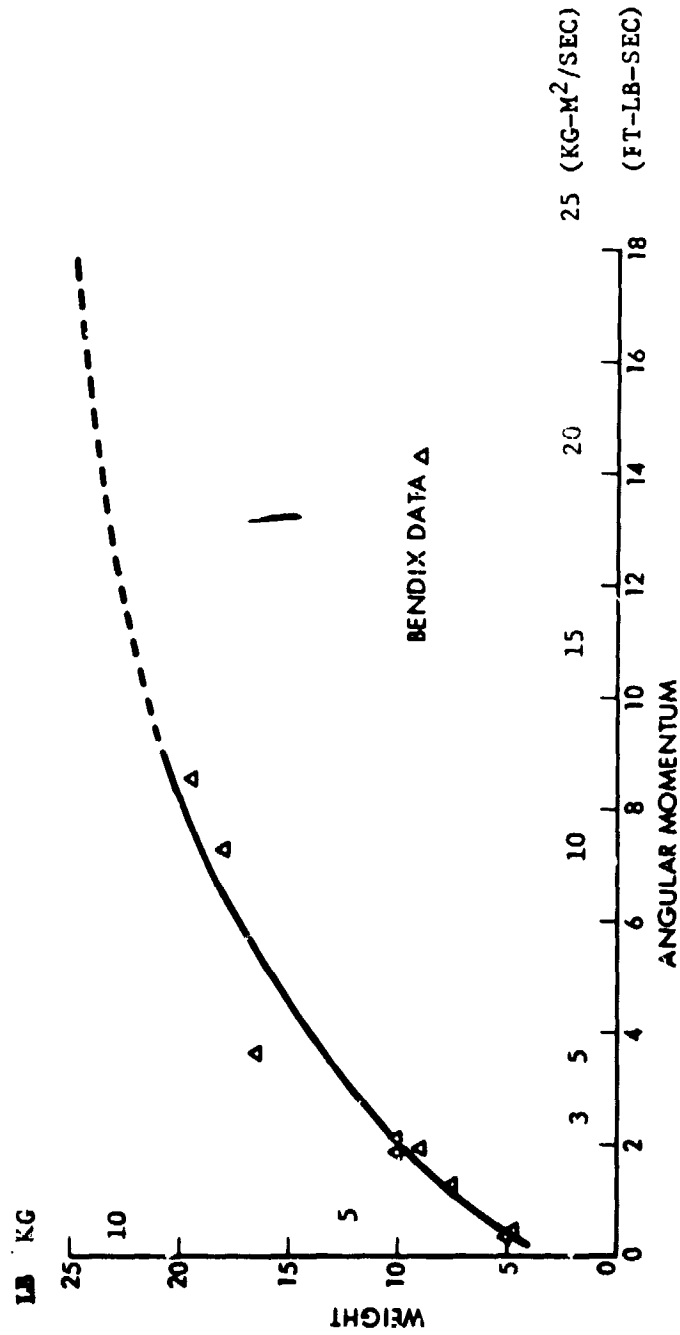


Figure 6-7 Reaction Wheel Weight

Table 6-4. Momentum Storage Subsystem Trade Data

Component	"T" (H = 12.6)			"V" (H = 12.6)			Grasp (H = 6.85)			T-Gyro (H = 12.6)		
	W lb (kg)	P (watts)	\$ (recur)	W lb (kg)	P (watts)	\$ (recur)	W lb (kg)	P (watts)	\$ (recur)	W lb (kg)	P (watts)	\$ (recur)
Momentum Wheel	19 (8.62)	4.4	50	14.3 (6.49)	3.9	50	10 (4.54)	3.5	30	19 (8.62)	4.4	50
Momentum Wheel	5 (2.27)	2	30	14.3 (6.49)	3.9	50	-	-	-	-	-	-
Horizon Sensor	-	-	-	-	-	-	10 (4.54)	8	150	-	-	-
Gyro	4.5 (2.04)	5	20	4.5 (2.04)	5	20	4.5 (2.04)	5	20	4.5 (2.04)	5	20
Electronics	12 (5.44)	8	100	12 (5.44)	8	100	12 (5.44)	8	100	12 (5.44)	5	75
Gimbals	-	-	-	-	-	-	8	10	25	-	-	-
Total	40.5 (18.37)	19.4	200	45.1 (20.46)	20.8	220	44.5 (20.19)	34.5	325	31.5 (14.29)	14.4	145

in these calculations are presented in Section 10. Flight and testing experience with reaction wheels (well over a million hours) with only one questionable failure indicates the reliability of these devices.

The "V plus one" configuration was selected for the baseline system as it has a substantial reliability advantage over the other systems and is the only one meeting the reliability goal.

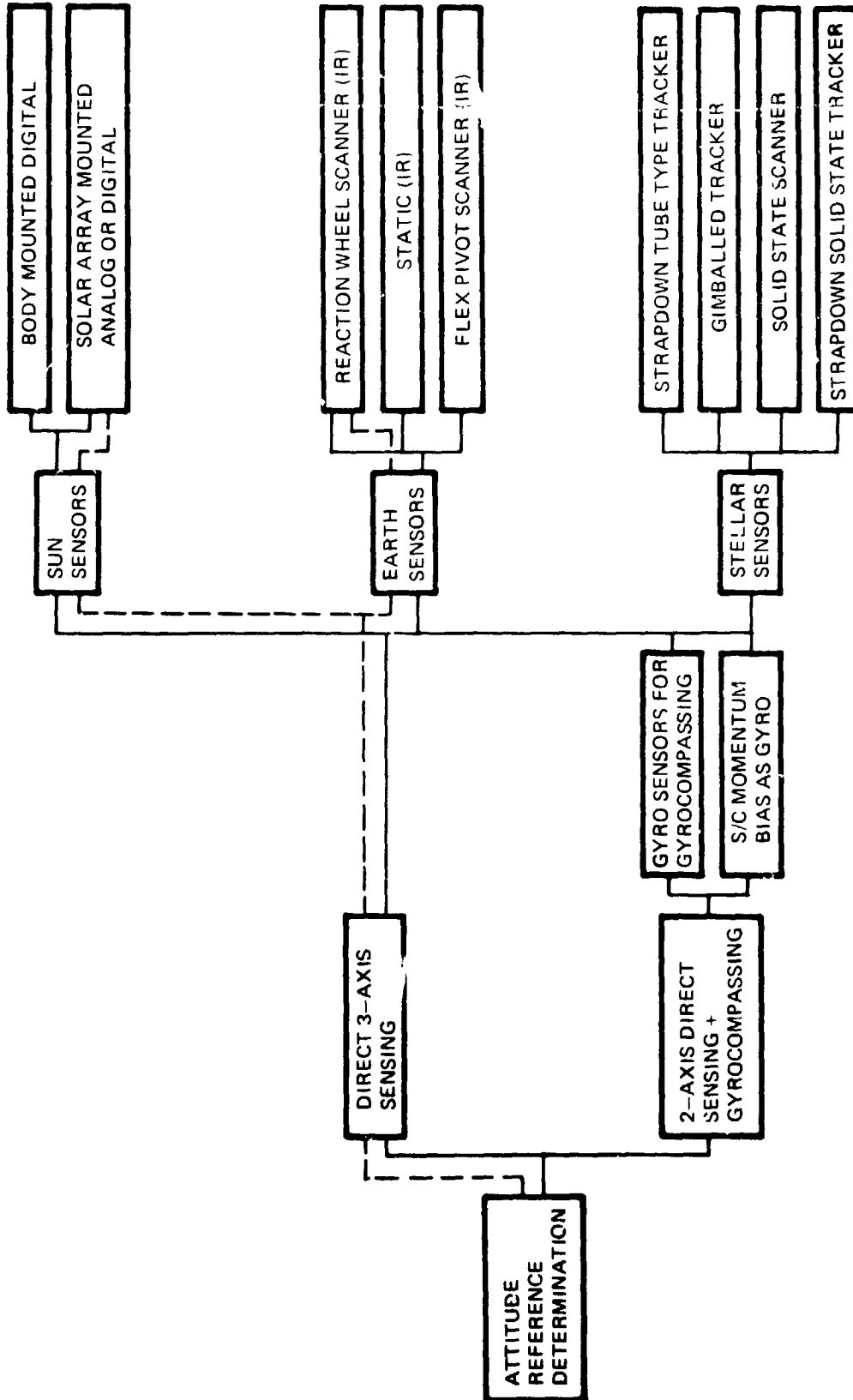
6.3.3 Attitude Determination Sensor Trades

A large family of space qualified sensors and techniques for attitude determination have been developed as indicated in Figure 6-8. "Direct 3-axis sensing" is selected over the "2-axis sensing plus gyrocompassing" for the baseline mode. This provides for faster and more accurate attitude determination updating following the attitude transients induced by antenna gimbaling disturbances. The gyrocompassing techniques have inherently long response time constants. A yaw gyro and small momentum bias incorporated into the baseline system for other reasons, permit both of the gyrocompassing techniques to be used for backup. The rationale for system selection is:

- Stellar Sensors--Polaris sensor is a good technique in principal but is expensive. Sensitive to stray light reflections from solar arrays.
- Earth Sensors--Reaction wheel scanned IR sensors are lighter and less expensive than the other IR techniques.
- Sun Sensors--The use of body mounted sensors requires an excessive number of sensors to obtain the required field-of-view due to the segmenting of the field-of-view by the antenna elements. The solar array mounting is therefore selected. Digital sensors are selected to provide accurate outputs through the required field-of-view (approximately $\pm 25^\circ$ (.436 rad) in yaw).

The major constraint in sensor selection is the need to obtain an adequate unobstructed field-of-view through the antennas and solar arrays. The selected baseline is the reaction wheel scanned horizon sensor providing pitch and roll information and the solar array mounted digital sun sensors providing pitch and yaw information. The horizon sensor data is used for onboard control and is telemetered for ground based attitude determination. Satisfactory operation can be achieved with a single sensor thereby providing redundancy. Redundant sun sensors are also provided. This data is only for ground based attitude determination. The sun sensor data facilitates the acquisition of the nominal attitude reference and also provides for rapid yaw updating in the attitude determination.

A wide bandpass yaw sensor is required for delta-V maneuvers and a gyro was selected for this purpose. The candidate gyro sensors considered are listed in Table 6-5. With conventional gyros reliability for a five year mission is a serious problem. The G-6C gas bearing gyro has the highest operationally proven reliability of any of the candidates as demonstrated in Tables 6-6 and 6-7. It is a two-degree of freedom gyro thereby enhancing



----- SELECTED BASELINE CONFIGURATION

Figure 6-8. Attitude Determination Subsystem Trades

Table 6-5. Yaw Sensing Gyro Candidates

Type	Supplier	Program	Units Produced
G6	NR	Minuteman	6000
K7	Northrop	C5A	600
GG334	Honeywell	ATS F&G Classified	100
GG134	Honeywell	Development	10
Alpha III	Singer-Kearfott	Development	10
Alpha II (Ball Bearing)	Singer-Kearfott	Mariner MVM 73 Viking Classified Others	1500

Table 6-6. G6 Gyro History--Minuteman

Program	Autonetics Recorded Gyro Run-Time	Gyro MTBF
Minuteman I	31,000,000 Hr	1,000,000
Minuteman II Block I	6,000,000 Hr	
Minuteman II Block II	2,000,000 Hr	
Minuteman III	2,800,000 Hr	

Table 6-7. Gyro and Momentum Wheel Comparison

Parameter	Units	G-6C	Bendix Wheel (Nimbus)
Weight	lb/kg	4.6/2.09	4.8/2.18
Power	watts	10	10
Momentum (max)	ft-lb-sec/ kg-m ² /sec	0.3/0.41	0.4/0.55
Torque	inch-ounce/ m-newt	2.0/0.014	2.0/0.014
MTBF	hour	1,000,000	100,000
Bearing type	--	Gas	Ball
Cost (recurring)	dollars	15K	30K

the system with additional pitch information. This gyro has the additional feature that its spin rate can be controlled through a reasonable range permitting its use as a momentum transfer device. Some of the characteristics of the G-6C compared with a Nimbus momentum wheel in Table 6-7. On the basis of these considerations the G-6C is selected for the baseline system.

For the spinning phase, body mounted (spin scanned) horizon sensors and digital sun sensors were selected. These sensors and the necessary computational algorithms were developed and used on several previous programs.

6.4 BASELINE SYSTEM DESCRIPTION

The baseline ASCS employs spin stabilization for the transfer orbit and synchronous orbit insertion (SOI). Shortly after SOI, the spacecraft is despun, stabilized about three axes, and maneuvered to acquire solar and horizon references. The performance requirements of the system are summarized in Tables 6-1 and 6-2. The spin stabilized and 3-axis-stabilized ASCS control modes are functionally independent and are described separately below. A functional flow diagram for the overall system is presented in Figure 6-9. The hardware component physical properties are summarized in Table 6-8. All components are existing flight qualified hardware with the exception of the horizon scanner assemblies which must be modified for operation at synchronous altitude.

6.4.1 Spin Stabilized Control Mode

The spin stabilized control mode requires active nutation control and the attitude precession maneuvers. These are functionally similar to those employed on previous spacecraft such as the ATS-V and make maximum use of previously developed spacecraft and ground station control hardware, technology, and operational procedures.

Table 6-8. TDRS ASCS Component Characteristics

	Dimensions inches (cm)	Power (Watts)		Weight lb (kg)
		Av.	Max.	
Mutation Sensing Accelerometers (2) (Sundstrand Data Control, Inc., PAL-5706)	2.3 x 1.7 x 1.2 (5.8 x 4.3 x 3.0)	2	2	0.6 (.27)
Spinning Horizon Sensors (2) (Barnes #13-210)	3.3 x 4.3 x 8 (8.3 x 10.9 x 20.3)	2.7	2.7	4.0 (1.8)
Spinning Sun Sensor (2) (Adcole #16765)	2.2 x 2.4 x 3.0 (5.6 x 6.1 x 7.6)	0.5	0.5	2.0 (.91)
Subtotal (Spinning)				6.6 (2.99)
Solar Aspect Sensors (2) (Adcole #15672)	3.7 x 3.8 x 0.9 (9.4 x 9.7 x 2.3)	0.5	0.5	4.5 (2.0)
Reaction Wheel/Earth Scanner Assemblies (2) (Ithaco/Bendix)	8.0 dia x 6.5 (20.3 dia x 16.5)	7	40	28.6 (13)
Electronics (NR)	10 x 5 x 6 (25.4 x 12.7 x 15.2)	8	45	12.0 (5.4)
Yaw Gyro & Nutation Damper (1)	5 x 6 x 6 (12.7 x 15.2 x 15.2)	5	10	6.0* (2.7)
Subtotal (Or-Orbit)				51.1 (23.1)
Total				57.7 (26.2)

* Including electronics

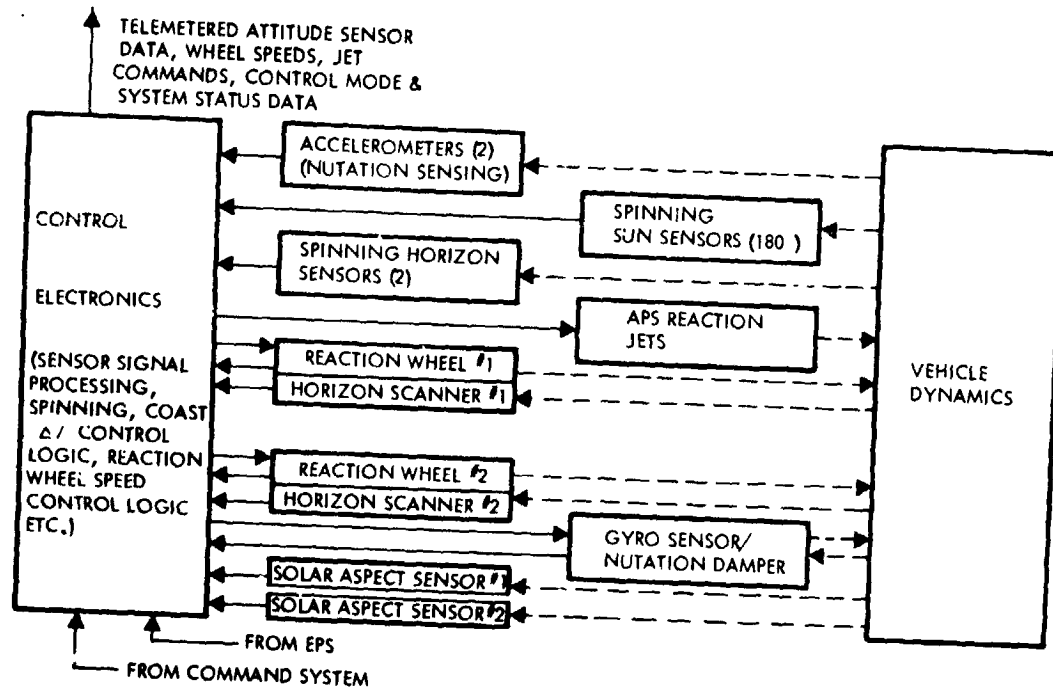


Figure 6-9. Attitude Stabilization and Control System

6.4.1.1 Active Nutation Control

Active nutation control (ANC) is required during the transfer orbit and apogee burn to correct nutation angle buildup. Nutation angle buildup can occur since spin is about a minor axis of inertia and, in the presence of energy dissipation sources, is unstable. The rate of nutation angle divergence is minimized through careful design of the TDRS subsystems to keep the energy dissipation at low levels. The dominant source of energy dissipation is the propellant motion.

An analysis of propellant sloshing effects on the stability of a spinning S/C was performed. Results obtained are presented in Appendix 6B. A "fluid-slug" propellant model for spherical tanks and the "energy sink" stability analysis technique were employed. The results indicate that the nutation divergence time constant will be greater than 80 hours for the assumed flight conditions. The analysis neglects the effects of the positive expulsion bladders and internal ridges in the tanks. The influence of these items on the stability is unknown and must be established. It is recommended that ground based tests of the energy dissipation due to propellant sloshing in these CTS tanks be performed in order to qualify their use for TDRS.

A functional block diagram of the ANC system is given in Figure 6-10. Nutation is sensed by a pair of linear accelerometers located near the outer periphery of the spacecraft and have sensitive axes parallel to the desired spin axis. Mounted in this fashion, the accelerometers provide outputs proportional to the angular acceleration about the transverse axes of the S/C.

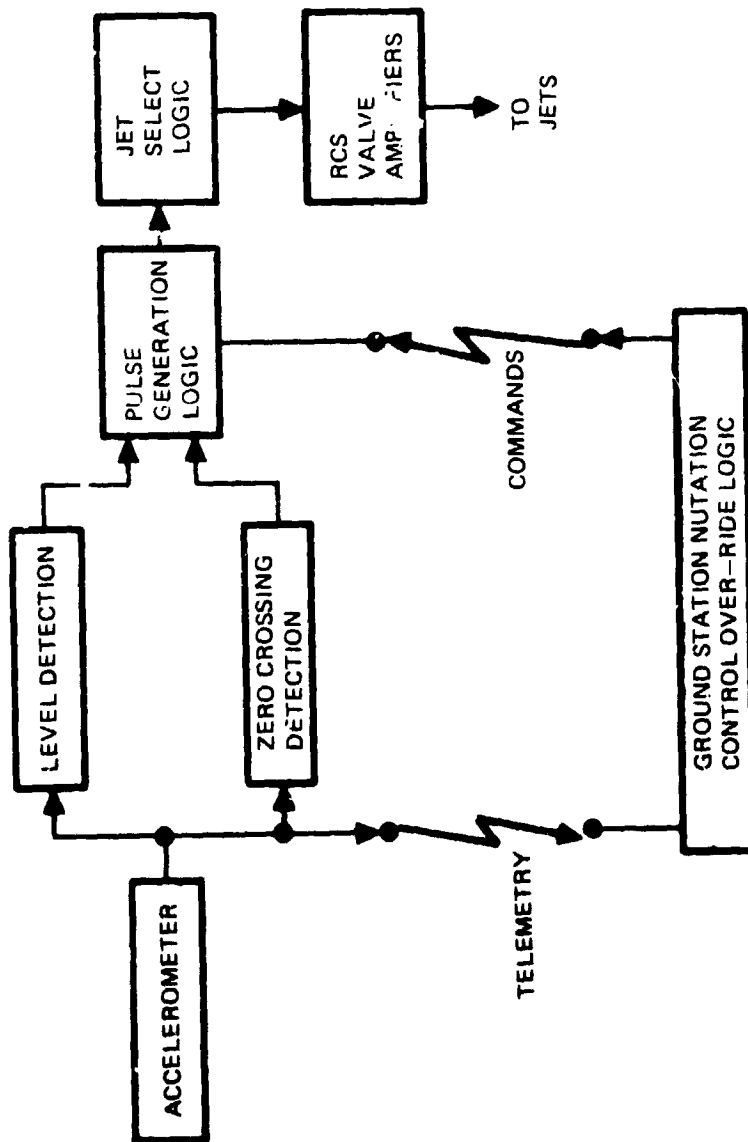


Figure 6-10. Active Nutation Control System Block Diagram

For given vehicle spin rates and inertia ratios, the nutation angle is proportional to the accelerometer outputs. As depicted in Figure 6-10 automatic ANC operation is initiated and cutoff by a level detector operating on the accelerometer signals. The jet pulses are phased at the proper place in the spin cycle by detecting the descending zero crossing of an accelerometer output. This crossing is easily detectable and defines when the transverse body rate is maximum about the sensed axis. The optimum time to apply jet pulses for rate damping is when the jet torque is parallel but opposite in sense from the body rate. The accelerometers are mounted along axes which are rotated slightly with respect to the body axes to compensate for the finite duration of the jet pulses. When enabled, the system provides automatic initiation of pulsing when the nutation angle exceeds approximately one degree and ceases operation when the nutation angle is below 0.3 degrees.

A ground over-ride ANC system is also provided and permits more flexible operation than is possible with the hardwired spacecraft ANC system. This system uses telemetered accelerometer data to determine the nutation amplitude and time phasing. The ground station control logic then generates the reaction jet pulse commands which are telemetered to the spacecraft and executed. The over-ride system compensates for the round trip signal transmission delays. The re-programmable control logic is particularly effective in adapting to off-nominal or unforeseen circumstances such as jet failures. This mode can reduce the nutation angle to less than 0.1 degree (1.745 mrad).

6.4.1.2 Attitude Precession

Re-orienting the spinning spacecraft to new attitudes requires precession control. This is achieved by commanding reaction jet torque pulses for approximately 60° (1.05 rad) of each spin cycle such that the time averaged torque produces precession to the desired inertial position. In the baseline reaction jet configuration eight pitch jets are available to provide torques normal to the spin axis. The proper inertial direction of the torque pulses during the spin cycle is achieved by phasing them with respect to the sun sensor pulses. To simplify the system mechanization, precession control is performed at the ground station. The signal delay in the telemetered sun sensor outputs and telemetered jet commands back to the S/C is compensated for. Some nutation may be excited by the precession thrust pulses and the ANC can be re-enabled to damp this out. An alternative technique is to use the accelerometer nutation sensor data to modulate the precession pulse widths permitting simultaneous precession and nutation damping. The 140° (2.44 rad) precession maneuver can be accomplished in slightly over an hour under nominal conditions.

6.4.1.3 Attitude Determination

Attitude determination during spin uses real time computer solution of algorithms defining S/C attitude as a function of sun and horizon sensor data. These sensors are all body mounted and are scanned by the spacecraft spin motion. The Adcole digital sun sensors provide a sun crossing pulse and a digital word for the sun line direction with respect to the spacecraft Z body axis. The Barnes horizon scanners produce square wave horizon crossing pulses defining the earth local vertical.

6.4.2 Three-Axis Stabilized Control System

To initiate synchronous orbit operations (3-axis stabilized flight), the spacecraft is despun (yaw jets) and the operational attitude reference is acquired. The sun and earth are acquired in that order. The S/C is inhibited from locking on the earth during the first acquisition scan maneuver in order to "map" the horizon radiance output of the sensors. Sufficient impulse for four additional acquisition maneuvers is budgeted to provide for inadvertent loss of reference.

The 3-axis stabilized attitude control concept selected in the trade studies is the "V plus one" system. The system employs two momentum wheels which are operated with a nominal speed bias and are oriented in a shallow "V" in the Y-Z plane (Figure 6-11). A G-6C gyro is included as the third wheel and performs the dual function of attitude sensing during delta-V maneuvers and momentum transfer for nutation damping in the event of a failure of either momentum wheel in the V pair. The selected momentum wheels were originally developed for the Delta PAC mission and are derivatives of the Nimbus roll reaction wheel/earth scanner assemblies. The horizon scanning of the infra-red bolometers is accomplished by the rotation of the momentum wheels. The assemblies are provided by Ithaco and the momentum wheels are manufactured by Bendix. The horizon scanners must be modified to scan the earth from synchronous altitude. With the present LDR antenna design a planar scan is preferable because it minimizes the interference with the antenna elements.

A control logic diagram for the coasting control of the "V" system is presented in Figure 6-12. Pitch and roll error data is derived from the horizon crossing pulses in the system electronics. Pitch control is achieved by driving the two momentum wheels in unison. Active nutation damping is provided by commanding the wheels differentially to transfer momentum into the Z body axis. A pure derivative network is utilized in the roll feedback path to obtain nutation damping which is greater than critically damped (i.e., no steady-state axis momentum) occurs. The de-stabilizing influence of pure roll data in this loop would result in larger transient overshoots due to antenna motion disturbances and would result in larger short term attitude errors. Since the short term attitude error requirement ($\pm 0.3^\circ$) (5.2 mrad) is more stringent than the long term pointing requirement ($\pm 0.935^\circ$) (16.4 mrad) no active roll steering terms are employed in the network. The pitch lead/lag network is similar to the Nimbus pitch control compensation. The control logic given in Figure 6-12 has been verified in simulations and has been breadboarded and operated on the air bearing table at NR. Other control logic mechanizations such as that of P. Hui at GSFC are potentially attractive.

For coasting control the canted yaw RCS jets provide the momentum dumping required for the roll axis control of the momentum bias system. The disturbance induced yaw attitude errors are controlled through the dynamics of the quarter-orbit coupling in the momentum bias system, i.e., yaw error couples into roll after approximately 90° (1.57 rad) of pitch rotation and is removed in the roll channel. Relatively tight tachometer feedback control loops provide a momentum command system rather than a torque command system.

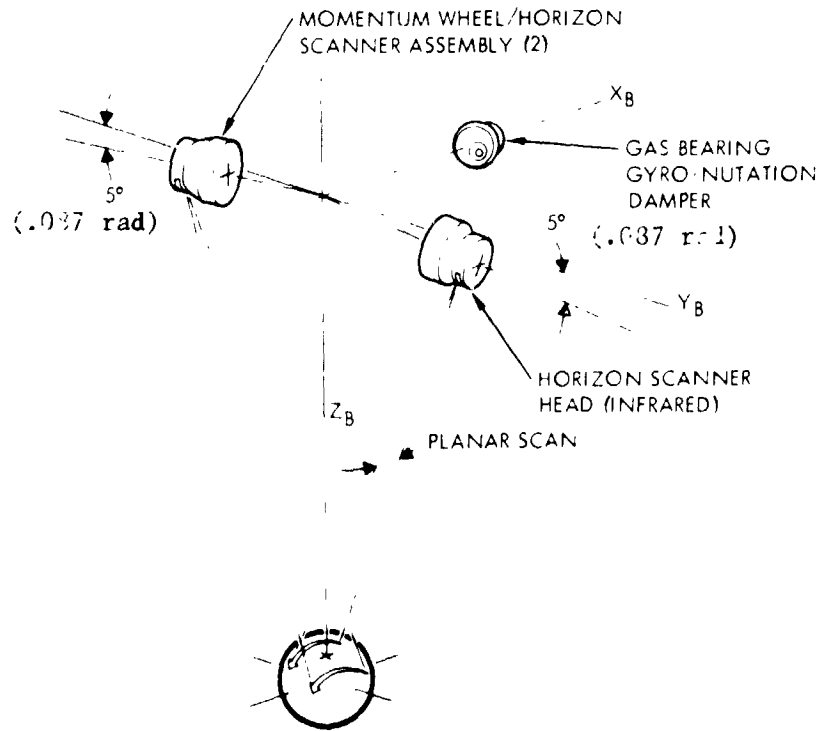


Figure 6-11. Momentum Storage Subsystem Arrangement

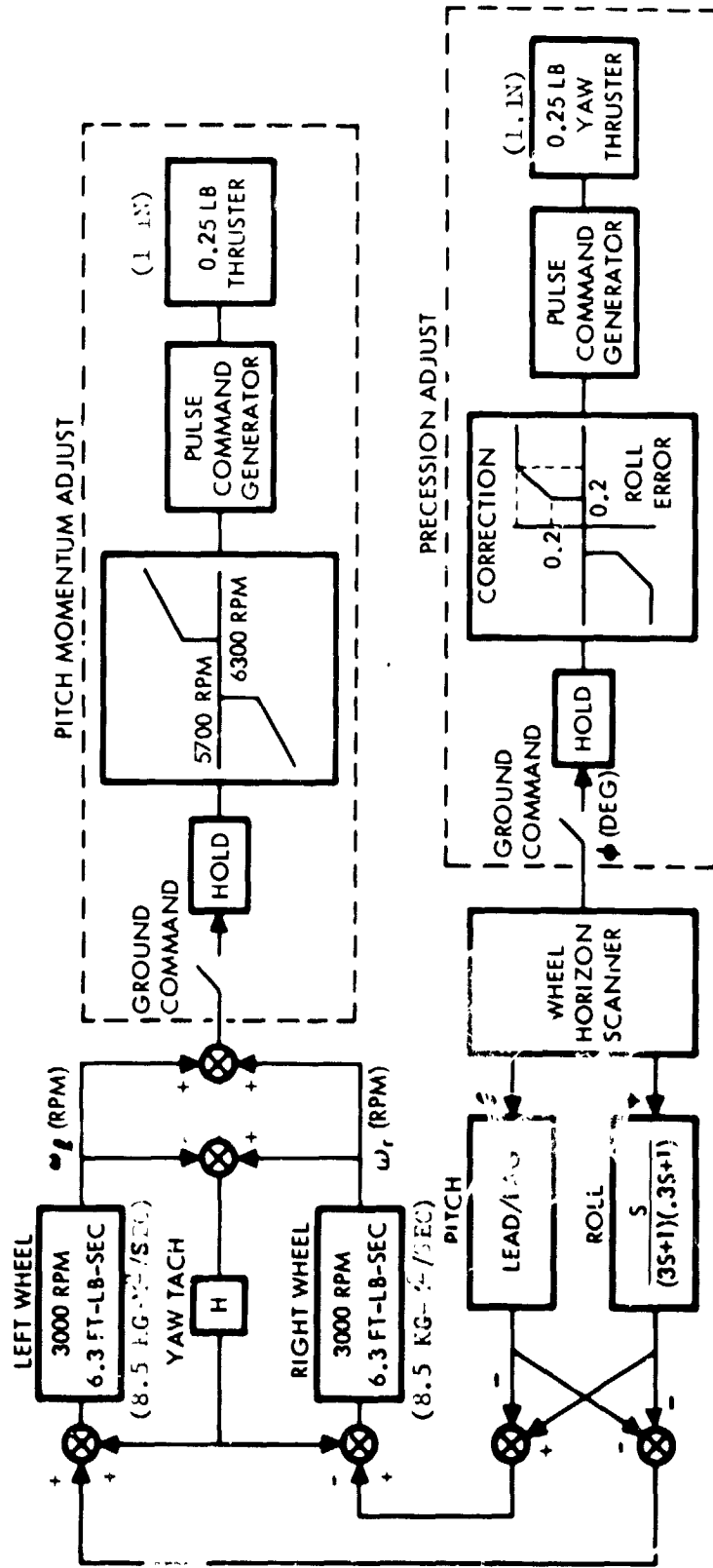


Figure 6-12. On-Orbit Stabilization and Control Logic

The pitch and yaw axis reaction jet momentum dumping control logic will normally be disabled and will be activated no more frequently than once per day. The momentum storage capacity was sized on this basis. Automatic momentum dumping at more frequent intervals is undesirable because of the larger power requirement of the reaction jet heaters and the jet pulsing duty cycle.

For coasting flight the momentum bias provides the necessary stiffness for passive yaw control. During delta-V maneuvers larger disturbance torques can occur due to the RCS thrust vector misalignment and mounting tolerances necessitating active three-axis control. This necessitates the addition of a wide bandpass yaw sensor and the G-6C gyro was selected for this purpose (see Figure 6-13). This gyro has the additional bonus feature that its spin rate can be modulated about the nominal spin rate providing momentum transfer capability. The gyro is mounted with its spin axis along the X axis of the S/C. This permits the two degree of freedom gyro to sense pitch and yaw attitude data as well as transferring momentum into the X axis. Momentum transfer into the X axis is desirable for nutation damping because the closure of a roll sensing control loop into X axis momentum transfer produces very stable nutation damping without the necessity of lead filtering to obtain this stability. Nominally this gyro will not be operated except for delta-V maneuvers. In the event of a momentum wheel failure the gyro will provide full time nutation damping. The gyro may also be turned on to augment attitude determination during the infrequent periods when the sun line and the nadir are nearly collinear.

6.5 APS PERFORMANCE REQUIREMENTS

The Auxiliary Propulsion Subsystem (APS) performance requirements imposed by its operation in conjunction with the ASCS are established in this section. This includes total impulse (propellant), thrust level, minimum impulse bit size and thruster configuration requirements necessary for attitude control and the performance of delta-V maneuvers.

6.5.1 Propellant Requirements

The APS must provide the impulse for the nine functions listed in Table 6-9.

The table also summarizes the propellant requirement, the impulse and the criteria on which the requirements are based. The calculations are based on the following conditions:

Precession Maneuver:

Precession angle, $\theta_0 = 140.5^\circ$ (2.53 rad) (nominally) + margin - 150° (2.62 rad)
 Spin rate, $W_s = 90$ RPM
 Spin moment of inertia, $I_s = 147$ ft-lb-sec² (200 kg-m²)
 Jet moment arm, $r_j = 3.13$ ft (.95 m)
 Number of jets nominally used, $n = 8$
 Specific impulse, $I_{sp} = 220$ sec



Figure 6-13. Minuteman Gyro/Nutation Damper

Table 6-9. Auxiliary Propulsion System Impulse Requirements & Criteria

Item	Criteria	Delta V ft-sec (m/sec)	Impulse lb-sec (newt-sec)	Hydrazine Weight, lb (kg)
1. Attitude Precession	Precess Spin Vector 150°, Spin Rate = 90 RPM, Jets on 60° of Rotation	--	1212 (5400)	5.5 (2.49)
2. Active Nutation Control	5 Times Due to Worst Expected Energy Dissipation Over 30 hr	--	121 (540)	0.7 (.318)
3. Despin	One Maneuver Required from 90 RPM	--	442 (1970)	2.0 (.907)
4. Local Vertical Attitude Acquisition	Initial Acquisition Plus 4 More	--	188 (840)	0.9 (.408)
5. Apogee Injection Correction	Correct In-Plane Errors Only with 3σ Probability	180 (54.7)	4350 (19,300)	19.8 (8.98)
6. Braking ΔV at Station Arrival	Remove Drift Rate of 5 deg/day	47 (14.3)	1100 (4900)	5.0 (2.27)
7. Longitude (E-W) Stationkeeping	Worst Location (7 ft/sec/yr)	35 (10.6)	818 (3640)	3.7 (1.68)
8. Momentum Dumping	Secular Momentum Buildup of 0.2 ft-lb-sec/day (.272 Kg-M ² /sec/day)	--	117 (520)	0.6 (.272)
9. Longitude Station	One Trip, 65° in 15 Days & Another, 130° in 30 Days	162 (49.2)	3770 (16,800)	17.1 (7.76)
Total				55.3 (25.1)

Active Nutation Control:

Nutation divergence time constant, $\tau = 10$ hr
 Nutation controlled in range of 1-2 deg (1.74 - 3.49 mrad)
 Time spent spin stabilized, $\Delta t = 30$ hrs
 Safety factor, SF = 5

Despin:

One maneuver performed (with yaw jets) from 90 RPM

 C³



Local Vertical Attitude Acquisition:

Five maneuvers required (initial + 4 more for possible loss of reference)
Pitch to acquire sun and precess momentum bias to acquire earth
Total maneuver equivalent to precessing momentum bias 450 deg

Apogee Injection Correction:

Based on apogee injection correction analysis performed for RMU
Correct "in-plane" errors only
Transfer orbit injection error covariance matrix from McDonnell Douglas
Apogee injection execution errors = 0.5%/axis (3 σ)
Correction magnitudes are not Gaussian distributions

Braking ΔV at Station Arrival:

SOI and apogee injection correction targeted to easterly drift
with longitude drift rate = 5 deg/day (.087 rad/day)

East-West Stationkeeping:

Sized to accommodate worst case geo-potential perturbations,
7 ft (2.6 M)/sec/year

Momentum Dumping:

Roll/yaw secular momentum buildup of 0.1 ft-lb-sec/day (.136 kg-m²/sec/day)
Pitch axis secular momentum buildup of 0.1 ft-lb-sec/day (.136 kg-m²/sec/day)
Total secular ΔH = 0.2 ft-lb-sec/day (.272 kg-m²/sec/day)

Longitude Station Changes:

Two trips at 4.33 deg per day (.0756 rad/day)

The initial spacecraft weight at booster separation is 788 lb (357.5 kg)
The specific impulse (I_{sp}) for hot firings is 220 seconds and for single pulse operation (momentum dumping and active nutation control) is 180 seconds.

6.5.2 Thruster Performance Requirements

An analysis of the thrust level and minimum impulse bit size requirements for each mission requirement was performed and the results are summarized in Table 6-10.

Table 6-10. Summary of APS Thruster Requirements for the Various Maneuvers

Maneuver	Thrust per Jet lb (newt)	Minimum Impulse per Jet lb-sec (newt-sec)	Number of Jets		Criteria
			Nominal	Contingency	
1. Attitude Precession	0.16* (.71)	**	8	6 or 4	Precess 140.5° (2.45 rad). Complete prior to 1st apogee (3 hr) w/4 jets.
2. Active Nutation	**	0.62 (2.74)	2	4 Without failed jets; other 2 with failed jets	Spin Vector Pointing Accuracy of 0.1° (1.75 mrad)
3. Despin	0.15 (.67)	**	2	1	Less than 1/2 hr with 2 jets.
4. Local Vertical Attitude Acquisition	0.028 (.925)	0.011 (.049)	2	1	Roll maneuver rate 0.5°/sec (8.7 mrad/sec) & roll att. error less than 0.3° (5.73 mrad)
5. Apogee Injection Correction	0.075 (.334)	**	4	2	Perform 3σ correction in single burn with negligible losses due to finite burn time (<4 hr) with 4 jets
6. Braking ΔV at Station	**	**	4	2	Perform 2 Hohmann transfer ΔV maneuvers in less than 4 hr/burn
7. Longitude Station Changes	0.00834 (.0360)	**	4	2	65° (1.13 rad) long. Change in 15 days, Hohmann trans. to and from circular drift orbit, single burn time <4 hr
8. Longitude Station-Keeping	**	0.0215 (.960)	4	2	Trajectory control within 200 ft (60.9 m)
9. Momentum Dumping	**	0.0035 (.0155)	2	1	Att. error less than 0.1° (1.74 mrad) due to dumping pulse disturbance

☐ = Constraining Requirement **Less constraining than for other maneuvers

* Minimum value

The spin vector precession maneuver imposes the largest thrust level requirement. The reaction jet configuration selected permits the nominal use of 8 jets to perform this maneuver, 6 jets with a single failure and 4 jets with two failures. The criteria is to complete the maneuver before first apogee so the orientation can be confirmed and accurately corrected prior to second apogee. The spinning horizon sensors are most accurate at this time and this spacecraft orientation. With an average thrust level of 0.26 lb (1.15N) (nominal), the 140.5° (2.47 rad) precession maneuver can be completed with four jets in 1.3 hours.

The reaction jet minimum impulse bit size is constrained by momentum dumping. The criteria adopted is that the attitude control system transient response be no greater than 0.1° (1.74 mrad) due to the granularity of the pulses of a jet pair. This produces a minimum impulse bit size requirement of less than 0.0035 pound-second (.0156 N-sec).

The number of on-off jet cycles were calculated and the results are presented in Table 6-11. The pitch jets are exercised more than the others and may have 16,600 pulse/jet. The calculations are based on nominal operation but are pessimistic in that the momentum dumping impulse requirements were estimated pessimistically. Also, the momentum dumping was assumed to be performed completely with minimum jet impulses which may also be somewhat pessimistic.

Table 6-11. Reaction Jet Duty Cycle (Number of On-Off Cycles per Jet)

Maneuver	Coasting		ΔV 's (Canted Jets)
	Pitch Jets	Yaw Jets	
1. Precession	7,000	-	-
2. Nutation Control	850	-	-
3. Despin	-	10	-
4. Local Vertical Acquisition	400	400	-
5. Apogee Injection Correction	-	-	600
6. Braking ΔV	-	-	100
7. Station Changes	-	-	500
8. Station Keeping	-	-	100
9. Momentum Dump	8,350	8,350	-
Totals	16,600	8,760	1,300

6.5.3 Reaction Jet Configuration

The selected reaction jet configuration is presented in Figure 6-5. Sixteen jets provide an initial thrust level of 0.275 lb (1.22N) per jet and 0.09 lb (.4N) at propellant depletion. The jet select logic is given in Table 6-12, and is based on the jet numbering system of Figure 6-14.

The requirements and constraints in selecting the jet thruster configuration are presented in Table 6-13. Physical interference and/or jet impingement on the antennas and solar arrays was found to be a dominant constraining factor. Locations on the plus and minus X axes were the only ones without substantial interference. Approximately 12 jet configurations using between 8 and 24 jets were synthesized and evaluated against the requirements of Table 6-13. In addition to satisfying the basic requirements the baseline reaction jet arrangement has the following key features:

1. The jets are in only two locations.
2. The system can handle the worst possible combination of two jet failures and still perform all mission functions (with increased propellant consumption in some cases).

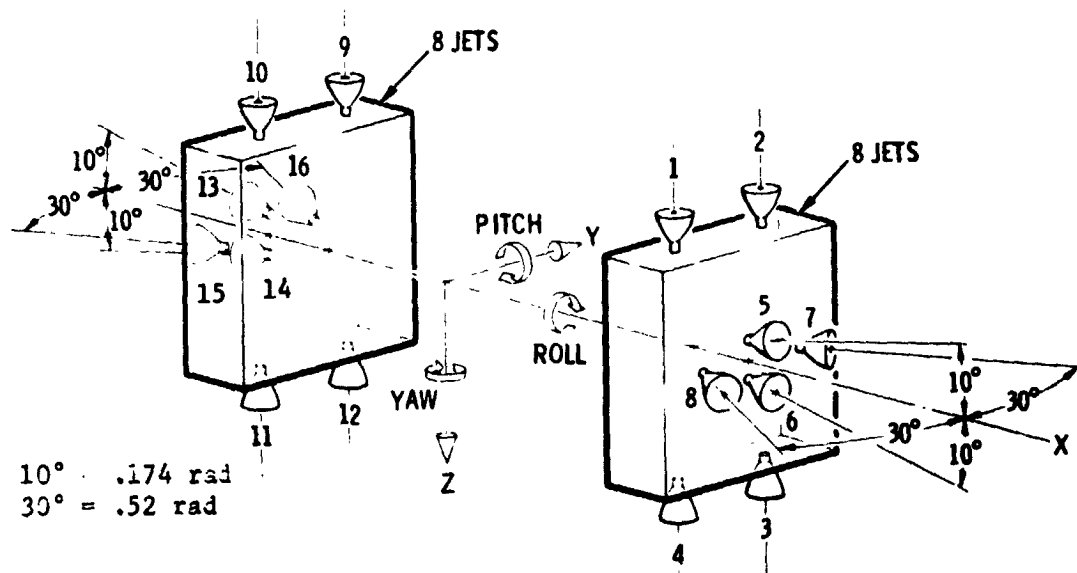


Figure 6-14. APS Engine Arrangement

Table 6-12. Jet Select Logic

Function		Roll		Pitch		Yaw	
		$-\phi$	$+\phi$	$-\theta$	$+\theta$	$+\psi$	$-\psi$
3-Axis Stabilization	Coast Control	Not Req.	Not Req.	(4+10) or (3+9)	(1+11) or (2+12)	(7+15)	(8+16)
	+ ΔV Control	(1+3) or (10+12)	(2+4) or (9+11)	13	14	15	16
	- ΔV Control	(1+3) or (10+12)	(2+4) or (9+11)	6	5	7	8
Spin	Precession			(3+4+ 9+10)	(1+2+ 11+12)		
	Despin						(8+16)

Table 6-13. Summary of APS Thruster Arrangement Requirements

<ul style="list-style-type: none"> • FORCES <ul style="list-style-type: none"> $+\dot{X}$, ΔV Maneuvers Only • TORQUES <ul style="list-style-type: none"> $+\dot{\theta}$ (ANC, Precession, 3 Axis Stab. Momentum Dumping, and ΔV's) $+\dot{\psi}$ (Despin, 3 Axes Stab. Momentum Dumping and ΔV's) $+\dot{\phi}$ (ΔV Maneuvers Only) • RELIABILITY <ul style="list-style-type: none"> Accommodate Two Jet Failures Without Compromising Mission • MINIMIZE SYSTEM COMPLEXITY <ul style="list-style-type: none"> Number of Jets, Plumbing, S/C Structure and ASCS Control Logic • MINIMIZE PROPELLANT CONSUMPTION <ul style="list-style-type: none"> Reasonable Moment Arms • REASONABLE THERMAL SHIELDING FOR HYDRAZINE JETS, LINES AND TANKS
--

7.0 PROPULSION SYSTEM

The TDRS propulsion system consists of the auxiliary propulsion system (APS) which performs all spacecraft maneuvers other than apogee injection, and the apogee motor which performs the apogee injection. The selected baseline concept for the APS is a blowdown monopropellant system using hydrazine with catalytic thrusters. In the design, emphasis was placed on extreme reliability and minimum cost. Complete redundancy is used throughout and all parts specified are existing, space proven hardware, resulting in a system reliability greater than 0.99.

The apogee motor selected, Thiokol's TE-M-616, was designed for compatibility with the Delta 2914 and first firing is expected in October 1972. For use with the TDRS, the nozzle must be shortened 6 in. (15 cm) (resulting in 7-lb (3.2 kg) reduction) and approximately 46 lb (20.k kg) of propellant offloaded. These changes will not require requalification.

7.1 APS REQUIREMENTS AND CRITERIA

The propellant requirements are shown in Table 7-1. Results of the analysis and trades which establish these requirements are presented in the previous section, Attitude Stabilization and Control. These requirements are generally conservative as they are based on 3-sigma variations conditions.

Table 7-1. Propellant Requirements

	Impulse lb-sec (N-sec)	Propellant lb (kg)	Propellant (Percent)
Precess to SOI Attitude (150°)	1212 (5400)	5.5 (2.50)	10.0
Nutation Control-Transfer Orbit (30 hours)	121 (540)	0.7 (.317)	1.3
Despin (from 90 RPM)	442 (1960)	2.0 (.907)	3.6
Acquire Local Vertical (5 times)	188 (840)	0.9 (.408)	1.6
Correct Apogee Injection Error (3σ)	4350(19,300)	19.8 (8.98)	35.8
Stop Drift at Final Station (5°/ day)	1100 (4900)	5.0 (2.27)	9.0
Longitud. Stationkeeping (5 yr)	818 (3650)	3.7 (1.68)	6.7
Momentum Dumping (5 yrs)	117 (520)	0.6 (.272)	1.1
Longitudinal Station Change 2-65° - 15 days	3700(16,800)	17.1 (7.76)	30.9
S/C Wt (incl. Spent Apogee Motor & N ₂ H ₄) = 788 lb (357.5 kg)		55.3 (25.08)	100.0

Nearly 66% of the propellant is allotted to two functions: apogee injection error correction (35.8%) and longitudinal station change (30.9%). Nearly one-third of the propellant is provided for a contingency condition (longitudinal station change) where it is all used only when failure occurs first in the west operational satellites and then is followed by a failure of the east satellite. Over 60% of the propellant is provided to ensure placement of the spacecraft at its final station (expected arrival in less than one month after launch) and less than 8 percent is expended over the remainder of the 5-year period in a normal mission (above the one-third provided for longitudinal station change in the event of satellite failure). The criteria used in selecting the Auxiliary Propulsion System (APS) are as follows:

- . High reliability and long life (5 years) capability
- . Low cost

7.2 ANALYSIS AND TRADE STUDIES

The propulsion trade studies conducted are depicted in the trade tree of Figure 7-1. To include all applicable systems in the trade, particularly those that could enhance or satisfy the long life requirements, propulsion functions were divided into short-term and long-term functions. Short-term functions are those performed in the first two months of the mission and long-term functions are those occurring thereafter.

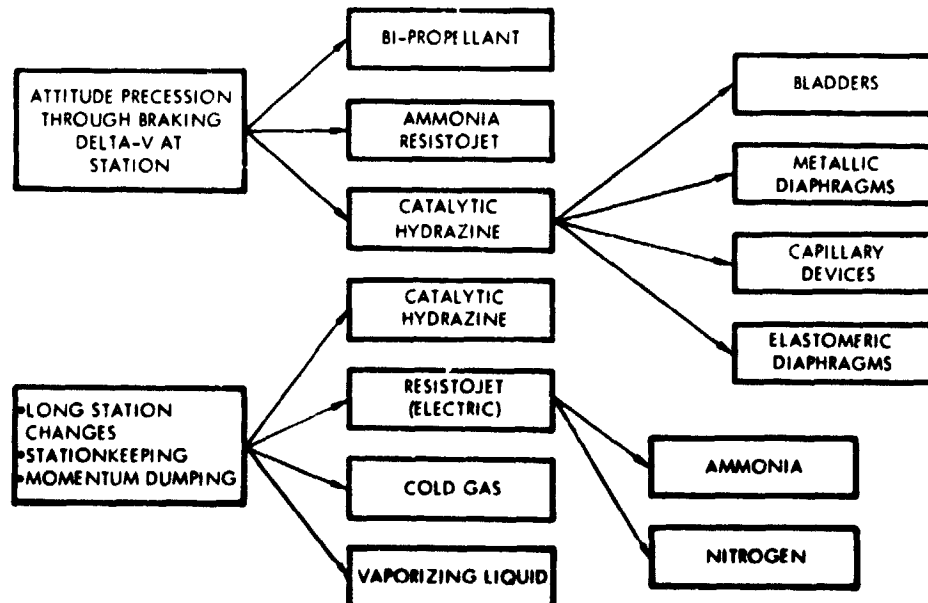


Figure 7-1. Auxiliary Propulsion System Trades

For the short-term functions, candidate propulsion systems include bipropellant, ammonia resistojet, and catalytic hydrazine. Candidates for the long-term functions include catalytic hydrazine, ammonia resistojet, and nitrogen resistojet. Other systems such as cold gas and vaporizing liquid were both too heavy and too low in performance. The results of this trade are summarized in Table 7-2. In the trade for the short-term functions, heavy weight and system complexity essentially ruled out the bipropellant approach. Although the ammonia resistojet system gives the lightest weight, the high power requirement (10 watts/millipound) of the resistojet as a result of the high thrust requirement (~ 0.150 lbf/0.667N) eliminates it from further consideration. The catalytic monopropellant hydrazine is best for the short-term functions and is recommended for the pre-operation maneuvers.

Table 7-2. Propulsion Trade Summary

PARAMETER	SHORT-TERM FUNCTIONS			LONG-TERM FUNCTIONS			REMARKS
	BIOPROPELLANT (NTO/MMH)	HYDRAZINE	AMM. RESISTOJET	AMM. RESISTOJET	NITROGEN RESISTOJET	CATALYTIC HYDRAZINE	
° PERFORMANCE (I_s)	High	Mod.	Mod.	Mod.	Low	Mod.	*If combined with the hydrazine system for the short-term functions, the increased sys. wt. would be due to the larger tank age to accommodate the added propellant. Based on a thrust level of 0.10#. **Risk is primarily in thrust-er development.
° WEIGHT Propellant Total System	Low Mod.	Mod. Low	Mod. Low	Mod. Mod.	High High	Mod. *	
° COMPONENT Total Number Availability	21 Off-the-Shelf	16 Off-the-Shelf	16 Limited	14 Limited	14 Limited	Off-the-Shelf	
° FLIGHT EXPERIENCE Extensive Moderate Limited None	 ✓ ✓	 ✓ ✓	 ✓ ✓	 ✓ ✓	 ✓ ✓	 ✓ ✓	
° POWER REQUIREMENT High > 500 Med 100 - 500 Low < 10 Watts	 ✓	 ✓	 ✓ ✓	 ✓ ✓	 ✓	 ✓	
° TECHNOLOGICAL RISK	Low	Low	Mod.	**Mod	**Mod	Low	
° DEVELOPMENT COST	Mod.	Mod.	Mod.	Mod.	Low	Mod	
° SELECTION RANKING	2	1	3	2	3	1	



In the trade study for the long-term functions, ammonia and nitrogen resistojets and catalytic hydrazine were considered. The nominal specific impulse of catalytic hydrazine and ammonia resistojets is about the same, except the ammonia resistojets provides higher performance if additional power is available to heat the ammonia vapor. Unlike monopropellant hydrazine, ammonia can be expelled from its storage tank by its own vapor pressure eliminating the need for bladders. The nitrogen resistojets system is considerably heavier because of its low I_{sp} (140 sec) and high storage pressure (4000 psi/ 27.6×10^6 N/m²). As shown in Table 7-2, the most favorable of the three systems is the catalytic hydrazine due to its low development risk, high performance, low power requirements, and the availability of flight-qualified components. Extensive investigations were conducted into the long life capabilities of propellant expulsion devices and concerns about potential failures have been overcome.

A comparison was made of propellant expulsion systems. The results of this trade are shown in Table 7-3. The candidate expulsion devices are elastomeric diaphragm/bladder, metallic (reversible) diaphragm, capillary (surface tension) device, and piston. Bellows tanks were not considered because of heavy weight and high cost. Of the four candidate expulsion devices, elastomeric diaphragms/bladders are presently the most widely used and have the most flight experience. Both butyl rubber and laminated Teflon were successfully used as bladder material in previous space missions. The Lunar Orbiter II propulsion system was maintained in space in a fully functional condition for 338 days before the spacecraft was commanded to crash on the moon. The Mariner IV hydrazine system was successfully operated after 1040 days in space. Other Mariner spacecraft propulsion systems have repeatedly operated in space for periods exceeding 600 days.

A material with substantial mechanical property improvements, EPT-10 (ethylene propylene terpolymer), has been developed in recent years. Extensive testing has been accomplished by Pressure Systems, Inc., in Los Angeles. Long-term soaking of the EPT-10 material in hydrazine is now in its third year with no deterioration. Satellite programs already committed to or seriously considering the use of EPT-10 are presented in Table 7-4.

Metallic diaphragms are produced by Arde, Inc., and consist of a thin, one-piece stainless steel shell reinforced by stainless steel hoop wires attached by brazing. The performance and weight of metallic diaphragms are highly competitive with elastomeric diaphragms/bladders. Reliable, lightweight, multicycle capability metallic diaphragms were successfully demonstrated in sizes from 6 in. to 33 in. (15.2 cm to 82.8 cm). Depending on the cone angle of the diaphragm (increased cone angle increases cycle life) up to 20 reversals have been demonstrated. Hemispherical diaphragms for spherical tanks have demonstrated up to three reversals. By the nature of its material of construction, metallic diaphragms will have a long shelf and operating life (up to 10 years is predicted by the manufacturer).



Table 7-3. Expulsion System Comparison

Characteristics	Elastomeric Bladder/Diaphragm	Metallic Diaphragm (ARDE)	Capillary Device	Piston (Rocketdyne)
<ul style="list-style-type: none"> o TECH. RISK Level of dev. Shelf life Dev. cost 	<p>High</p> <p>Potentially good</p> <p>Low</p>	<p>Medium</p> <p>Excellent</p> <p>Medium</p>	<p>Medium</p> <p>Excellent</p> <p>Medium</p>	<p>Low</p> <p>Good</p> <p>Medium</p>
<ul style="list-style-type: none"> o DYNAMIC CHAR. Sensitive to slosh Slosh self-damaging Vibration sensit Accel. sensit. 	<p>Yes</p> <p>No</p> <p>No</p> <p>Yes</p>	<p>No</p> <p>Yes</p> <p>No</p> <p>No</p>	<p>Yes</p> <p>No</p> <p>No</p> <p>Yes</p>	<p>No</p> <p>Yes</p> <p>No</p> <p>No</p>
<ul style="list-style-type: none"> o PERFORMANCE Expulsion eff. % Cycle life 	<p>98</p> <p>Multi-cycle capability</p>	<p>98</p> <p>Three reversals demonstr. for hemispherical diaphragm</p>	<p>99</p> <p>Unlimited</p>	<p>95</p> <p>Multi-cycle capability</p>
<ul style="list-style-type: none"> o STRONG POINTS 	<p>Much dev. & flight experience.</p> <p>Proven life 3 years in space</p>	<p>Good compatibility.</p> <p>Not sensitive to slosh</p>	<p>Good compatibility</p>	<p>Positive displacement</p>
<ul style="list-style-type: none"> o POTENTIAL PROBLEM AREAS OR WEAK POINTS 	<p>Five-year life not yet proven</p>	<p>Flight experience is minimal and is limited to short duration missile application</p>	<p>Subject to propellant slosh. Hard to check out design on the ground</p>	<p>Subject to jamming due to sloshing and leakage. Heavy configuration</p>

Table 7-4. Positive Expulsion Tanks with EPT-10 Diaphragms for Hydrazine Service

Program	Tank Diameter		Operating Pressure		Design Life (Yrs)
	inch	(cm)	psi	(kilg-newtons/m ²)	
Viking Lander	22.25	(56.5)	364	(2510)	3
Acro/Erno	9.59	(24.4)	610	(4206)	3
ATS F&G	16.5	(41.9)	400	(2758)	5
Pioneer	16.5	(41.9)	535	(3689)	3
P-95 (MIL)	22.25	(56.5)	350	(2413)	3
MVM	16.5	(41.9)	380	(2620)	1
CTS	13.0	(33.0)	396	(2730)	7
*Jupiter/Saturn					> 4-1/2

*Firm selection not yet made but considers EPT-10 as prime candidate.

Capillary propellant retention and control is another method of providing propellant to the engine under a zero-g environment for long times. For a three-axis stabilized spacecraft where the propellant tank system must provide propellant to a series of thrusters in various directions, the design for total propellant retention and supplying the gas-free propellant through a single tank outlet is within the present state-of-the-art. Since there are no moving parts in capillary devices, cycle life is unlimited. One weak point of the capillary technique is that it requires a fairly complex and costly test program to qualify it for flight.

The use of pistons for positive displacement of the propellant represents one of the oldest and most commonly used expulsion devices in the industry. However, this technique has two weak points: (1) it is inherently heavy due to the degree of rigidity that must be maintained in the tank design and (2) it is subject to leakage from seal deterioration. Flight experience of this method is unavailable since none has been used in satellite application.

The results of the expulsion system comparison indicate that an elastomeric diaphragm tank is the best choice. Encouraging test results on the EPT-10 material at PSI, indicate five-year life will be demonstrated by the time the final design phase of TDRS is implemented. In

light of this possibility, a catalytic hydrazine system is used for both the short-term and long-term functions. In the event a positive expulsion device fails to satisfy the five-year life requirement of the TDRS, then an independent ammonia resistojet system will be used to perform the long-term functions (those occurring after station arrival). This duplicate system, if required, will impose only a minor weight penalty of approximately 15 pounds. (6.80 kg).

7.3 SUBSYSTEM DESIGN

7.3.1 Description

The baseline Auxiliary Propulsion Subsystem (APS) is a blowdown system using monopropellant hydrazine and is shown schematically in Figure 7-2. Gaseous nitrogen is used as the pressurant. The blowdown ratio (as constrained by the existing tank size, the total propellant requirement, and the final tank pressure) is 3.35 to 1. Two Canadian Communication Technology Satellite (CTS) tanks are used to store both propellant and pressurant. Two fill/drain valves, one per tank, are provided for separate nitrogen servicing and one fill/drain valve is provided for propellant servicing. Each tank is equipped with an elastomeric (EPT-10) diaphragm for positive propellant expulsion and to separate the pressurant from the propellant.

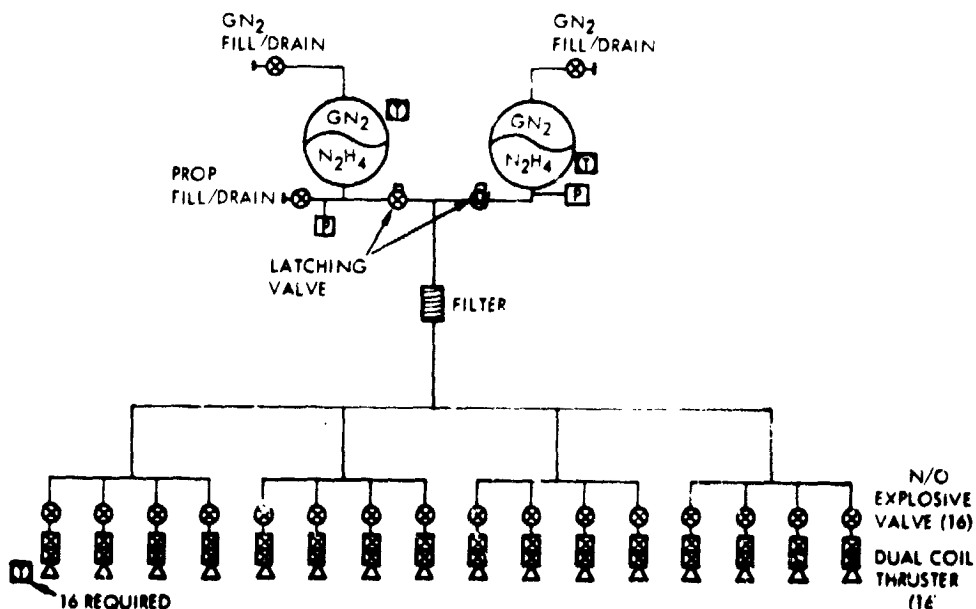


Figure 7-2. Auxiliary Propulsion System Baseline Configuration

Propellant tank isolation is accomplished with the latching valves on one side, as shown in Figure 7-2.

To maintain balance to minimize spacecraft stability and control requirements, propellant is simultaneously drawn from both tanks by opening the latching valve prior to operating the thrusters. A high capacity, low micron rating, etched disc filter located upstream of the thrusters, filters all harmful contaminants from the propellant. Each of the 16 thrusters is equipped with a propellant flow control valve operated by a torque motor. The torque motor valve features dual seats in series to protect the system against internal leakage caused by contamination, and dual coils, wired in parallel, to protect against coil failure. The valve is designed to prevent a leak failure of one poppet. Each coil can actuate both poppets. However, the response time is slightly longer if only one coil is operating. In addition to the redundant thruster valve, each thruster assembly has a normally open explosive valve that is closed when the thruster valve fails open and causes a "run-away" thruster. Eight thrusters, capable of operating in a thrust range of 0.275 lbf to 0.090 lbf, are assembled in each of two identical modules. Each thruster is thermally controlled (with heaters) to permit operation at temperatures ($\approx 300\text{F}$) which enhance thruster operating performance and catalyst bed life.

The baseline APS configuration will be instrumented to measure tank temperature and pressure as well as thrust chamber temperature. The on-off position of the latching valve will also be instrumented. The tank temperatures and pressure measurements are used to calculate the quantity of consumed propellant throughout the mission and to predict thruster performance. When the APS is not in operation and the latching valve is closed, the pressure measurement may also be used as a tank leak detector.

Thruster temperature sensors are used primarily to identify a failed thruster valve.

7.3.2 Performance

Tank pressure as a function of propellant consumed and its corresponding thrust level is shown in Figure 7-3. The maximum tank pressure of 350 psi ($2.3 \times 10^6 \text{ N/m}^2$) was based on the constraints of tank size and the desired final pressure of 100 psi ($.69 \times 10^6 \text{ N/m}^2$) to the thrusters. The thrust-pressure relationship is based on actual demonstrated performance by the selected Hamilton Standard thruster.

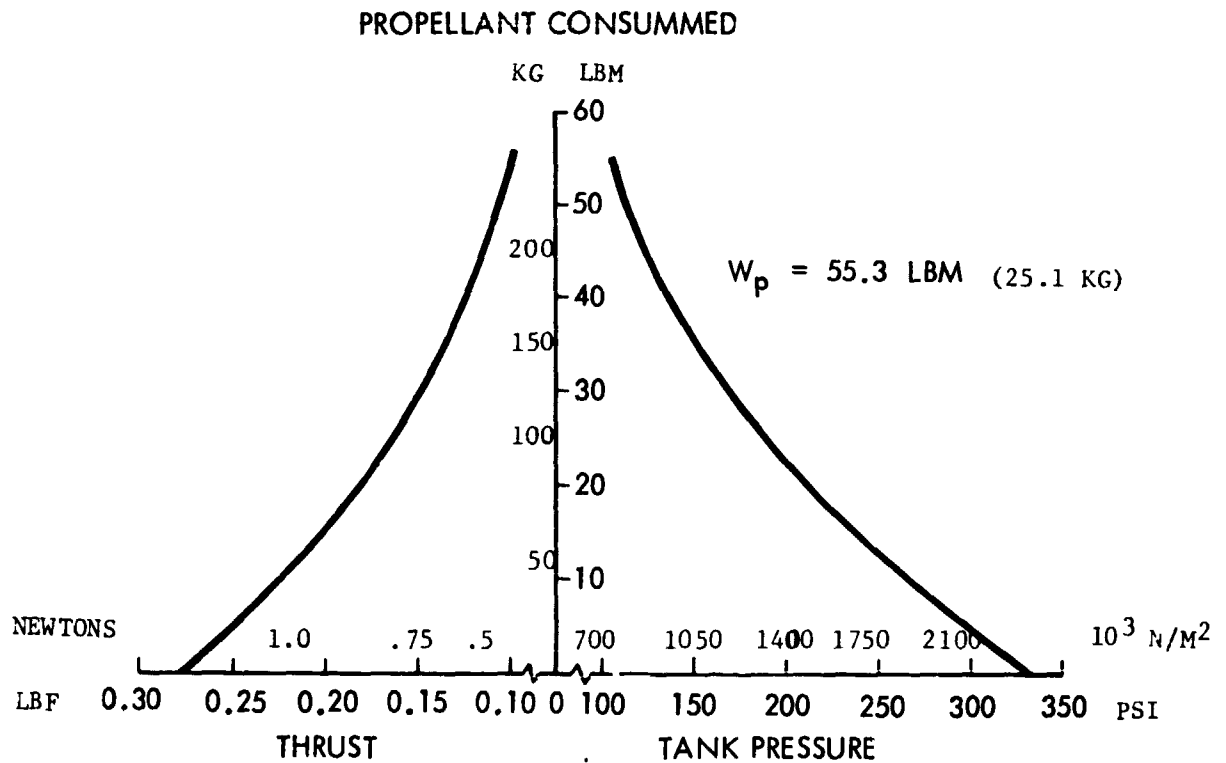


Figure 7-3. Thrust-Pressure versus Propellant Consumed

7.3.2.1 Component Selection

The hardware list for the baseline system is shown in Table 7-5. Except for the normally open explosive valve, all components are the same as those selected for the Canadian Communication Technology Satellite (CTS). The criteria used for the component selection are:

- . meet performance requirements
- . flight qualified
- . low cost

Each of the selected components is discussed below and the manufacturer and previous users identified.

Table 7-5. APS - Hardware List

Component	Manufacturer	No. Reqd.	Weight		Previous Use
			lb	(kg)	
GN ₂ fill/drain	TRW	2	0.6	(0.27)	Intelsat IV, RAE-B
Prop. tank with EPT-10 diaph.	PSI	2	11.0	(4.99)	CTS
Latching valve	HRM	1	0.6	(0.27)	Similar to SMS and RAE-B
Expl. valve, N/O	Pyronetics	17	6.8	(3.08)	Qual. for manned S/C
Prop. fill/drain	TRW	1	0.3	(0.14)	Intelsat IV, RAE-B
Filter-15μ ABS	Vacco	1	0.4	(0.18)	Surveyor, Intelsat IV, Mariner, Saturn, LEM
Press. transducer	Bourns	2	0.6	(0.27)	Saturn, Scout, Shrike
Temp. transducer (tanks)	Gulton	2	0.6	(0.27)	Apollo
Temp. transducer (thrusters)	Genisco	16	0.4	(0.18)	
Thruster	Ham. Std.	16	9.6	(4.35)	CTS, Solraa
Wiring and lines		-	3.0	(1.36)	
Thruster housing		2	1.5	(0.68)	
Trapped propel.		-	3.0	(1.36)	
Total			38.0	(17.4)	
GN ₂			0.6	(0.27)	
Propellant			55.3	(25.08)	
Total			94.3	(42.8)	

Propellant Tank Assembly

The propellant tank is the same as the CTS tank shown in Figure 7-4 except for the attachment points. The tank is now in development by Pressure Systems, Inc., and delivery of the first unit is expected in October, 1972.

The tank is basically a 13-in. (33 cm) diameter sphere with an EPT-10 elastomeric diaphragm for positive propellant expulsion. It consists of

two forged and finished machined hemispheres of 6 AL-4V titanium. The two halves are TIG welded together at the girth point which also retains and seals the hemispheric elastomeric diaphragm. The diaphragm separates the tank into two compartments, one for the hydrazine and the other for the gaseous nitrogen. The diaphragm is made of ethylene propylene terpolymer, EPT-10. This material has shown superior mechanical properties over other materials such as Teflon and butyl rubber, and is widely used in other spacecraft with monopropellant hydrazine systems. Programs already committed to EPT-10 or strongly considering it as the prime candidate are summarized in Table 7-4.

Fill and Drain Valves

The fill and drain valve (Figure 7-5) is a TRW design fabricated by VACCO in earlier productions. It is identical to a qualified unit in INTELSAT IV, except for end fitting sizes. The valve has a manually operated mechanical (non spring-loaded) shutoff with redundant sealing. Sealing is created by seating a tungsten carbide ball into a seat within the stainless steel body. The ball is held captive in a poppet which is actuated closed or open by rotation of the adjusting cap. Poppet sealing with the valve open during fill and drain (vent) operations is achieved by an O-ring and backup ring forming the poppet/body seal. Torquing the adjusting cap to a prescribed value assures sealing.

The pressurant and propellant Fill and Drain valves are identical except for the size of the fitting which will be different to avoid filling errors.

Latching Valve

The selected Hydraulic Research latching valve is shown in Figure 7-6. It permits the pressure measurement of one tank (when the system is shut-down) and isolates the same tank if it leaks. This valve is also used on the CTS and is similar to the units presently being qualified for the SMS and RAE-B programs.

The latching valve is torque-motor actuated with latching forces supplied by a magnetic circuit in both the open and closed positions. The torque motor is isolated from the fluid by a torque tube which is also the primary valve spring. The motor contains two coils, wound in opposite directions: one coil for valve opening and the other for valve closing. The valve is seated by utilizing a stainless steel poppet housing with an elastomeric poppet face. The elastomer is an ethylene propylene/HYSTL composite developed by TRW. The configuration also features a swivel design which ensures optimum alignment. Valve position is indicated by a hermetically sealed micro-switch, mounted to the top frame and actuated by an extension from the valve flapper.

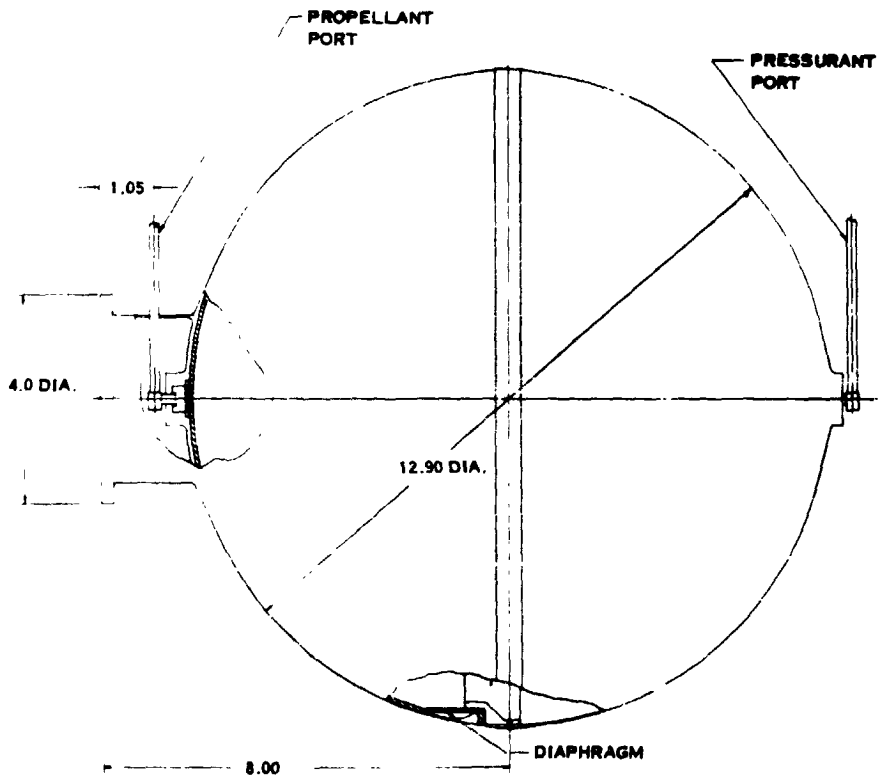


Figure 7-4. Pressurant/Propellant Tank

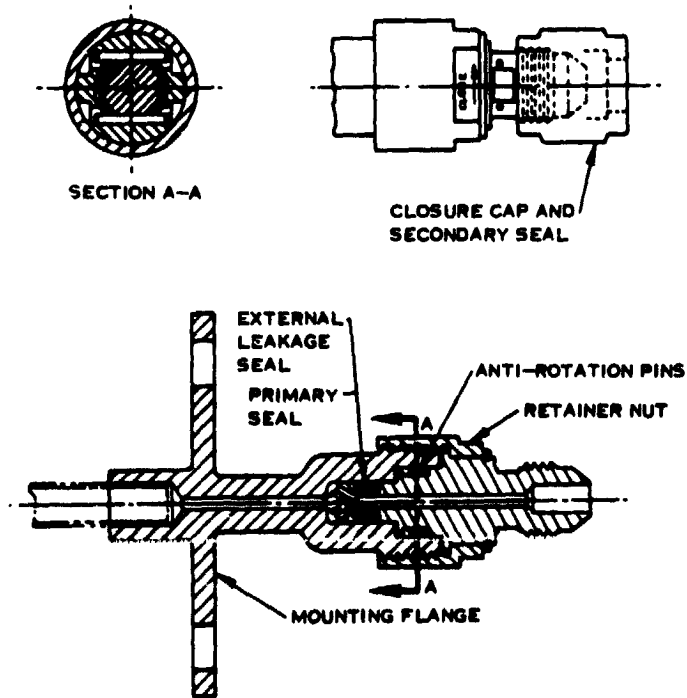


Figure 7-5. Fill and Drain Valve



Space Division
North American Rockwell

Explosive Valve

The explosive valve, manufactured by Pyronetics, Inc., (Figure 7-7) isolates an individual thruster in case of a thruster valve open failure. In this case, both seats must fail before the explosive valve need be actuated.

Explosive valves are inherently very reliable because of their design simplicity. The pyrotechnic initiator used to actuate the valve is of the "1 amp-1 watt no-fire" type. This valve requires a power supply in excess of 1 amp or 1 watt to make it fire; therefore, initiation by stray current or EMI is unlikely. Thousands have been static tested or flight tested in the last decade in support of both manned and unmanned spacecraft without any mishaps. In addition to the built-in safety of the initiator, safety gates can be provided in the firing circuit such that a completed circuit is possible only if all conditions are satisfied.

The valve materials include 300 series CRES for the body and ports, 440C CRES for the ram and Teflon for the ram seal. The valve design eliminates pressure surges in the line during actuation since fluid is not stored in the valve element. Also, valve operation is not affected by line pressure because the ram is isolated from the propellant flow. The valve is supplied with weld fittings or tube fittings and is qualified for use on a manned spacecraft.

Propellant Filter

The line filter, made by Vacco Industries (Figure 7-8) is identical to the one used in Intelsat IV. The one filter used in the TDRS protects the downstream thruster valves and injectors from harmful contaminants. The Vacco filter consists of a multi-segmented filter element welded into a titanium body. The element is comprised of stacked etched filter discs. The depth of etch in each disc can be held with such precision that a multi-segmented filter can meet filtration requirements unobtainable by any other type element. This filter concept has also been used on Surveyor, Lunar Orbiter, LEM/Apollo, Saturn, and Mariner.

Thruster Assembly

The thruster assembly is similar to the nominally rated 0.10-1b (.45N) thrust engine qualified by Hamilton Standard for the NRL/SOLRAD X satellite and selected for the Canadian CTS. The only difference is in the propellant flow valve. For TDRS, a Hydraulic Research (HR) torque motor operated, dual seat, dual coil valve is proposed. It was chosen over the normally equivalent Wright Components solenoid valve because of its redundant features and the subsequent elimination of a single failure point condition. The valve is similar to the unit qualified for the Sky-net, NATOSAT and Intelsat IV and used on the CTS with the High Thrust Engine. The proposed HR valve (Figure 7-9) is normally closed. Two

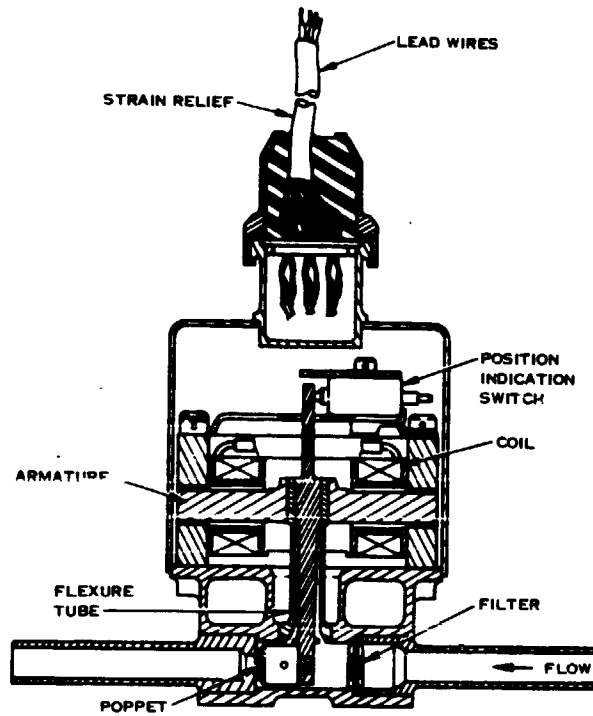


Figure 7-6. Latching Valve

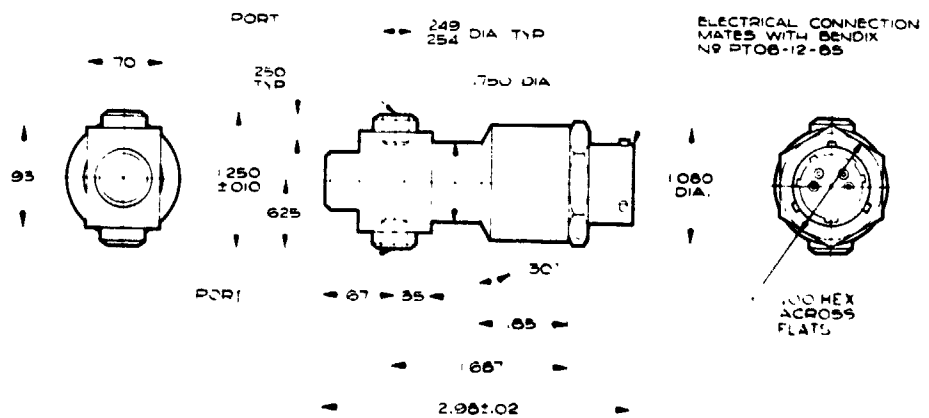


Figure 7-7. Explosive Actuated Valve (N/O)

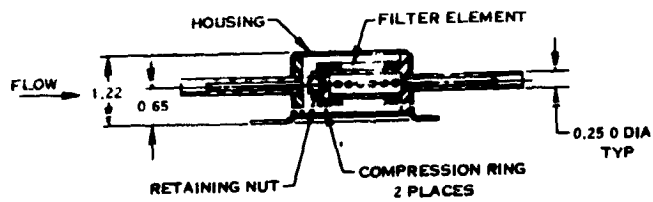
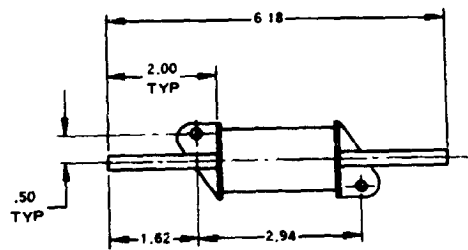


Figure 7-8. Propellant Filter

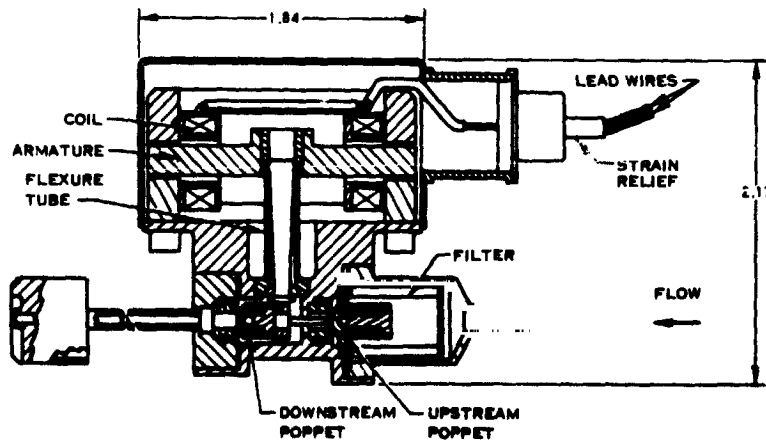


Figure 7-9. Thruster Valve

metal-to-metal flat-lapped poppets and seats in series provide redundancy in the prevalent fail-open mode. The downstream poppet is actuated directly by the flapper, which is an integral part of the armature. The upstream poppet is mechanically opened by a pin connected to the flapper. The torque motor consists of two pole pieces, two coils in parallel, four permanent magnets, and an armature which is an integral part of the flapper and flexure tube. The permanent magnets generate sufficient flux to overcome the spring force and keep the valve poppets closed. When current is passed through the coils, the magnetic flux in the armature is biased and the armature moves to the open position. Failure from contamination must occur in both poppets before the valve becomes totally incapacitated. Similarly, the two coils in parallel must fail before the valve can fail closed.

Each thruster assembly is thermally controlled to maintain a catalyst temperature of 300F (149C) to overcome possible pressure overshoot due to cold starts and to eliminate the possible formation of liquid in the catalyst bed. The sizing of the heater and the determination of the power requirements for its operation are presented in Section 9.0.

7.4 DESIGN CONSIDERATIONS

7.4.1 Operating Life

The performance of monopropellant hydrazine is well characterized. The areas of uncertainty in terms of demonstrating operating life lie primarily in the expulsion system and catalyst bed. Encouraging progress has been made in the development of the EPT-10 diaphragm by Pressure Systems, Inc., and metallic diaphragm by Arde, Inc. The results thus far indicate that a proven 5-year expulsion system can be expected before the implementation time frame of the TDRS as discussed in Section 7.2.

Reports from early hydrazine thruster testing indicate that the single most important factor which could limit the life expectancy of the subsystem is the number of cold starts which cause low catalyst bed temperature at ignition. Apparently, long ignition delays, caused by the decreased activity of the catalyst at lower temperatures, results in excessive accumulation of liquid hydrazine in the reactor bed causing extreme overpressure which is detrimental to both the reactor bed and the catalyst pellets. Although cold start is a recognized constraint, monopropellant hydrazine thrusters have been successfully tested in the continuous mode for many hours and in the pulse mode in excess of one (1) million cycles. Damage to the catalyst due to cold starts can be prevented by the incorporation of active thermal control directly on the catalyst bed. This minimizes the startup pressure overshoot that damages the catalyst and significantly increases life expectancy.

7.4.2 Thrust Vector Alignment

In an idealized symmetrical thrust chamber, the thrust vector action line coincides with the thrust chamber longitudinal axis. The thrust vector of an actual thrust chamber deviates slightly from the longitudinal axis due to tolerances in manufacture and assembly, and the asymmetric expansion of the exhaust gases during thruster operation. These two effects are termed geometric and dynamic thrust vector misalignment respectively.

The geometric misalignment can be estimated from a dimensional analysis of manufacturing tolerances and assembly procedures. In this analysis, the true reference points are the common mounting interfaces of the thruster and the spacecraft.

Dynamic thrust misalignment can be caused by several factors, none of which can be determined analytically. These factors are the random fluctuations in gas flow through the chamber; asymmetry of the chamber throat, expansion nozzle, and nozzle exit about the chamber axis; and deviation of the throat plane and exit plane from perpendicular to the chamber axis. Dynamic misalignment can be determined only by hot firings of the thrusters.

Results of a series of tests by Rocketdyne using 25-1b (111 N) Gemini engines showed 3-sigma standard deviation values of 0.22 degrees (first series of nine tests) and 0.057 degrees (second series of nine tests). A representative dynamic misalignment value for the TDRS hydrazine thrusters is not available, but a slight improvement is expected because of their small size.

7.4.3 Performance Verification

The in-flight performance of the monopropellant hydrazine system is determined from pressure and temperature measurements of the pressurant and propellant. Temperature sensors will be provided at each of the propellant tanks, and as a backup, a pressure transducer will be provided at the tank outlet manifold. The combined pressure and temperature information is also used to calculate the unused propellant quantity (using the PVT technique).

As a diagnostic aid to determine thruster failure the temperature of each thruster can be measured. If a thruster valve fails open, the catalyst bed will continue to register a high temperature; pinpointing the troubled thruster for immediate corrective action.

7.5 APOGEE MOTOR

The apogee motor selected to inject the TDRS spacecraft into synchronous orbit is a modified TE-M-616 presently in development by



Thiokol Chemical Corporation for the Canadian Communication Technology Satellite. Forty-six pounds (20.8kg) of propellant are off-loaded and the nozzle length reduced 6 inches (15.2 cm). The nozzle length reduction results in a reduced Isp of 283 sec., and a burnout weight of 50 pounds (22.7 kg). The modified motor characteristics and performance are shown in Tables 7-6 and 7-7.

The motor case consists of the hemispherical ends and a short cylindrical section connecting these two ends and is made of 6Al-4V titanium. The nozzle is submerged into the motor and is constructed of tape-wrapped carbon phenolic. The nozzle throat is made of Graph-I-Tite G-90. The motor is ignited by a remotely located safe and arm (S&A) device firing through contained detonating fuse lines into two through-bulkhead initiators. Two initiators located in the forward end of the motor provide redundancy. The ignition system can accept either a Minuteman S&A device or an existing Thiokol electromechanical S&A device with minor modification.

The propellant is of the high energy "H" series variety, cast with an eight-point internal star configuration. The motor is designed for propellant off-load up to 10 percent by cutback technique without modifying motor hardware or requalification testing.

Development of the CTS apogee motor is progressing according to schedule. The first sea level development firing is scheduled for October, 1972, and the first altitude firing in November, 1972. Complete qualification testing is expected in March, 1973.

Table 7-6. Modified CTS Motor Performance and Weight Data

MOTOR PERFORMANCE

Burn time/action time (t_b/t_a), sec	37.06/34.90 sec	
Ignition delay time (t_d), sec	0.108 sec	
Burn time avg cham. press. (P_b)	433 psia	2.98×10^6 N/m ²
Action time avg. cham. press (P_a)	420 psia	2.89×10^6 N/m ²
Maximum chamber pressure (P_{max})	493 psia	3.4×10^6 N/m ²
Total impulse (I_T)	196,000 lb-sec	$.870 \times 10^6$ N-sec
Burn time impulse (I_b)	187,500 lb-sec	$.834 \times 10^6$ N-sec
Motor specific impulse (I_{mo})	262 sec	
Propellant specific impulse (I_{sp})	283 sec	
Burn time average thrust (F_b)	5700 lb	25,400 N
Action time average thrust (F_a)	5360 lb	23,600 N
Maximum thrust (F_{max})	6400 lb	28,400 N
Discharge coefficient (C_d)	0.959	

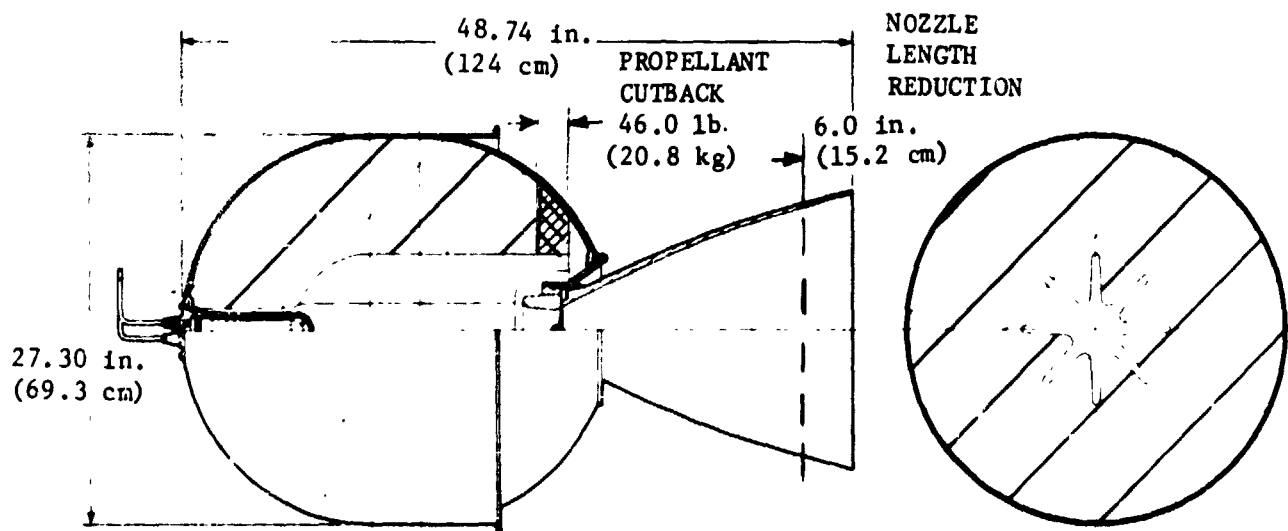
WEIGHTS

	LB	KG
Total loaded	746.0	338.4
Propellant	688.0	312.1
Case assembly	22.60	10.3
Nozzle assembly	25.78	11.8
Igniter assembly	4.60	2.1
Internal insulation	12.62	6.7
External insulation	0.0	--
Liner	0.33	0.2
Miscellaneous	1.86	0.8
Burnout	50.00	22.6
Propellant mass fraction, including S&A/SMDC	0.919	0.4
Propellant mass fraction, excluding S&A/SMDC	0.922	0.4

TEMPERATURE LIMITS

	DEGREES F	DEGREES C
Operation	20 to 100	7 to 38
Storage	20 to 100	7 to 38

Table 7-7. CTS Motor Characteristics



CASE

Material	6414V Titanium
Minimum ultimate strength	165,000 psi (1135×10^6 N/m ²)
Minimum yield strength	155,000 psi (1065×10^6 N/m ²)
Hydrostatic test pressure	590 psi (4×10^6 N/m ²)
Hydrostatic test pressure/maximum pressure	1.00
Yield pressure/hydrostatic test pressure	1.25
Nominal thickness	0.035 in. (.089 cm)

NOZZLE

Body material	Carbon Phenolic
Throat insert material	Graph-I-Tite G-90
Initial throat diameter	2.89 in. (.073 m)
Exit diameter	15.88 in. (.402 m)
Expansion ratio	30.5
Expansion cone half-angle, degrees	14.07
Type	Fixed contoured
Number of nozzles	1

LINER

Type	TL-H-304
Density	0.046 lb/in. ³ (1275 kg/m ³)

Table 7-7. CTS Motor Characteristics (Cont)

PROPELLANT CHARACTERISTICS

Burn rate at 500 psia (r_b)	0.233 in./sec (.59 cm/sec)
Burn rate exponent (n)	0.28
Density	0.0641 lb/in. ³ (1780 ..g/m ³)
Temperature coefficient of pressure (π_k), percent deg F	0.12
Characteristic exhaust velocity (C*)	5080 ft/sec (1550 m/sec)
Effective ratio of specific heats (Chamber)	1.146
(Nozzle exit)	1.16

CURRENT STATUS

Development

IGNITER

Thiokol model designation	TE-P-641-01
Type	Pyrogen
Recommended firing current, amperes	5.0
Circuit resistance, ohms	1.0
Number c ⁶ squibs	2

PROPELLANT

Propellant designation and formulation	TP-H-3135
--	-----------

PROPELLANT CONFIGURATION

Type	Internal Burning-8-Point Star
Web	8.16 in. (20.8 cm)
Web fraction, percent	60.5
Silver fraction, percent	2.58
Propellant volume	10.620 in. ³ (.174 m ³)
Volumetric loading density, percent	
Web average burning surface area	1272 in ² (.82 m ²).

8.0 ELECTRICAL POWER SUBSYSTEM (EPS)

This section describes the baseline TDRS electrical power subsystem (EPS) design. The EPS generates, conditions, distributes and controls electrical power as required by the TDRS subsystem and telecommunication services. As a general utility service the EPS delivers regulated 28-volt dc power. A small portion of the 28-volt power is converted to 18-volts for specific loads. All other nonstandard power conditioning is part of the user equipment. Major EPS assemblies are shown in Figure 8-1. The baseline consists of solar arrays for primary power generation, nickel cadmium batteries for array power utilization by subsystem loads.

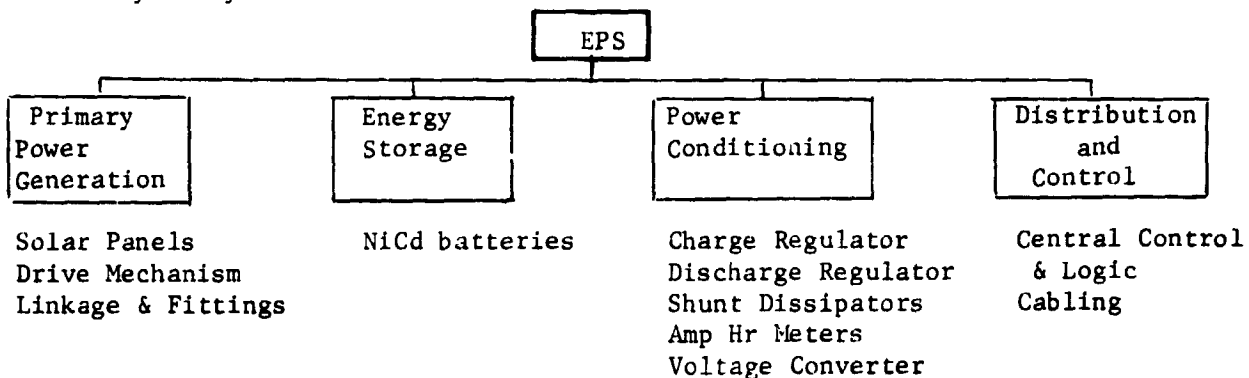


Figure 8-1 TDRS Major EPS Assemblies

8.1 EPS SUMMARY

The selection of the EPS concept was driven by consideration of geosynchronous orbit characteristics, transfer orbit requirements, and normal operational requirements. A summary of the major design drivers for the EPS is given in Table 8-1.

Figure 8-2 shows the sun eclipse periods which occur twice per year at the equinoxes in March and September. Each eclipse season extends for approximately 45 days with a maximum sun eclipse time of 72 minutes and an average eclipse time of 53 minutes.

The baseline EPS was designed to the power requirements presented in Section 8.1.2. Updated requirements were tabulated in terms of servicing the Shuttle with MDR voice transmission. Additional detailed power tabulations are given in Appendix 8B. The baseline provides for one Ku- plus one S-band in the MDR forward links. The design at beginning of life can support two S-bands (an increase of 32 watts over the baseline) by utilizing the contingency (6 w) and degradation allowance (66 w) for the solar array space environmental effects. It is expected that dependence on S-band will decline with mission time.

Table 8-1 EPS Major Design Drivers

Description	Driver
Program	
Launch Date	1977
Orbit	Geosynchronous
Mission/Operational	
Lifetime	5 years
Transfer orbit time	Up to 27.5 hours
Configuration	
Integration	Subsystem integrated to permit replacement by alternates with greater capability and minimum impact
Spacecraft	3 axis stabilized
Booster	Delta 2914
Electrical Power Subsystem	
Reliability apportionment	0.95 (5 years)
Eclipse season	See Figure 8-2
Daylight power	
Eclipse power	See Table 8-3
Transfer orbit power	

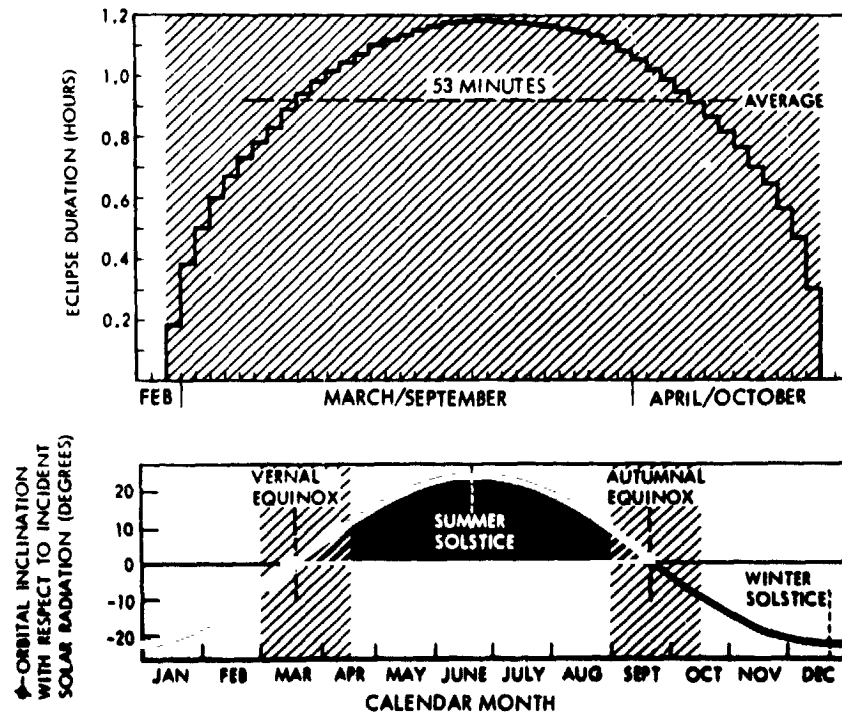


Figure 8-2 Eclipse Periods

The solar panels can readily be increased 25% in width over the baseline size at a weight penalty of 15 lb (7 kg), providing a 25% increase (100 w) in available power. This amount will readily support two S-band links at the end of the mission. Using the above logic it is concluded that the NR TDRS design is capable of servicing the shuttle in this time period.

8.1.1 Alternative Concepts

The requirement for a 3 axis stabilized spacecraft drives the EPS to select a deployed solar array for most efficient utilization of available area. Other solar array concepts were not studied within the scope of this study. Because of a constraint to utilize only flight proven technology and hardware (where possible) nickel cadmium batteries were selected for the energy storage requirements. Other techniques have been evaluated in past studies, e.g., regenerative fuel cells and energy wheels (reference Shuttle Launched Modular Space Station); however, while a considerable amount of technology development is going forward on these devices, and a potential weight savings exists, only NiCd batteries are presently available for flight hardware.

Figure 8-3 shows a trade tree that summarizes the trade offs that were made before defining the EPS baseline. Major study effort was given to the energy storage (secondary battery) in defining its configuration. Cell sizes of 4, 6, 12 and 15 ampere hour and configurations of 1, 2, 3 and 4 batteries were compared. The selection of two batteries for the baseline was made after an examination of the impact of a battery failure and weight trade offs. With two batteries, the loss of one still permits a load of 115 watts (e) for a full 72 minutes eclipse sufficient to operate one forward LDR and one forward MDR link. The selection of a 12 ampere hour cell size results from the comparison of battery voltages with the main bus voltage. Each battery cell has a charge voltage (end of charge) of approximately 1.5 volts/cell. The requirement for a 28-volt bus dictates a battery configuration of 18 cells or less in series. Commonly, battery configurations from 15 to 18 cells are used in the direct energy transfer concept. This concept was found to be most efficient for the TDRS mission since it permits direct transfer of solar array power to the loads without any in line power conditioning. Note: The majority of time (all but 80.2 hours per year) is spent in direct sunlight with spacecraft loads supported directly from the solar array. Based on a 16 cell battery and two batteries in the subsystem, then a cell size of 12 ampere hours is selected for the total energy requirements.

A range of battery requirements from 218 to 349 watt-hours were considered in the tradeoffs. These varied from minimum telecommunication capability of one LDR forward link and no MDR forward link to a full two-forward link capability normally provided during sunlight periods. For these conditions, tradeoffs showed battery weight to range from 35 lb to 62 lb (15.9 to 28.1 kg). Considering the weight impact on payload it was decided that the design points should be to provide one LDR forward link and one MDR forward link during the full eclipse period. In the event of a battery failure, then the design

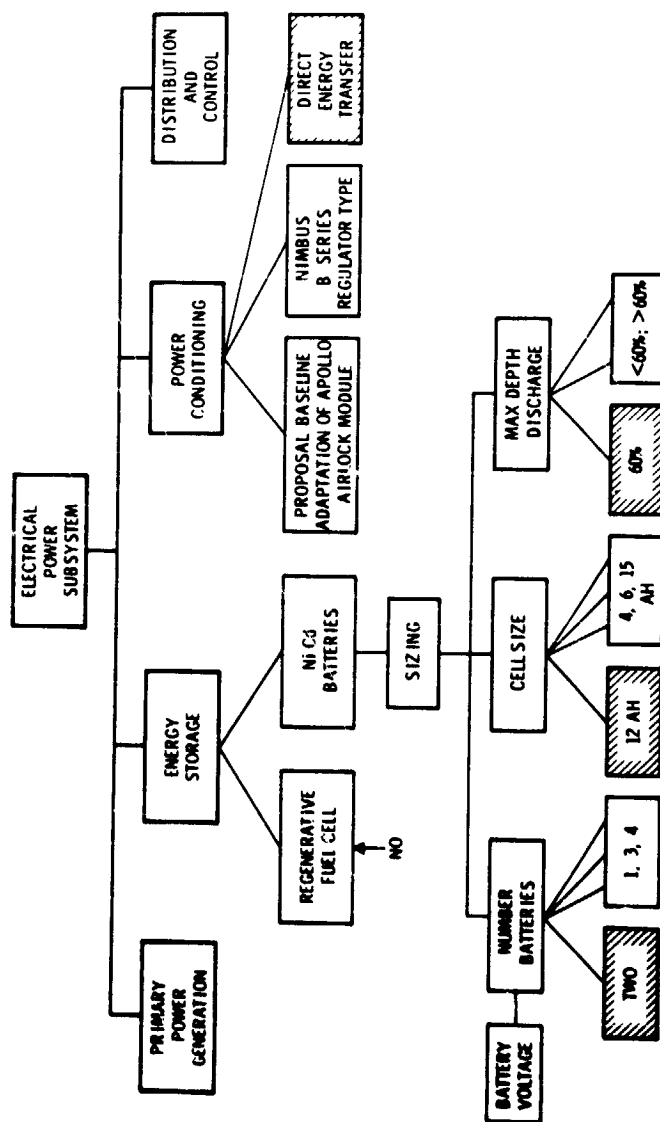


Figure 8-3 EPS Trade Tree



point reduces to only one MDR forward link. Figure 8-4 demonstrates the various capability combinations during maximum eclipse possible between LDR and MDR forward links. As shown, the selected baseline battery configuration (total energy storage of 460 watt hours) provides an energy storage requirement of 276 watt hours at a 60% (maximum) depth of discharge for the worst eclipse conditions.

Description of the EPS includes preliminary design and physical and performance characteristics. Each assembly description covers sizing requirements, performance capability, and physical installation data, and growth considerations.

8.1.2 Requirements

Subsystem level requirements are given in this paragraph. Assembly level data are presented in the following subsections.

8.1.2.1 EPS Performance Requirements

Table 8-2 summarizes the EPS sizing requirements. Detailed power requirements are tabulated in Table 8-3. This is the sizing model used for baseline concept definition.

An average power of 300 watts (e) must be provided throughout a 24-hour sunlight period. This supports telecommunication capability of two forward links for both medium data rate (MDR) and low data rate (LDR) transmitters, with a 25-percent duty cycle for one-voice LDR forward link as well as full return links. During eclipse the power level is reduced to 213 watts (e) which supports one forward LDR and one forward MDR (S-band). The impact on load profile to provide on LDR forward link voice communication is shown by Figure 8-5. The requirements used in generating the profile of Figure 8-5 are listed in Table 8-4. Sensitivity of the system to S-band voice and effects of the time voice is used is shown in Appendix 8B.

Figure 8-5 shows the time required to charge the NiCd batteries toward mission end of life (~ 5 years) during a maximum eclipse period. A typical load power profile is used based on two LDR forward links with one of the links on a voice transmission 25 percent of the 24 hours, and the second link transmitting data. It is assumed that the TDRS is communicating with the Space Shuttle in low earth orbit 16 times per day for periods of 22-1/2 minutes each. The array power shown (400 watts) is based on end of life (EOL) and allows 66 watts for degradation and 6 watts for contingency.

The required load includes power conditioning and distribution losses of 12.5 percent for daylight loads and 9 percent for eclipse loads. 85 watts of solar array power is available for battery charging during periods when there is no voice transmission. A battery charging circuit loss of 17 percent is used to obtain available power at the battery for charging. At an average cell charge voltage of 1.42 the charge current is 1.55 amps or approximately a C/8 rate (parallel battery charging). During the eclipse period and including the last daylight voice transmission the battery is discharged to 47.2 percent of rated capacity. Using battery charge time data presented in Appendix 8A,

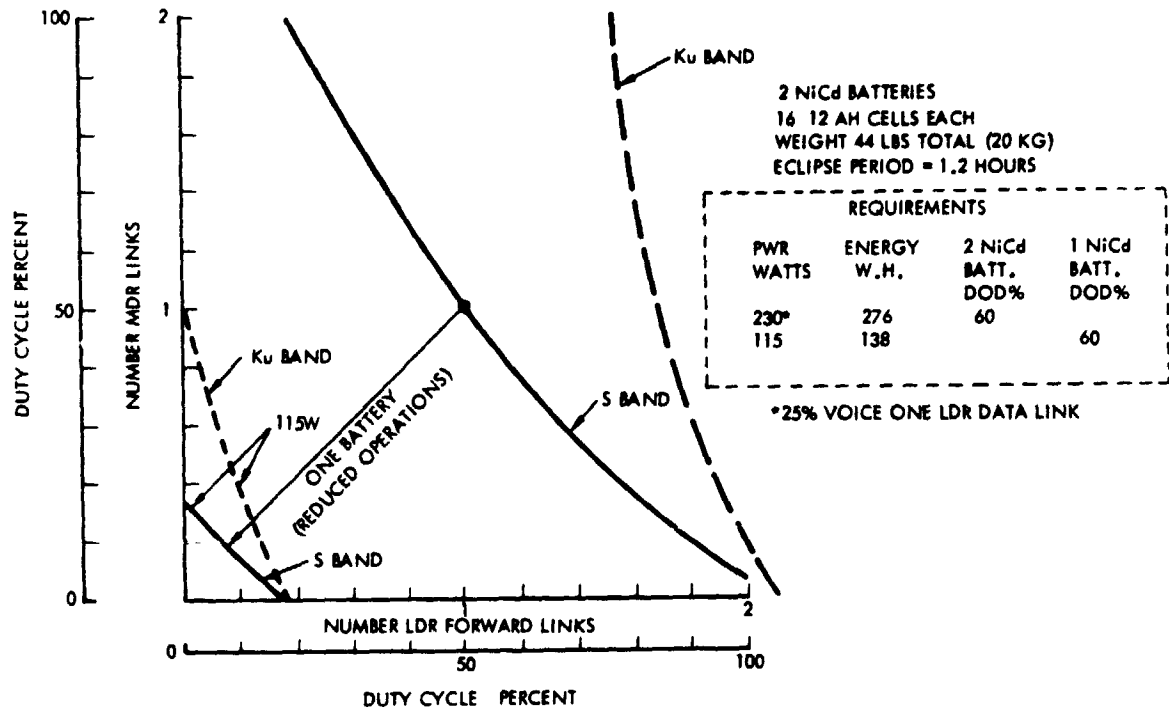


Figure 8-4. Battery Requirements - Maximum Eclipse Period - 2 NiCd Batteries

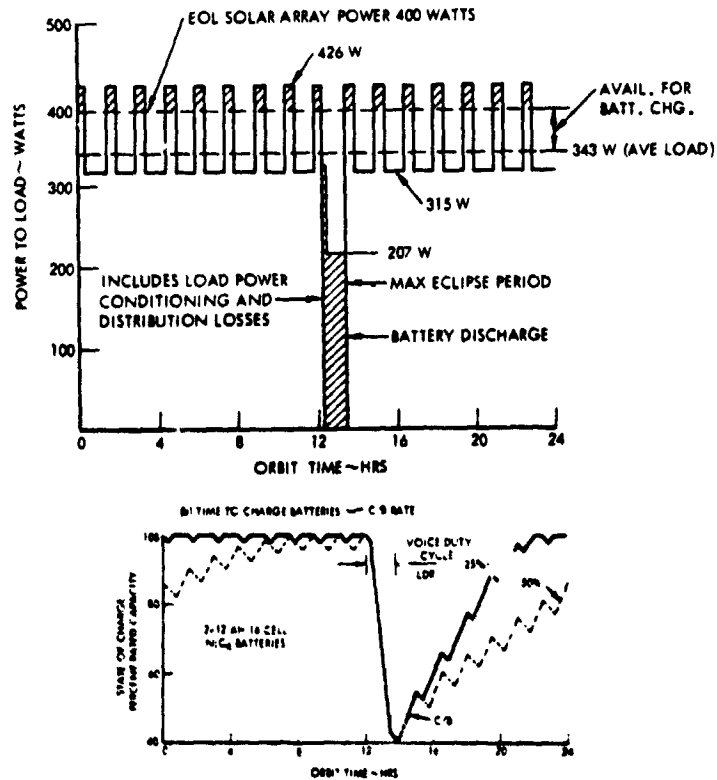


Figure 8-5. Time Required to Charge Batteries

Table 8-2. EPS Sizing Requirements

Identification Assy/Component	Description	Requirement
Primary Power Generation Solar panel Drive Mechanism	Transfer Orbit Avg. subsystem load Normal Operations Total array power Array specific power Array specific heat Solar cell characteristics Orientation Power transfer	See Table 8-3 466 watts B.O.L. 10.35 watts/ft ² B.O.L. (111.5 watts/m ²) 0.22 Btu/ft ² °F (0.692 watts/m ² °F) 125 ma (45 mv) 28°C Single axis (360°/day continuous) + 6° from sunline 16.7 amps (28 vdc)
Energy Storage Secondary batteries	Transfer Orbit Energy requirement Normal Operations Eclipse load, average/peaks Energy Voltage (nominal) Discharge Charge	Supplement solar array as required (not to exceed 276 watt-hours) See Figure 8-3 276 watt-hours 1.2 volts/cell 1.42 volts/cell
Power Conditioning Charge regulator Discharge regulator Shunt dissipator Amp-hr meter Voltage converter	Battery Charge Voltage range Current (range) Current (nominal) Current (maximum) Output Voltage Modulation range Dissipation level (continuous rating) Maximum current Solar array bus voltage Maximum Minimum Accuracy Current range (nominal) Charge Discharge Voltages Input Output Rating	16.5 to 24.5 vdc 2.91 to 1.96 amps 2.11 amps (at 1.42 volts per cell) 6.0 amps 28 volts - 1 volt (with battery input voltage range 16.0 to 24.5 volts) Over 437.5 watts 184 watts 6.35 amps dc ±2 percent 0 to 2.91 amps 0 to 12.0 amps 28 ± 1 volt 18 ± 1 volt 68.6 watts
Distribution and Control Central Control and Logic Cabling	Functions Functions Current capability	Mode control (array shunting; battery charge regulator; and battery discharge boost regulator) 16.7 amps (at nominal 28 vdc)

Table 8-3. Electrical Load Chart (watts)

Subsystem	Daylight		Eclipse		Transfer Orbit	Comment
	Average	Peak	Average	Peak		
Attitude Stab. and Control****	16.5	100.5	13.5	85.5	5.2	VHF transmitter on standby
Heaters	2.0	25.2	1.0	25.2	10.4	
TT&C	10.5	14.5	10.5	14.5	14.5	
Telecomm. Services**	(249.3)		(179.4)			25 percent voice 100 percent data
LDR						
Receive	9.1	9.1	9.1	9.1		
Transmit #1*	64.0	137.6	64.0	137.6		
Transmit #2**	40.4	40.4				
Divider	11.4	11.4	11.4	11.4		
MDR No. 1						S-band
Receive	6.2	6.2	6.2	6.2		
Transmit #1 (S-band)	47.5	190.0	47.5	190.0		
Antenna track and control element	7.0	24.0	7.0	24.0		
MDR No. 2						Ku-band
Receive	6.2	6.2	6.2	6.2		
Transmit #2 (Ku-band)	13.2	13.2				
Antenna track and control element	7.0	24.0	7.0	24.0		
TDRS-GS						
Receive	5.3	5.3	5.3	5.3		
Transmit	11.0	49.0***	11.0	49.0***		
Antenna track and control element	--	9.5	--	9.5		
Frequency Source	4.8	4.8	4.8	4.8	4.8	
TDRS Tracking Transponder	7.9	7.9	--	--		
Ku-Band Acq. Beacon	8.3	8.3	--	--		
Solar Panel Drive and EPS						
Central Controls	15.7	33.2	8.5	29.2	5.2	
Contingency	6.0					
Subtotal	300.0		213.0		40.1	
Battery Charge	48.0					
Power Condit./Line Losses	52.0		17.0		3.9	
Total	400.0		230.0		44.0	
Array Output E.O.L.	400.0					
Degrad. Allowance (5 years)	66.0					
Array Output B.O.L.	466.0					
Battery Load			230.0			

* Includes 25 percent duty cycle voice (23.6 watts) + power conditioning for voltage conversion
 ** Telecom. values taken from Table 4-3 with power conditioning requirements added where applicable.
 *** 10 dB added for operation during heavy rain.
 **** Based on 20% duty cycle - yaw gyro and nutation damper



Table 8-4. Telecommunication Service Low Data Rate Voice Transmission Power Requirements (Watts)

Orbit	Full Sunlight	Sun Eclipse
Telecommunication Mode (LDR)	One S- plus one Ku-band	One S-band
Attitude Stab. and Control Heaters } TT&C }	29.0	25.0
MDR No. 1	60.7	60.7
MDR No. 2	26.4	13.2
TDRS-GS	16.3	16.3
Frequency Source } Tracking Beacons }	21.0	4.8
Solar Array Drive } Controls }	15.7	8.5
Subtotal	169.1	128.5
LDR No. 2 (Data)	60.9	20.5
Subtotal	230.0	149.0
LDR No. 1	137.6 (voice)	137.6 (voice)
	40.4 (data)	40.4 (data)
Total	367.6	286.6
Duty Cycle	25 percent	75 percent
Average	300	213

the time required to return the batteries to full charge is 5.2 hours with worst case battery temperature of 78°F.

Table 8-5 shows estimated battery life for the operating conditions shown by Figure 8-5. The estimates shown are based on the available number of discharge cycles as a function of depth of discharges data given in Appendix 8A where results are shown for battery cycle life based on the least squares fit curve and the -3 sigma line. It is assumed that the battery life use is a cumulative effect of the number of cycles at different depths of discharge. For example, at 2 percent depth of discharge and using the -3 sigma line 18,000 charge/discharge cycles are indicated. The batteries will be required for peaking in the mode shown by Figure 8-5 between the fourth and fifth mission year. This results in 5470 battery cycles. The ratio of 5470 to 18,000 results in 30.2 percent of battery life used in this operating mode. The battery life used during eclipse is based on 90 eclipses per year for five years based on a maximum depth of discharge of 60 percent and an average of 45 percent.

Table 8-5. Estimated Battery Life Consumed in 5 Years

No. Peaking Batteries	2	2	1	1
Batt DoD Peaking %	2	2	1	4
Batt Peaking Cycles	5470	5470	2735	2735
Battery Life Criteria Peaking ⁽¹⁾	MEAN	-3 σ	MEAN	-3 σ
Allowable Cycles Peaking	50,000	18,000	45,000	16,500
Batt Life Used Peaking %	10.9	30.2	6.1	16.6
Batt Life Used Eclipse % ⁽²⁾	20.2	20.2	20.2	20.2
Total Batt Life Used	31.1	50.4	26.3	36.8

(1) Figure 8A1 (Appendix)
(2) Based on average depth of discharge of 45% during 10 eclipse periods and -3 σ cycle life curve from (1)

Based on the -3 sigma line the battery life used during eclipses is 20.2 percent. The two lifetime depletions added together indicates 50.4 percent of battery life used. These are obvious uncertainties in using the above approach to estimate battery life, since the charge/discharge cycle allowable at very low depths of discharge are primarily an extrapolation. Since a substantial margin in battery life used exists when compared with 100 percent depletion for worst case assumptions, the above approach is adequate at this time.

Other variations in operating mode of the telecommunications service were considered. Table 8-6 shows MDR variations of 2 S-bands, 2 Ku bands, and 1 S-band + 1 Ku band in the forward link. The impact on average power is shown to range from 54.1 watts to 119 watts.

Table 8-6. Variations in MDR Power Requirements (Watts)

Item	2 S-Bands		2 Ku-Bands		1 S + 1 Ku-Band	
	Average	Peak	Average	Peak	Average	Peak
MDR No. 1						
Receive	6.2	6.2	6.2	6.2	6.2	6.2
Transmit	47.5	190.0*	14.5	14.5	47.5	190.0*
Antenna Track	7.0	24.0	7.0	24.0	7.0	24.0
MDR No. 2						
Receive	6.2	6.2	6.2	6.2	6.2	6.2
Transmit	45.1	45.1	13.2	13.2	13.2	13.2
Antenna track	7.0	24.0	7.0	24.0	7.0	24.0
Totals	119.0		54.1		7.1	

*Instantaneous peak powers for voice

8.1.2.2 Transfer Orbit

An average power of 44 watts must be provided through prelaunch, boost, parking orbit, and transfer orbit when the solar array is not deployed. However, in its stowed configuration, the solar cells face outward and supply power after shroud jettison. Table 8-7 summarizes the energy requirement variations of primary interest.

Table 8-7. Transfer Orbit Energy Requirements

Power Level (Average)	Duration	Energy W.H.	Description
44 watts	16 hrs. 15 min.	715	Descending node launch* and 2nd apogee
	27 hrs. 15 min.	1210	Descending node launch and 3rd apogee

*Baseline profile

Total dependence on batteries during this period has the disadvantage of a critical time limit as well as heavier batteries. To supplement and/or remove the battery dependence (time criticality), the EPS baseline utilizes the solar array in the stowed configuration.

Table 8-8 summarizes the calculated efficiencies used in the subsequent sizing of the EPS. The battery charging efficiencies as a function of charge rate is shown in Figure 8-6.

Table 8-8. EPS Component Efficiency
(Sizing Model)

Identification Assy/Component or Line	Voltages		Efficiency Factor
	Input	Drop	
Solar Panel			0.94 (2350 cells/m ²)
Design Packaging			0.942 (41°C)
AVE Temp Effect			0.95
Glass Loss			0.98
Assy Loss			0.95
Off Opt. OPS			0.857 (5 years)*
Radiation Degrad.			0.95
Design Margin			
Isolation Diode	30.8	0.8	
Power Transfer & Line Losses To Load		1.0 (Max)	
Charge Regul.	28.0	Min 1.5	.90 (Nominal)
Boost Regul.	19.2		.925 (Nominal)
			(0.85 Min E.O.L.)
A. H. Meter	24.0		.95
Voltage Converter	28.0		.85
Battery Charge			(See Figure 8-6)

* $\frac{V_{pm}}{V_{pmo}} = 0.95$ $\frac{I_{pm}}{I_{pmo}} = 0.903$

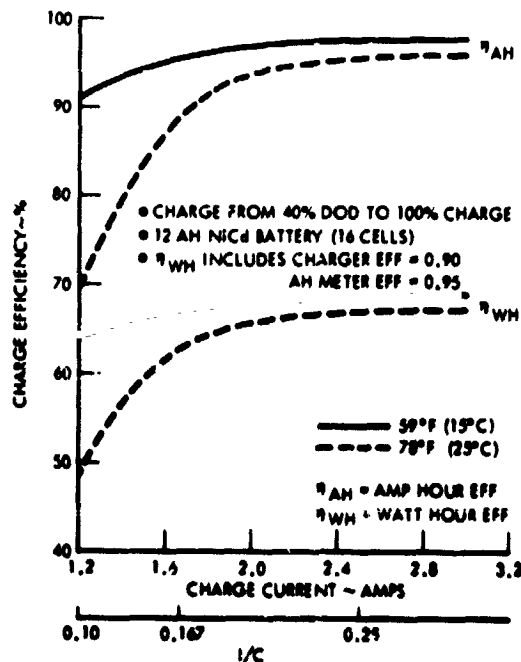


Figure 8-6. Average Battery Charge Efficiencies

8.1.3 EPS Description

The EPS block diagram is shown in Figure 8-7. Power is supplied directly from the solar array to the loads with a central regulated 28 ± 1 volt bus. Voltage regulation is accomplished by a shunt regulator operating as a variable load across lower sections of the solar array panels. Each solar array panel is approximately 22.5 ft^2 (2.09 m^2) for a total area of 45 ft^2 (4.18 m^2). Based on 10.35 w/ft^2 (115 w/m^2), beginning of life (BOL) power output of 466 watts is expected with an end of life (EOL) power output of 400 watts (allowing for space radiation effects over the five years operating life). By shunting only a portion of the solar array and locating the shunts on the array, the net thermal dissipation is substantially reduced. Full functional redundancy is built into each solar array orientation drive, with an independent drive provided for each solar array panel. The solar array drive and power transfer assembly orients the solar array panels normal to, and steps it to follow the spacecraft sunline and transfer power to the central bus. Electrical power and signals are transmitted between the rotating array and the spacecraft through slip rings with redundant brushes.

The central power control unit controls the various EPS operational modes. It operates by detecting the difference between the main bus and reference voltage levels. The difference error is amplified and used to drive the system functions (i.e., supply regulated power, provide control of battery charge and to dispose of excess power generated by the solar array). Since the solar array is a constant power source to supply larger amounts of power to subsystem loads, battery charging must be inhibited and/or the boost regulator activated to supply power from the batteries. The regulator has a nominal rating of 230 watts based on the tabulated night time load. The charge regulator is basically a series dissipative regulator controlled by external stimuli to provide desired output voltage and current conditions for charging the battery. The ampere-hour meter provides state of charge information for telemetry. The ampere-hour meters monitor the input and output ampere-hours of the nickel cadmium battery. This device multiplies replaced or charging power by a charge efficiency characteristic of the battery which varies with battery temperature. Each meter integrates battery current with time and keeps track of the ampere-hours in the battery.

The voltage converter is required to provide 18.0 volts to the LDR for data transmission. This converter operates from the 28-volt regulated bus and supplies an output of 18 volts with a rating of 68.6 watts based on the LDR transmitters load requirements. The weight includes an active redundant unit.

A battery charging allowance of 48 watts (net to the batteries) is sufficient to permit parallel charging of the two batteries. Several charge characteristics will be available to permit more rapid battery charging, depending upon the availability of solar array power. This will be done by setting a charge current limit and permitting any charge current to that limit. A weight summary of the EPS is shown in Table 8-5. As shown, the weight breakdown of 155.6 lb (70.6 kg) is made up of three major items: (1) solar array, 58.6 lb (26.6 kg), (2) power conditioning and distribution, 52.7 lb (23.9 kg), and (3) energy storage, 44.3 lb (20.1 kg).

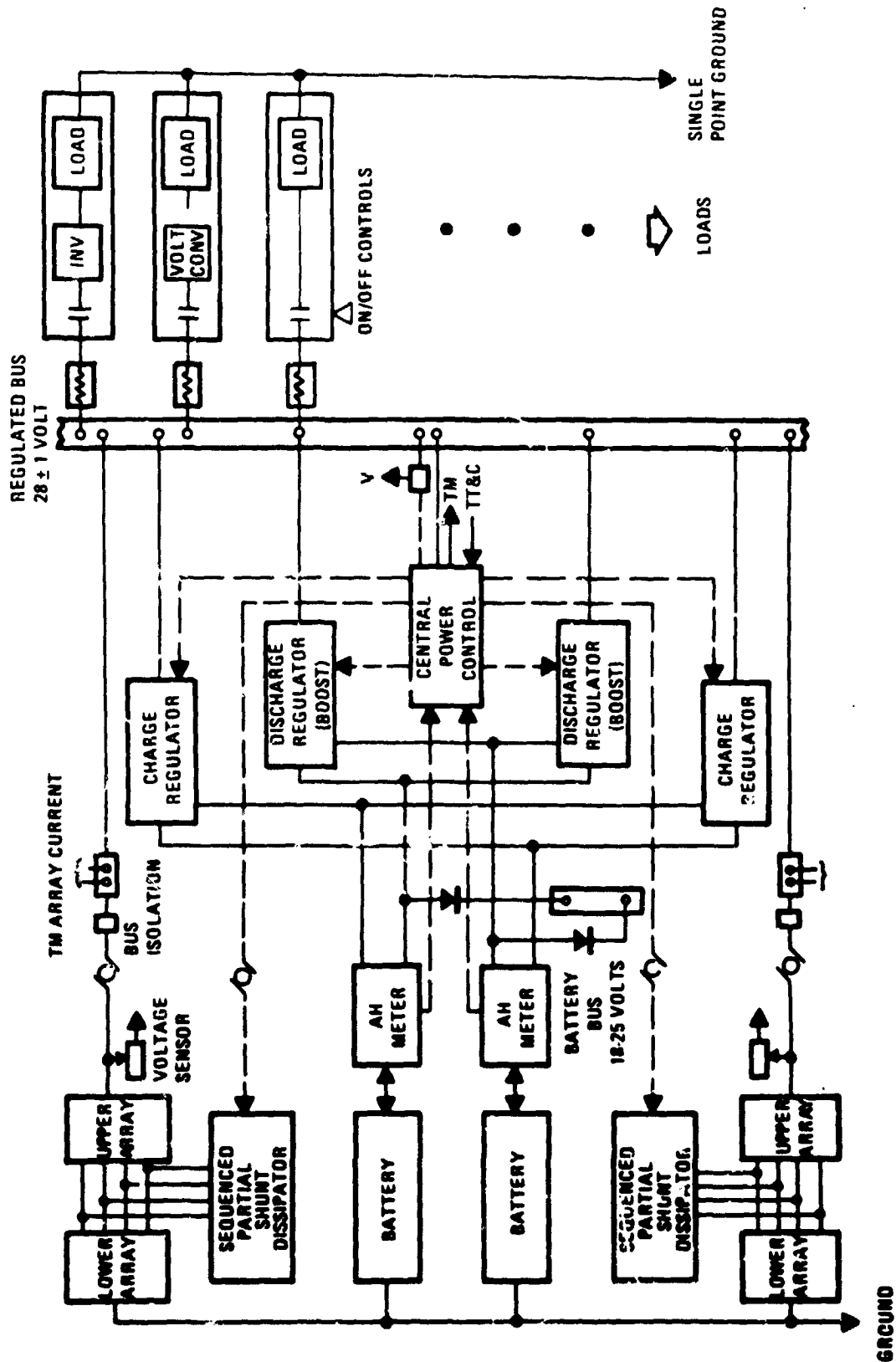


Figure 8-7. Electrical Power Subsystem Block Diagram

Table 8-9 Electrical Power Subsystem Weights

Components/Assemblies	Weight		Potential Supplier
	Kg	lb	
<u>Solar Array</u>	(26.6)	(58.6)	
Panels (2)	17.5	38.6	EOS, Ferranti
Drive Mechanism (2)	6.8	15.0	BBRC, SPAR, GE
Linkage and Fitting (2)	2.3	5.0	NR
<u>Power Conditioning & Distri.</u>	(23.8)	(52.7)	
Charge and Discharge	5.1	11.3	
Central Control and Logic	2.3	5.1	GE
Packaging	2.2	4.9	
Shunt Dsssipators	1.1	2.4	
Amp Hr Meters	1.8	4.0	Fngr. Magnetics
Power Conditioner Voltage	2.3	5.0	
Cabling	9.1	20.0	NR
<u>Energy Storage</u>			
Batteries (2)	(20.1)	44.3	GE
Total	70.5	155.6	

8.2 PRIMARY POWER GENERATION ASSEMBLY

The primary power generation assembly consists of the solar arrays to convert solar energy to electrical power; drive mechanism to orient the solar panels normal to the sunline, and transfer power to the spacecraft load bus; and the necessary linkage and fittings for attachment to the spacecraft.

8.2.1 Solar Array Function and Description

Figure 8-8 shows the selected solar array characteristics. Additional detail is shown in Figure 5-4. The solar cells generate electrical power at 32.4 volts (BOL 41C) based on 45 mv per cell and 72 cells in series. Using an estimated voltage degradation factor of 0.95 reduces this voltage to 30.8 volts at the end of life (five years).

Each panel is divided into 12 six-cell (parallel) strings. A separate shunt dissipation circuit is used for each of the 6-cell strings. The tap point between the upper and lower sections of a single string is located at 50 percent of the total string length. This is based on array performance upon emergence from eclipse when the array is coldest. At this minimum temperature (-121 C) at no load conditions (i.e., cell open circuit voltage of 0.71 volts/cell) the 50 percent tap results in a voltage of 25.6 volts or well below and adequate to prevent excessive bus voltage. Utilizing a proposed design by General Electric (reference 8-1) the highest shunt dissipation occurs at the no-load condition and has a value of 18 watts per string. To avoid maximum dissipation if all strings operated simultaneously, the shunt circuits are operated in three-step sequences.

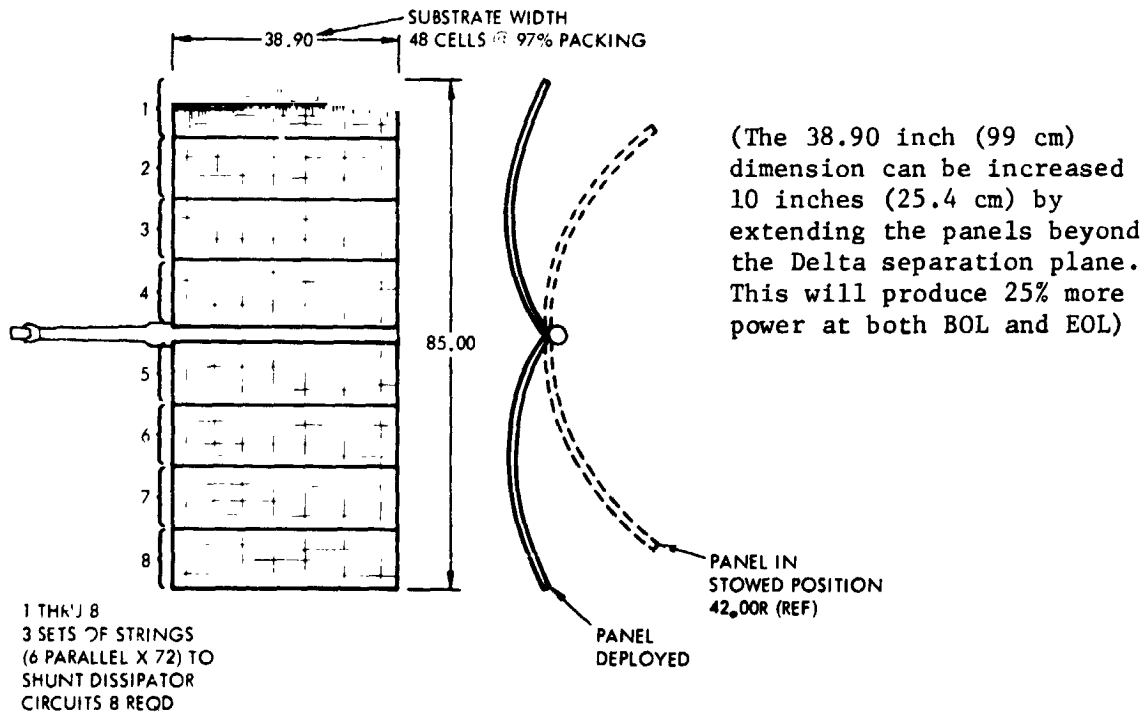


Figure 8-8 Solar Panel Array Configuration

Considering a single 3-circuit group, circuit No. 1 first operates to saturation, then circuit No. 2 and finally No. 3. The saturation drop across each shunt circuit is 1.5 volts and has a dissipation of 2.4 watts. The maximum dissipation for each 3-circuit group then occurs when two circuits are saturated and the third operates at maximum dissipation for a total of 23 watts. For eight 3-circuit groups, the highest dissipation is 184 watts.

Figure 8-9 shows the schematic of the shunt dissipator for 12 strings representing one solar panel (wing) i.e., one half of the total solar array.

Power across the rotating interface is achieved by slip rings with redundant brushes similar to the NIMBUS slip ring assembly. Six brushes are provided on every power ring; any two brushes could fail without any degradation in performance. Each brush is provided with a separate lead and connector pin to enhance its reliability. Oversize brushes provide life and current density margin. Brush slip rings are selected because of their excellent flight proven reliability. Life is not a problem based on a highly conservative design. Using slip rings permit continuous 360 degree rotation of the array.

The selected solar array configuration consists of two panels (wings), each having a nominal area of 27.5 ft² (2.09 m²) (projected area) with a total of 5784 cells per panel (i.e., 10,368 cells for the complete solar array).

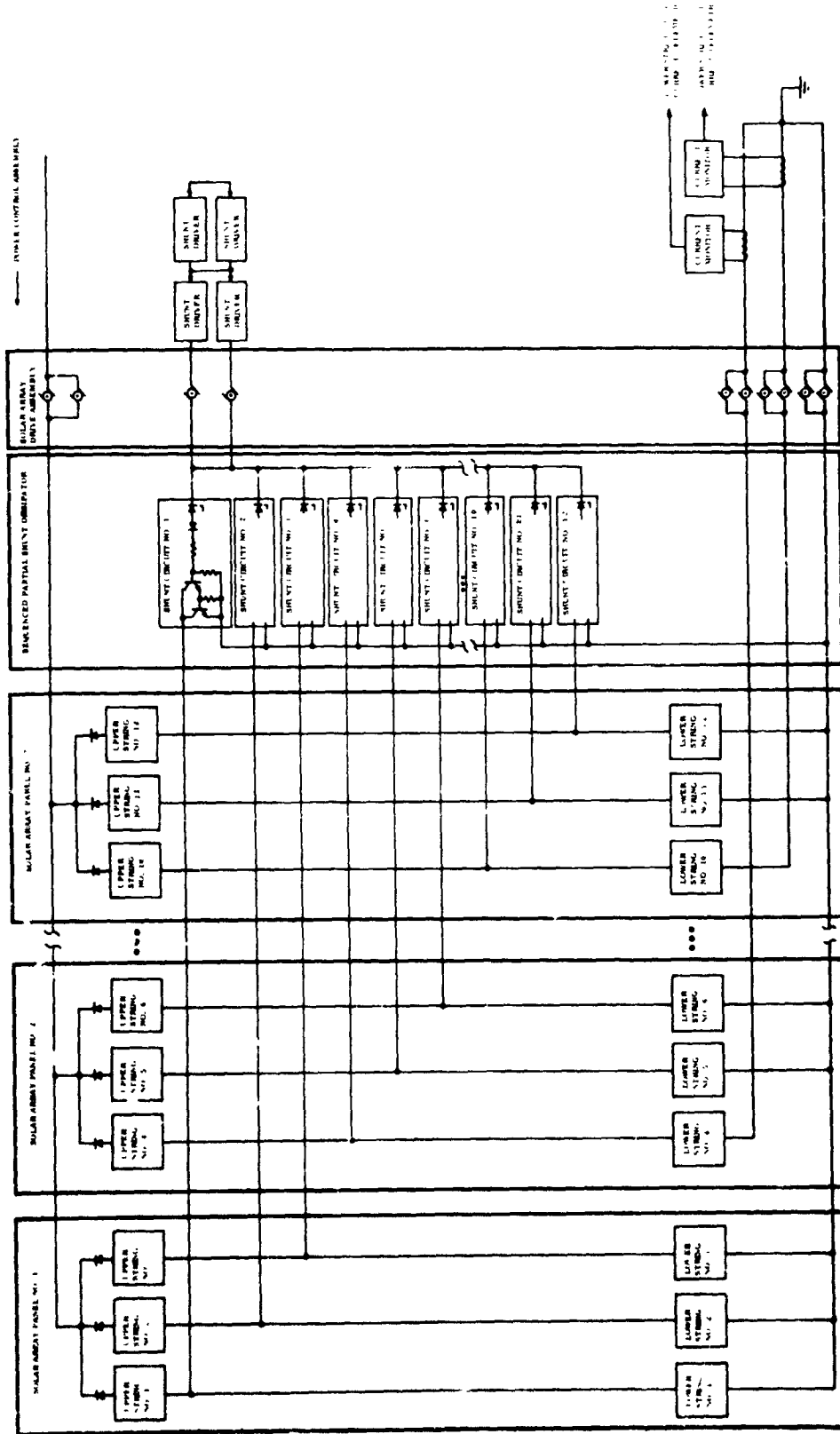


Figure 8-9. Schematic of Shunt Dissipator

8.2.2 Solar Array Assembly Characteristics

The characteristics of the selected solar array assembly are given in Figure 8-10. Computer simulation was used to generate temperature and power profiles taking into account thermal inputs and albedo from the earth. The temperature profile shown is based on a panel specific heat of $0.22 \frac{\text{Btu}}{\text{ft}^2 \cdot ^\circ\text{F}}$. This corresponds to approximately 0.84 lb/ft^2 as shown in the plot of solar array panel eclipse temperature vs thermal capacitance in Figure 8-11. A detailed weight statement of the solar array assembly is given in Table 8-10.

Table 8-10 Solar Array Assembly Weight Summary

Array Area, Total	45 FT ² (4.2 m ²)	
Cover Glass Material	Fused silica	
Solar Cells	Silicon N/P	
Coating	TiO ₂	
Solder	Machine pressed	
Substrate	Al. honeycomb	
Type		
ITEM	Weight	
	(lb)	(kg)
Cover Glass	5.55	2.52
Adhesive	0.43	.20
Solar Cells	6.69	3.03
Solder	0.97	.44
Cell to Sub. Adhesive	0.99	.45
Wiring, Term. Bds. Intl. Conn.	3.85	1.75
Subtotal	18.48	8.49
Substrate	20.12	9.14
Subtotal	38.6	17.5
Solar Array Drive System (Housing, shaft, drive motor, bearings, lubrication and slip rings) (2)	15.0	6.8
Linkage and Fittings (2)	5.0	2.3
Total	58.6	26.6

The estimated performance of the solar array is based on a total of 10,368 cells at $60 \frac{\text{mw}}{\text{cell}}$ or a gross array power of 620 watts. Degradation factors shown in Table 8-8 were applied to reduce the array power to 482 watts, i.e., $620 \text{ watts} (0.79) = 482 \text{ watts} (41\text{C})$. A correction factor of 0.97 was applied for effects of a curved surface to further reduce the expected array power to 466 watts (B.O.L.). End of life power is calculated to be 400 watts based on a space radiation degradation factor of 0.857, i.e., $466 \text{ watts} (0.857) = 400 \text{ watts E.O.L.}$ The radiation reduction factor results from radiation flux of 2.2×10^{14} (1 Mev) electrons/cm² (5 years), and obtained from Figure 8-12. A cover glass thickness of 12 mils was selected to

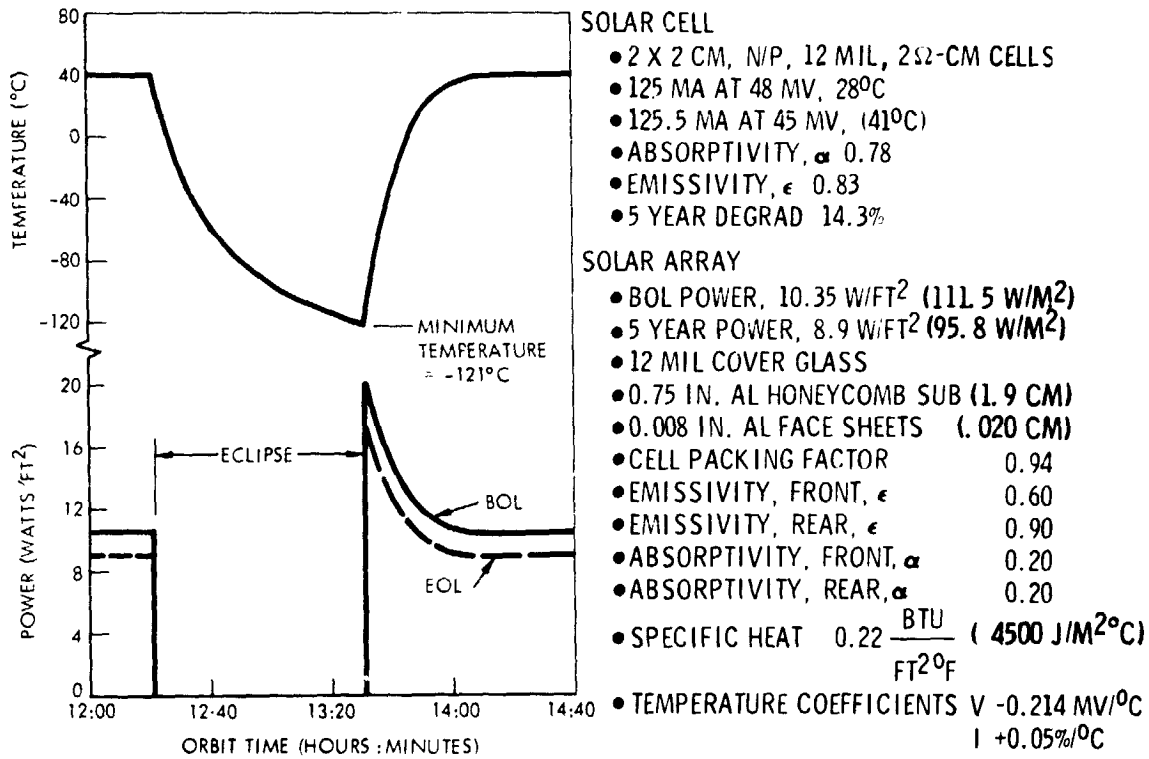


Figure 8-10 Solar Array Characteristics

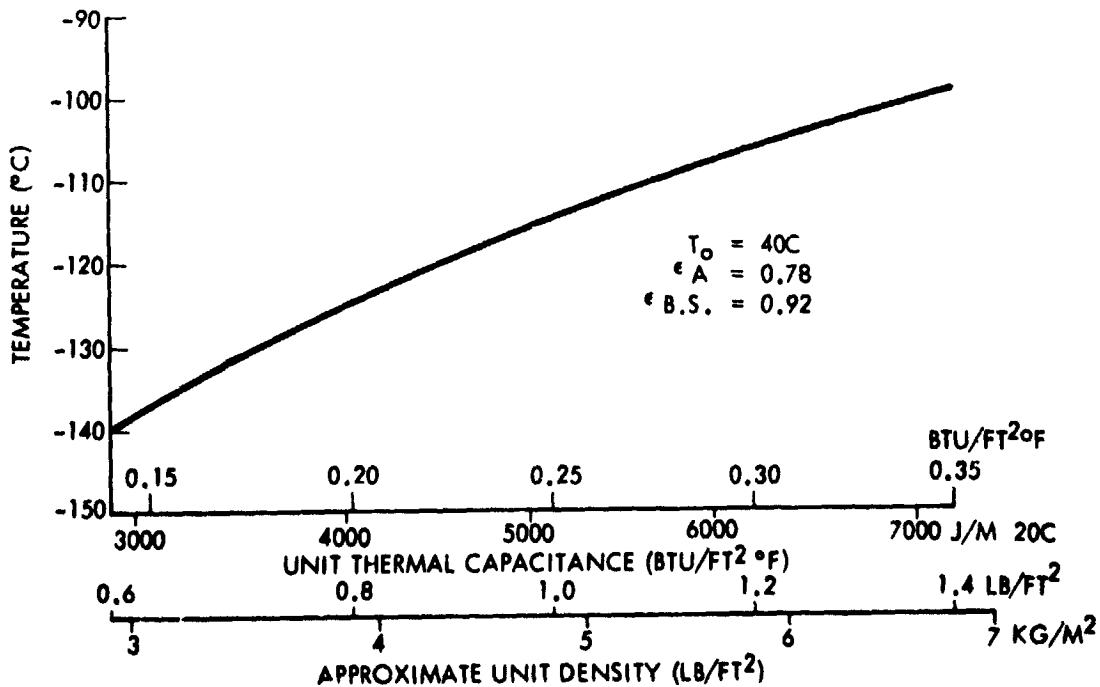


Figure 8-11. Solar Array Panel Eclipse Temperature vs Thermal Capacitance

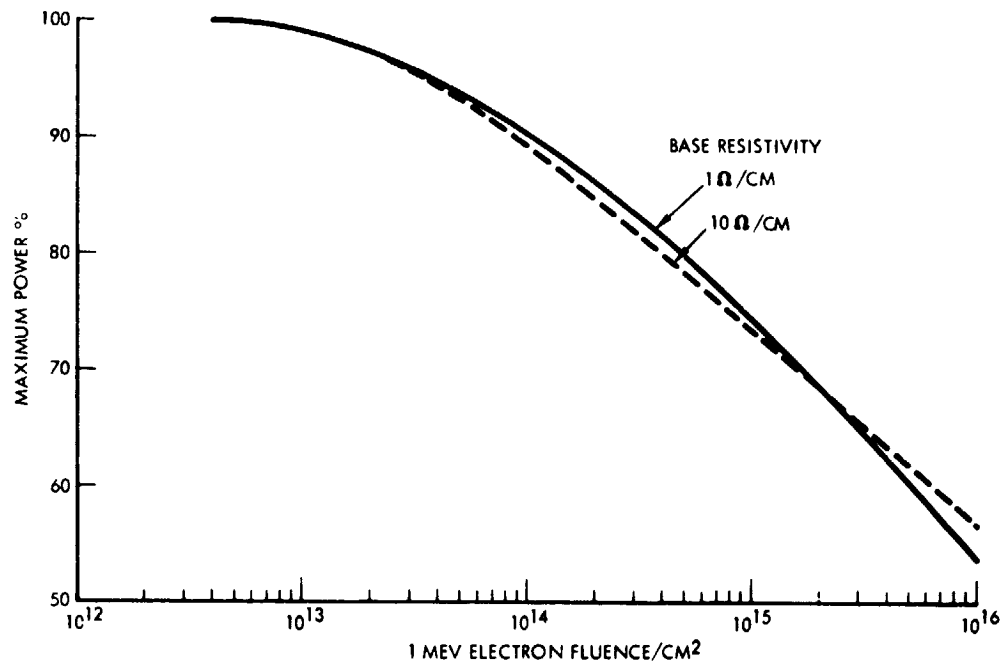


Figure 8-12. Degradation of Maximum Power of Hoffman N/P Si Solar Cells Under 1 mev Electron Bombardment

optimize utilization of available area based on less radiation degradation and considering the fact that a heavier mass provides less temperature extremes during maximum solar eclipse. There was an approximate 1.5 ft² (.14 m²) area savings which co-pensated for the lighter weight of the 6-mil cover glass.

8.2.3 Operational Constraints and Growth Considerations

The solar array assembly will not result in any operational constraints during normal mission modes. As shown in Figure 8-3, there is a variation in sunline inclination and array performance as a function of earth position, i.e., +23.5° (.41 rad) inclination from the sun at summer and winter solstice. The decrease in available power during these extremes is compensated by the reduced requirement in battery charging since during this period the spacecraft is in full 24-hour sunlight. This battery charging savings of 48 watts (net) more than compensates for the approximately 30-watt lower array power (reference Table 8-11).

Present solar array packaging constraints limit the array to a total of 45 ft² (4.18 m²). The Thor Delta will allow a 10-inch (25.4 cm) extension aft of the separation plane, providing 25% increase in solar array area. This is not incorporated into the baseline design. A minor modification in array configuration to include an additional fold increases the available area to 82 ft² (7.6 m²). Detailed system analysis of these modifications would be necessary to implement the change.

Table 8-11. Array Performance Factors

Parameter	Earth Position	
	Equinox	Perihelion
Solar constant w/m^2	1396	1351
Temperature (deg C)	41	33
Angle of incidence	0°	23.5° (.41 rad)
Array performance w/ft^2 (w/m^2)	10.35 BOL (111.5)	9.6 BOL (103.5)
	8.9 EOL (95.6)	8.25 EOL (88.9)

Continual effort to improve solar cell efficiency is underway by various organizations. This is evidenced by recent announcements by IBM on an 18-percent SaAs cell and by Comsat on a 14-percent silicon solar cell. The more near-term availability of the Comsat cell could increase the power level per unit array area by 20 to 30 percent over the selected (baseline) conventional N/P silicon solar cell. This would provide either an area and weight reduction and/or increased design margin for TDRS. Mass production techniques must be developed together with achieving complete performance testing prior to considering these cells as state of art.

The improvement in cell performance of the Comsat cells is attributed primarily to three significant changes in the conventional N/P silicon solar cell mechanism:

1. Formation of a shallower junction depth in the order of 0.1 micron which increases the blue spectrum response of the cell.
2. Use of a titanium oxide anti-reflective coating to provide a better match and higher transmission of blue light.
3. Grid configuration change and increase in number of grid lines by an order in magnitude from the standard configuration of six.

Limited operational test data indicate that these cells may be about 30 percent better in performance than the conventional silicon N/P silicon cell at end of life (5 to 7 years in earth synchronous orbit).

8.3 ENERGY STORAGE ASSEMBLY

This section defines the energy storage assembly requirements, characteristics, and operational constraints. Analysis and trades leading to energy storage definition are in Appendix 8B.

8.3.1 Function and Description

The energy storage assembly supplies electrical power to spacecraft loads during sun eclipse periods of the orbit, supports peak loads in excess of solar array power available during sunlight periods, and augments available solar array power during the transfer orbit. At equatorial synchronous altitudes, two 45-day eclipse seasons occur each year. Figure 8-2 shows the eclipse period varies from zero to a maximum of 1.2 hours. Total dark time for each season is approximately 40 hours, providing an average daily eclipse of 53.5 minutes. Table 8-12 summarizes spacecraft energy requirements during eclipse as a function of forward communication data links used. Power required includes spacecraft subsystem, telecommunication services, and power conditioning losses. Maximum data link utilization (4 on) during the maximum eclipse period requires 348 watt-hours of energy (i.e., 291 watts x 1.2 hours). In order to obtain acceptable battery weights, one S-band data link was taken as the baseline. A five-year operational lifetime requires 450 charge-discharge cycles of varying depths of discharge from the batteries. These two factors dictated a choice of two nickel-cadmium batteries (230-watt-hour capacity each). To obtain five-year operational life with an adequate margin, a maximum depth of discharge of 60 percent rated capacity was used.

Figure 8-13 shows spacecraft operational constraints when operating on battery power. This is a graphical representation of data in Table 8-12. For example, at a 60-percent depth of discharge (two batteries) the following telecommunication services may be provided at worst case eclipse.

- . Two S-band continuous plus 14 percent LDR duty cycle
- . One S plus one Ku-band continuous, plus 35 percent LDR duty cycle
- . One S-band continuous plus 50 percent LDR duty cycle (baseline)
- . Two Ku-bands continuous plus 70 percent LDR duty cycle

In case of battery failure, one Ku-band (with no LDR) could be continuously operated for 72 minutes to 60-percent battery depth of discharge. In the event of a battery failure it is planned to reduce spacecraft operations to reduce fixed loads by 10.9 watts (i.e., no array orientation, etc.). The dark period for one-half of the eclipse season is 56 minutes or less. 148 watts of power is available from a single battery for a period of 56 minutes when discharged 60 percent. Therefore, for approximately one-half of the eclipse season, a single battery will allow continuous operation of one S-band or one LDR forward link.



Table 8-12. Eclipse Period Maximum Energy Requirement (1.2-Hour Maximum Eclipse Period)

		← REDUCED OPS →												
DATA LINKS	LDR MDR • S-BAND • KU-BAND	0	1	2	0	1	2	0	1	2	0	1	0	0
CONSTANT		101.4	101.4	101.4	101.4	101.4	101.4	101.4	101.4	101.4	101.4	101.4	90.5	90.5
LDR			64.0	104.3		64.0	104.3		64.0	104.3		64.0		
MDR														
• S-BAND					47.5	47.5	47.5				14.5	14.5		47.5
• KU-BAND														
SUBTOTAL	POWER COND. $\eta = .915$	101.4	165.4	205.7	148.9	212.9	253.2	115.9	179.9	90.5	105.0	138.1		
TOTAL (WATTS)		111.0	181.0	225.0	161.0	230.0	276.0	126.0	197.0	99.0	115.0	150.0		
WATT-HOURS REQUIRED		133	218	270	193	276	331	151	236	119	138	180		
DATA LINKS	LDR MDR • S-BAND • KU-BAND	2	0	1	2	0	1	0	1	0	0	1	1	2
CONSTANT		101.4	101.4	101.4	101.4	101.4	101.4	101.4	101.4	101.4	101.4	101.4	90.5	90.5
LDR				64.0		64.0	64.0		64.0	64.0		64.0		
MDR														
• S-BAND					47.5	47.5	47.5				27.7	27.7		14.5
• KU-BAND														
SUBTOTAL	POWER COND. $\eta = .915$	220.2	163.4	227.4	267.7	194.0	258.0	129.1	193.1	145.3	185.6			
TOTAL (WATTS)		241.0	177.0	247.0	291.0	212.0	282.0	141.0	210.0	159.0	210.0	210.0		
WATT-HOURS REQUIRED		269	212	296	249	254	339	169	252	191	252	252		

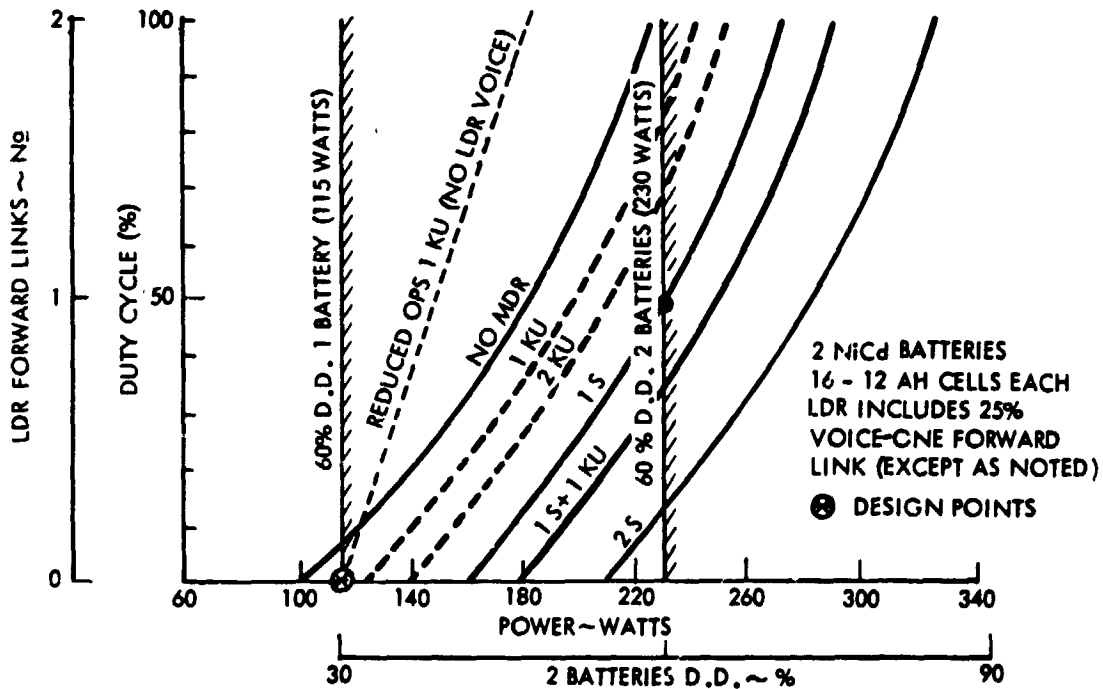


Figure 8-13. Baseline Battery Capability Maximum Eclipse

8.3.2 Assembly Characteristics

8.3.2.1 Physical and Performance Characteristics

Characteristics of the selected battery cell are summarized in Table 8-13. The cells are nickel-cadmium, 12 ampere-hour, manufactured by General Electric. They are rectangular and hermetically sealed with stainless steel containers and covers. The terminals are insulated from the cell cover by ceramic seals, and the terminals protrude through the cover with solder tabs welded to the top. The cell incorporates an auxiliary electrode for charge control. The reaction of oxygen (produced on charge) with the active material of the auxiliary electrode produces a voltage in direct proportion to the oxygen pressure and, consequently, the amount of charge returned to the cell. The auxiliary electrode is welded to the inner surface of the cell container.

8.3.2.2 Interface Requirements

Performance of the batteries will be monitored and controlled by ampere-hour meters, central power control unit, and boost discharge regulators. Battery charge will be controlled by a regulator which in turn is controlled by the central power control. The above components are included in the power conditioning assembly and are discussed in Section 8.4.

Table 8-13. Nickel-Cadmium Battery Cell Characteristics
(GE Catalog No. 42B012AB53)

CAPACITY @ 2 HOUR RATE	12	AH
CELL WEIGHT	1.12	LBS (.51 KG)
CASE MATERIAL	301	STAINLESS STEEL
RECOMMENDED CHARGE RATE @ 25°C, 16 HOURS	1.2	AMPS
RECOMMENDED MAXIMUM CHARGE - CONTINUOUS @ 25°C	1.5	AMPS
TEMPERATURE RANGE - STORAGE **	-40°C to 50°C	
TEMPERATURE RANGE - CHARGE	-10°C to 40°C	
TEMPERATURE RANGE - DISCHARGE	-10°C to 40°C	
MAXIMUM CONTINUOUS DISCHARGE	120	AMPS
IMPEDANCE	2-4	MILLIOHMS
CELL LEAKAGE RATE	LESS THAN 1X10 ⁻⁸ CC/SECOND OF HELIUM	

RECOMMENDED -10°C to 15°C**

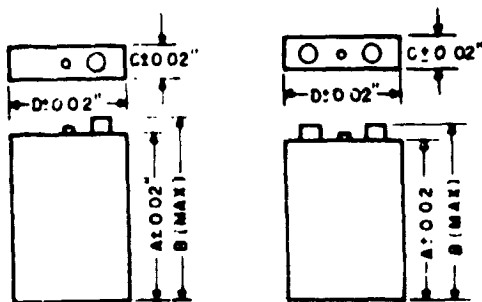


FIG-1

FIG-2

A	B	C	D
4.03	4.64	.891	2.99

NICKEL-CADMIUM BATTERY CHARACTERISTICS

TYPE	HERMETICALLY SEALED
NUMBER CELLS	16
NOMINAL RATINGS	
AMP HOURS	192
WATT HOURS (@ 1.2 V/CELL)	230
DISCHARGE VOLTAGE (C/2 RATE)	19.2
CHARGE VOLTAGE (MAX)	24
CHARGE TERMINATION	SIGNAL ELECTRODE
OPERATING TEMPERATURE, MAX (SOLITICES)	75°F (24 C)
OPERATING TEMPERATURE, MIN (EQUINOXES)	65°F (18 C)
LIFE (DESIGN GOAL @ 60% D.D. MAX)	5 YEARS
WEIGHT	22.15 LB (10.1 KG)
DIMENSIONS, INCHES	7.8 x 8.0 x 6.5
VOLUME	.24 CUBIC FEET (.0068 M ³)

8.3.3 Growth Considerations

A possibility for increased battery performance is indicated by data presented by Figure 8-14, which indicates that nominally rated 12-ampere-hour cells actually have a higher capacity. The average for a population of 419 cells was 14.4 AH. If a 14.4 ampere-hour battery were to be built using nominal 12 AH cells, the principal effect would be increased cost because of the higher cell selectivity required.

CELL CAPACITY (A.H.)	12.0
TOTAL CELLS TESTED	419
AVERAGE CELL CAPACITY	14.42
STANDARD DEVIATION (σ)	.73 (5.05%)

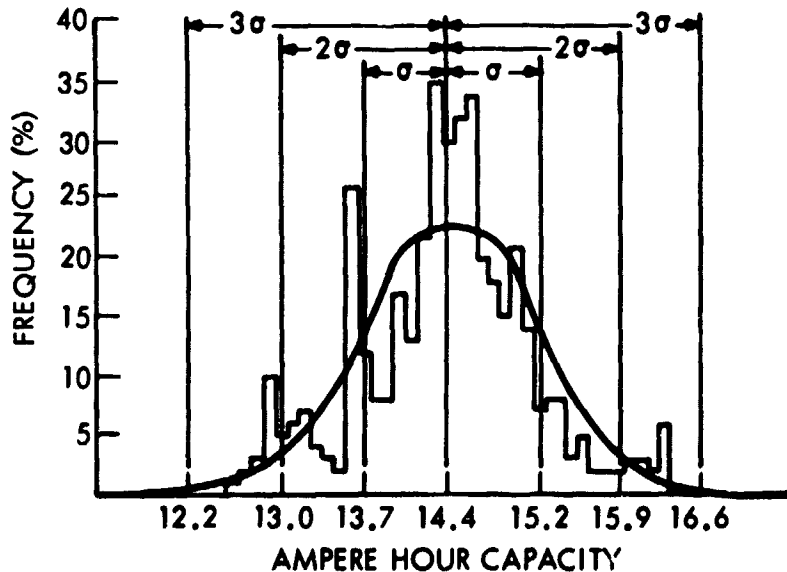


Figure 8-14. Statistical Data for Nominal 12-Ampere-Hour Cells

8.4 POWER CONDITIONING ASSEMBLY

The baseline power conditioning concept is based on design data supplied by General Electric Space Division, Valley Forge, Pa. (Reference 8-3).

8.4.1 Function and Description

Power is supplied directly from the solar array to the loads with regulation accomplished by a shunt regulator. The power conditioning assembly provides continuous regulation, control of battery charging/discharging and disposal of any excess power generated by the solar array. These functions are accomplished by the central control unit which modulates the operation of a shunt regulator, battery charge regulators, and a battery discharge regulator in response to small changes in the regulated level of the main distribution bus. Ampere hour meters included in the design assure that battery state of charge knowledge is available since load sharing between batteries and solar



array during normal daylight operations is necessary to allow sizing around 24-hour average power requirements. The power conditioning assembly consists of: (1) charge regulator; (2) boost regulator; (3) central control unit; (4) shunt dissipators, and (5) ampere-hour meters. The shunt dissipator consists of mounting plates on the boom and the partial shunt dissipation elements.

To supply larger amounts of power than the 24-hour average, battery charging is stopped to divert the allotted 48 watts to the loads. If still more power is required the boost regulator is activated to supply power from the batteries.

The central control circuit detects any significant difference between bus and reference voltage levels. Difference error is amplified and used to drive separate circuits for controlling shunt operation, charge regulator and boost regulator operation. For the baseline concept, at the maximum positive deviation of one percent, the shunt regulator is driven to a full-on condition, absorbing maximum power to prevent over-voltage. At lower positive bus voltage deviations, the shunt power is decreased and at a deviation of +0.3 percent, the shunt is full-off. The charger is operational from full-on to full-off corresponding to bus voltage deviations from 0.3 to -0.3 percent. At -0.3 percent, the array just satisfies the load demand without battery charge or discharge. With increased load demand, the boost regulator is gradually turned on to a full-on setting at -1.0 percent deviation. For TDRS application these tolerances are about a factor of 4 better than required.

The central control circuit detects any significant difference between bus and reference voltage levels. Difference error is amplified and used to drive separate circuits for controlling shunt operation, charge regulator and boost regulator operation. For the baseline concept, at the maximum positive deviation of one percent, the shunt regulator is driven to a full-on condition, absorbing maximum power to prevent over-voltage. At lower positive bus voltage deviations, the shunt power is decreased and at a deviation of plus 0.3 percent, the shunt is full-off. The charger is operational from full on to full off corresponding to bus voltage deviations from 0.3 to -0.3 percent. At -0.3 percent, the array just satisfies the load demand without battery charge or discharge. With increased load demand, the boost regulator is gradually turned on to a full on setting at -1.0 percent deviation. For TDRS application, these tolerances can be further expanded by about a factor of 4.

The charge regulator is controlled by external stimuli to provide desired output voltage and current conditions for charging the battery. The controlling factors are:

1. Current limit - the regulator limits the charge current to 6.0 amperes.
2. Taper charge regime - the charge regulator reduces current in relation to the charging voltage in accordance with the characteristics TBD. Ground command selectivity of one of TRD charge taper characteristics permits charging to be adjusted as a function of battery life and state of health.
3. Redundancy - Active block redundancy can be employed for the charge regulator with automatic switchover and back up by ground command.



The boost regulator supplies battery power to the regulated bus in response to the signal level from the central control. The regulator has a nominal rating of 190 watts and regulates within 28 ± 1 volt for input voltages in the range of 16.0 to 24.5 volts and can be modulated by pulse width modulation circuitry over the entire range including peaks. Redundancy is provided by an active standby unit with automatic transfer by a fault sensing circuit.

Eighteen volts are supplied to the LDR transmitters from a converter operating from the 28 volt regulated bus. An 85 percent efficiency is used through the rectifier filter and regulator. The reference concept permits energizing this load by relay control switches contained in the central power control unit. The relay switches response to the following signals:

1. Independent "on" and "off" signals by on board logic and/or ground command.
2. "Off" signals if the load exceeds the maximum rated value by a nominal 50 percent for 100 milliseconds or when an equivalent energy overload occurs for a shorter time. Each circuit breaker fraction can be overridden by ground command.
3. Sequential "off" signals if the main bus drops to 26 volts or less and persists through a 100 millisecond interval.
4. "Off" signal if the battery voltage decreases below a selected threshold level for 100 milliseconds. The threshold levels are selected by ground command.
5. Restoration is accomplished by ground command.

8.4.2 Power Conditioning Assembly Characteristics

The bulk of power conditioning components is in a single housing in quadrant 4 on the Y axis as shown in Figure 5-6. A packaging concept for these components is shown in Figure 8-15. Exceptions to this single housing are the ampere hour meters located near the batteries and the shunt dissipator panels mounted on the solar array booms. Weight summary is shown in Table 8-14.

The electrical interfaces for the power conditioning are:

Shunt control - the central control unit supplies a shunt control signal to the shunt dissipator through the solar array drive assembly (slip rings)

Battery - the central control unit provides positive, and return lines to the battery and signal lines for the battery temperature sensor.

Telemetry & command - The central control provides the telemetry information and receives and responds to the required commands.

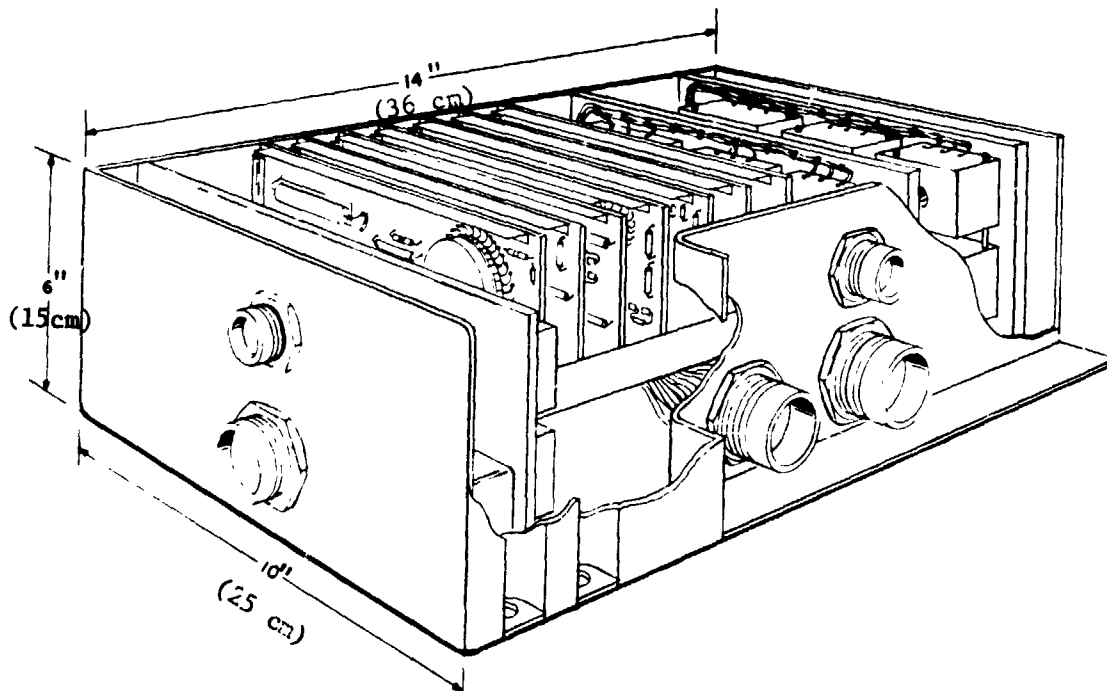


Figure 8-15. Power Conditioning Packaging Concept

Table 8-14. Power Conditioning Assembly Weight Summary

Item	Weight	
	lb	(kg)
Boost regulators (2)	10.0	4.5
Charge regulators & failure detector (2)	0.8	0.4
Boost failure detector	0.5	0.2
Voltage detector	0.6	0.3
Voltage & current telemetry	1.5	0.7
Shunt driver & central control	0.6	0.3
Brackets & relays	1.8	0.8
Stud mounted components	0.6	0.3
Container & covers	2.5	1.1
Internal wiring	1.0	0.5
Connectors	1.4	0.6
Subtotal	21.3	9.7
Voltage converter (2)	5.0	2.2
Shunt dissipators *	2.4	1.1
Ampere hour meters (2)	4.0	1.8
Total	32.7	14.8

*Installation weight penalty included in the boom
(components hard-mounted to the boom)

8.4.3 Operational Constraints and Growth Considerations

Present requirements can be met with state of art technology. The present developments indicate that regulation can be held at ± 2 percent (i.e., $\pm .56$ volts) over a 5 year period. In 1969 a direct energy transfer power subsystem similar to the TDRS baseline was breadboarded and tested for NASA Goddard (Figure 8-16) which provides good confidence in the efficiencies, voltage regulation, etc.

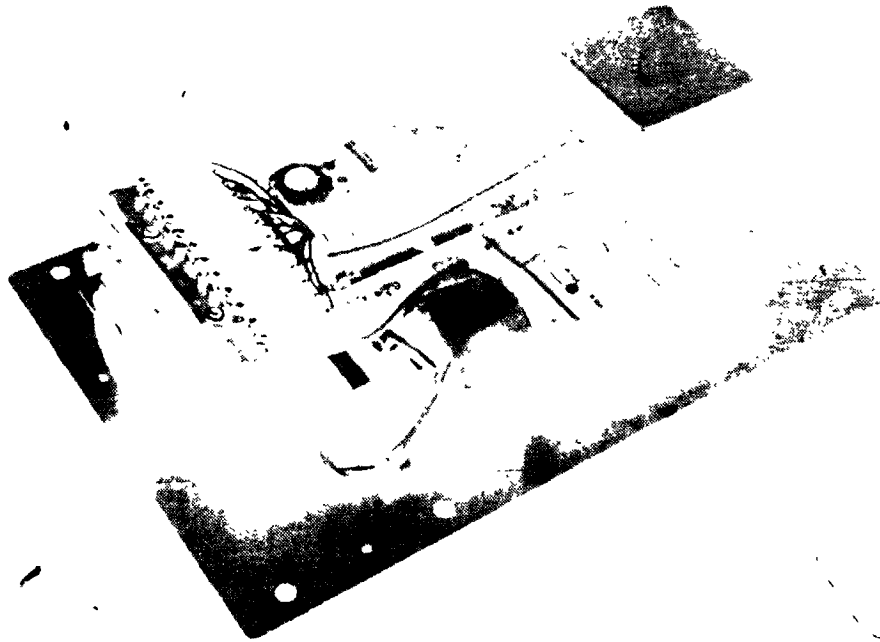


Figure 8-16. Breadboard Parts Regulator Unit



8.5 DISTRIBUTION, CONTROL AND WIRING ASSEMBLY

Electrical power must be distributed from the generation source to the user equipment. This design provides for its own stability under transient and overload conditions and includes capability to adjust for changing loads to support different payload requirements.

8.5.1 Function and Description

The distribution concept employs spacecraft proven technology of 28 vdc. Requirements for other voltages and a.c. will be satisfied by individual provisions at the user end. A detailed design was not accomplished during this phase of study. Circuit protection and switching design is state-of-the-art and will use solid state power controllers for loads less than 10 amperes and hybrid power controllers for larger loads will be utilized. These units will use solid state elements for control and protection, and electromechanical elements for power switching.

8.5.2 Assembly Characteristics

Power distribution weight allowance for cabling was estimated at 20 lb (9.1 kg). The electrical distribution block diagram is shown in Figure 8-8. A single main bus connects all loads with the exception of high current users such as pyrotechnics for apogee engine firings which are connected to a separate battery bus. General purpose loads can be removed to preserve essential loads and limit the demand for power to the available power source under specific power failures. Specified fuses will be packaged together to conduct average and peak load currents without interruption. Fuse requirements are to be determined.

8.6 EFFECT OF BATTERY CAPABILITY ON TDRS VOICE TRANSMISSION

Table 8-15 a and b shows the TDRS power requirements for full sunlight and sun eclipse period as a function of no voice communication and with voice for both low data rate and medium data rate transmission.

Figure 8-6(a) shows a load power profile based on the requirements of Table 8-15(a) (LDR). The values shown are source power required since electrical power conditioning and distribution losses are included. The profile presented is based on a voice duty cycle of 25 percent through the maximum eclipse period. The number of voice transmissions is based on communication with the shuttle once during each of its earth orbits (16 in a 24-hour period). The 25 percent LDR voice duty cycle selected results in 18 minutes of transmission before sun eclipse, 4.5 minutes during eclipse, and 22.5 minutes immediately afterwards. The energy required results in a 60 percent depth of discharge for the two NiCd batteries (maximum allowed).

Figure 8-6b shows the time required to recharge the batteries with continued voice transmission. The charge time is based on mission end of life (EOL) solar array power, when 85 watts of solar array power is available for battery charging when there is no voice communication. The time required to retain the batteries to 100 percent state of charge is 8 hours for 25 percent voice and 19 hours for 50 percent voice duty cycles after eclipse. However, voice transmission during maximum eclipse periods must be limited to 25 percent LDR voice duty cycle so that the battery 60 percent depth of discharge limit will not be exceeded.

Figure 8-17 gives the time required to recharge the batteries as a function of voice duty cycle for both LDR and MDR during the season for maximum eclipse periods. The charge time is limited only by the 85 watts of solar array power available to the battery at the end of five years. LDR voice transmission requires 26 watts in excess of available solar array power and MDR needs an excess of 96 watts. The larger MDR requirement will not allow voice transmission during eclipse and shuttle orbits immediately before and after the eclipse without exceeding the allowable 60 percent depth of discharge. However, some small amount of LDR voice transmission may be allowed (25 percent).

A 50 percent voice duty cycle during daylight an LDR requires a 5.3 percent battery depth of discharge. The same depth of discharge allows an 18 percent voice duty cycle on MDR.

Assuming an average 45 percent (maximum 60 percent) battery depth of discharge during 10 eclipse seasons (450 cycles), the estimated battery life consumed is 20 percent. This is based on 2200 cycles allowed by the -3 sigma curve of Figure 8A-1. The same curve shows 16,000 charge-discharge cycles

Table 8-15. Telecommunication Service Transmission Power Requirements (Watts)

(a) Low Data Rate Voice

Orbit	Full Sunlight		Sun Eclipse	
Telecommunication Mode (MDR)	1S + 1Ku Band		1S Band	
Attitude Stab & Control Heaters TT&C	29.0		25.0	
MDR #1	60.7		60.7	
MDR #2	26.4		13.2	
TDRS-GS	16.3		16.3	
Frequency Source, Tracking Beacon	21.0		4.8	
Solar Array Drive Controls	15.7		8.45	
Subtotal	169.1		128.45	
LDR #1 (Data)	60.8		20.47	
Subtotal	229.9	229.9	148.92	148.92
LDR #2	137.6 (Voice)	40.4 (Data)	137.6 (Voice)	40.4 (Data)
Total	367.5	270.3	286.5	189.3
N _{pc & o}	0.862	0.860	0.915	0.915
Source Power	426	315	314	207

(b) Medium Data Rate Voice

Orbit	Full Sunlight		Sun Eclipse	
Telecommunication Mode (MDR)	1S + 1Ku Band		1 S Band	
Attitude Stab & Control Heaters TT&C	29.0		25.0	
LDR #1 (Data)	60.8		60.8	
LDR #2 (Data)	40.4		16.3	
TDRS-GS	16.3		16.3	
Frequency Source, Tracking Beacon	21.0		4.8	
Solar Array Drive Controls	15.7		8.45	
Subtotal	183.2	183.2	115.35	115.35
MDR #1	217.7 (Voice)	60.7 (Data)	217.7 (Voice)	60.7 (Data)
MDR #2	26.4	26.4	13.2	13.2
Total	427.3	270.3	346.25	189.3
N _{pc & o}	0.86	0.86	0.915	0.915
Total	496	315	376	207

- ① 16-12 AN NiCd CELLS TEMP. = 78°F (25°C)
- ② SOLAR ARRAY POWER TO BATTERIES DURING CHARGE PERIODS = 85 WATTS ~ C/8
- ③ η CHARGER X η A.H. METER = 0.83
- ④ 16 VOICE TRANSMISSIONS PER DAY EXCEPT AS NOTED
- ⑤ MAXIMUM GEO-SYNCHRONOUS ECLIPSE PERIOD

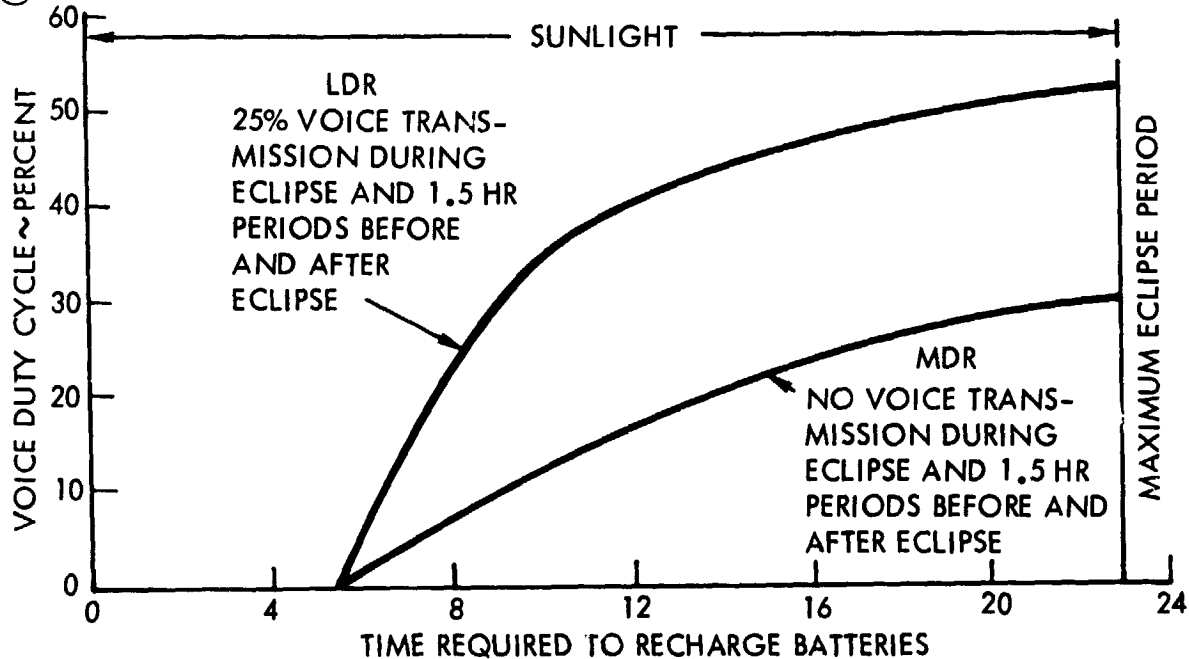


Figure 8-17. TDRS Voice Transmission Battery Capability

allowable at 5 percent depth of discharge for the -3 sigma curve and a median value of 43,000 cycles. Allocating 80 percent battery life to the 5 percent DOD 12,800 cycles would be allowed based on the conservative -3 sigma curve. Using the above approach to estimating battery life, the battery capability permits operating one-half of the mission duration (5 years) at 50 percent voice duty cycle on LDR and 18 percent voice duty cycle on MDR. Again, the above analysis is based on an EOL solar array power.

Figure 8-18 shows allowable continuous voice transmissions during non-eclipse seasons. Battery power required is based on 4 watts available from the solar array (EOL) and is adjusted for the difference between direct solar array to load losses and battery-to-load losses. The effect of estimated battery lifetime as a function of battery depth of discharge is related to total voice transmission time with continuous voice transmission time. In obtaining the data shown, 20 percent of battery life is allocated to the 10 mission eclipse seasons. Maximum mission voice transmission time results when battery depth of discharge is held to a range of 20 to 25 percent for either the LDR or MDR.

The figure shows, for the noneclipse season, the total mission transmission time and percent of total five-year life the TDRS can transmit voice as a function of continuous voice transmission time, the percent of battery DOD, and the time required to fully recharge the batteries.

The assumptions made in this analysis are conservative since they are based on maximum eclipse period of 72 minutes end of life power capability (66 watts more at beginning of life), and the minus 3 sigma battery values. The capabilities shown are for one TDRS spacecraft and will be increased if both operational spacecraft are considered.

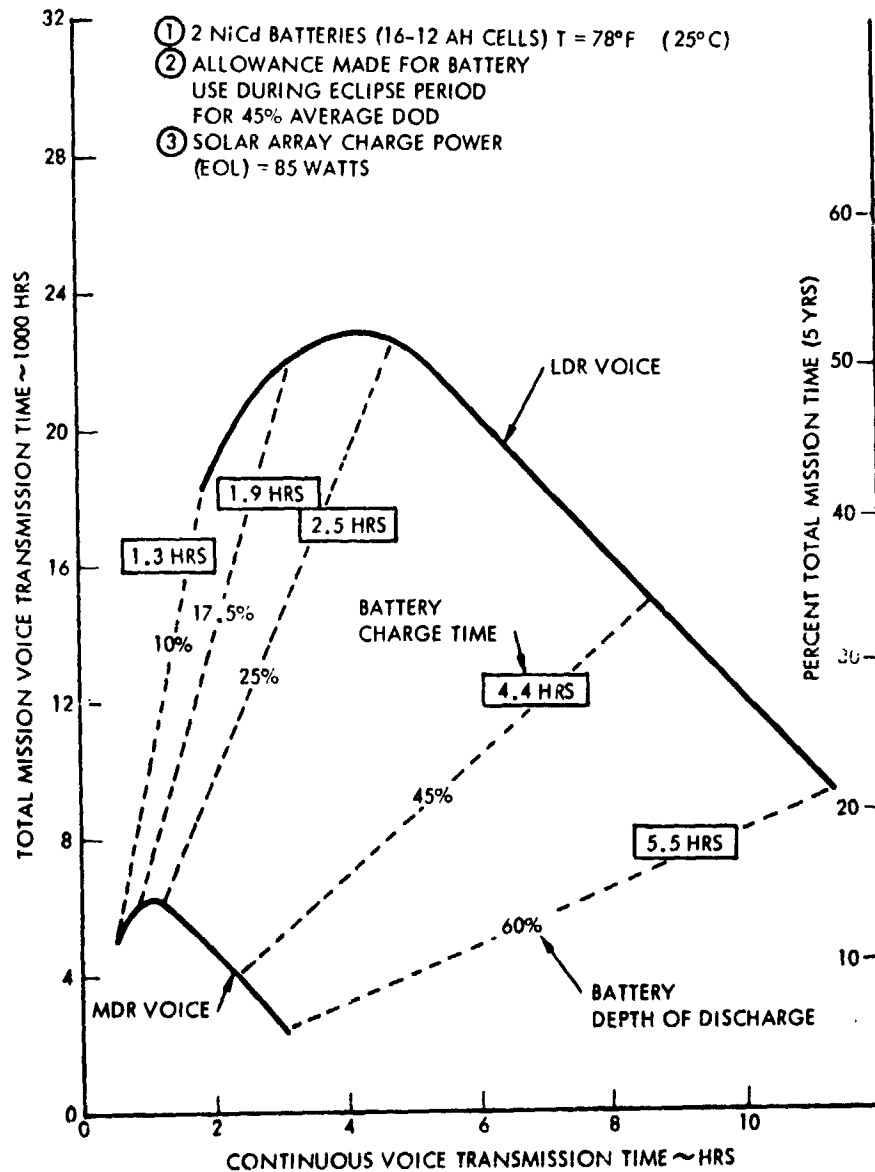


Figure 8-18. TDRS Voice Transmission Sunlight Period (Non-Eclipse Season)



Space Division
North American Rockwell

REFERENCES

- 8-1 Proposal for Power Control Subsystem, SDN-22470, General Electric Valley Forge, Pa., October 18, 1971
- 8-2 Programmers Guide to NR Spacecraft Mission Simulations Computer Programs YN0002, YN0003, YN0004, North American Rockwell, Space Division, SD 72-SA-0044, 31 March 1972
- 8-3 U.S. Government Memorandum - Recommendations for Use of Nickel Cadmium Battery in Synchronous Orbit Application, F. E. Ford, 9 February 1969



9.0 THERMAL CONTROL

The thermal control subsystem maintains design temperature limits of all equipment and manages heat load rejection from the TDRS body. The system accommodates induced heat loading from the apogee burn and motor case heat soakback and from a broad range of equipment power dissipation. The system is sized for a combination of operational and standby housekeeping modes, seasonal changes, and the long mission duration. The design employs standard techniques similar to those used on other satellites, but considers seasonal solar load variations on louvered radiator panels. During transfer orbit and eclipse standby operation when power dissipation is minimal, makeup heating maintains the RCS at operational temperatures. The system performs during all mission phases without constraining attitudes, maneuvers, or durations.

9.1 REQUIREMENTS

The thermal control system requirements consist of (1) mission natural environments, (2) operational induced environments, and (3) design temperature requirements of performance and reliability.

9.1.1 Mission Requirements

The mission thermal requirements are summarized for each mission phase in Table 9-1. The environmental heat loadings were evaluated for each phase from accepted design criteria, the Delta 2914 booster design requirements for user spacecraft, and mission and operational analysis. The apogee motor case heat soakback was evaluated from case temperatures measured in test firings upon solid motors with similar case and liner designs. Radiant solar loads were evaluated for end of life optical properties of thermal control coatings.

9.1.2 Heat Rejection Loads

The electrical and electronic power load is dissipated as heat and must be properly managed to achieve a thermal balance for temperature control. The power dissipation loads produced within the TDRS body are itemized in Table 9-2 according to mission/operational phase, subsystem, and quadrant location. Specific dissipation loads occurring outboard of the body are omitted from this analysis because they have negligible effect upon body heat balance. These outboard loads are separately considered in section 9.4. Makeup heating loads required for components of the RCS propulsion system are also omitted from the analysis of the body heat balance for two reasons: (1) the thruster chamber and valve heating power leaks directly to the space heat sink because of the exposure of these components in the thruster modules; (2) the platform or spacecraft temperature is the effective environment for platform mounted components, such as the tanks

Table 9-1. Mission Thermal Requirements

PHASE	DURATION	ENVIRONMENT	CONSIDERATIONS	REQUIREMENTS
PRE-LAUNCH CHECKOUT	HOURS AS REQ'D.	HOT OR COLD DAY FULL POWER LOAD	AIR FLOW PROVISIONS	PROVIDE DUCT PORTS
LAUNCH AND ASCENT	4 MINUTES	DELTA FAIRING HEAT SOAK-BACK, DEPRESSURIZATION	FAIRING RISES TO +400F	JETTISON FAIRING, PROVIDE VENT
PARKING ORBIT	20 MINUTES	100 NM EARTH ORBIT. MIN POWER LOADS	FIXED ATTITUDE, NON-UNIFORM HEATING. STORED PANELS AND ANTENNAS	
TRANSFER ORBIT	26 HOURS	SOLAR, W EARTH EMISSION & ALBEDO NEAR PERIGEE. MINIMUM POWER LOADS	90 RPM SPIN-UP, THRUST AXIS ATTITUDE ORIENTATION MANUEVER FOR S.O.I.; STOWED CONFIGURATION	LIMIT COOLDOWN OF TDRS AND APOGEE MOTOR
INSERTION AND PRE-OPERATIONS	1 ~ 2 HRS	SOLAR, POWER-UP	DEPLOYMENT OF PANELS & ANTENNAS	APOGEE MOTOR CASE HEAT SOAKBACK INTO S/C
SYNCHRONOUS ORBIT	5 YRS	SOLAR, OPERATIONAL NOMINAL AND REDUCED POWER LOADING.	FIXED EARTH ORIENTATION. ONCE A DAY ROLL TO SUN. 26° SEASONAL OUT OF ORBIT PLANE SUNLINE CHANGE UP TO 72 MINUTE ECLIPSE.	MAINTAIN SUBSYSTEMS DESIGN TEMPERATURE. REJECT HEAD LOADS. LIMIT ECLIPSE COOL-DOWN.

and lines. Since the dissipation loads are the major variables affecting TDRS temperature, the temperature must first be evaluated to establish the need for direct heating of components.

The estimated exothermal battery (discharge) load is included in the eclipse budget for the beneficial heating and the significant relative amount. In all other respects, this accounting agrees with the baseline electrical power load.

The dissipation loads in each quadrant within the TDRS body is required for detailed equipment temperature analysis and is discussed in Section 9.2.5. The results of the analyses are included in Table 9-2 and show the requirement to make minor relocations of some high power dissipation equipment to equalize power dissipation around the spacecraft. The equipment relocations required for temperature control affect a LDR transmitter, and the panel mounted power conditioners and controllers. These minor relocations can be incorporated in refinements of the baseline design.

Power loads during ground hot checkout are assumed to equal the beginning of life capability of the solar array. This loading establishes requirements for conditioned airflow in the Delta shroud.

Table 9-2. Thermal Control System Heat Rejection Loads (WATTS)

Phase	Transfer Orbit	Synchronous Orbit*				Eclipse**	Housekeeping (Spare)				
		Quad					Quad				
		1	2	3	4		1	2	3	4	
System	System Subtotal				System Subtotal					System Subtotal	
ACS Reaction Wheels Horizon Sensors Gyro Electronics Mod	5.2	3.00 0.25	3.00 0.25	3.00 0.25	3.00 0.25	13.5	3.0 0.25	3.0 0.25	3.0 0.25	3.0 0.25	16.5
<u>PROPULSION</u>	***	***	-	-	1.0***	0.5	0.5	0.5	0.5	2.0	
<u>ITGC</u>	5.3			5.3	5.3	5.3			5.3	5.3	
<u>LDR</u> <u>RCVR</u> <u>XMTR</u>	-	2.25 26.2	2.25 52.4	4.5 26.2	113.8	73.5	-	-	-	-	
<u>MDR</u> <u>RCVR</u> <u>XMTR</u> Antenna Track & Control	-	5.7 27.6 14.0		5.7 27.6	80.5	40.2	-	-	-	-	
<u>TDSS-GS</u>	-	11.7			11.7	11.7					
<u>FREQ SOURCE</u>	4.8		4.8 *****		4.8	4.8		4.8		4.8	
<u>IDSS TRACKING TRANS.</u>	-		7.9		7.9	7.9					
<u>EPS</u> Solar Panel Drive EPS Central Control Power Conditioner/ Losses Battery Exothermal	- 5.2 3.9	1.63 3.1 23.4	1.63 3.1 23.4	1.63 3.0	6.5 9.2 46.8	6.5 5.2 17.0	1.63 1.1 2.0	1.63 1.1 2.0	1.63 3.0	6.5 5.2 3.9	
	24.4	90.38	72.53	63.03	303.1	206.6	8.48	13.28	8.88	13.68	44.2

*Baseline - MDR:2 S-band, 2-LDR
 **Baseline - Battery Failure MDR:1 S-band, 1 LDR
 ***Valve & Chamber & Tank HTRS Omitted
 ****Valve HTRS @ 50%, Chamber & Tank HTRS Omitted
 *****Quad 2 Freq. Source Active Only



9.1.3 Temperature Limits

The design temperature limits of the electronics and propulsion equipment establish thermal control system design requirements. Subsystem temperature limits presented in Table 9-3, are representative of values used on previous satellites and on other high reliability long lifetime programs such as Minuteman. The limits are consistent with operation and/or survival for all subsystems during the mission phases preceding synchronous orbit operation, Table 9-1.

The TDRS upper temperature limit is due to the need of the communications equipment to provide high reliability, light weight and efficiency; therefore, the operational temperature limit of the communications subsystem electronics is assigned at 40C. The survival limit of 50C is assigned to preclude derating of solid state components for reason of elevated environment.

The TDRS lower design temperature of 40F (4 C) is due to the freezing point of hydrazine. The limit applies to all APS components to provide continuous operational capability. APS component upper temperature limits consider system pressure as well as vapor pressure and thruster heat soakback to valve seats. RCS thruster catalyst chambers are conditioned to 300F (149C) to ensure reliable starts.

The battery temperature limits are established from stringent requirements to limit energy storage degradation. Battery life is extended by maintaining temperature below 75F (24C) while undergoing trickle charge.

General structure temperature limits are established from considerations of materials and bonding limits. Masts, booms, and antenna feed supports and dishes have temperature levels and gradients consistent with pointing error budgets.

9.1.4 Design Constraints and Problem Areas

The thermal control design is affected by the TDRS packaging and design configuration and by two mission phases where the electrical power load is turned down.

The TDRS packaging and design configuration impose the following constraints on thermal control:

1. Recession and retention of the apogee motor case entails attenuation of the case heat soakback into the TDRS ordinarily avoided by end mounting and ejection.
2. The TDRS toroidal body offers limited heat sink area for efficient heat rejection due to the daily periodic solar incidence; i.e., the body has limited north and south facing planes which tend parallel to the sunline and receive solar loads only during summer and winter solstice, respectively.

Table 9-3. Temperature Requirements of TDRS Components (English Units)

System/Component	Allowable Temperature °F			
	Operational		Survival	
	Maximum	Minimum	Maximum	Minimum
<u>AS&C</u>				
Reaction Wheels	185	165	190	120
Gyro	185	165	190	120
Horizon Sensors	120	30	140	0
Solar Sensors	85	- 50	105	- 65
Electronics	100	0	120	- 65
<u>PROPULSION</u>				
Tanks	100	0	120	- 10
Lines and Valves	110	40	145	- 10
Thrusters	145	5	-	0
Apogee Motor	100	20	00	20
<u>EPS</u>				
Batteries	75	30	100	10
Control & Logic	150	35	170	0
DC voltage reg.	150	35	170	0
Battery Charge Reg.	150	35	170	0
Load Reg.	160	20	180	- 20
Solar Cell Array	150	- 150	240	- 200
Struts	260	- 225	-	-
Drives	260	- 70	320	- 75
<u>COMMUNICATIONS</u>				
LDR RCVR	105	30	122	- 65
Xmtr.	105	30	122	- 65
Antenna	150	- 150	240	- 200
MDR RCVR	105	30	122	- 65
Xmtr. (S)	105	30	122	- 65
Xmtr. (Ku)	105	30	122	- 65
Antenna	150	- 150	240	- 200
Antenna Track Rec & Serve	150	- 150	240	- 200
<u>TDRS/GS</u>				
Rcvr	105	30	122	- 65
Xmtr.	105	30	122	- 65
Antenna	150	- 150	240	- 200
Antenna Track Rec & Serve	150	- 150	240	- 200
Frequency Source	105	30	120	10

Table 9-3. Temperature Requirements of TDRS Components (English Units) (Cont)

System/Components	Allowable Temperature °F			
	Operational		Survival	
	Maximum	Minimum	Maximum	Minimum
<u>TT&C</u>				
Logic	105	30	122	- 65
Transceiver	105	30	122	- 65
<u>TDRS TRACKING</u>				
Rcvr	105	30	122	- 65
Xmtr	105	30	122	- 65
Antenna	150	- 150	240	- 200
Switching Network	105	30	122	- 65
<u>THERMAL CONTROL SYSTEM</u>				
Insulation TDRS	250	- 200	250	- 200
Insulation Apogee Motor	600	- 200	-	-
Louvers	130	- 50	150	- 65
Coatings	200	- 200	250	- 300

- The TDRS equipment shelf layout, required for static and dynamic balance, separates heat dissipation equipment from heat sink surfaces. The separation results in large temperature differences in order to transfer the heat for rejection. Additionally, the large tanks and momentum wheels block radiant interchange between quads.

The transfer orbit lasts 28 hours until third apogee insertion. Electrical power is reduced during transfer orbit because of the inefficiency caused by (1) array folding, (2) spin, (3) precession attitudes which can reduce solar energy, (4) the extended duration which constrains battery power supply. The TDRS cools to below the 40°F allowable limit of the APS requiring additional insulation and makeup heaters on all APS components.

Table 9-3A. Temperature Requirements of TDRS Components (International Units)

System/Component	Allowable Temperature °C			
	Operational		Survival	
	Maximum	Minimum	Maximum	Minimum
<u>AS&C</u>				
Reaction Wheels	85	74	88	49
Gyro	85	74	88	49
Horizon Sensors	49	-1	60	-18
Solar Sensors	29	-46	40	-18
Electronics	38	-18	49	-18
<u>PROPULSION</u>				
Tanks	38	-18	49	-23
Lines and Valves	43	4	63	-23
Thrusters	63	-15	-	-18
Apogee Motor	38	-7	38	-7
<u>EPS</u>				
Batteries	24	-1	38	-12
Control & Logic	66	2	77	-18
DC voltage reg.	66	2	77	-18
Battery Charge Reg.	66	2	77	-18
Load Reg.	71	-7	82	-29
Solar Cell Array	66	-101	116	-129
Struts	127	-143	-	-
Drives	127	-57	160	-60
<u>COMMUNICATIONS</u>				
LDR RCVR	40	-1	50	-18
Xmtr.	40	-1	50	-18
Antenna	66	-101	116	-129
MDR RCVR	40	-1	50	-18
Xmtr. (S)	40	-1	50	-18
Xmtr. (Ku)	40	-1	50	-18
Antenna	66	-101	116	-129
Antenna Track Rec & Serve	66	-101	116	-129
<u>TDRS/GS</u>				
Rcvr	40	-1	50	-18
Xmtr.	40	-1	50	-18
Antenna	66	-101	116	-129
Antenna Track Rec & Serve	66	-101	116	-129
Frequency Source	40	-1	49	-12

Table 9-3A. Temperature Requirements of TDRS Components (Cont.)
(International Units)

System/Components	Allowable Temperature °C			
	Operational		Survival	
	Maximum	Minimum	Maximum	Minimum
<u>TT&C</u>				
Logic	40	-1	50	-54
Transceiver	40	-1	50	-54
<u>TDRS TRACKING</u>				
Rcvr	40	-1	50	-54
Xmtr	40	-1	50	-54
Antenna	66	-101	116	-129
Switching Network	40	-1	50	-54
<u>THERMAL CONTROL SYSTEM</u>				
Insulation TDRS	121	-129	121	-129
Insulation Apogee Motor	316	-129	-	-
Louvers	54	-46	66	-54
Coatings	93	-129	121	-184

The spare TDRS is maintained in a standby mode. The reduced house-keeping power load alone is insufficient to achieve a balance with the heat leakage at the allowable limit temperature. This operation results in platform temperatures colder than occurring at the end of transfer orbit and consequently larger amounts of makeup heating power. The differing make-up heater sizing imposes additional heater monitoring and control operations. This make-up power is readily available on the spare since solar panels are deployed and equipment is not operating.

9.2 SYSTEM DESCRIPTION

The TDRS thermal control requirements and design are similar to those of other 3-axis stabilized satellites. The baseline design employs standard techniques and consists of: (1) louvered radiators for management of heat rejection and temperature control, (2) insulation for heat retention, or attenuation of heat soakback, (3) makeup heaters for RCS system components. The sizing and performance of the first and second items are presented in this section. The RCS heaters are described in detail in Section 9.4. The results of detailed temperature analysis of equipment within quads 1 and 2 are also presented.

9.2.1 Louver Radiator

The thermal actuated louvers used on TDRS are individually actuated by bi-metallic thermostats similar to previous spacecraft applications such as Mariner, Pegasus, and Pioneer. In these applications, the panels are shaded from the sun by the vehicle or shields. The performance of the protected louvered radiator is well established by tests. The use of a shield, configured either as an overhead canopy or an enclosing shadow casting fence, reduces heat rejection performance and necessitates oversizing and weight penalties. For TDRS, the shield design is constrained by the folded solar arrays.

The TDRS orbit inclination and the seasonal solar variation results in a maximum angle of $+23\ 1/2^\circ$ (.41rad) between the sunline and the TDRS XZ plane during summer solstice, and -26° (.45rad) during winter solstice. Placing the louvers on the north and south facing surfaces limits solar incidence. However, the TDRS curved periphery and the daily inertial rotation subjects the radiators to varying amounts of solar energy. Although the antenna dishes shadow the louvers for short periods, this benefit was excluded in sizing the louvers.

The TDRS unshielded louver configuration presents the following problems:

1. Accounting for the solar loading absorbed by the radiator base, including the trapping by the louver blades.
2. Designing the actuator housing so the bimetallic spring responds primarily to the base temperature.
3. Providing a thermal control coating to the radiator base which rejects heat efficiently, reflects solar energy, and is stable for 5 years.

The heat rejection characteristics and performance of thermal louvers has been investigated analytically in Reference 9-1 and extended in Reference 9-2. Reference 9-1 presented rejection capability over all solar and blade positions for a diffuse base and specular blades. Reference 9-2 also presents performance for an all specular system. The full open blade position is the basis for louver sizing. The TDRS has 14.4 ft² (1.34 m²) of louvers divided equally between the four quads.

The performance data used for sizing is shown in Figure 9-1. The distributed performance of the TDRS configuration is shown in Figure 9-2 for three extremes of seasonal solar incidence and TDRS orbital position. In these positions, the sun is most incident on the louver system of one quad. The total performance of each quad louver radiator is integrated from the distributions and is listed in Table 9-4.

Table 9-4. Performance of Louver Radiator (Radiation Base Temp, 86F/30C)

Condition	Season	Sunline Position	Heat Rejection (Watts)		
			Quad 1 (or 3)	Quad 2 (or 4)	Subtotal Quad 1 & 2
1.	Solstice	Lies in XY plane 26° (.45 rad) to Z axis	44.4	115.6	160
2.	Solstice	Lies in YZ plane 26° (.45 rad) to X axis	80.5	80.5	161
3.	Equinox	Lies in XY plane	84	139	223

It is a design objective for each quad to have independent heat rejection capability, since radiant heat transfer of the equipment loads may require large temperature differences. The individual quad heat rejection capability meets the load requirements shown in Table 9-2, except quad 1.

For conditions 2 and 3, the 90 watt heat load of quad 1 is shared and rejected adequately by the adjacent quad 2 to meet the summed load requirement as indicated in Table 9-4. In condition 1, while the available capability exists in quad 2, it is estimated that not more than 15 or 20 watts can be transferred by radiative interchange within the black coated reradiative TDRS enclosure. In this case an over temperature condition will result to increase the louver rejection and intraquad heat transfer until the deficit is made up. To provide for an additional rejection and transfer of 30 watts, a louver panel temperature of 20F (-7C) is estimated. The same temperature increase also occurs on the equipment.

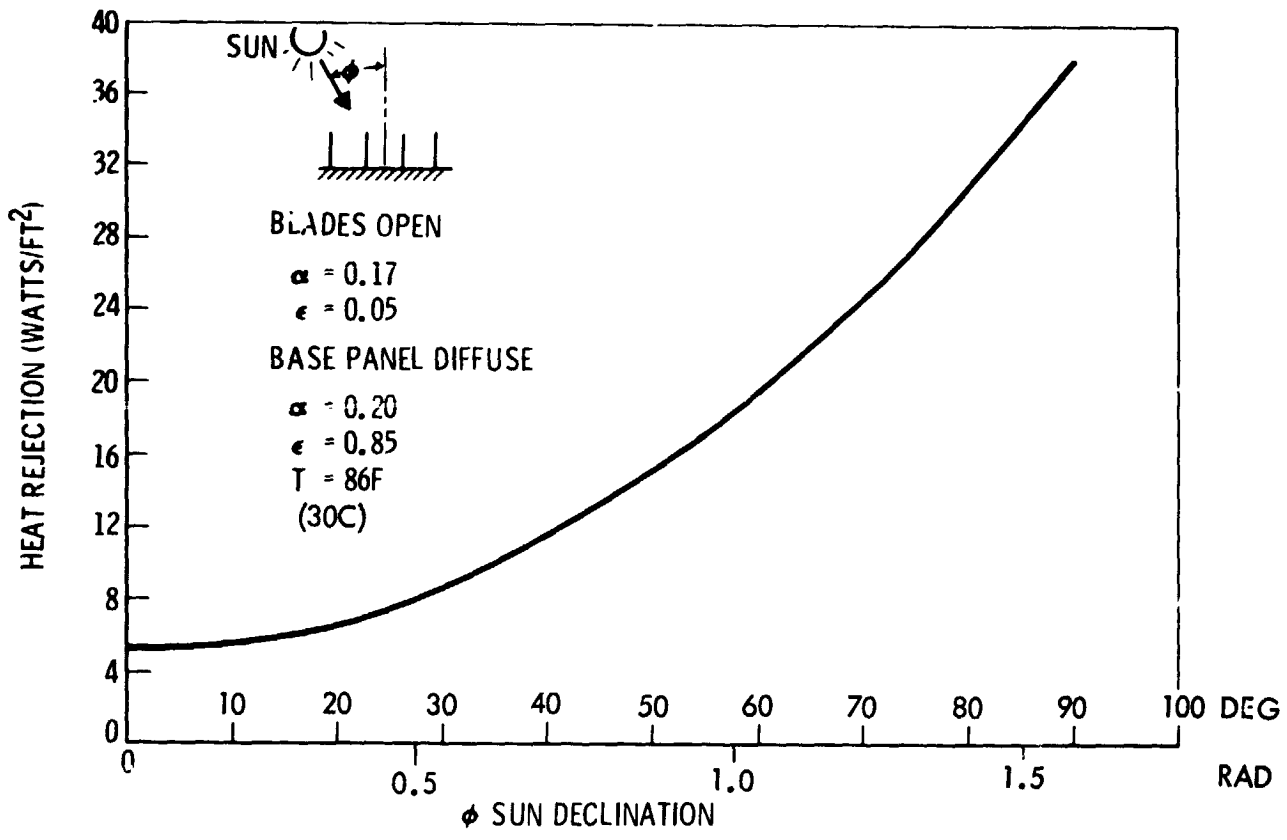


Figure 9-1. Louver Panel Heat Rejection Versus Sun Angle

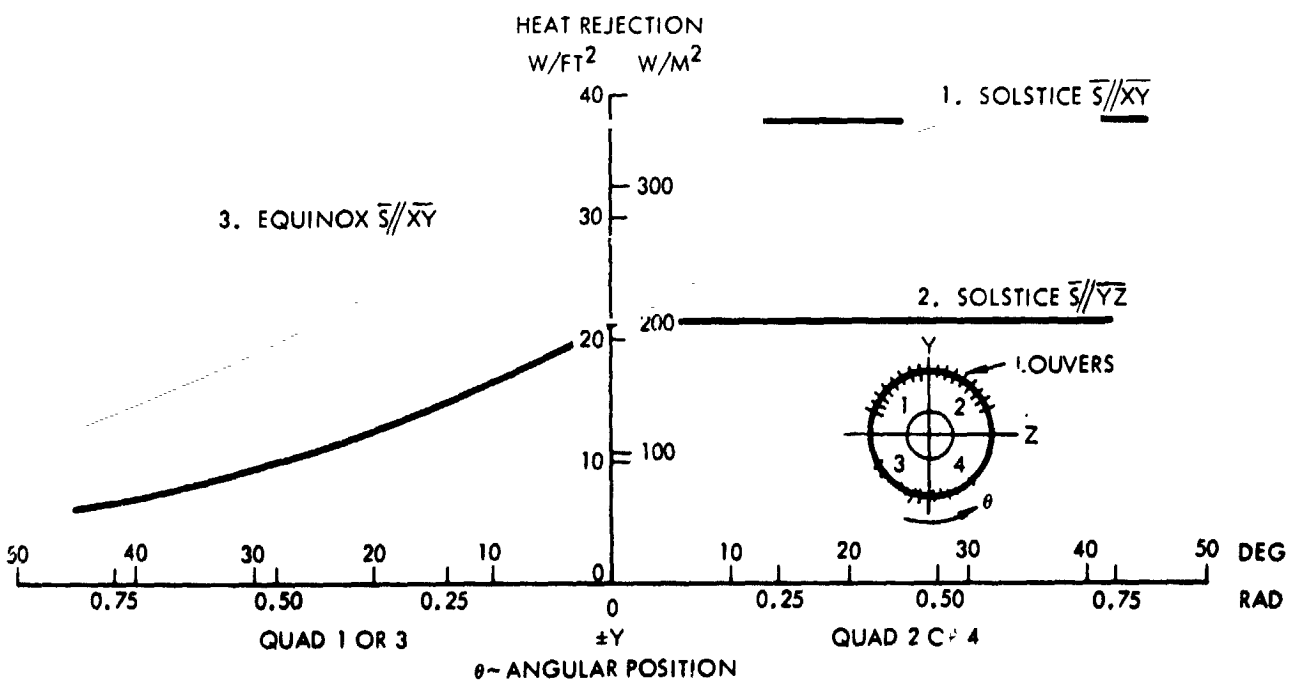


Figure 9-2. TDRS Louver Radiator Heat Rejection



A 20 F (11 C) temperature difference between equipment and louvers was allowed for transfer of the heat loads. The additional increase of temperature causes quad 1 equipment to attain survival temperature limits presented in Table 9-3. This condition occurs for a few hours per day during the month of summer solstice on quad 1. The condition is considered marginally acceptable and within the design capability of the electronic and power equipment.

Several approaches for alleviation of the problem are:

1. Relocate equipment to achieve a more uniform quad loading.
2. Increase intra-quad heat transfer by providing doublers to conduct heat.
3. Increase louver radiator area.
4. Increase heat rejection capability by providing a radiation window.
5. Increase louver heat rejection efficiency in this attitude by providing a fixed shadow shield over the hot spot.

The fifth approach was selected for the baseline. A short fixed shadow shield parallel to the blades in the middle of the panel provides an adequate increase of heat rejection. This approach is preferred because heat leakage is not increased during cold soak phases and the weight increase is least.

9.2.2 Multilayer Insulation

The TDRS body is insulated with multilayer insulation on all surfaces other than the louvers and small areas such as the horizon sensor ports and connectors. A blanket of 20 ply of aluminized 1/4 mil mylar, embossed and perforated, will be tailored to the TDRS body. Post and grommet retainer mounting will be used. A thermal coating of aluminized FEP film is the blanket outer layer.

Because of the uncertain heat leakage through seams, joints, and penetrations, the effective emittance of the blanket is estimated to be between 0.01 and 0.02. Steady state heat balances of the TDRS were determined using these values of insulation effective emittance. The louver heat rejection temperatures were also described by an effective emittance temperature relation shown in Figure 9-3.

The heat balances determine the relationship between the TDRS temperature and the power dissipation loads. The results are shown in Figure 9-4 during daylight and eclipse hot and cold environments. Figure 9-4 shows a power load greater than 90w is necessary to maintain temperature control by the louvers. For smaller power loads, the temperature depends on

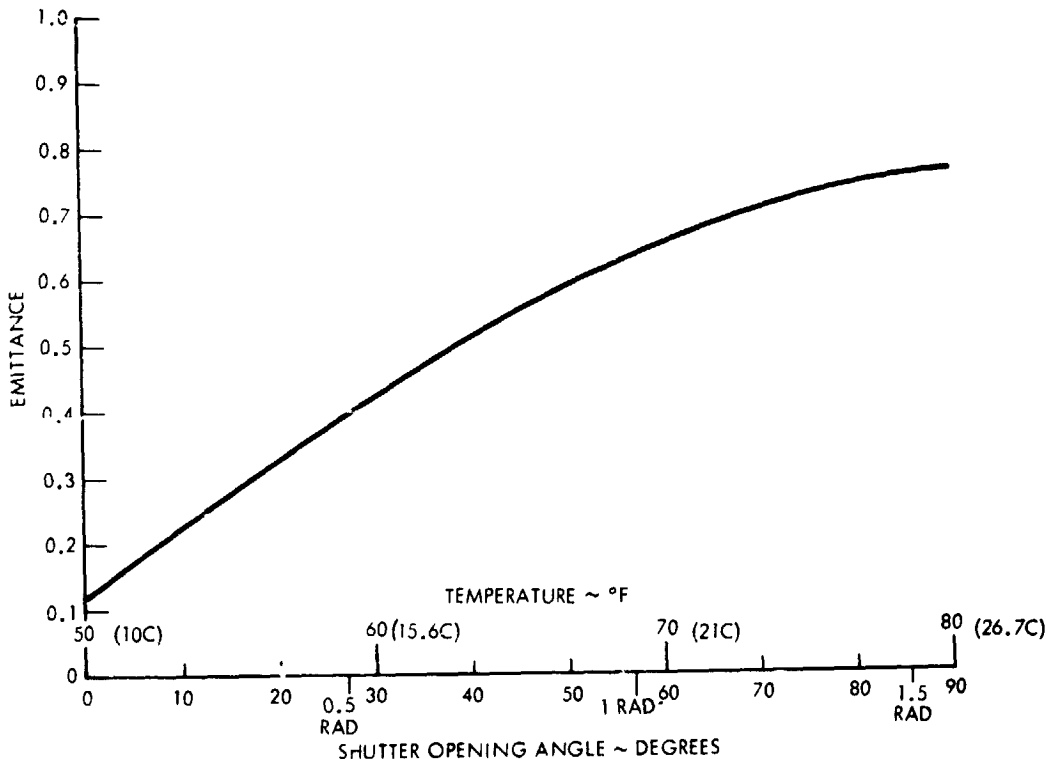


Figure 9-3. Louver Operating Characteristics

insulation performance. The temperature is uncertain within a 20F (11C) band due to the undetermined insulation performance. The TDRS daylight and eclipse loads are well within the louver temperature control range. The spare TDRS power load is insufficient to balance the heat leakage at required temperature. The RCS is affected by this condition and makeup heating is sized accordingly.

A transient temperature analysis was performed on the TDRS during transfer orbit. The temperature at the end of transfer orbit is shown in Figure 9-5. Starting at 70F (21C), the TDRS cools during the 30-hour transfer. The cool-down depends primarily on the thermostat actuation temperature range and power dissipation load and secondly upon the sun attitude, which determines the solar array temperature. Although the arrays are folded, the louver panels and insulation leak heat at a reduced rate. Closure of the louver blades over an elevated temperature range retains heat within the TDRS longer. The power load offsets the heat leak and the temperature decline is reduced as the power is increased. A load of 50 watts is required to maintain 40F (4C) over all precession solar angles. Constraining the angle between the sunline and spin axis above 60 angular degrees will prevent cool-down at the 24.4-watt transfer load. Otherwise, makeup heating is required upon the RCS components.

In Figure 9-6, the required values of parameters for the TDRS to arrive on station and begin operations within allowable temperature are shown. Also shown, is the power available from the spun-up array. It is

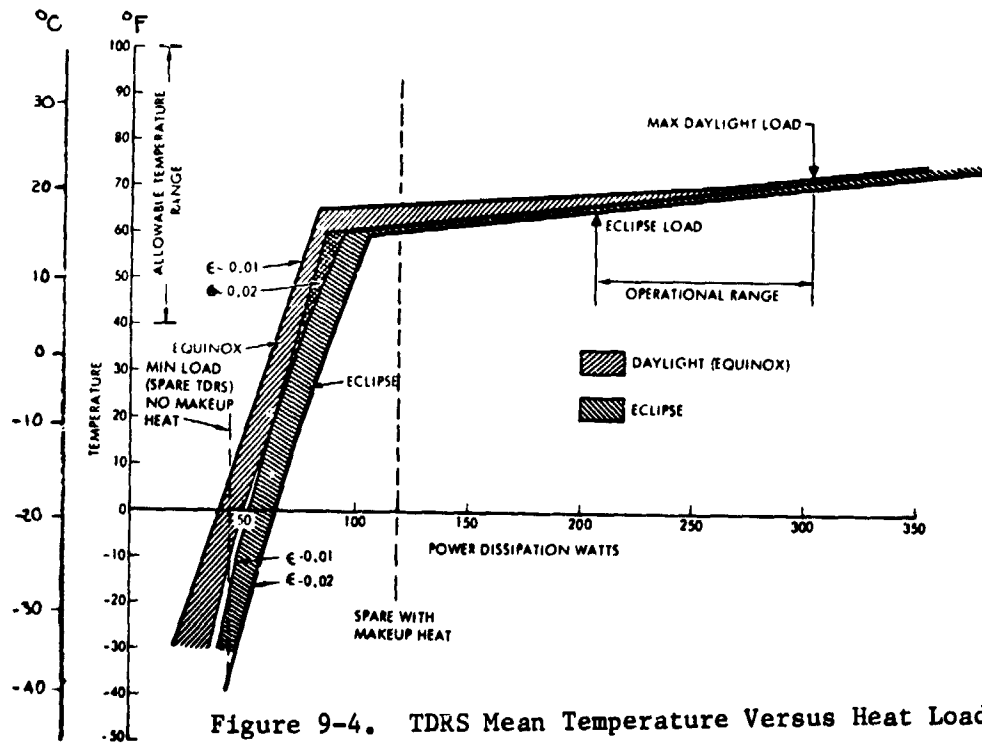


Figure 9-4. TDRS Mean Temperature Versus Heat Load

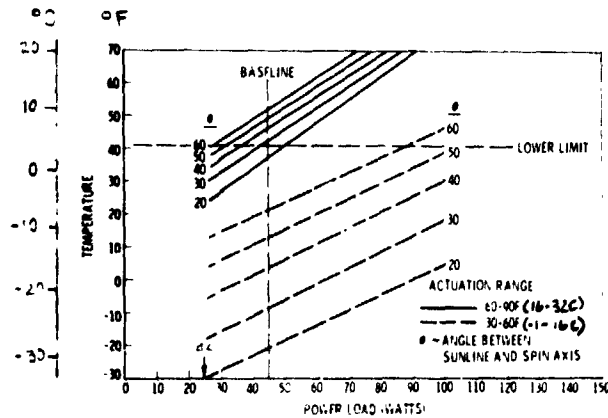


Figure 9-5. Temperature at End of Transfer Orbit Versus Power Load

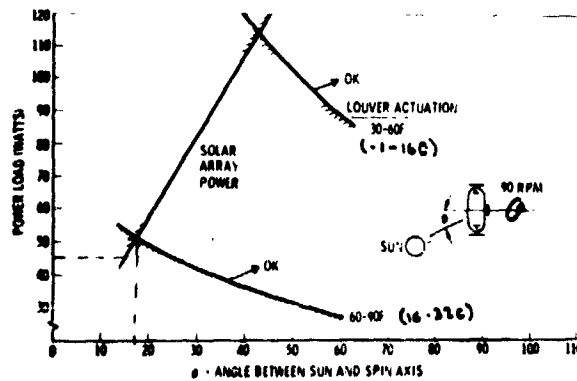


Figure 9-6. Transfer Orbit Attitude to Maintain 40 F

seen in Figure 9-6 that adequate power is available over all required precession angles for the louver range 60 - 90F (16 - 32C).

9.2.3 Thermal Control Coatings

Selection of thermal coatings requires consideration of stability of the optical properties in the space environment during the 5 year mission. In-situ laboratory tests and flight experiments have been conducted and it was found that particle radiation causes the most severe degradation. Two areas on TDRS require solar reflector coatings and are critical: (1) louver base panel, (2) TDRS body. Candidate coatings for these areas are: Z-93 paint or back surface microquartz mirrors (OSR) for the louvers; aluminized FEP or Kapton for the TDRS body. For the TDRS, the Z-93 is used in the louver baseline. It is estimated that the degraded EOL solar absorption values will produce slight acceptable operating temperature increases. The OSR coating is very stable, but louver performance is less. Further study is required to make a final selection between the coatings for EOL requirements and heat rejection performance. For the TDRS body, the degraded EOL solar absorptance of either aluminized film is acceptable for the heat gain is attenuated by the insulation blanket.

9.2.4 Equipment Component Placement

The TDRS orbit and attitude requirements are such that the best heat rejection area is centered about the Y axis, on the celestial north or south faces of the body. The LDR and MDR transmitters, power conditioners, and controllers are the relatively large power dissipaters and must be placed on or near the heat sink thermal control surfaces. Preliminary analysis of the TDRS quadrant configuration established the intraquad radiant heat interchange for the limiting temperature conditions. The heat load of quad 1 and 4 are largest but these quads contain equipment which have higher temperature limits. The heat loads of quad 2 and 3 are least, consistent with the moderate temperature limit requirements of the batteries. The heat rejection requirements of the quad louvers were discussed in section 9.2.1. The louver areas are specifically oversized on the quads 2 and 3, relative to quads 1 and 4 so as to operate at the required lower temperature levels.

A thermal math model was developed to establish equipment location and preliminary temperatures. The math model consists of 53 nodes and 278 radiation resistors and is constructed to simulate the characteristics of a TDRS quad. It was conservatively assumed that conductive heat transfer occurs only on the heavy platform, with radiation occurring between viewing surfaces. Quads 1 and 2 were each investigated because of the large loading with respect to the temperature limits. Two mounting arrangements were analyzed: Case 1 - platform mounted equipment as shown in Section 5, Figures 5-5, 5-6; and Case 2 - transmitters and power control panel relocated to face and be closer to the louver panels. The results of the thermal analyses are shown in Table 9-5 for the worst hot case environment of summer solstice.

Table 9-5. Equipment Temperatures (Summer Solstice)

Quad	Equipment	Case 1		Case 2			
		Mounting Location	Temp.		Mounting Location	Temp.	
			°C	°F		°C	°F
1.	RCS TANK	Fig 5-5, 5-6 Platform	50	122	Platform	37	98
	TDRS/GS RCVR.		53	128		40	104
	TDRS/GS XMTR		53	127		30	102
	MDR RCVR.		58	136		37	99
	MDR XMTR.		63	144	Moved near louder panel	34	94
	TDRS/GS ANT. ELECT.		53	128	Platform	37	99
	MDR ANTENNA ELECT.		53	127	Near louver panel	33	92
	EPS POWER COND. MODULE		67	153	Near louver panel	33	92
	ACS REACTION WHEEL		57	134	Platform	41	107
	2.		RCS TANK	Fig 5-5, 5-6 Platform	44	112	Platform
TDRS TRACK XMTR		48	118			27	80
FREQ SOURCE		47	117			25	77
LDR RCVR		52	127			28	83
LDR XMTR		52	127		Near louver panel	25	77
TDRS TRACK RCVR		41	107		Platform	23	74
ACS REACTION WHEEL		46	114			28	83
ACS HORIZON SENSOR		48	118			26	78
Battery		48	117			24	76
EPS POWER COND. MOD.		55	132		Near louver panel	25	77
ACS ACCELEROMETER		41	107		Platform	24	76

Comparing temperature values of these two cases shows case 2 meets temperature requirements, whereas case 1 does not. Therefore the LDR and MDR transmitters, MDR antenna electronics, and EPS power components module must be relocated adjacent to the louvers near the Y-axis. In addition, other equipment items must be relocated to equalize quad power loads as follows:

1. Relocate the ACS electronics and the power meters from quad 1 and quad 2 to quads 3 and 4.
2. Relocate the LDR transmitter from quad 4 to quad 3.
3. Provide conduction straps as required to aid heat transfer between equipment and louvers.

These relocations can be readily accommodated and still maintain balance, function, and wiring relationships.



9.3 ALTERNATE CONCEPTS

To provide temperature control and heat rejection of the TDRS, two alternate design concepts to the baseline were considered and rejected. These are:

1. Heat rejection and control of maximum temperature with a passive thermal design employing a solar reflector coating of second surface mirrors, and control of minimum temperature with insulation, capacitance, and makeup heating as required.
2. Heat rejection and control of temperature with the use of variable conductance heat pipe radiators and insulation.

9.3.1 Passive Design

The passive thermal design is preferred for its inherent reliability, but is limited in temperature control performance. The temperature control performance is directly related to the power dissipation load variation. With temperature limits of 40-100F (4-38C), the allowable power profile turndown ratio is proportional to emissive power ratio, 1.7:1. The TDRS power loads, Table 9-1, shown for daylight and eclipse operation are in a ratio of 1.5:1 and amenable to passive design. The passive design is inadequate, however, for the transfer orbit and for the spare TDRS.

Since the passive design incorporates a fixed cold bias, makeup heating is required for loads smaller than the minimum rejection load to maintain the lower limit temperature. The weight associated in providing makeup heating power is considerable during transfer orbit because of the impact to the EPS. Additional energy storage would be required to provide the power and increase battery weight. While this concept is used on outboard equipment, it is unsatisfactory for the TDRS body.

9.3.2 Variable Conductance Heat Pipe Radiator

The newly developed VCHP is able to modulate heat rejection while holding load temperature fixed. Typical design performance has been reported in Reference 9-3 as follows: heat load range 1-65 watts, control temperature variation 1.5°F (.83°C). This concept was considered recently for application to small satellites as well as large manned space stations. The results of design studies have indicated performance and weight advantages for the concept over pumped fluid radiators, and performance advantages over louvered radiators. In addition to the performance versatility, the ability to transfer heat with a small temperature difference makes the VCHP attractive for TDRS design.

Disadvantages of this concept are: (1) high cost, (2) reservoir volume requirements, (3) design integration, (4) leakage contamination, and (5) energy dissipation. Because of the preliminary developmental status and experience, and moderate thermal control system requirements, the heat pipe concept was rejected in favor of the proven louvered radiators.

9.4 SUBSYSTEMS THERMAL CONTROL

The thermal control of the APS, solar arrays, antennas, apogee motor, and the excess power dissipation panel is discussed in this section. Each subsystem has unique thermal requirements and designs separate from the TDRS body.

9.4.1 APS

The APS must be maintained operational after arming. All components are subjected to cold environments as described in Section 9.2, or from direct exposure to space (i.e., thrusters). The thrusters and valves are affected by firing heat soakback, while the other APS components are affected by apogee motor case heat soakback.

9.4.1.1 Thrusters

The thermal design requirements of the thrusters are derived from engine performance requirements. These are:

1. Condition catalyst beds to 300F (149C) for firing events with minimal power demand.
2. Minimize heat loss to the natural environment.
3. Minimize heat soakback to the TDRS from engine firing, electrical heater, and direct solar heating.

The significant thermal design characteristics are:

1. Radiant heat shield. The exposed engine surfaces other than the nozzle exit port are sheathed by the concentric shield. Inner and outer shield and engine surfaces are plated to be highly reflective in order to minimize radiant emission from the thrust chamber and the catalyst bed.
2. Thermal Standoff. The thrust chamber is supported to the mounting bracket by thermal standoffs consisting of thin-walled cylinders with staggered perforations to reduce conductive area and increase conductive path length by providing a tortuous heat path. The thermal resistance is 167°F/Btu/hr.
3. Catalyst Bed Heater. A redundant heater is directly mounted to the rear of the catalyst bed thrust chamber to provide direct heating. Some cooling is provided at the heater location through fuel cooling at the injector.

To warm the catalyst bed to 300 F (149 C) operating temperature requires heating power amounts of 0.67 watts. Heater warmup rate was determined and 2.3 hours are required before operation with a heater rate of 0.67 watt, while 22 minutes is required with a 2-watt heater.

The effect of heat soakback under combined conditions of engine firing, heater activation, and direct solar heating raises valve temperature to maximum values. The maximum platform temperature of 114 F (40 C) was conservatively used. A temperature map of the engine, mount, and valve is shown in Figure 9-7. The heat soakback to the TDRS amounts to 4 watts. The valve remains near the spacecraft ambient, well within allowable limit.

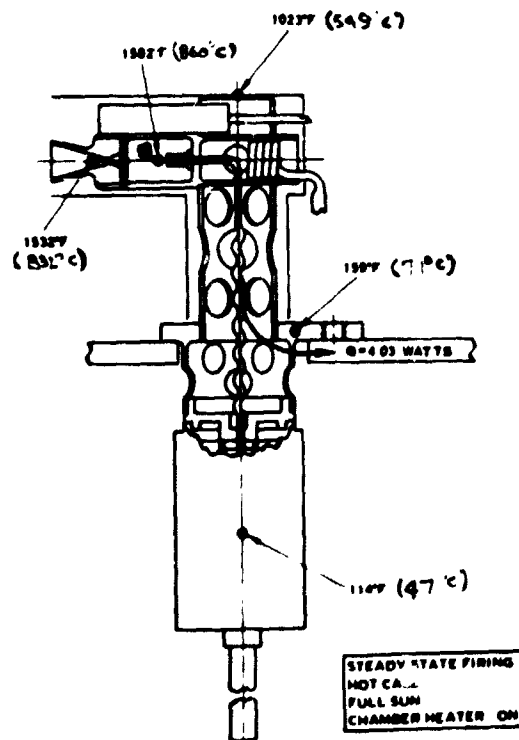


Figure 9-7. Thruster Temperature Distribution



9.4.1.2 Valves, Tanks, and Lines

During regular synchronous orbit the TDRS platform temperature is warm and provides a compatible environment for these components. During transfer orbit, and housekeeping operation of the spare TDRS, the platform temperature is below the allowable limit of 40F (4C). To prevent overcooling and propellant freezing, these components are heated electrically.

The thermal design features are:

1. The tanks are plated with a low emittance coating (gold) to limit radiative loss. The low conductance standoff mounting incorporates fiberglass plastic isolation separator washers.
2. The propellant lines are wrapped with a low emittance goldized Mylar tape to limit radiative transfer. The line mountings are standoff clamps with inserts of low conductance material such as Nylon or Teflon.
3. The valves and filter are standoff mounted from the platform with fiberglass insulation washers. A low emittance gold coating is applied to valve and support surfaces.
4. Thin flexible patch heaters are attached to components directly or to connective mounting structure. All heaters have redundant resistive elements and are wired for automatic or ground controlled override operation.
5. The heater circuits upon activation are operated by bimetallic thermostat switches (Klixon) saddle mounted to the propellant lines adjacent to the component.

The required heating power for the valves and tanks was determined from the combined radiative and conductive heat loss to the platform at the holding temperature. The thruster propellant valve heaters were sized to include the heat leakage to space from the thruster module as well. The required heating power for the APS tank is shown in Figure 9-8. The additional weight and power is summarized in Table 9-6.

9.4.2 Solar Array Panel

The solar array panel temperature limits (Table 9-3) are established from operational requirements of energy conversion efficiency and mechanical integrity. The temperature profile during each mission phase was evaluated. During phases of long steady conditions, temperatures were evaluated by a steady state heat balance. Eclipse and maneuvers were evaluated by transient heat transfer analyses.

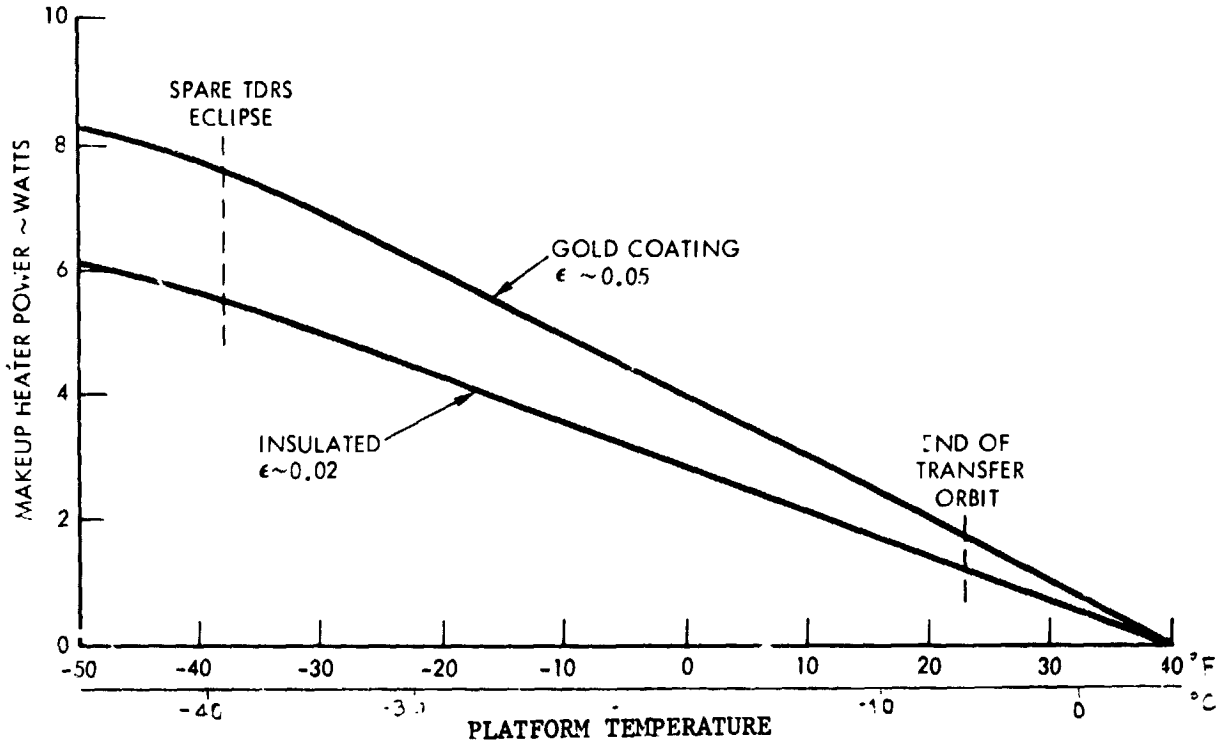


Figure 9-8. Required Heating Power for Propellant Tank

Table 9-6. APS Thermal Design Requirements

Component	No. Req'd.	Weight (lb)	Power (W)	
			Transfer Orbit	Spare Eclipse
Explosive Valve Set Heater	4	0.10	6.8	30.0
Thruster Valve Heater	16	0.36	5.0	15.9
Tank Heater	2	0.16	3.6	15.2
Line Heater	AR	0.66	1.3	5.7
Filter Heater	1	0.06	0.5	2.2
Latching Valve Heater	1	0.06	0.05	2.2
Explosive Valve Heater	1	0.06	0.5	2.2
Insulation Spacers	AR	0.20	-	-
Heater Wiring and Switches	AR	1.34	-	-
		3.0 (1.36 kg)	18.2W	73.4W

9.4.2.1 Ascent

The Delta fairing is aerodynamically heated and radiates heat to the opposing panels. The fairing thermal profile rises to 400F (204C) and the fairing inner surface emittance is given as 0.1. The panel temperature rise at fairing ejection was 11F (-12C).

9.4.2.2 Earth Parking and Transfer Orbit

The array temperature will vary during the parking orbit for two reasons:

1. The parking orbit phase is brief (~ 20 minutes) due to transfer orbit insertion on the first descending mode.
2. The solar heating varies because of the fixed attitude relative to the local horizon. Since the earth parking orbit mean heating load is within the range of the variation of the transfer orbit load, these phases will be assumed contiguous.

The TDRS spin axis is precessed from the perigee attitude to the apogee attitude. Depending upon the launch time, the included angle between the sunline and apogee motor thrust vectors varies between 19.3° and 160° (.337 rad and 2.79 rad). The panel temperature is shown in Figure 9-9 as a function of solar attitude. The portion of the panel folded over the body has negligible backside radiation to the space sink, while the portion of the panel extended aft of the body has partial backside view to space. The exposure causes the extended panel to run cooler up to an angle of 90° (1.57 rad) where the sun begins to be incident on both sides of the panel as it rotates.

9.4.2.3 Synchronous Orbit Pre-Operations

Between despin and panel deployment a portion of the panel is occluded by the body. The exposed extended panel cools rapidly if occluded and can attain minimum allowable temperature. Figure 9-10 shows the duration to attain limit temperature depending upon solar attitude which fixes the initial temperature at despin. At least 70 minutes are available to deploy the panel before cooling to the minimum operational limit, -120C.

On the other hand, a portion of the panel folded over the body is insulated continuously and warms rapidly because of the lack of backside radiation to the space sink. The radiation equilibrium temperature of 240F(116C) which is attained is within the allowable temperature.

9.4.2.4 Synchronous Orbit

During synchronous orbit, the deployed array acquires a steady operating temperature. The maximum array temperature occurs during equinox and is 40C. The minimum array temperature also occurs during equinox eclipse. To prevent cool down below the lower limit temperature, the thermal capacitance must be adequate. The array temperature versus unit area capacity is shown in Figure 9-11 with the baseline design value indicated.

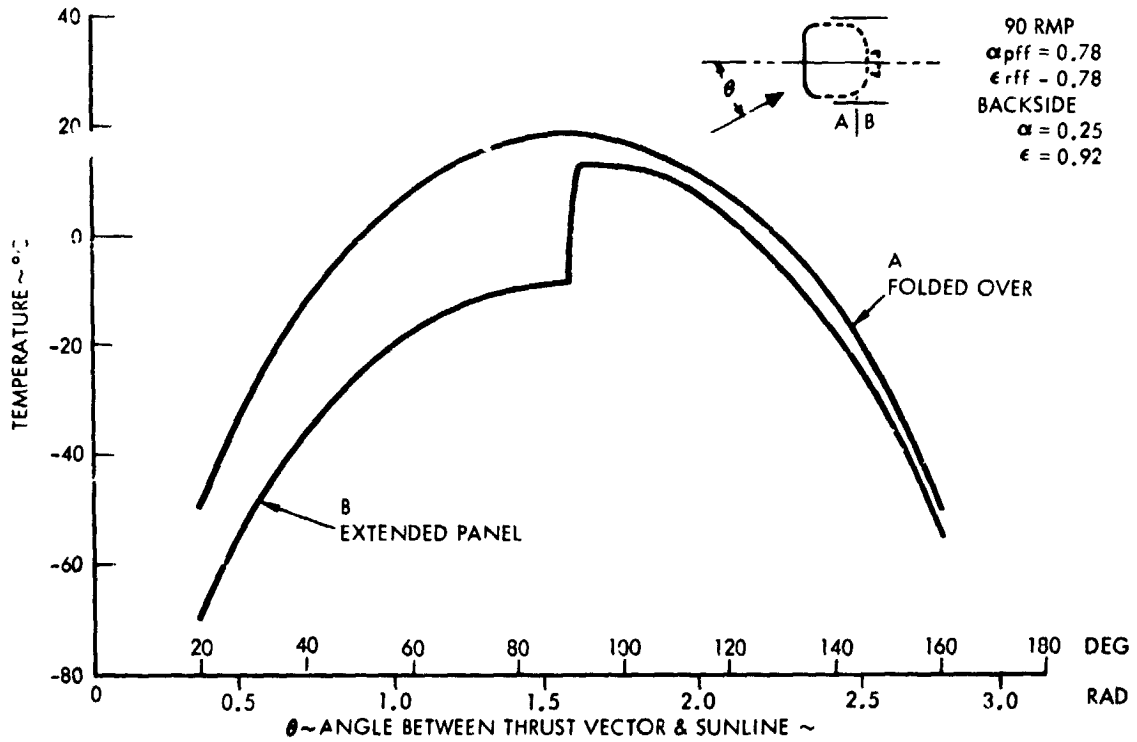


Figure 9-9. Solar Array Panel Temperature Transfer Orbit

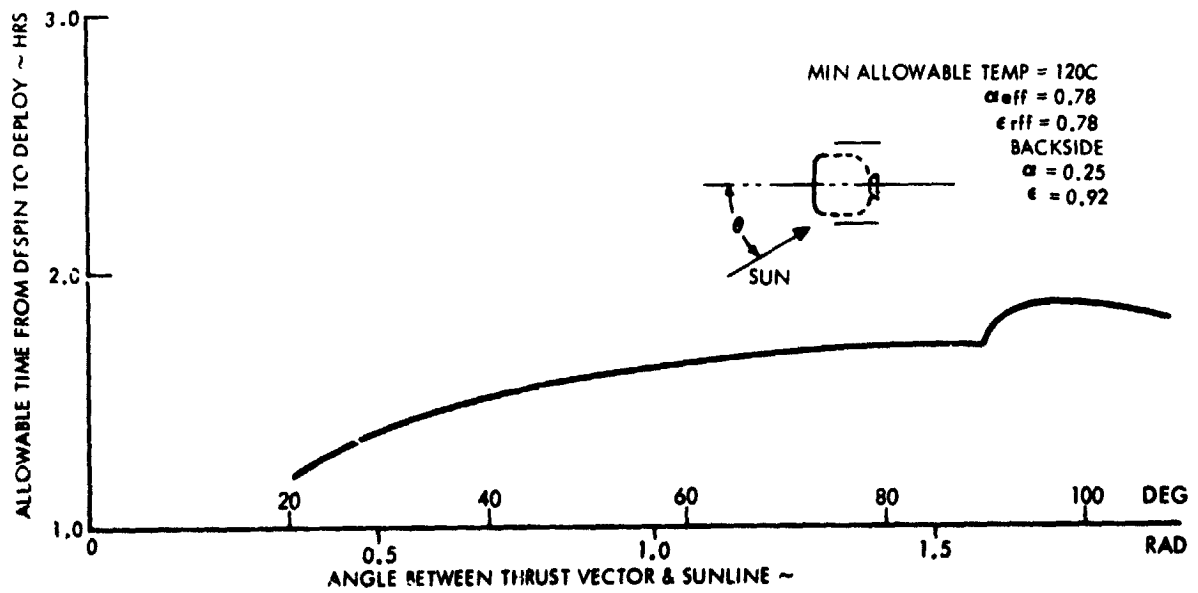


Figure 9-10. Solar Array Panel Allowable Duration from Despin to Deployment

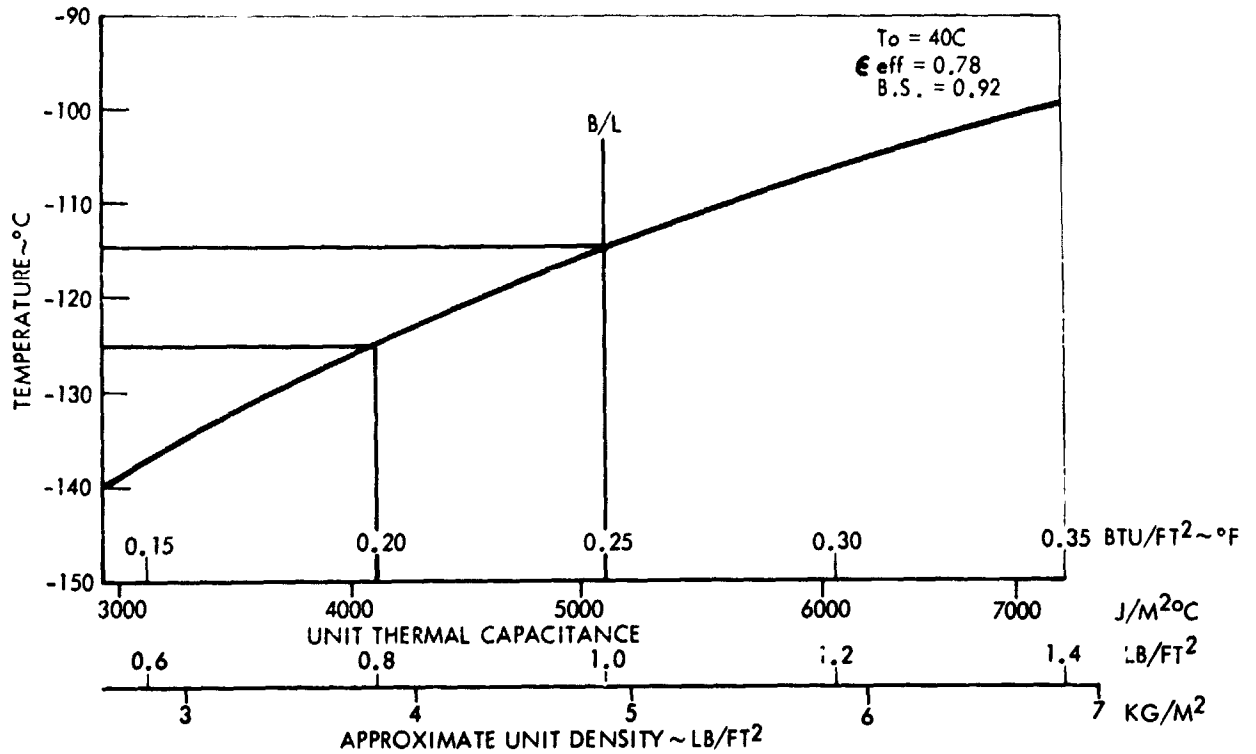


Figure 9-11. Solar Array Panel Eclipse Temperature Versus Thermal Capacitance

9.4.3 Antennas

The TDRS antennas are honeycomb sandwich dishes, and mesh and disk arrays. The antenna dish requires a low epsilon, low alpha coating to passively maintain a uniform allowable temperature over its surface. Insulation is required upon the mast and feed support, to maintain alignment. The mesh and disk array thermal characteristics are adequate to maintain allowable temperatures.

9.4.4 Apogee Motor

The design for control of the apogee motor temperature during transfer orbit is to depend upon its large mass and thermal capacitance and minimize heat loss. Multi-ply insulation is used to close out the annular tunnel opening around the motor, and to cover the nozzle exit openings. The nozzle exterior is wrapped with aluminized tape. In addition, the tunnel is lined with high temperature insulation to limit heat soak back after motor ignition. An analysis conducted for the worst case sun angle throughout the transfer orbit indicated the design is adequate to hold the temperature within limits with no constraints on the transfer orbit sun angle or launch window.

To minimize heat soakback from the expended motor case body, a three layer blanket of high temperature insulation, aluminum foil or Kapton, lines the tunnel and the mounting ring area. The motor case temperature is 600F (316C) at burnout and analysis shows the equipment platform does not exceed 120F (49C).



9.4.5 Excess Power Dissipation

Excess power is dissipated to the space sink. A separate shunt dissipation circuit is used for each array cell string. The greatest shunt dissipation occurs at the no-load condition and amounts to 100W per panel.

The temperature difference from the junction to the case of the dissipation transistors is about 1°C per watt of dissipation. For each transistor dissipation load of 18 watts, the case temperature should be limited to 92°C to limit the junction temperature to 110C, which is an acceptable junction temperature for the required service. Another temperature difference is required to transfer the heat dissipation from the cases to the radiator mounting surface. Taking into account the fin effectiveness of the radiator, a temperature difference of 10°C is estimated between the case temperature and the average radiator temperature; the radiator will operate at 82°C to limit junction temperature at 110°C.

The array mast is baselined as the radiator. The dissipation transistors are directly mounted to the array mast which is 2" d. Applying a solar reflective coating, such as Z-93 or S-13G, provides adequate emission while minimizing the solar heat loading to the sun facing masts. At 82°C, the radiated power to the space sink under equinox solar loading is 0.42 w/in² (.065 w/cm²). The required area is 240 in² (.154 m²), equivalent to a length of 38 in. (.97 m) along each mast.

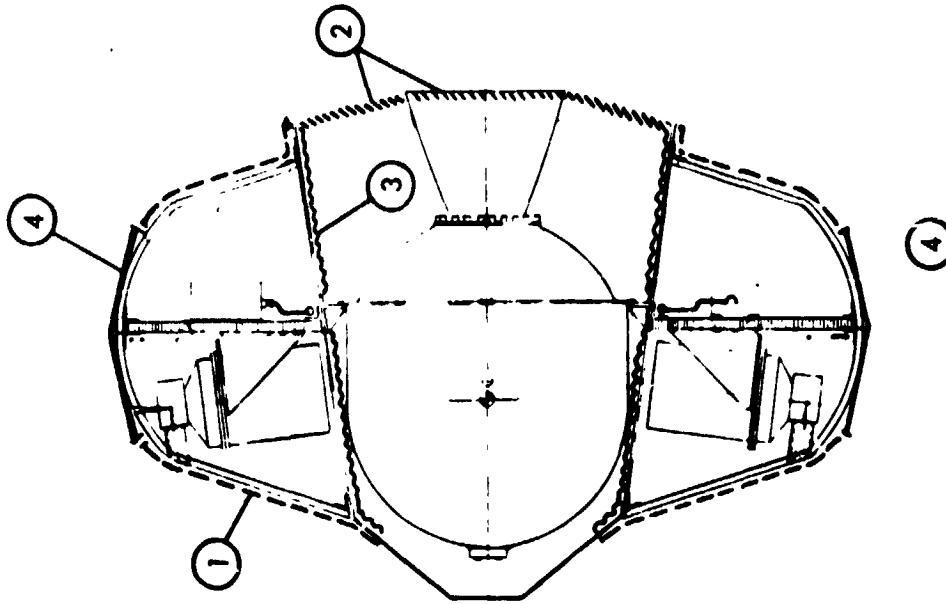
If further constraints preclude the use of the integrated mast radiator, a separate radiator panel will be provided. For the same emissive temperature and factor, the radiative power from one space facing side is 0.52 w/in² (.081 w/cm²). The required area is 1-1/2 ft² (.124 m²).

9.5 SYSTEM DEFINITION

The baseline thermal control system, as described in the previous section is shown in Figure 9-12. Component weights and location are also indicated.

REFERENCES

- 9-1. Parmer, J. F. and Buskirk, D. L., "The Thermal Radiation Characteristics of Spacecraft Temperature Control Louvers in the Solar Space Environment", AIAA Paper 67-307.
- 9-2. Eby, Robert J., et al, "Thermal Control of ATS F & G", ASME Paper 71-Av-28.
- 9-3. Hinderman, J. D., and Waters, E. D., "Design and Performance of Non-Condensable Gas Controlled Heat Pipes", AIAA Paper 71-120.



MISSION PHASE	CRITERIA	CONCEPT	WT. LB (KG)
TRANSFER ORBIT	$N_2H_4 > 41F (5C)$ BATTERY $> 32F (0C)$ ELECTRONICS $> 40F (5C)$ APOGEE MOTOR $> 20F (-7C)$	MULTI-LAYER INSULATION ①	5.5 (2.5)
		INSULATION ②	0.7 (0.32)
INSERTION BURN	$< 120F (149C)$	HIGH-TEMP INSULATION ③	7.3 (1.05)
SYNCHRONOUS OPS ECLIPSE	ELECTRONICS $< 100F (38C)$ BATTERY $75F (24C)$ RCS $> 40F$, ELECT. $> 30F (-16C)$ HEAT LOAD REGULATION	LOUVERS ④	12.3 (5.6)
		HEATERS	3.0 (1.36)
ALL	BATTERY & PROPELLANT		23.8 (10.8)

Figure 9-12. Thermal Control Subsystem

10.0 RELIABILITY

Reliability goals were established for the TDRS and subsystems, and subsystem qualitative and quantitative reliability analyses were performed. In addition, the definitions and reliability design criteria were defined for program guidance and are included in Appendixes 10A and 10B.

Based on experience with other spacecraft designs and after analysis of mission and system requirements, reliability goal of 0.8 for five years of orbital operations was established for the TDRS satellite and allocated to the subsystems. Rationale for goal selection and allocation is contained in Section 10.2. Predictive analyses and periodic design reviews were conducted to indicate areas requiring reliability improvement or areas where increased reliability would be most fruitful. A failure mode and effects analysis (FMEA) was conducted to define and minimize or eliminate single failure points and equipment criticalities. The results of the FMEA are contained in Section 10.3.

The baseline subsystem designs meet or exceed the established reliability goals in all cases except telecommunications subsystem. The objective of minimizing single failure points was also accomplished successfully.

The following sections contain the detailed results of the reliability analysis together with substantiating documentation.

10.1 DEFINITIONS

The following definitions were developed for specific application to the TDRSS. Additional definitions of a more general nature which also apply are in Appendix 10A.

Mission Success - Ability to service 20 low data rate and 2 medium data rate users on the return link and 2 medium and 2 low data rate users simultaneously on the forward link for a period of five years. Reduced forward link capability is permitted during periods of eclipse.

TDRS Reliability - The probability of each satellite performing the required functions for a period of five years in orbit, given a successful launch and orbital injection.

Single Failure Point (SFP) - Failure of a single component which would preclude attainment of full mission success. (A single point failure is not necessarily of a mission critical nature which terminates the mission but in some instances only degrades the overall mission capabilities. It is to be noted that the definition of mission success is for capabilities in excess of the requirements in the SOW.)

Redundancy - The use of more than one means of accomplishing a given function where more than one must fail before the function cannot be performed. A program goal was established to eliminate all single-failure points by redundancy where feasible but not to protect against double failures except in some special cases where this can be done at little cost.

10.2 RELIABILITY GOALS AND CRITERIA

The TDRSS consists of two operating satellites and one spare, all located in synchronous orbit. The operational concept entails phasing out some existing ground stations as the performance and dependability of the TDRSS is demonstrated.

Communications satellite studies (DOMSAT) conducted at NR and other companies indicate a five year reliability in the range of 0.8 is a practical upper limit with current technology and dependent on the complexity of the telecommunications subsystem.

Available data indicate many varying satellite designs have attained or surpassed a five-year orbital lifetime. Attaching probabilities to these satellite operations is difficult because of the wide variance in design, particularly the payload, and because successful operation of a limited sample size is statistically insignificant. Data based on various satellite analytical studies is shown in Figure 10-1. The bottom curve indicates Thermal Electric Outer Planet Mission Spacecraft (TOPS) reliabilities with a scientific payload developed by the Jet Propulsion Laboratory. The DOMSAT curve is based on analytical work conducted at NR/SD. The Electric Propulsion Stage Goal also was developed at NR/SD; however, this goal does not include a payload or the solar electric propulsion.

The major reliability goal in the TDRS design effort was to provide a satellite reliability of 0.8. This goal was established in conjunction with the GSFC Project Office after preliminary reliability analyses showed the relationship between satellite reliability and the probability of having one or two satellites remaining at the end of five years. This relationship is shown in Figure 10-2 which also shows the effects of the original number of satellites purchased. In developing the curves a booster reliability of 0.95 and an apogee motor reliability of 0.98 were used.

The curves show the probability of mission success where mission success is defined as the ability of each TDRS to service 20 LDR users and two MDR users on the return link and two LDR and two MDR users simultaneously on the forward link. Reduced forward link capability is permitted during eclipse. This capability exceeds that required in the statement of work and a higher probability of success can be obtained using the SOW capability required of one MDR user on forward and return and one LDR user on forward link. An even higher reliability will occur for reduced operation below the SOW

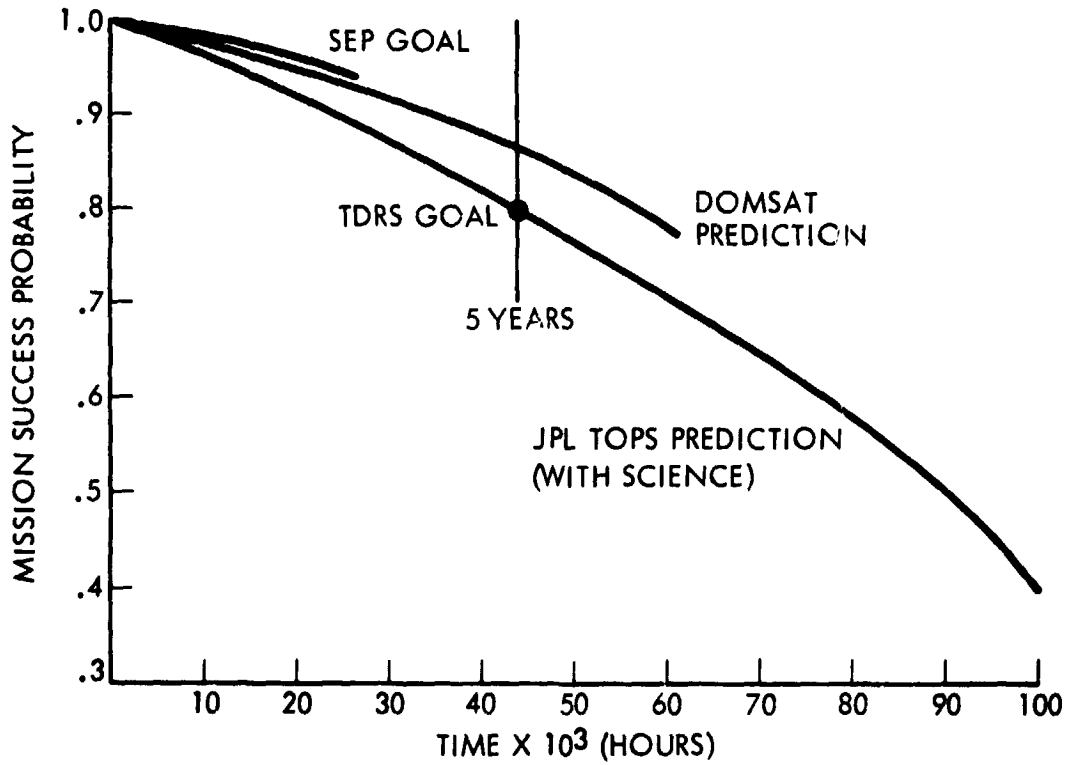


Figure 10-1. Satellite Reliability Estimates

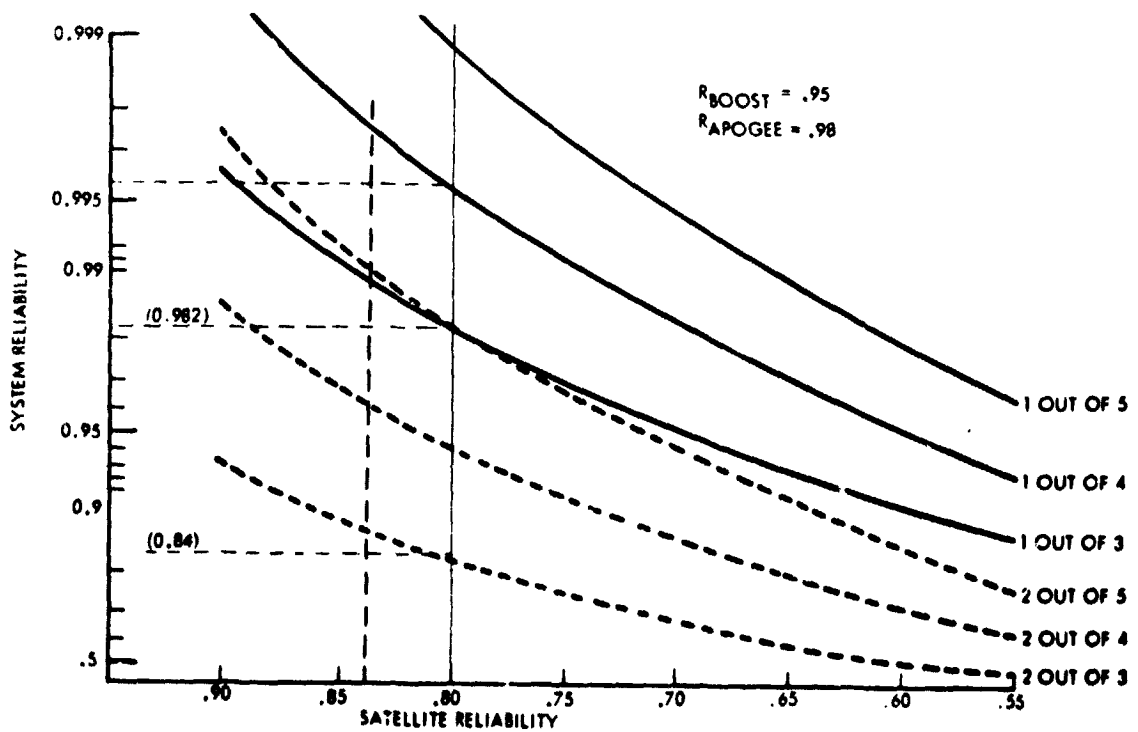


Figure 10-2. System Reliability Versus Satellite Reliability

capability since the satellite in nearly all cases degrades gracefully, allowing mission continuation.

Subsystem reliability analyses show that for the excess capability discussed above, the satellite reliability is 0.804 and for the SOW capability the satellite reliability is 0.844.

Table 10-1 shows the system reliabilities taken from Figure 10-2 of one or two spacecraft remaining in full operation at the end of five years for these satellite reliabilities.

Table 10-1. Probability of Mission Success

Satellite Capability	Probability of Success			
	Excess Capability		SOW Capability	
	1	2	1	2
No. of S/C in Full Operation				
Initial No. of satellites				
3	.983	.840	.990	.880
4	.996	.950	.998	.965
5	.999	.983	.9995	.991

These high goals were achieved by adhering to a design philosophy throughout the spacecraft of eliminating or minimizing single point failures, using high reliability components, and using redundancy whenever necessary. The weight margins provided by the creative and unique design approaches permitted the use of redundancy in all critical areas.

The 0.8 reliability goal was apportioned to the subsystems, based on equipment complexity and mission operating requirements. The results of this apportionment are shown in Table 10-2 along with the analytical prediction.

Table 10-2. Preliminary Subsystem Reliability Goals

Subsystem	Initial Allocation	Analytical Prediction
Tracking, telemetry, & command	0.96	0.966
Communications	0.96	0.915
Structure & mechanisms	0.98	0.999
Attitude control	0.96	0.962
Auxiliary propulsion	0.98	0.997
Electrical power	0.95	0.962
Thermal control	0.99	0.999
Total Satellite	0.80	0.804

The reliability goals can be accomplished with present technology and at this time no new technology will be used on the program. If, in the future, it is decided to apply new technology to attain substantial improvements in payload performance, a qualification program will be instituted to assure that this new hardware is space qualified for a five year mission and meets the reliability requirements.

Attainment of satisfactory subsystem performance will be accomplished when all subsystem operations support the spacecraft and communication payload to achieve mission success.

10.3 SUBSYSTEM ANALYSIS

A failure mode and effects analysis (FMEA) of each TDRS subsystem was conducted to determine failure modes and the effect of potential failures on TDRS mission success. The FMEA was complemented by a reliability predictive analysis using exponential distribution. The combined results defined potential problem areas where redundancy or a modified design approach was indicated. Logic diagrams based on subsystem schematic layouts were developed to support the FMEAs and quantitative analyses. The details of the analyses are contained in the following sections. A summary of failure rates and reliability calculations is shown in Appendix 10C. A single failure point summary together with supporting rationale for retention is contained in Section 10.4.

10.3.1 Telecommunications

10.3.1.1 Communications

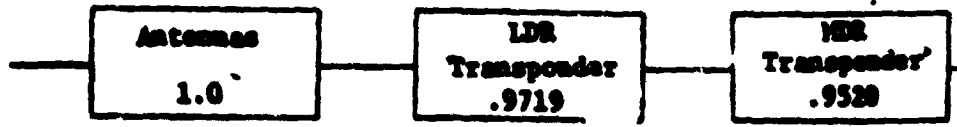
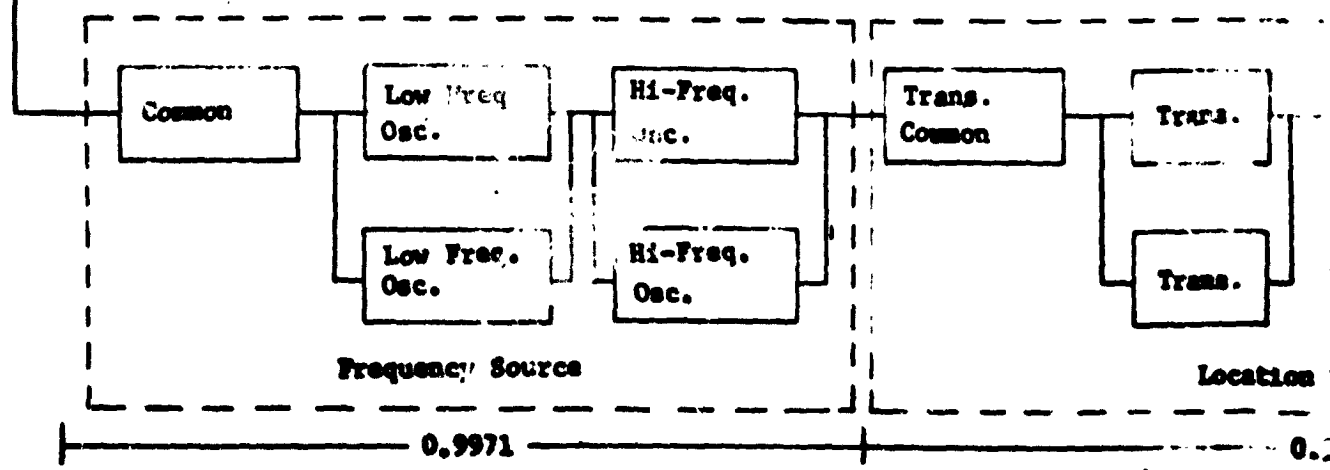
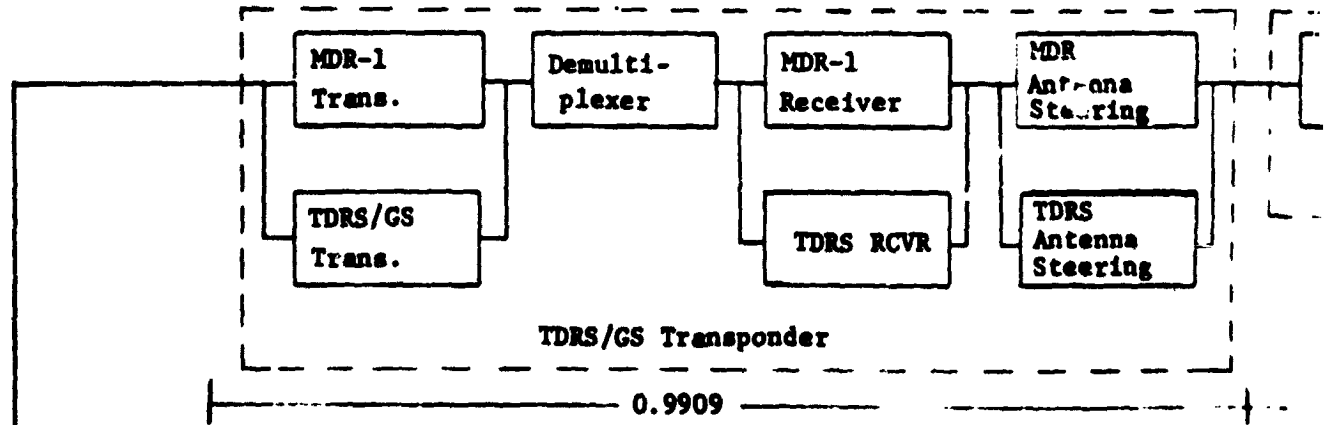
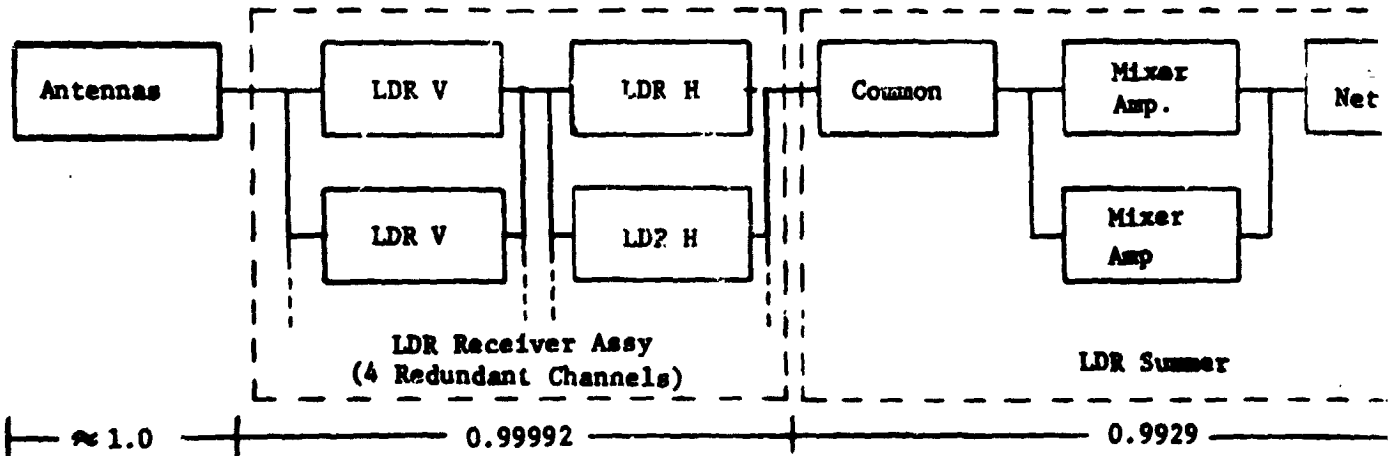
The communications subsystem consists of the LDR transponder, the MDR transponder, the TDRS/GS transponder, a frequency source, a location transponder, a beacon, and the TDRS antennas. Figure 10-3 shows a reliability logic diagram of the overall system and major components.

The LDR transponder contains four horizontal and four vertical channels together with the associated summer and divider circuitry and transmitter phase shifters. The reliability model assumes that the system is still operative, although degraded, if at least one horizontal and one vertical channel is available.

The MDR transponder consists of two groups, each containing an antenna, an MDR transmitter, and MDR receiver. Using the configuration specified in the SOW, the two groups are redundant, resulting in a reliability of 0.994 for the function. However, providing the excess capability of servicing two MDR users simultaneously, the reliability analysis assumed the two groups to be in series, since both are required for mission success, giving a reliability of 0.952.

The TDRS/GS transponder is comprised of the TDRS transmitter, the TDRS receiver, and the TDRS antenna. The transmitter consists of a Video module section and a VCO assembly, each with redundant units. The receiver has multiple redundant sections. In the event of a failure affecting the TDRS transmit function, the MDR-1 transmitter provides a backup mode as shown in Figure 10-3. The function can be performed with either the MDR-1 or the TDRS antenna system.

OLDOUT FRAME



$$R_{Total} = R_{ANT} \times R_{LDRTR.} \times R_{MDRTR.} \times R_{TDRS.} \times R$$

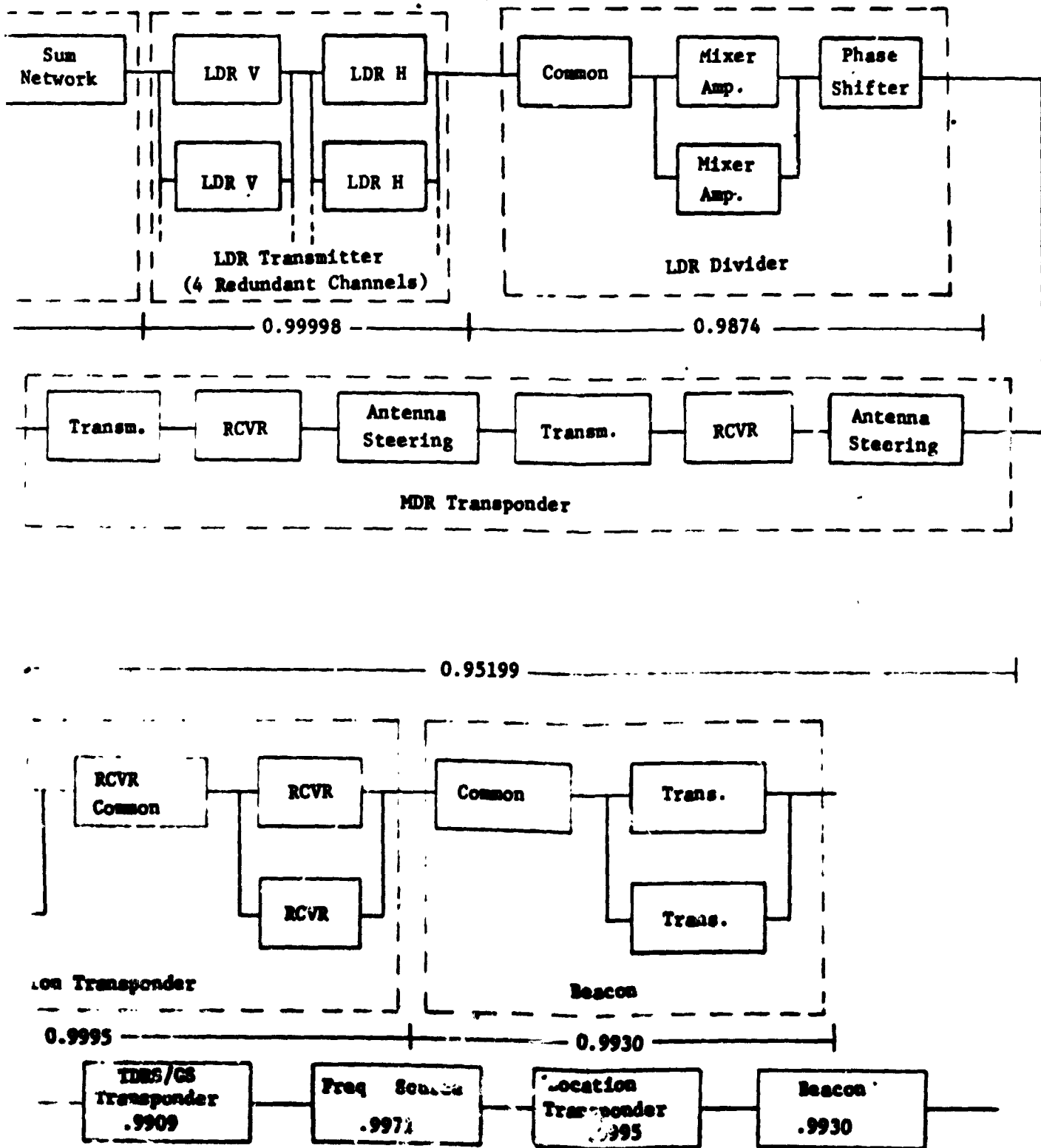


Figure 10-3. Reliability Diagram of Communications Subsystem

10-7,10-8

The MDR-1 receiver provides redundancy to the recovery function.

The frequency source provides high and low frequency oscillations, each redundant with the capability of independent selection.

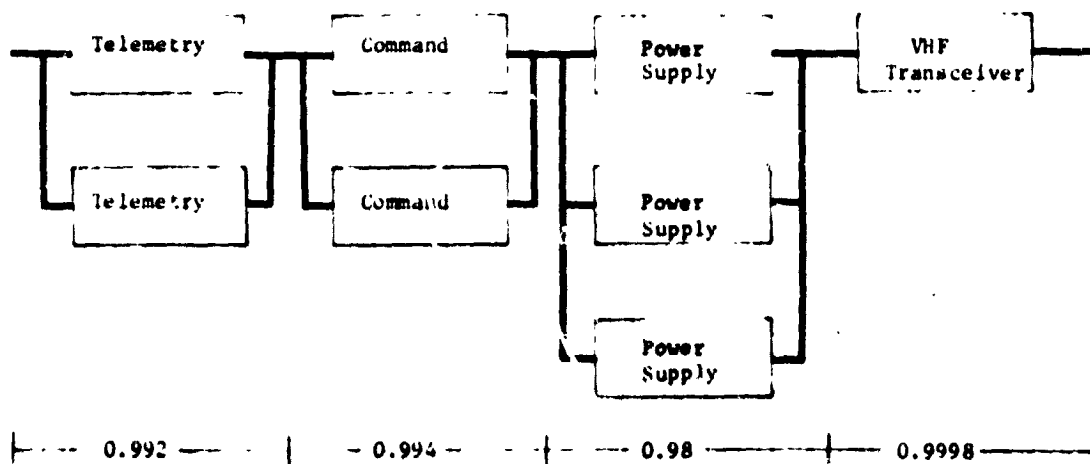
The location transponder consists of redundant transmitters and receivers with cross-strapping. The reliability calculations are based on the assumption that the location transponder will not exceed 2000 hours of operation during the five-year mission.

The reliabilities of the system major assemblies are indicated in Figure 10-4. The overall system reliability is 0.9151. This probability is increased to 0.9608 if the MDR functions are considered redundant. The probability of an antenna failing after deployment is considered to be negligible; however, discrete probabilities associated with antenna drives have been included. Appendix 10-C contains a listing of the failure rates used in the analysis together with more detailed reliability logic diagrams. A 10% contingency was applied to the failure rate summation for each component to allow for any additional parts required during more detailed design definition.

An FMEA of the communications system was conducted. The results, (Table 10-3) revealed no single failure points other than the components listed in the reliability logic diagrams as "common." A discussion of these components is contained in Section 10.4.

10.3.1.2 Tracking, Telemetry, and Command

This function, shown in Figure 10-4, consists of telemetry, command, power supplies, and a VHF transceiver, with complete redundancy for all elements of



$$R_{TOTAL} = R_T \times R_C \times R_{PS} \times R_{VHF} = 0.9161$$

Figure 10-4. Reliability Logic Diagram of Tracking, Telemetry and Command Subsystems

FOLDOUT FRAME

Table 10-3. Failure Mode Effects Analysis

ITEM IDENTIFICATION/ QUANTITY	FUNCTION	FAILURE MODE	CRIT. CATEGORY	FAILURE EFFECT	ALTERNATE MEANS OF OPERATION	REMARKS
PROGRAM: TDSS SUBSYSTEM: COMMUNICATION						
CRITICALITY I: SINGLE FAILURE PRECLUDES MISSION SUCCESS CRITICALITY II: ALL OTHER FAILURES						
<u>LDR TRANSPONDER</u>						
LDR RECEIVER/SUMMER/8	RECEIVES LOW DATA RATE SIGNALS FROM USER SATELLITES	LOSS OF FUNCTION	II	SLIGHT SIGNAL DEGRADATION	USE REMAINING CIRCUITS	
LDR TRANSMITTER/DIVIDER/8	TRANSMITS LOW DATA RATE COMMANDS TO USER SATELLITES	LOSS OF FUNCTION	II	SLIGHT SIGNAL DEGRADATION	USE REMAINING CIRCUITS	
RF SWITCH (COMMON)/4	SWITCHES TO REDUNDANT CIRCUITS IN CASE OF MALFUNCTION	FAILS TO TRANSFER	II	NONE	USE REDUNDANT PATHS	ALL RF SWITCHES WILL EITHER BE REDUNDANT OR SWITCHES WITH REDUNDANT COILS WILL BE UTILIZED
POWER DIVIDER (COMMON) 16	PASSIVE DIVISION OF POWER	LOSS OF FUNCTION	I*	LOSS OF SIGNAL	NONE	
<u>MDR TRANSPONDER</u>						
MDR TRANSMITTER/2	TRANSMITS MEDIUM DATA RATE COMMANDS TO USER SATELLITES	LOSS OF FUNCTION	II	CAN COMMUNICATE WITH ONLY ONE USER AT ANY GIVEN TIME	USE REDUNDANT UNIT	WITH THE EXCEPTION OF TWO POWER DIVIDERS ALL PARTS WITHIN THE MDR TRANSMITTER ARE COMPLETELY REDUNDANT. TWO FAILURES HAVE TO OCCUR BEFORE ONE MDR LINK CAPABILITY IS LOST.
MDR RECEIVER/2	RECEIVES MEDIUM DATA RATE SIGNALS FROM USER SATELLITES	LOSS OF FUNCTION	II	CAN COMMUNICATE WITH ONLY ONE USER AT ANY GIVEN TIME	USE REDUNDANT UNIT	WITH THE EXCEPTION OF ONE DIPLEXER EACH IN THE KU AND S BAND RECEIVER ALL PARTS ARE REDUNDANT. TWO FAILURES HAVE TO OCCUR BEFORE ONE MDR LINK CAPABILITY IS LOST.
MDR MOTOR (ANTENNA DRIVE)/8	DRIVES GIMBAL MECHANISM	LOSS OF FUNCTION	II	LOSS OF REDUNDANCY	USE REDUNDANT UNIT	
GIMBAL MECHANISM; 2 AXIS (COMMON)/2	GIMBALS MDR ANTENNA TO POINT AT USER SATELLITES	LOSS OF FUNCTION	I*	LOSS OF ONE MDR LINK	USE TIF SECOND MDR LINK	ALL PREDOMINANT FAILURES HAVE BEEN PROTECTED BY REDUNDANCY COMM. SS. WILL DEGRADE TO ONE MDR LINK CAPABILITY.
RF SWITCH (COMMON)/18	SWITCHES TO REDUNDANT CIRCUITS IN CASE OF MALFUNCTION	FAILS TO TRANSFER	II	NONE	USE REDUNDANT PATHS	ALL RF SWITCHES WILL EITHER BE REDUNDANT OR SWITCHES WITH REDUNDANT COILS WILL BE UTILIZED.
POWER DIVIDER (COMMON)/4	PASSIVE DIVISION OF POWER	LOSS OF FUNCTION	I*	LOSS OF ONE MDR LINK	USE SECOND MDR LINK	COMM. SS. WILL DEGRADE TO ONE MDR LINK CAPABILITY.
DIPLEXER (COMMON)/4	FILTERS INCOMING SIGNALS	LOSS OF FUNCTION	I*	DEGRADED MDR LINK CAPABILITY	USE SECOND MDR LINK	
<u>TDSS/CS TRANSPONDER</u>						
TDSS/GS TRANSMITTER/1	TRANSMITS DATA TO GROUND	LOSS OF FUNCTION	II	LOSS OF REDUNDANCY	SWITCH TO MDR TRANSMITTER FOR BACKUP	
TDSS/GS RECEIVER/1	RECEIVES DATA FROM GROUND	LOSS OF FUNCTION	II	LOSS OF REDUNDANCY	SWITCH TO MDR RECEIVER FOR BACKUP	



SPACE TRANSMITTER TRANS/SS TRANSMITTER/1	TRANSMITS DATA TO GROUND	LOSS OF FUNCTION	II	LOSS OF REDUNDANCY	SWITCH TO MDR TRANSMITTER FOR BACKUP	
TRANS/GS RECEIVER/1	RECEIVES DATA FROM GROUND	LOSS OF FUNCTION	II	LOSS OF REDUNDANCY	SWITCH TO MDR RECEIVER FOR BACKUP	
RF SWITCH (COMMON)/1	SWITCHES TO REDUNDANT CIRCUITS IN CASE OF MALFUNCTION	FAILS TO TRANSFER	II	NONE	USE REDUNDANT PATHS	ALL RF SWITCHES WILL EITHER BE REDUNDANT OR SWITCHES WITH REDUNDANT COILS WILL BE UTILIZED.
TRANS DRIVER (ANTENNA DRIVER)/2	DRIVES COMBAL BEAM ANTENNA	LOSS OF FUNCTION	II	LOSS OF REDUNDANCY	USE REDUNDANT UNIT	
FEEDBACK MECHANISM; 1 AXIS (COMMON)/1	POINTS TOWARDS ANTENNA TO LAUNCH	LOSS OF FUNCTION	II	LOSS OF REDUNDANCY	SWITCH TO MDR DISH FOR BACKUP	THE ANTENNA POINTING OPERATION IS PERFORMED ONLY ONCE DURING THE 5 YEAR MISSION.
FREQUENCY SOURCE LOW FREQUENCY SOURCE /2	PROVIDES LOCAL OSCILLATOR REFERENCE SIGNALS	LOSS OF FUNCTION	II	LOSS OF REDUNDANCY	USE REDUNDANT UNIT	
HIGH FREQUENCY SOURCE /2	PROVIDES LOCAL OSCILLATOR REFERENCE SIGNALS	LOSS OF FUNCTION	II	LOSS OF REDUNDANCY	USE REDUNDANT UNIT	
RF SWITCH (COMMON)/13	SWITCHES TO REDUNDANT CIRCUITS IN CASE OF MALFUNCTION	FAILS TO TRANSFER	II	NONE	USE REDUNDANT PATHS	ALL RF SWITCHES WILL EITHER BE REDUNDANT OR SWITCHES WITH REDUNDANT COILS WILL BE UTILIZED.
LOCATION TRANSMITTER LOCATION TRANSMITTER/2	TRANSMITS ACQUISITION & TRACKING BEACON SIGNALS	LOSS OF FUNCTION	II	LOSS OF REDUNDANCY	USE REDUNDANT UNIT	
LOCATION RECEIVER/2	RECEIVES TRACKING BEACON & ORDER WIRE	LOSS OF FUNCTION	II	LOSS OF REDUNDANCY	USE REDUNDANT UNIT	
RF SWITCH (COMMON)/2	SWITCHES TO REDUNDANT CIRCUITS IN CASE OF MALFUNCTION	FAILS TO TRANSFER	II	NONE	USE REDUNDANT PATHS	ALL RF SWITCHES WILL EITHER BE REDUNDANT OR SWITCHES WITH REDUNDANT COILS WILL BE UTILIZED.
AMPLIFIER (COMMON)/2	FILTER RF SIGNALS	LOSS OF FUNCTION	II	LOSS IN TRACKING ACCURACY	USE SINGLE CHANNEL RANGING WITH EITHER KU BAND OR VHF	
BEACON BEACON TRANSMITTER/2	TRANSMITS ACQUISITION SIGNAL	LOSS OF FUNCTION	II	LOSS OF REDUNDANCY	USE REDUNDANT UNIT	
RF SWITCH (COMMON)/2	SWITCHES TO REDUNDANT CIRCUITS IN CASE OF MALFUNCTION	FAILS TO TRANSFER	II	NONE	USE REDUNDANT PATHS	ALL RF SWITCHES WILL EITHER BE REDUNDANT OR SWITCHES WITH REDUNDANT COILS WILL BE UTILIZED.

*A DETAILED JUSTIFICATION FOR RETAINING THESE SINGLE POINT FAILURES IN THE DESIGN IS PRESENTED IN SECTION 10.4.



the subsystem. A failure rate of 2.5×10^{-6} was selected for the transceiver, which operates primarily during the first hundred hours after launch. During the remainder of the mission the unit was considered as back up for the Ku-band telemetry and command channels. The reliabilities listed for the remainder of the components are based on data included in Appendix 10C. The single failure points identified in the FMEA (Table 10-4) are discussed in Section 10.4.

10.3.2 Structure and Mechanisms

Spacecraft structures reflecting extensive testing and many millions of hours of space operations have demonstrated extremely high reliabilities; reliabilities that are considerably higher than the remainder of the subsystem. Therefore the reliability of the TDRS structure has been assumed as 1.00 in the analysis. The remainder of the subsystem consists of the mechanisms which deploy the solar arrays, MDR antennas, and LDR antennas. The three sets of mechanisms are similar in that each consists of loaded springs held in place by locking latches until released by solenoids. Microswitches are provided to indicate full deployment. In addition, the LDR antennas include a STEM erection system and cables to deploy the antennas.

The baseline design consists of a solenoid for each locking latch. Redundancy is provided by either a dual solenoid assembly or a single solenoid with dual coils and redundant springs to preclude deployment failure caused by a single malfunction, thus eliminating single failure points in this subsystem.

Figure 10-5 contains the top level reliability logic diagram for the mechanisms, together with the reliability estimate of 0.99968. No formal FMEA was conducted; however, no credible single failure points exist.

10.3.3 Attitude Control

Attitude control is provided by a combination of two reaction wheels and a gyro together with sensors, scanners, and associated electronics as described in Section 6. Two redundant inverters are included in this subsystem to provide alternating current for the gyro.

The attitude control system performs two functions using different combinations of components for each function. During the transfer orbit and synchronous orbit injection, when the TDRS is spinning, the accelerometer, spinning horizon sensor and sun sensor, plus the control electronics provide the signals for firing the appropriate thrusters. In synchronous orbit the TDRS is 3-axis stabilized and utilizes a combination of reaction wheels, a gyro, sensors, and control electronics. The system employs considerable redundancy and has no single failure points which could jeopardize the mission.

Figure 10-6 contains the subsystem reliability logic diagrams. The results of the FMEA are shown in Table 10-5. A reliability of 0.962 is predicted for this subsystem which was allocated a goal of 0.96.

10.3.4 Auxiliary Propulsion Subsystem (APS)

This subsystem described in Section 7, uses hydrazine stored in two propellant tanks containing an expulsion bladder pressurized by gaseous nitrogen. Sixteen thrusters provide ΔV maneuvers and pitch and yaw control. All maneuvers can be performed by combinations of various thrusting modes in the event



Table 10-4. Failure Mode Effects Analysis

PROGRAM: TDMS
SUBSYSTEM: TRACKING, TELEMETRY & COMMAND

CRITICALITY I: SINGLE FAILURE PRECLUDES MISSION SUCCESS
CRITICALITY II: ALL OTHER FAILURES

ITEM IDENTIFICATION/ QUANTITY	FUNCTION	FAILURE MODE	CRIT. CATE- GORY	FAILURE EFFECT	ALTERNATE MEANS OF OPERATION	REMARKS
TELEMETRY/2	CONDITIONS & FORMATS SPACECRAFT MEASURE- MENTS	LOSS OF FUNCTION	II	LOSS OF REDUNDANCY	USE REDUNDANT UNIT	
COMMAND/2	DECODES & PROCESSES COMMAND SIGNALS	LOSS OF FUNCTION	II	LOSS OF REDUNDANCY	USE REDUNDANT UNIT	
POWER SUPPLY/3	PROVIDES CONDITIONED POWER TO SUBSYSTEM	LOSS OF FUNCTION	II	LOSS OF REDUNDANCY	USE REDUNDANT UNIT	
VHF TRANSMITTER/2	TRANSMITS TELEMETRY DATA TO GROUND	LOSS OF FUNCTION	II	LOSS OF REDUNDANCY	USE REDUNDANT UNIT	
VHF RECEIVER/2	RECEIVES VHF SIGNALS FROM THE GROUND	LOSS OF FUNCTION	II	LOSS OF REDUNDANCY	USE REDUNDANT UNIT	
RF SWITCH (COMMON)/4	SWITCHES TO REDUNDANT CIRCUITS IN CASE OF MALFUNCTION	FAILS TO TRANSFER	II	NONE	USE REDUNDANT PATHS	ALL RF SWITCHES WILL EITHER BE REDUNDANT OR SWITCHES WITH REDUNDANT COILS WILL BE UTILIZED.
DIPLEXER (COMMON)/1	ISOLATES RECEIVER & TRANSMITTER PORTS OF ANTENNA	LOSS OF FUNCTION	I*	LOSS OF COMMUNICATION WITH SPACECRAFT	NONE	THIS FAILURE IS ONLY CRITICAL DURING THE INITIAL 30 HRS OF FLIGHT, UNTIL THE KU LINK IS OPERATIONAL. FROM THIS POINT ON THE VHF IS USED AS A BACKUP ONLY.

*A DETAILED JUSTIFICATION FOR RETAINING THESE SINGLE POINT FAILURES IN THE DESIGN IS PRESENTED IN SECTION 10.4



Figure 10-5. Reliability Logic Diagram of Structure and Mechanisms

of up to any two individual thruster failures. The thrusters contain an ignition catalyst and dual series propellant valves to minimize leakage and provide increased reliability. Figure 10-7 shows the subsystem reliability logic diagram and Table 10-6 contains the results of the FMEA. The reliability logic diagram shows the two tanks to be redundant for the purpose of the predictive analysis and the calculations to obtain the subsystem reliability numbers. It is assumed in the analyses that if a failure occurs in the tank system it would happen after orbit injection correction (approximately 30 hours after launch). This is a reasonable assumption, since extensive tests and checkout prior to launch assure a reliable working subsystem. In addition, the probability of a failure like a tank or line rupture within the first 30 hours is extremely small (estimated at 0.99999+).

Once orbit injection occurs, enough fuel is left in a single tank to achieve mission success with capability for one station change of 65° (1.13 rad) in 20 days if 2σ of allotted fuel for the apogee motor injection correction has been used or one station change of 65° (1.13 rad) in 40 days if all of the allotted fuel (3σ) is used. Furthermore, it is very unlikely that both a failure of the APS and the utilization of 3σ fuel will occur on the satellite requiring a station change, thus justifying the analytical approach taken.

10.3.5 Electrical Power

The electrical power system (EPS) described in Section 8 consists of two solar array assemblies, solar array drive assemblies, two NiCd batteries, battery chargers, regulators, various electrical control and measuring components, distribution, and associated wiring. A reliability block diagram of the system is shown in Figure 10-8. Table 10-7 contains the failure mode, effects, and criticality analysis. The FMEA revealed two Criticality I or single failure point items; (1) loss of rotating function of the solar array drive assembly, and (2) an open failure of the bus isolator. These two potential single failure points have been retained in the design. Justification for their retention is contained in Section 10-4.

The reliability goal for the electrical power system (Table 10-2) is 0.95 for five years. The predicted reliability is 0.955, which slightly exceeds the goal.

10.3.6 Thermal Control

The thermal control subsystem consists of passive insulation (i.e., paint and aluminized TFE Teflon), thermostat-actuated louvers, and heaters for the

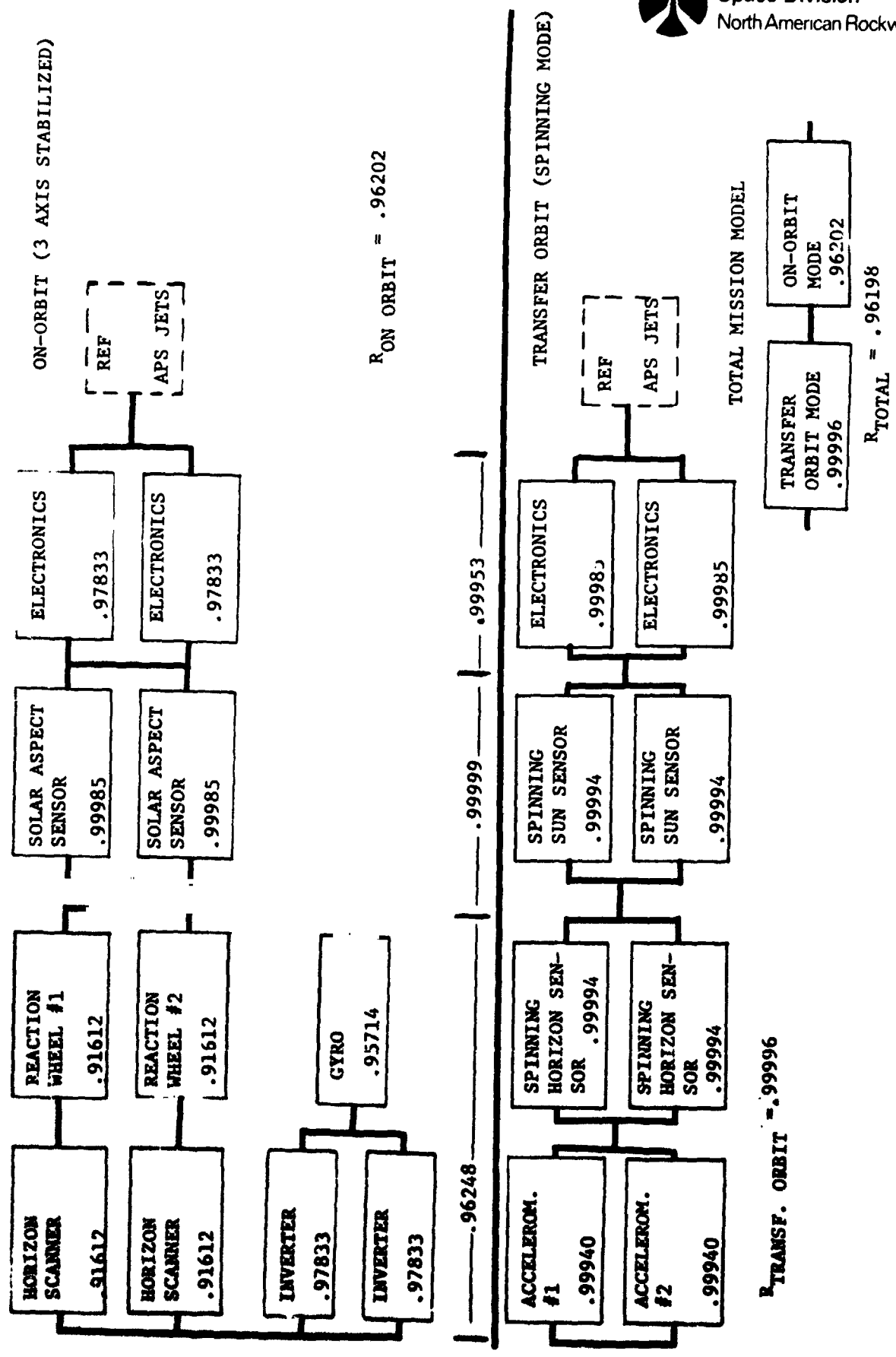


FIGURE 10-6. RELIABILITY LOGIC DIAGRAM
ATTITUDE CONTROL SUBSYSTEM



Table 10-5. Failure Mode Effects Analysis

PROGRAM: TDMS
SUBSYSTEM: ATTITUDE CONTROL

ITEM IDENTIFICATION/ QUANTITY	FUNCTION	FAILURE MODE	CRIT. CATE- GORY	FAILURE EFFECT	ALTERNATE MEANS OF OPERATION	REMARKS
TRANSFER ORBIT (SPINNING MODE)						
ACCELEROMETER/2	SENSES ACCELERATION FOR ROTATION COM- TROL	LOSS OF FUNCTION	II	REDUCTION OF RE- DUNDANCY	USE OF REDUNDANT SENSOR	
SPINNING HORIZON SENSOR/2	USED IN DETER- MINATION OF S/C ORIENTATION	LOSS OF FUNCTION	II	REDUCTION OF RE- DUNDANCY	USE OF REDUNDANT SENSOR	
SPINNING SUN SENSOR/2	USED IN DETER- MINATION OF S/C ORIENTATION	LOSS OF FUNCTION	II	REDUCTION OF RE- DUNDANCY	USE OF REDUNDANT SENSOR	
ELECTRONICS	PROVIDES CONTROL & LOGIC REQUIRED FOR FIRING APPROPRIATE JETS	LOSS OF FUNCTION	II	REDUCTION OF RE- DUNDANCY	USE OF REDUNDANT CIRCUITRY	
ON ORBIT (3 AXIS STABILIZED MODE)						
SOLAR ASPECT SENSOR/2	ACQUIRES SUN AFTER SPACECRAFT IS DE- SPIN	LOSS OF FUNCTION	II	REDUCTION OF RE- DUNDANCY	USE OF REDUNDANT SENSOR	
HORIZON SCANNER/2	UTILIZED IN SPACE- CRAFT STABILIZATION	LOSS OF FUNCTION	II	REDUCTION OF RE- DUNDANCY	USE OF REDUNDANT SENSOR	
REACTION WHEEL/2	PROVIDES ROTATION DAMPING & MOMENTUM STIFFNESS	LOSS OF FUNCTION	II	REDUCTION OF RE- DUNDANCY	USE OF REDUNDANT WHEEL & GYRO	
GYRO /1	ROTATION DAMPING, PITCH & YAW SENSING	LOSS OF FUNCTION	II	REDUCTION OF RE- DUNDANCY	USE OF THE TWO REACTION WHEELS	
ELECTRONICS	PROVIDES CONTROL & LOGIC FOR THE GYRO & FIRING OF AP- PROPRIATE JETS	LOSS OF FUNCTION	II	REDUCTION OF RE- DUNDANCY	USE OF REDUNDANT CIRCUITRY	
INVERTER/2	PROVIDES POWER FOR REACTION WHEELS	LOSS OF FUNCTION	II	REDUCTION OF RE- DUNDANCY	USE OF REDUNDANT CIRCUITRY	

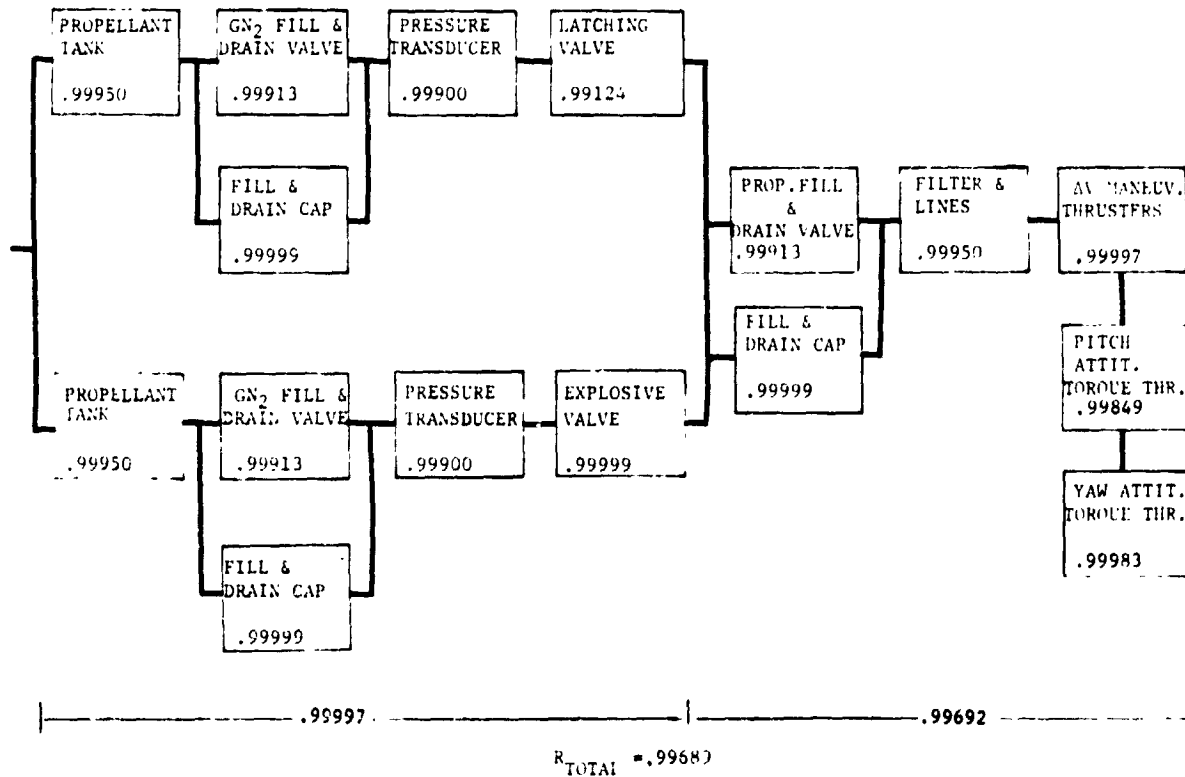


Figure 10-7. Reliability Logic Diagram of Auxiliary Propulsion Subsystem

thruster assemblies. The latter are included in the auxiliary propulsion section. In addition, a special microquartz radiation window is placed in a cutout of the surface insulation for battery cooling. There are approximately 100 louvers operating in pairs, which augment the thermal control provided by the insulation. This type of louver has provided reliable operation on the Mariner spacecraft, Nimbus, and other satellites. The failure of one or more pairs is not critical since other louvers will adjust and thus compensate for an open or closed failure. This redundant, or compensatory capability enhances the reliability. The reliability of the overall thermal subsystem is estimated to be in excess of 0.999.

10.4 SINGLE FAILURE POINT SUMMARY

As defined in Section 10.1, a single failure point is a failure of one component which precludes attainment of mission success, where mission success is the ability to service 20 LDR and 2 MDR users for a period of five years. Not all single point failures identified below are "mission critical." A failure of an EPS SFP would not terminate the mission but only degrades the overall mission capabilities.

Table 10-8 shows seven basic single failure point hardware items. Retention of these SFPs is justified by the following rationale:

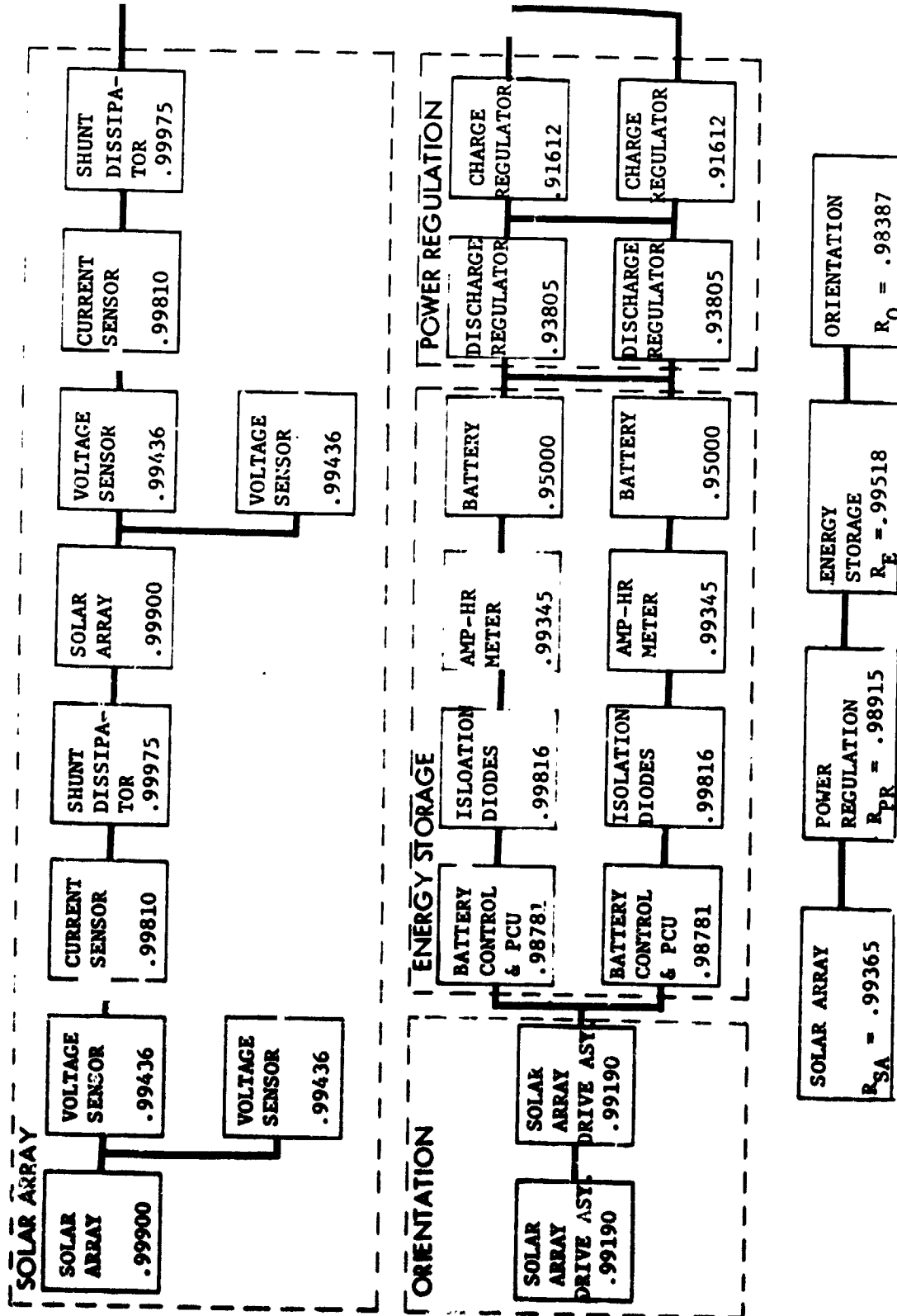


PROGRAM: TDRS
SUBSYSTEM: AUXILIARY PROPULSION

Table 10-6. Failure Mode Effects Analysis

ITEM IDENTIFICATION/ QUANTITY	FUNCTION	FAILURE MODE	CRIT. CATE- GORY	FAILURE EFFECT	ALTERNATE MEANS OF OPERATION	REMARKS
PROPELLANT TANK/2	PROPELLANT & PRESSUR- ANT STORAGE & EXPUL- SION	RUPTURE, LEAKAGE DIAPHRAGM LEAKAGE	II	LOSS OF PROPELLANT	USE SECOND TANK FUEL	
PROPELLANT FILL & DRAIN VALVE/1	FILL TANKS, DRAIN DURING GROUND OPERATIONS	EXTERNAL LEAKAGE	II	DECREASE OF PERFOR- MANCE, LOSS OF PRESSURE	NONE	
CH ₂ FILL & DRAIN VALVE/2	PRESSURIZES PRO- PELLANT TANKS	EXTERNAL LEAKAGE	II	LOSS OF PROPELLANT	ENERGIZE LATCHING VALVE TO ISOLATE LEAK & USE SECOND TANK FUEL	MANUAL VALVE, CLOSED PRIOR TO LAUNCH. FLIGHT CAP PROVIDES BACKUP SEAL TO PRECLUDE LEAKAGE.
PRESSURE TRANSDUCER/2	PRESSURE SENSING	EXTERNAL LEAKAGE	II	LOSS OF PRESSURE	NONE	MANUAL VALVE, CLOSED PRIOR TO LAUNCH. FLIGHT CAP PROVIDES BACKUP SEAL TO PRECLUDE LEAKAGE.
LATCHING VALVE/1	ISOLATES ONE PRO- PELLANT TANK	INTERNAL LEAKAGE, FAILS OPEN FAILS CLOSED	II	LOSS OF PROPELLANT	USE SECOND TANK FUEL	
EXPLOSIVE VALVE/1 (TANK)	ISOLATES ONE PRO- PELLANT TANK	FAILS TO CLOSE	II	CANNOT ISOLATE TANK	NONE	
FILTER/1	PREVENTS CLOGGING OF THRUSTER ASSY	FAILS TO CLOSE	II	LOSS OF ONE TANK	USE SECOND TANK FUEL	DESIGN DOES NOT PROVIDE FOR 2ND ORDER FAILURE, I.E., VALVE CLOSURE REQUIRED ONLY IF TANK RUPTURES OR LEAKS.
EXPLOSIVE VALVE/16 (THRUSTER)	PERMANENT SHUTOFF OF GIVEN THRUSTER	CLOGGING	I*	LOSS OF PROPELLANT CAPABILITY	NONE	
TEMPERATURE TRANS- DUCER/2 (TANK)	MONITORS TANK TEMP.	FAILS TO CLOSE	II	LOSS OF PROPELLANT	NONE	DESIGN DOES NOT PROVIDE FOR 2ND ORDER FAILURE, I.E., VALVE CLOS- URE REQ'D ONLY IF THRUSTER FAILS OPEN.
THRUSTER ASSEMBLY/16	ΔV MANEUVERS, PITCH & YAW ATTITUDE CONTROL	LOSS OF FUNCTION	II	LOSS OF DATA	NONE	
TEMPERATURE TRANS- DUCER/16 (THRUSTER)	MONITORS CATALYST TEMPERATURE	LOSS OF FUNCTION	II	REDUCTION OF RE- DUNDANCY	SELECT ALTERNATE SET OF JETS	
VALVE/16	MAINTAINS DESIRED CATALYST TEMPER- ATURE	LOSS OF FUNCTION	II	CANNOT DETERMINE BURNWAY THRUSTER ASSY	NONE	DESIGN DOES NOT PROVIDE FOR 2ND ORDER FAILURE, I.E., IDENTIFICATION OF THRUSTER REQ'D ONLY AFTER THRUSTER FAILURE HAS OCCURRED.
LINES & FITTINGS	CORRECT SUBSYSTEM COMPONENTS	RUPTURE, EXTERNAL LEAK	I*	DEGRADED THRUSTER PERFORMANCE	USE REDUNDANT JETS IF REQUIRED	

* A DETAILED JUSTIFICATION FOR RETAINING THESE SINGLE POINT FAILURES IN THE DESIGN IS PRESENTED IN SECTION 10.4



$$R_{TOTAL} = R_{SA} \times R_{PR} \times R_E \times R_O = .96235$$

Figure 10-8. Reliability Logic Diagram of Electrical Power Subsystem

Table 10-7. Failure Mode Effects Analysis

PROGRAM: TONS		SUBSYSTEM: ELECTRICAL POWER		CRITICALITY I: SINGLE FAILURE PRECLUDES MISSION SUCCESS		CRITICALITY II: ALL OTHER FAILURES	
ITEM IDENTIFICATION/ QUANTITY	FUNCTION	FAILURE MODE	CRIT. CATE- GORY	FAILUREE EFFECT	ALTERNATE MEANS OF OPERATION	REMARKS	
SOLAR CELL ARRAY ASSEMBLY/2 (UPPER & LOWER ARRAY)	TO PROVIDE ELECTRICAL ENERGY	BREAK OF POWER CABLE BETWEEN CELL ASSY AND SLIP RINGS (1 WIRE)	II	LOSS OF 12.5% AVAIL- ABLE SOLAR ENERGY	HEAVIER UTILIZATION OF BATTERIES AND TIGHTER ENERGY MGT. FROM GROUND	LOSS OF ONE CELL STRING IN EITHER ASSY NOT CRITICAL SINCE IT REPRE- SENTS A LOSS OF < 1% OF TOTAL SOLAR ENERGY	
VOLTAGE SENSOR/3	MONITORS ARRAY & BUS OUTPUT VOLTAGES	LOSS OF FUNCTION	II	PARTIAL LOSS OF DATA	OPERATE WITH RE- MAINING SENSORS		
ISOLATION DIODE/24 (SOLAR ARRAY)	ISOLATES SOLAR ARRAYS	FAILS OPEN FAILS SHORT	II II	PARTIAL LOSS OF AVAILABLE SOLAR ENERGY (APPR. 4%) PARTIAL LOSS OF AVAILABLE SOLAR ENERGY (< 1%)	NONE NONE	TIGHTER ENERGY MGT. FROM GROUND TOWARD END OF MISSION LIFE	
CURRENT SENSOR/2	MEASURES CURRENT FLOWING TO BUS	LOSS OF FUNCTION	II	PARTIAL LOSS OF DATA	OPERATE WITH RE- MAINING SENSOR		
SHORT DISSIPATOR/24	REGULATES SOLAR ARRAY OUTPUT VOLTAGE	FAILS OPEN FAILS SHORT	II II	PARTIAL LOSS OF REGULATION PARTIAL LOSS OF SOLAR ENERGY (APPR. 4%)	REDUNDANCY IN DIS- SIPATOR PERFORMS FUNCTION NONE	TIGHTER ENERGY MGT. FROM GROUND TOWARD END OF MISSION LIFE	
CHARGE REGULATOR/2	CONTROLS ALL BATTERY CHARGING FUNCTIONS	LOSS OF FUNCTION	II	LOSS OF RE- DUNDANCY	SECOND UNIT WILL PERFORM FUNCTION		
DISCHARGE REGULATOR/2 (BOOST REGULATION)	CONDITIONS BATTERY OUTPUT VOLTAGE	LOSS OF FUNCTION	II	LOSS OF RE- DUNDANCY	SECOND UNIT WILL PERFORM FUNCTION		
BATTERY/2	TO PROVIDE ELECTRICAL ENERGY	FAILS OPEN FAILS SHORT	II II	LOSS OF ONE BATTERY SHORT WILL BURN OUT ISOLATION DIODES OR COM- PLETELY DIS- CHARGE UNIT	SECOND UNIT WILL PERFORM FUNCTION SECOND UNIT WILL PERFORM FUNCTION		
AMPERE-HOUR METER/2	MONITORS BATTERY DIS- CHARGE TIME AND CURRENT	LOSS OF FUNCTION	II	PARTIAL LOSS OF DATA	OPERATE WITH RE- MAINING SENSOR		
ISOLATION DIODE (BATTERY)/4	ISOLATES BATTERIES	FAILS OPEN FAILS SHORT	II II	PARTIAL LOSS OF CUR- RENT CARRYING CAPA- BILITY CREATES SLIGHT UN- BALANCE IN BATT. BUS LOAD SHARING	REMAINING PARALLEL DIODE CARRY ADD'L LOAD SEQUENTIAL CHARG- ING OF BATT. IN PLACE OF PARALLEL		
CENTRAL POWER CONTROL/1	PERFORMS ALL SUB- SYSTEM CONTROL FUNCTIONS	LOSS OF FUNCTION	I:	LOSS OF INTERNAL REDUNDANCY	REDUNDANT COMPO- NENTS WILL PERFORM FUNCTIONS		



FOLDOUT FRAME

OUTPUT VOLTAGE	FUNCTION	DUNDANCY	SECOND UNIT WILL PERFORM FUNCTION
(1) 2.1 REGULATION) BATTERY/2	FAILS OPEN FAILS SHORT	II II	SECOND UNIT WILL PERFORM FUNCTION SECOND UNIT WILL PERFORM FUNCTION
AMPERE-HOUR METER/2	LOSS OF FUNCTION	II	OPERATE WITH REMAINING SENSOR
ISOLATION DIODE (BATTERY)/4	FAILS OPEN FAILS SHORT	II II	REMAINING PARALLEL DIODE CARRY ADD'L LOAD SEQUENTIAL CHARGING OF BATT. IN PLACE OF PARALLEL
CENTRAL POWER CONTROL/1	LOSS OF FUNCTION	II	REDUNDANT COMPONENTS WILL PERFORM FUNCTIONS
SOLAR ARRAY DRIVE ASSEMBLY 2	LOSS OF ROTATING FUNCTION LOSS OF POWER TRANSFER FUNCTION	I* II	HEAVIER UTILIZATION OF BATTERIES REDUNDANT SLIP RINGS WILL PERFORM FUNCTION
BUS ISOLATOR/2	FAILS OPEN FAILS CLOSED	I* II	NONE NONE
			GRACEFUL DEGRADATIONS ALLOW FULL RETURN LINK AND PARTIAL FORWARD LINK OPERATION DESIGN DOES NOT PROVIDE FOR 2ND ORDER FAILURE, I.E., OPERATION OF ISOLATOR REQUIRED ONLY IF SHORT IS PRESENT

* A DETAILED JUSTIFICATION FOR RETAINING THESE SINGLE POINT FAILURES IN THE DESIGN IS PRESENTED IN SECTION 10.4.

Table 10-8. Single Failure Point Summary

Subsystem	Failures Identified
Tracking, Telemetry and Command	1A. Diplexer (1) 1B. Diplexer (4)
Communications	2. Power Divider (10) 3. Gimbal Mechanism (2)
Structure and Mechanisms	0
Attitude Control	0
Electrical Power	4. Solar Array Drive (2) 5. Bus Isolator (2)
Propulsion	6. Filter (1)
Thermal Control	7. Lines and Fittings 0
Total SFPs	23

Diplexer. One diplexer is used between the transceiver and the antenna of the TT&C and the other four in the Ku- and S-band receiving circuits. Loss of the TT&C diplexer, during the first thirty hours after launch, is critical since it is required for VHF communications with the spacecraft. Thereafter, the VHF link is only used to back-up the Ku-link. Loss of the diplexers in an MDR is not critical since the second MDR link can perform the function and still maintain the SOW requirements. The likelihood of a diplexer failure is very remote. It consists exclusively of passive elements and no diplexer failures have been reported. Due to the extremely high reliability of this component it is considered justified to retain this design.

Power Divider. Power dividers are used in several telecommunication circuits. The dividers consist of passive elements which are highly reliable. Since the probability of failure is negligible, duplication of the power dividers is unnecessary.

Gimbal Mechanism. A failure of one of the two MDR gimbals degrades one MDR link by eliminating antenna motion in one of the two axes. To preclude mechanism failure, a simple redundant design was adopted to eliminate predominant failure modes. Gimbal mechanisms of similar design have been successfully flown in space for many years, indicating high reliability. Duplication of gimbal mechanisms adds weight, is costly and is not considered justified.

Solar Array Drive Assembly. The loss of rotating capability of either solar array reduces the power by 35 percent, thus degrading the mission. Dual wired stepper motors and redundant slip rings were incorporated. Potential suppliers indicated similar hardware was flown successfully in space for extensive time periods and the probability of failure is very small. A duplication of the gearing, bearing, and seals was considered unjustified since it would substantially increase the subsystem weight and complexity.

Bus Isolator. The failure of the bus isolator in the open position causes a loss of half the available power and degrades the mission. It is very unlikely that after extensive tests and checkout performed prior to launch a faulty component can be overlooked, especially since no spacecraft power would be available. The reliability of such a device, like a fuse, is very high and once determined to be functioning properly it is unlikely to fail. Due to the small probability of failure it is considered justified to retain this design.

Filter. The clogging of the filter results in loss of thrusting capability which precludes the successful completion of the mission. Extensive precautions during ground handling will be implemented to assure a contaminant free subsystem prior to launch. The filter is chosen so that only very large particle can clog the system. Particles of this nature could only be generated if an explosion or similar deterioration takes place.

Lines and Fittings. A rupture or external leak of the lines or fittings causes the loss of all propellant which precludes the successful completion of the mission. A failure of this nature is unlikely since all lines and fittings are brazed and thoroughly checked and verified prior to launch. Adequate precautions will be taken prior to launch to assure no leaks in the subsystem.

10.5 RELIABILITY PROGRAM FOR IMPLEMENTATION PHASE

The following elements are recommended for the Phase C reliability program of the TDRS:

1. Reliability Program Management
2. Quantitative Analyses
3. Failure Mode and Effects Analysis/Single Failure Points
4. Parts Program
5. Failure Reporting/Corrective Action
6. Design Specifications
7. Design Review
8. Test Support

Reliability Program Management. Reliability management will establish and maintain an effective reliability program that is planned, integrated and developed in conjunction with other program functions to permit the most economical achievement of overall program objectives. The following products will be generated.

- a. Reliability Program Plan
- b. Internal Controls and Visibility
- c. Subcontractor/Supplier Reliability Control
- d. Customer Visibility
- e. Cost Control

Quantitative Analysis. Apportionment of required system probability of mission success to each function will be updated and refined. The reliability of hardware items and other system elements supporting each function will be determined. The following end products are anticipated:



Space Division
North American Rockwell

- a. System/Subsystem Numerical Requirements
- b. Numerical Assessment of Design Against Requirements
- c. Quantitative Reliability Trade Study Comparisons
- d. Definition of Reliability Problem Areas

Failure Mode and Effects Analysis (FMEA). Update and refine FMEAs to identify potential system weaknesses, furnish design guidance and provide data for design review considerations. FMEAs will be generated to:

- a. Identify potential problem areas and single failure points (SFP)
- b. Generate pertinent preventive information
- c. Assure timely implementation of curative measures
- d. Document rationale for accepted SFP risk

Parts Program. The parts program will assure the selection, control and proper application of preferred parts including selection controls, specifications, qualification, derating, application review, parts accountability and parts in off-the-shelf hardware. Maximum use will be made of parts that are qualified and minimum qualification testing of new parts is anticipated.

Failure Reporting and Corrective Action. This task involves the implementation of a closed loop system for collecting, analyzing and recording all failures occurring during tests at the prime contractor, suppliers, and launch site prior to turnover to the customer. The products generated are the following:

- a. Documentation of all failures
- b. A thorough investigation of failed components
- c. Failure analysis
- d. Timely program status
- e. Cost effective corrective action
- f. Documented problem histories

Design Specifications. This element provides the reliability requirements for end item CEI specifications and for all subsystem and equipment specifications, which would include all procurement, subsystem, CEI and system specifications.

Design Review. The reliability support to design and program reviews accomplished by this task, assures all imposed requirements are met.

Qualification Test Support. This task supports the preparation and review of the integrated test plan and assures reliability objectives and compatibility with environmental requirements are included. A qualified status list is also maintained.